

## PDF hosted at the Radboud Repository of the Radboud University Nijmegen

The following full text is a publisher's version.

For additional information about this publication click this link.

<http://hdl.handle.net/2066/19054>

Please be advised that this information was generated on 2017-12-05 and may be subject to change.

# **Polymers and Block Copolymers of Isocyanopeptides**

Towards Higher Structural Order in Macromolecular Systems

Jeroen Cornelissen



# **Polymers and Block Copolymers of Isocyanopeptides**

Towards Higher Structural Order in Macromolecular Systems

Een wetenschappelijk proeve op het gebied van de  
Natuurwetenschappen, Wiskunde en Informatica

## **PROEFSCHRIFT**

ter verkrijging van de graad van doctor  
aan de Katholieke Universiteit Nijmegen,  
volgens besluit van het College van Decanen  
in het openbaar te verdedigen op woensdag 21 november 2001,  
des namiddags om 1.30 uur precies

door

**Jeroen Johannes Lambertus Maria Cornelissen**

geboren op 12 augustus 1972 te Veghel



**Promotor:** Prof. dr. R. J. M. Nolte

**Copromotor:** Dr. N. A. J. M. Sommerdijk  
Eindhoven University of Technology

**Manuscriptcommissie:** Prof. dr. E. W. Meijer  
Eindhoven University of Technology

Dr. P. C. J. Kamer  
University of Amsterdam

Dr. A. P. H. J. Schenning  
Eindhoven University of Technology

The work described in this thesis was supported financially by the Council for Chemical Sciences of the Netherlands Organization for Scientific Research (CW-NWO).

ISBN 90-9014942-2

Cover: Lidwien van der Horst, Sandra Cornelissen – de Wit

# Table of Contents

<b>Chapter 1</b>	<b>General Introduction</b>	<b>1</b>
1.1	Introduction	1
1.2	Polyisocyanides	3
1.3	Chiral Macromolecular Architectures: Tertiary Structure	15
1.4	Aim and Outline of the Thesis	21
1.5	References	22
<b>Chapter 2</b>	<b>Synthesis and Characterization of Polyisocyanides Derived from Alanine and Glycine Dipeptides</b>	<b>27</b>
2.1	Introduction	27
2.2	Results and Discussion	28
	2.2.1 Alanyl-alanine derived polyisocyanopeptides	28
	2.2.2 Polyisocyanopeptides based on alanine and glycine	37
2.3	Conclusions	40
2.4	Experimental Section	41
	2.4.1 General methods and materials	41
	2.4.2 Single crystal X-ray resolution of L,L-IAA	42
	2.4.3 Compounds	43
2.5	References and Notes	48
<b>Chapter 3</b>	<b>Conformational Analysis of Dipeptide Derived Polyisocyanides</b>	<b>49</b>
3.1	Introduction	49
3.2	Results and Discussion	51
	3.2.1 Side chain hydrogen bonding	51
	3.2.2 Unfolding of the secondary structure	58
	3.2.3 Determination of the helix sense	62
	3.2.4 Effects of the side chain configuration	66
	3.2.5 Lyotropic liquid crystalline phase	68
3.3	Conclusions	70
3.4	Experimental Section	71
	3.4.1 General methods and materials	71
	3.4.3 Powder X-ray diffraction	72
	3.4.4 Compounds	72
3.5	References and Notes	73
<b>Chapter 4</b>	<b><math>\beta</math>-Helical Polymers from Isocyanopeptides</b>	<b>75</b>
4.1	Introduction	75
4.2	Results and Discussion	77
	4.2.1 Synthesis and characterization of L,L,L-PIAAA	77
	4.2.2 Conformational analysis of L,L,L-PIAAA	79

4.2.3	Retention of the $\beta$ -helical architecture in an aqueous environment	82
4.3	Conclusions	88
4.4	Experimental Section	89
4.4.1	General methods and materials	89
4.4.2	Synthesis	
4.5	References and Notes	91
<b>Chapter 5</b>	<b>Helical Superstructures from Polystyrene-Polyisocyanopeptide Block Copolymers</b>	<b>93</b>
5.1	Introduction	93
5.2	Results and Discussion	94
5.2.1	Synthesis and characterization	94
5.2.2	Aggregation behaviour	100
5.3	Conclusions	105
5.4	Experimental Section	106
5.4.1	General methods and materials	106
5.4.2	Synthesis	107
5.5	References and Notes	109
<b>Chapter 6</b>	<b>Block Copolymers Based on Polyisocyanopeptides and Carbosilane Dendrimers</b>	<b>111</b>
6.1	Introduction	111
6.2	Results and Discussion	112
6.2.1	Synthesis and characterization	112
6.2.2	Self-assembling properties	116
6.2.3	Effect of $\text{Ag}^+$ ions on the self-assembling properties	117
6.3	Conclusions	121
6.4	Experimental Section	121
6.4.1	General methods and materials	121
6.4.2	Compounds	122
6.5	References and Notes	124
	<b>Summary</b>	<b>125</b>
	<b>Samenvatting</b>	<b>133</b>
	<b>Dankwoord</b>	<b>141</b>
	<b>List of Publications</b>	<b>145</b>
	<b>Curriculum Vitae</b>	<b>146</b>

# CHAPTER 1

## General Introduction

### 1.1 Introduction

In the course of evolution Nature has developed a multitude of biomacromolecules tailored to deal with complicated tasks such as information storage, support of tissue, transport, and the performance of localized chemical transformations. Although large numbers of researchers in the fields of chemistry and physics have been, and still are, pursuing the same goals using synthetic systems, nucleic acids and proteins still outclass Man-made materials. This has made an increasing number of scientists over the last decades turn their eye to Nature in order to design and synthesize increasingly precise nanoscopic and even mesoscopic structures using polymeric materials.

For the structuring of matter Nature uses the self-assembly of both low and high molecular weight compounds as a tool. Many biological architectures, of which the dimensions may range over several orders of magnitude, for their robustness rely on two structural components: the  $\alpha$ -helix and  $\beta$ -sheet structures of peptides. It is the secondary structure of these two components which, in a delicate interplay between steric, hydrophobic, electrostatic and hydrogen bonding interactions, give rise to the tertiary structure of Nature's main building blocks, the proteins. In order to achieve the high levels of organization, information must be built-in into the smallest building blocks, *i.e.* the amino acids. Indeed these building units do contain this information in the form of chirality, hydrogen bonding capacity, steric demands, electrostatic properties, hydrophilic or hydrophobic character or metal ion binding capability. Supramolecular chemistry since its early days has been inspired by biological assembly

methods and has already delivered a large number of (chiral) architectures of macromolecular size based on these secondary interactions.<sup>1,2</sup> The same principles, when applied to polymer chemistry, allow the construction of large, complex, but precise macromolecular architectures.

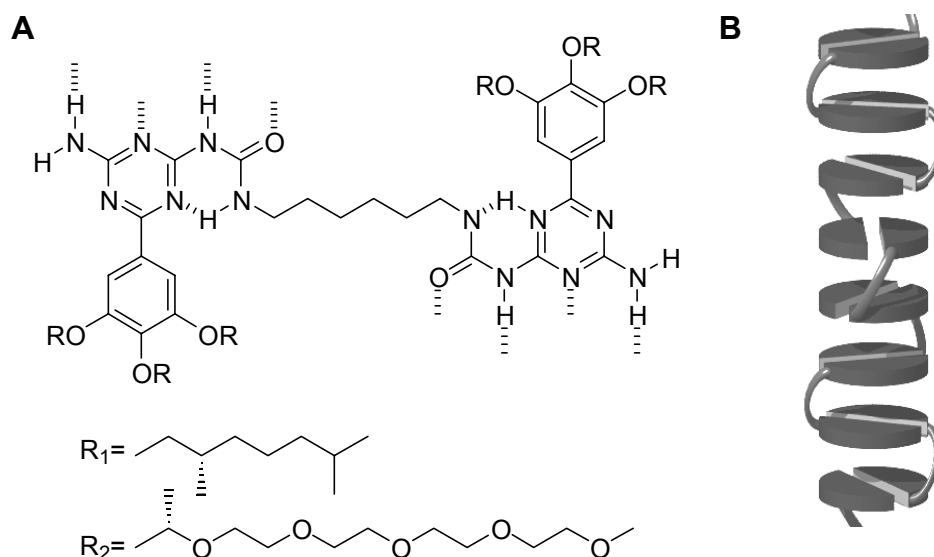


**Figure 1** (A) Structure of dimeric hydrogen bonding units able to form helical self-assembled polymers in organic ( $R_1$ ) or aqueous ( $R_2$ ) solution, (B) schematic representation of a right-hand helical self-assembled polymer.

By building-in structural information researchers have designed and synthesized self-assembling low molecular weight surfactants preprogrammed to form chiral superstructures such as “cigars”, twisted ribbons,<sup>3</sup> helices,<sup>4</sup> tubes,<sup>5</sup> braids,<sup>6</sup> boomerangs,<sup>7</sup> and superhelices in aqueous media<sup>8,9</sup> Comparable structures were generated by the aggregation of other low molecular weight compounds in organic solvents.<sup>10,11</sup> One other important principle to be learned from Nature, is that when the structural dimensions of the architectures enter the multi-micrometer domain, different levels of organization are involved, *e.g.* as in collagen, which consists of polypeptide strands that are organized in triple helices (tropocollagen) that assemble to form fibrils and ultimately generate the collagen fibers.<sup>12</sup> Several accounts of similar hierarchical order have also been reported for aggregates of synthetic low molecular weight compounds.<sup>13</sup> Another feature to be learned from Nature is the influences external stimuli as pH, ionic strength, temperature etc. have on assembling processes, as for example the coiling of DNA.<sup>14</sup> The double helix of DNA exemplifies Nature’s ability to construct complex chiral structures in an aqueous medium by making use of both

hydrogen bonding and hydrophobic interactions. Inspired by this phenomenon Sijbesma and Meijer used dimeric building blocks equipped with fourfold hydrogen bonding units to obtain true polymeric structures in solution based on supramolecular interactions. By the interplay between the stacking of the aromatic hydrogen bonding units and the incorporated enantiomerically pure solubilizing side chains they were able to generate helical self-assembled polymeric architectures in organic solvents as well as in aqueous media (Figure 1).<sup>15</sup>

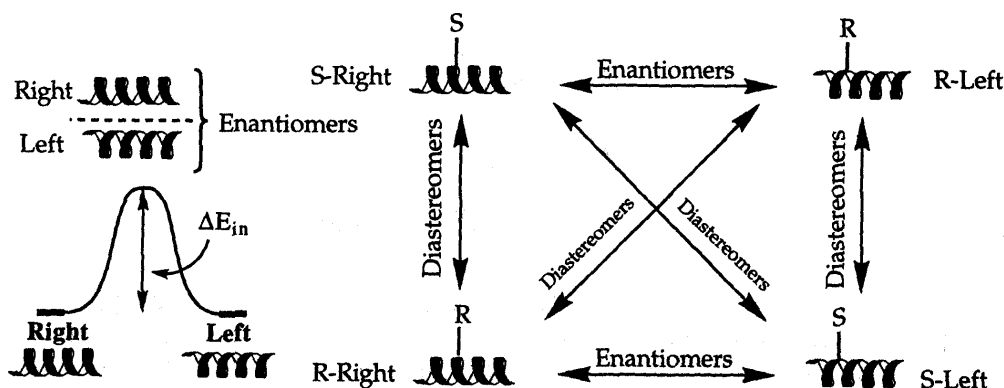


**Figure 2** Energy relationships between helical polymers.<sup>16</sup>

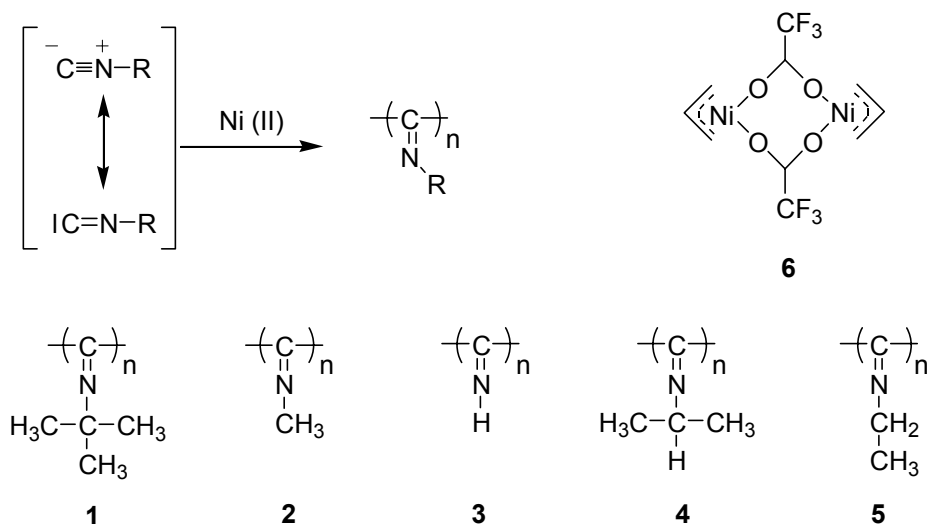
## 1.2 Polyisocyanides

### 1.2.1 Chiral Macromolecules: Secondary structure

A chiral organization *within* a macromolecule in most cases is present as a helical conformation of the polymeric backbone. The properties of such macromolecules are highly dependent on the helix inversion barrier ( $\Delta E_{in}$ ). The screw sense of one particular strand is stable at room temperature when this helical inversion barrier is high ( $> \sim 85$  kJ/mol). The two screw senses may be in equilibrium when the barrier is lower ( $< \sim 40$  kJ/mol).<sup>16</sup> In the case of achiral side chains the left- and right-handed helices are enantiomers, having equal free energies. When the polymer contains chiral side chains, the helices are diastereomers and consequently have different free energies (Figure 2). Polymers with low helix inversion barriers have dynamic properties which can be used to build chiral architectures that respond to interactions with small molecules, light, or to subtle changes in monomer composition or temperature. When the helix inversion barrier of the polymer is high, the helical conformation is usually formed under kinetic

conditions. This implies that upon incorporation in the growing chain each monomer contributes to the helix, and is sterically locked into its conformation.

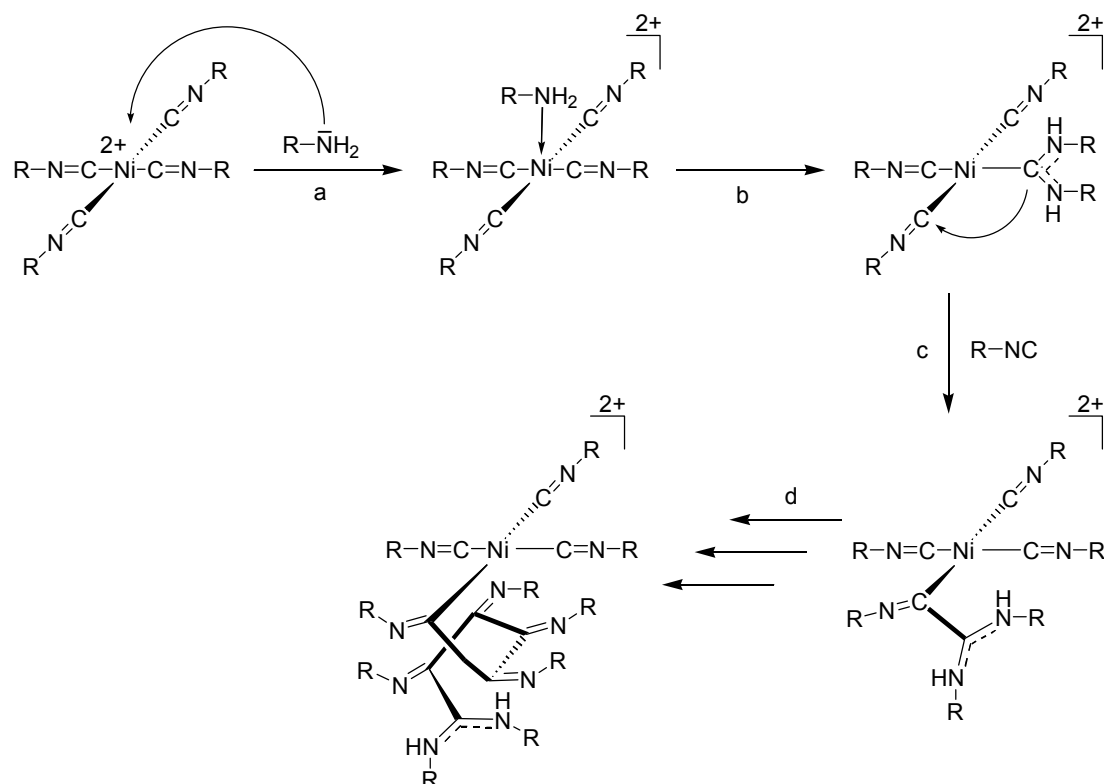
Examples of the first class of helical polymers comprise polyisocyanates,<sup>17,18</sup> polyacetylenes,<sup>19,20</sup> polyanilines<sup>21,22</sup> and polysilanes.<sup>23</sup> Polymers having a high helix inversion barrier are limited to fewer examples such as bulky poly(methacrylate esters),<sup>24,25</sup> polyaldehydes<sup>26,27,28</sup> and polyisocyanides. In the next sections recent developments in the field of polyisocyanides will be discussed in more depth.<sup>29</sup>



**Scheme 1** The nickel(II) catalyzed polymerization of isocyanides.

## 1.2.2 Mechanism of polymerization

Polymers of isocyanides have the unusual feature that every carbon atom in the main chain is provided with a substituent (Scheme 1). It was already proposed by Millich<sup>30</sup> that these macromolecules would have a helical conformation as the result of a restricted rotation around the single bonds constituting the polymeric backbone. Until Nolte's report on the applicability of Ni(II) as a catalyst for the polymerization of isocyanides, routes towards polyisocyanides were limited.<sup>31</sup> This transition metal catalyst allowed the polymerization of the sterically demanding poly(*tert*-butyl isocyanide) (**1**), which subsequently could be resolved by chromatography into the left- and the right-handed helical forms using poly((*S*)-*sec*-butyl isocyanide) as the stationary phase.<sup>32</sup> These experiments confirmed the structural proposition of Millich and provided the first example of an optically active polymer solely based on the stable helical conformation of the backbone.<sup>33</sup>



**Scheme 2** The ‘merry-go-round’ mechanism in Ni(II) catalyzed isocyanide polymerization.

The nickel(II) catalyzed polymerization of isocyanides proceeds relatively fast, a remarkable observation given the steric crowding that is introduced upon formation of the polymer chain. The driving force for the reaction is the conversion of a formally divalent carbon in the monomer into a tetravalent carbon in the polymer, the heat of polymerization being 81.4 kJ/mol.<sup>33</sup> For this polymerization reaction a *merry-go-round mechanism* has been proposed. Upon mixing of the isocyanides with the Ni(II) catalyst a square-planar complex is formed (Scheme 2), which in some occasions can be isolated when bulky isocyanides are used. The subsequent attack by a nucleophile on one of the isocyanide ligands is the initiation step of the polymerization reaction. Via coordination to the nickel (step a) this nucleophile migrates to the isocyanide and a carbene-like intermediate is observed (step b). In the presence of a chiral bias (introduced in the monomer or in the nucleophile) there is a preference for reacting with specifically one of the two neighboring isocyanide monomers on the nickel. After this step the free coordination position is occupied by an isocyanide from solution (step c) and the reaction sequence continues in the direction of the initial step (i.e. one particular helical sense is formed) and each rotation around the nickel adds one turn to the helix (step d).



In the absence of a chiral bias there is an equal probability of attack of the carbene-like carbon atom on both neighboring ligands leading to a racemic mixture of helical polymers. The easy formation of the tightly coiled helix is explained by the preorganizing effect of the nickel center: only a slight rearrangement of bonds is required to form the polymer molecule.

The *merry-go-round mechanism* of isocyanide polymerization can be used to explain and predict a number of the properties of polyisocyanides.<sup>33</sup> However, work by Deming and Novak indicated that some aspects of the mechanism are more complex and involve the reduction of Ni(II) to Ni(I) during the polymerization reaction. Using ESR, cyclic voltammetry, and magnetic susceptibility measurements it was shown that when an excess (10 equivalents) of *tert*-butyl isocyanide is added to NiCl<sub>2</sub>, the isocyanide acts as a reductant and an inactive nickel(I) catalyst is formed. Under atmospheric conditions this reduced catalyst is reoxidized by oxygen to the more active nickel(II) species. The optimum oxygen concentration appears to be at 1 atm of air, at high oxygen contents no polymerization occurs; instead, the nickel catalyzes the oxidation of the isocyanide to the isocyanate.<sup>34</sup> Taking into account these observations Deming and Novak investigated the electron-deficient  $\eta^3$ -allylnickel trifluoroacetate (**6**) as a polymerization catalyst. They found it to be a highly active system (Table 1) which, in a noncoordinating solvent, displayed living chain-growth behavior.<sup>35</sup>

**Table 1. Molecular Weight Characteristics of Selected Polymers<sup>35</sup>**

monomer	catalyst	Conditions	yield (%)	$M_n$	$M_w/M_n$
<i>tert</i> -C <sub>4</sub> H <sub>9</sub> NC	<b>6</b>	N <sub>2</sub> , neat	100	2200	1.03
C <sub>6</sub> H <sub>5</sub> CH(CH <sub>3</sub> )NC	NiCl <sub>2</sub>	N <sub>2</sub> , H <sub>2</sub> O	75	13220	1.45
C <sub>6</sub> H <sub>5</sub> CH(CH <sub>3</sub> )NC	NiCl <sub>2</sub>	Air, H <sub>2</sub> O	100	7420	1.64
C <sub>6</sub> H <sub>5</sub> CH(CH <sub>3</sub> )NC	<b>6</b>	N <sub>2</sub> , toluene	100	24000	1.15

Detailed kinetic and mechanistic investigations have been carried out by Deming and Novak employing this type of Ni-catalyst. In toluene a linear relation was found between the monomer conversion and the degree of polymerization, as well as between the catalyst to monomer ratio and the molecular weight, for a system consisting of **6** and  $\alpha$ -methylbenzyl isocyanide (for racemic as well as for pure enantiomers).<sup>35</sup> It also appeared possible to copolymerize a second isocyanide monomer (e.g. **1**) after

complete consumption of the first one. Different kinetic behavior was observed under a N<sub>2</sub> atmosphere compared to an O<sub>2</sub> rich environment. Under N<sub>2</sub>, the polymerization was found to be first order in monomer, obeying the rate expression:  $v_p = k_{\text{obs}}[\text{catalyst}][\text{monomer}]$  with  $k_{\text{obs}}(298\text{K}) = 3.7(1) \times 10^{-2} \text{ L}\cdot\text{mol}^{-1}\cdot\text{s}^{-1}$ . Under O<sub>2</sub> the rate was found to be zero order in monomer ( $v_p = k_{\text{obs}}[\text{catalyst}]$ ) with  $k_{\text{obs}}(298\text{K}) = 5.1(1) \times 10^{-2} \text{ s}^{-1}$ .<sup>36</sup> Although these rate constants are comparable, in such cases a zero-order reaction will appear faster than a first-order reaction, due to the lack of rate dependence on monomer concentration. The differences in transition-state were examined by determination of thermodynamic activation parameters performing an Eyring analysis of the rate constants.<sup>37</sup> More kinetic data have been reported by Deming and Novak investigating substituent effects on the monomer<sup>38</sup> and by Hong and Fox using functional isocyanides.<sup>39</sup> An in depth discussion of the mechanistic parameters based on these results is beyond the scope of this chapter and therefore the reader is referred to the work cited.<sup>40</sup>

### 1.2.3 Computational studies

The conformation of polyisocyanides has been the subject of several computational studies. Using the extended Hückel theory Kollmar and Hoffmann showed that repulsion between the lone pairs of the imino groups in a polyisocyanide chain favours a departure from a planar structure.<sup>41</sup> Similar repulsive effects are known to be operative in polyketones as was reported by Cui and Kertesz who found a new type of helical Peierls-like distortion for polyketone and polyisocyanide. They suggested that as a result of the existence of partially filled crossing bands a helical structure is formed.<sup>42</sup> Calculations by Kollmar and Hoffman on the series of polymers **1**, **2** and **3** indicated that steric effects are more important than electronic effects in determining the polymer structure. For the hypothetical polymer **3** a broad range of helical conformations was predicted, in contrast to **1** for which the authors proposed a rigid 4/1 helix. According to this theoretical analysis, polymer **2**, which only is moderately sterically restricted, may adopt two helical structures with different dihedral angles.

Huige and Hezemans<sup>43,44</sup> have performed extensive molecular mechanics calculations using the consistent force-field method on various oligo- and polyisocyanides. The hexadecamer of *tert*-butyl isocyanide was calculated to have a helical middle section and disordered ends. The dihedral angle N=C-C=N in the middle section was found to be 78.6° and the number of repeat units per helical turn was 3.75.

The latter number is in agreement with circular dichroism calculations using Tinoco's exciton theory (3.6 – 4.6) and De Voe's polarizability theory (3.81). The molecular mechanics calculations further predicted that the less bulky polymers **4** and **5** form helical polymers as well, whereas a disordered structure was calculated for poly(methyl isocyanide) (**3**).

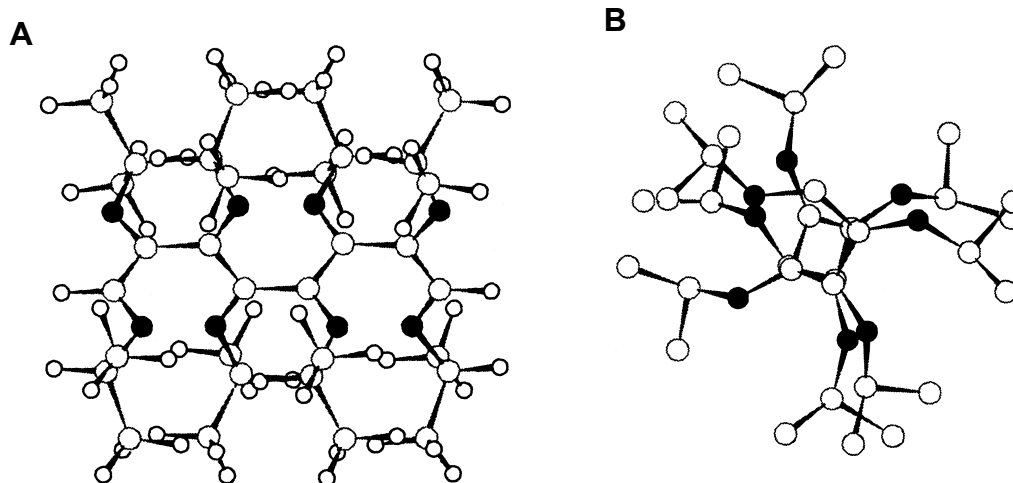
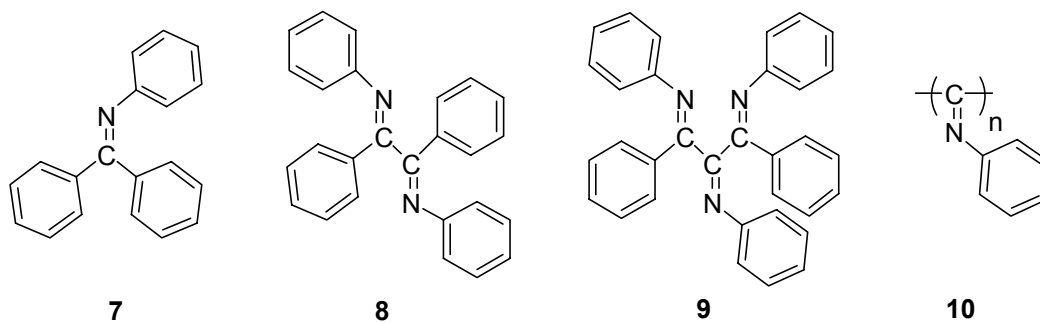


**Figure 3** Models of (A) the *syndio* conformation and (B)  $4_1$  helical conformation of poly(isopropyl isocyanide) **4**.<sup>45</sup>

Clericuzio et al. recently published *ab initio* and molecular mechanics studies on octameric oligoisocyanides. These calculations, in contrast to the aforementioned ones, showed the so-called *syndio* conformation to be the minimum energy geometry although the  $4_1$  conformation was recognized as a local minimum (Figure 3).<sup>45</sup> The obtained set of data was used to tentatively explain some of the features in the UV/vis, CD and  $^{13}\text{C}$  NMR spectra of compounds prepared by Salvadori's<sup>46</sup> and Green's group.<sup>47</sup> Regarding properties such as optical absorptions at long wavelengths, low intensity of CD bands and the chemical shift dispersion of backbone carbon atom resonances, the calculations were found to fit the experimental results. Nevertheless, the outcome of the calculations is the thermodynamic minimum conformation of the polymer backbone, whereas the polymerization is kinetically controlled, possibly leading to a different conformation. However, if the helix inversion barrier is not too high, the  $4_1$  helix imposed during polymerization reaction may unfold to give the proposed *syndio* conformation.



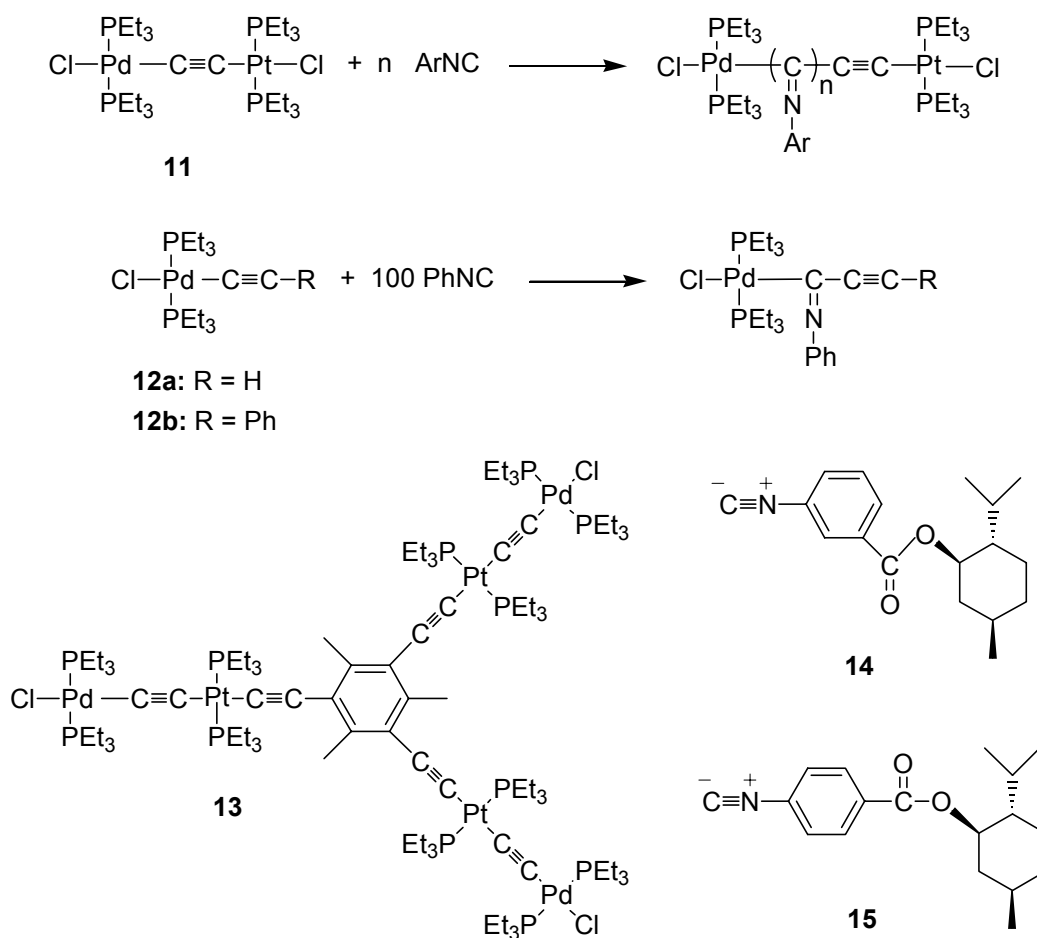
#### 1.2.4 Conformational studies

In depth studies towards the absolute conformations of polyisocyanides are limited. Green and coworkers<sup>47</sup> found, using  $^{13}\text{C}$  NMR and light scattering experiments, a limited persistence length ( $\sim 3$  nm) for polyisocyanides without bulky substituents. By means of NMR techniques Spencer et al.<sup>48,49</sup> studied oligoimine compounds **7-9** as model compounds for polymer **10**. In particular for the triimine **9** the conformational analysis is in line with the model of Clericuzio et al.<sup>45</sup> (*see above*). In the case of polymer **10** a combination of GPC, light scattering and X-ray diffraction showed that the native polyisocyanide has rigid rod character, but slowly precipitates from solution as a random coil. Using UV/vis spectroscopy, the Arrhenius activation energies for this rod to coil transition were determined in different solvents;  $E_a(\text{CCl}_4) = 44$  kJ/mol,  $E_a(\text{THF}) = 51$  kJ/mol and  $E_a(\text{CH}_2\text{Cl}_2) = 70$  kJ/mol.<sup>50</sup> These data indeed suggest that the helix inversion barrier for **10** is not sufficiently high to have a stable helical conformation at room temperature, but that as a result of the *merry-go-round mechanism* initially the  $4_1$  helix is formed as the kinetic product. Helical poly(*tert*-butyl isocyanide) (**1**), obtained by chiral resolution,<sup>32</sup> retains its optical activity even at elevated temperatures.<sup>51</sup> This enabled the use of this polyisocyanide as a chiral absorbent in liquid column chromatography although a different procedure was used for preparing it in the optically active form.<sup>52</sup>

#### 1.2.5 Screw-sense-selective polymerization

Several procedures have been established in the past for the helix-sense-selective polymerization of isocyanides.<sup>33</sup> For the introduction of a chiral bias, required for the discrimination of the otherwise enantiomeric helical senses, three distinct approaches can be applied. One is the use of a chiral monomer, which makes the left- and right-handed helices diastereotopic and as a result one of the two will be energetically favorable (Figure 2). A second approach involves the use of a chiral catalyst or a chiral

initiator in which case during the initiation of the polymerization there will be a preference for the formation of one particular helical sense that will be retained upon propagation due to the helix inversion barrier. The first approach has been employed in numerous cases; the accounts of the use of optically active Ni-catalysts are limited.<sup>53</sup> The third approach is the selective restraining of the growth of one particular helix by addition of a sterically encumbered optically active co-monomer to an achiral one. Polymerization of a fast propagating isocyanide of the latter type (e.g. phenyl isocyanide, 4-methoxyphenyl isocyanide) in the presence of the slowly polymerizing (*S*)-isocyanoisovaleric acid, leads to the formation of *P*-helical high molecular weight homopolymers of the former isocyanide and *M*-helical copolymers with a substantially lower degree of polymerization. Upon co-polymerization, the bulky chiral monomer prefers to be included into *M*-type helices and slows down their propagation, while the *P*-helices continue to grow fast and consequently consume the majority of the achiral monomer.<sup>54</sup>



**Scheme 3** Polymerization of isocyanides by a dinuclear  $\mu$ -ethynediyl Pd-Pt complex.

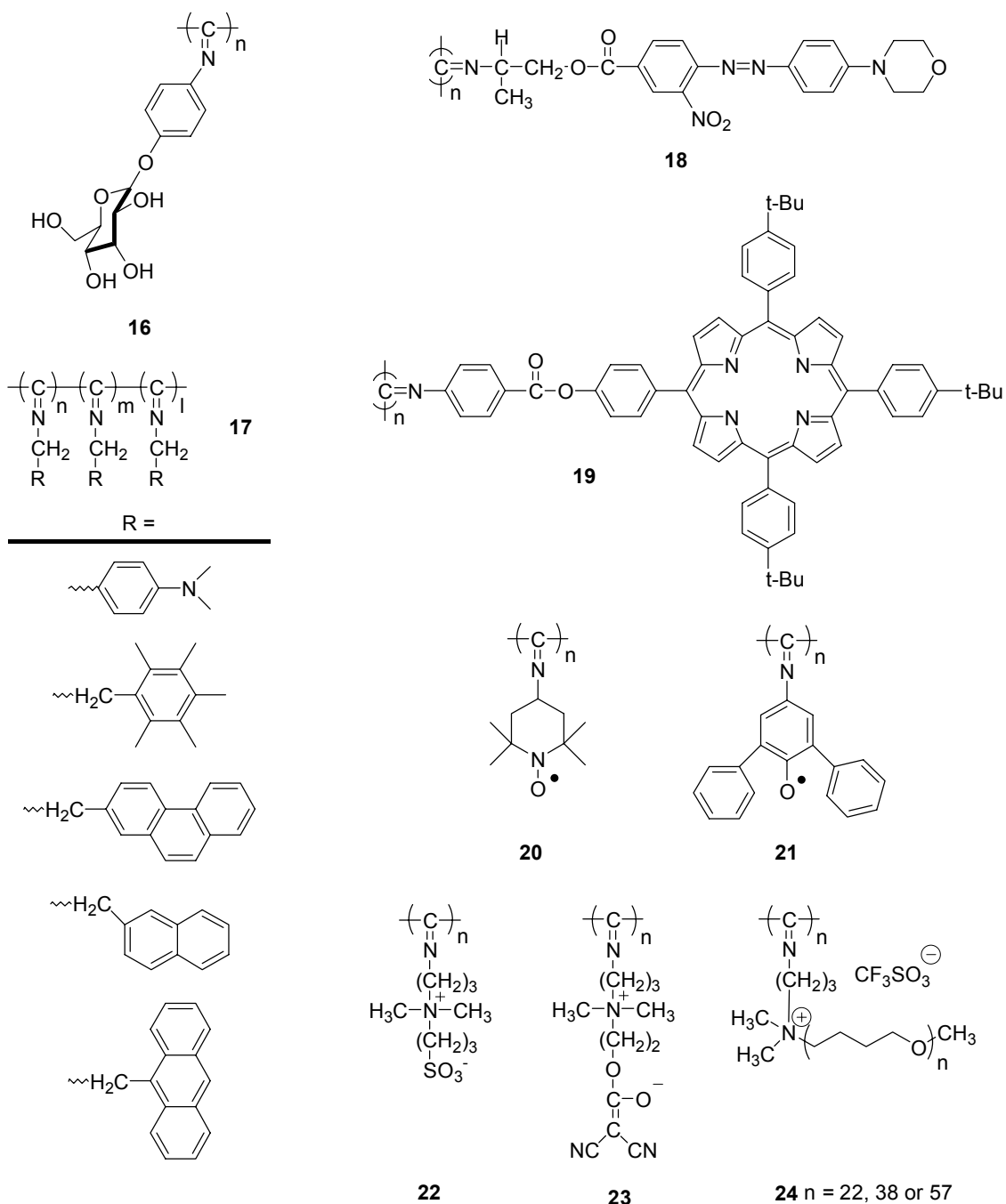
### 1.2.6 Pd-Pt dinuclear polymerization catalyst

An alternative to the nickel catalyzed synthesis of polyisocyanides has been developed by Takahashi and coworkers.<sup>55</sup> They found that the dinuclear  $\mu$ -ethynediyl Pd-Pt complex **11**<sup>56</sup> is active in the polymerization of aryl isocyanides,<sup>57</sup> but not when alkyl isocyanides are used. The isocyanides exclusively insert in the Pd-C bond, not in the Pt-C bond.<sup>58</sup> The importance of the Pt-C bond, however, is highlighted by the fact that only one isocyanide monomer is inserted in complex **12** although a hundred fold excess was used. The living nature of the catalyst was shown by the formation of block copolymers, which was possible since the active Pd end groups remained connected to the polymer when all monomers were consumed. Using this feature it proved to be possible to initiate the polymerization of an achiral isocyanide with an oligomer prepared from an optically active isocyanide.<sup>59</sup> This procedure, however, was only applicable for initiating complexes of which the oligomer exceeds a critical degree of polymerization and the optical activity is only retained in the case of sterically demanding achiral isocyanides. Initiators may carry multiple Pd-Pt  $\mu$ -ethynediyl units as was demonstrated by preparation of polyisocyanides from **13**.<sup>60</sup> A detailed study on the helix-sense-selective polymerization using chiral oligomer complexes derived from isocyanides **14** and **15** gave some interesting results.<sup>61</sup> First, the optical activity of the polymers, expressed in their optical rotation and CD effects, drastically increased in going from the *meta* substituted aryl isocyanides **14** to the *para* substituted ones **15**. Secondly, the rate constants for propagation were independent of the chirality of the monomer, i.e. having the same or the opposite chirality as the monomer building up the initiating oligomer. This suggests thermodynamic rather than kinetic control over the helical sense, which contradicts with the high helix inversion barrier previously proposed for helical polyisocyanides. However, the observation of a non-linear relation between the optical purity of the isocyanide and the induced helical sense in the polymer<sup>62</sup> (majority rules concept) confirms this suggestion. These observations, indicate that factors other than steric interactions may be operative during the synthesis of these particular polyisocyanides.

### 1.2.7 Polyisocyanides having functional side groups

Hasegawa et al. reported on glycosylated poly(phenyl isocyanide)s primarily to study the recognition of lectins by these polymers,<sup>63</sup> as well as the adsorption and self-organizing properties of these polymers (in particular **16**) on a hydrophilic surface.<sup>64</sup>

Molecular dynamics calculations indicated that in this case additional stabilization of the helical backbone by hydrogen bonding between side chain residues takes place. Due to the high saccharide density along the rigid polyisocyanide backbone the binding affinity of lectins was approximately 100 times lower than for flexible glycoproteins.



Hong and Fox<sup>39</sup> synthesized block copolymer **17** with a rigid backbone to spatially organize chromophores and quencher groups in order to study directional electron transfer and energy migration.<sup>65</sup> Excimer formation, which is a complication

observed in flexible polymeric systems, is depressed, and long-living charge separated states are observed. Both features are in line with the rigid character of the polymer, despite the absence of limiting steric interactions close to the backbone imine groups. Extensive nonlinear optical studies have been performed by Persoons and coworkers<sup>66,67</sup> on **18**<sup>68</sup> and related compounds.<sup>69,70</sup> Second-harmonic light was generated by Langmuir-Blodgett films of these polyisocyanides but not by spin coated or cast films. This NLO activity probably results from a side chain orientation realized at the air water interface. In solution the orientational correlation between the side chain chromophores led to unexpectedly high first hyperpolarizabilities (exceeding  $5000 \times 10^{-30}$  e.u.). The breaking of centrosymmetry, which is required for a second-order nonlinear response, was attributed to the consistent angle of  $\sim 60^\circ$  these chromophores make with the axis of the helical backbone, rather than to the helical organization itself.

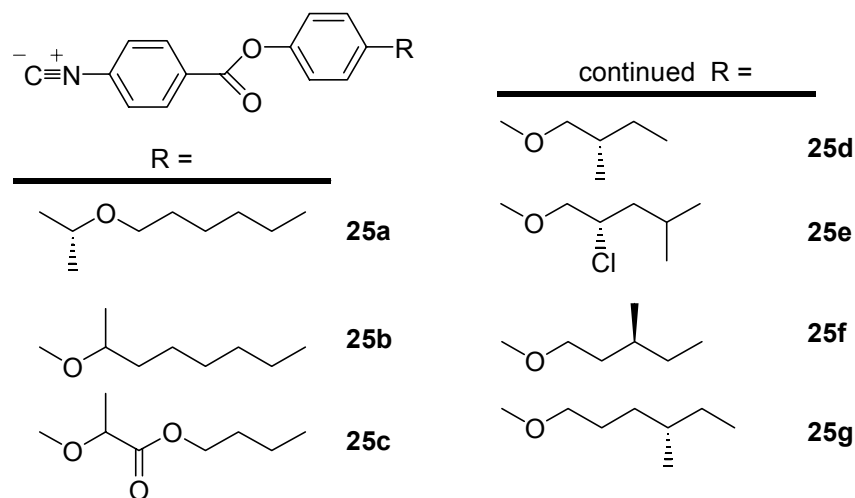
Recently, isocyanides containing a porphyrin group have been polymerized using the Pd-Pt  $\mu$ -ethynediyl catalyst discussed above (e.g. **19**).<sup>71</sup> Longer polymers (DP>30) show a distinct splitting of the Soret band, indicating a stacking of the porphyrins connected to the helical backbone. Other investigations towards polyisocyanides with potential applications as functional devices or specialty materials comprise the polymers **20**<sup>72</sup> and **21**,<sup>73</sup> designed as macromolecular ferromagnets, however, no paramagnetic bulk behavior was found.<sup>74</sup>

Galim and coworkers have synthesized the zwitterionic polymers **22** and **23** as potential lyotropic liquid crystals and as complexing agents for alkali metal salts.<sup>75</sup> Although only local ordering phenomena were found, the persistence length of the polyisocyanides was increased by a factor of 2, compared to poly(dizwitterionic methacrylates). The same group also prepared the ‘super-hairy’ polymer **24** which behaved as a cationic polyamphiphile.<sup>76</sup> Further applications for these polymers e.g. as lyotropic or thermotropic polymeric materials may be foreseen. Polyisocyanides with cholesterol-containing pendant groups have been reported to display thermotropic liquid crystalline properties.<sup>77</sup>

It was demonstrated that a stereocenter positioned far away from the reactive isocyanide group as in the optically active form of monomer **25b** can still induce chirality in the main chain of polyisocyanides resulting in the formation of an excess of one particular helix.<sup>78,79,80</sup> Kinetic control over the helix-sense in the polymerization of **25b** was confirmed by the non-cooperative transfer of chirality from the monomer to the macromolecule, e.g. a linear relation was found between the *ee* present in the isocyanide



and the optical activity in the polymers formed.<sup>81</sup> The kinetic inhibition of the growth of one particular handedness using (*S*)-2-isocyanovaleric acid<sup>184</sup> (*see above*) is used to force **25b** and **25c** in a macromolecular helicity with a screw sense opposite to that of the one preferred by homopolymers of these isocyanides. Using this procedure it is possible to create diastereomeric helices that include monomeric building blocks of identical absolute configuration but have opposite helical secondary structures.

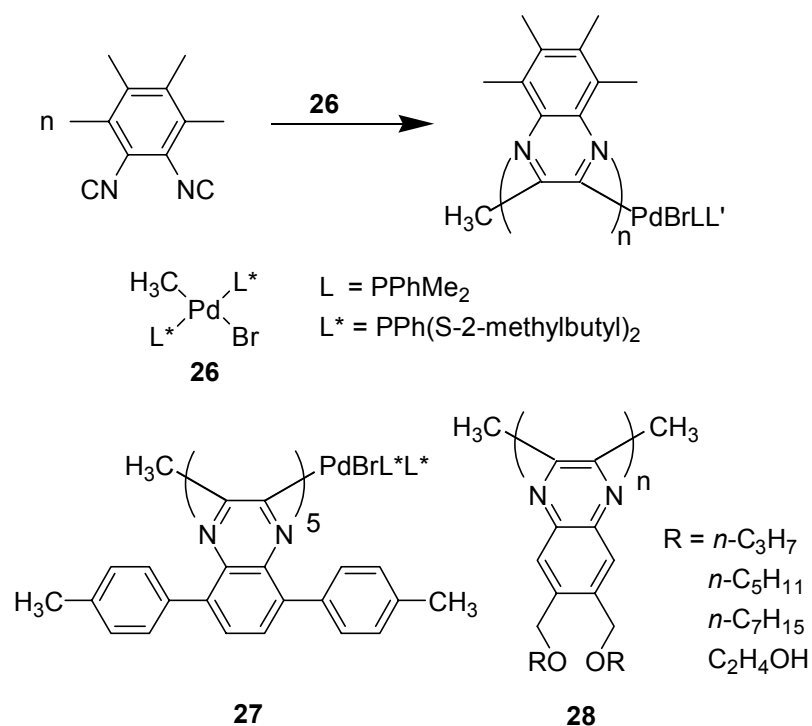


### 1.2.8 Poly(2,3-quinoxaline)s

The palladium catalyzed polymerization of 1,2-diisocyanoarenes has been reported to result in the formation of a different type of helical polyisocyanide (Scheme 4), referred to as a poly(2,3-quinoxaline).<sup>82</sup> Using Pd-complexes (**26**) with chiral phosphine ligands (e.g. bis{(*S*)-2-methylbutyl}phenylphosphine) as catalysts in the polymerization of 1,2-diisocyno-3,6-di-*p*-tolylbenzene did not lead to polymers with a large excess of one handedness, but it was possible to separate the optically pure pentamers **27**. Because these oligomers still contained the Pd(II) center it was possible to subsequently use these compounds as initiators for the helix-sense-selective polymerization of other 1,2-diisocyanoarenes.<sup>83</sup> The chiral selectivity is caused by the helical oligomer and not by the phosphine substituent as was demonstrated by ligand exchange experiments.<sup>84</sup> When a chiral Pd catalyst derived from an optically active binaphthyl compound was used, the X-ray structure of a stable and rigid helical structure of the growing {oligo(quinoxaliny)}palladium(II) complex could be solved.<sup>85</sup> The helical conformation of poly(2,3-quinoxaline)s was confirmed through empirical calculations. Two minimal energy conformations were determined, from which the theoretical CD

spectra based on the exciton theory were calculated. It was found that the experimental CD spectrum for (+)-poly(2,3-quinoxaline) was in agreement with the spectrum calculated for a right-handed helix with a dihedral angle of  $135^\circ$  between the planes of adjacent quinoxalines.<sup>86</sup>

Homopolymers and block copolymers of poly(2,3-quinoxaline)s containing functional side chains (**28**) have been prepared employing the Pd(II) catalyzed helix-sense-selective polymerization.<sup>87,88,89</sup> Recently it was reported that side chains can be modified without the quenching of the living site of the polymer.<sup>90,91</sup> The helical induction by the 1,1'-binaphth-2-ylpalladium(II) complexes has been investigated in detail, mainly using NMR techniques. It was found that the choice of substituents on the binaphthyl groups had a pronounced effect on the diastereomeric formation of the oligomeric intermediates of which the screw-sense was maintained in the further helix-sense-selective propagation steps.<sup>92</sup>



**Scheme 4** Palladium(II) catalyzed polymerization of 1,2-disocynoarenes to polyquinoxalines.

### 1.3 Chiral Macromolecular Architectures: Tertiary Structure

The interaction between chiral molecules may lead to superb properties and well-defined function as is exemplified in Nature by the high tensile strength in the  $\alpha$ -helical

coiled-coil superstructure in myosin and the storage of genetic information in the double helix of DNA. The design and synthesis of chiral superstructures in synthetic macromolecular systems is currently being studied by various groups. In the generation of such tertiary structures two distinct categories may be distinguished which will be discussed in the following sections: the self-assembly of chiral polymers that do not have a secondary structure in solution, leading to the formation of aggregates with induced chirality and the self-assembly of helical macromolecules in solution leading to chiral hierarchical structures.

#### 1.4.1 Chiral architectures from non-helical polymers

Association of stereoregular polymers belongs to this category since for a number of these so-called stereocomplexes a helical superstructure is found.<sup>93</sup> The formation of such macromolecular complexes can be achieved using different secondary interactions of varying strength,<sup>99</sup> although vanderWaals forces are the most frequent observed. In particular the complexation between isotactic (*it*-PMMA) and syndiotactic poly(methyl methacrylate) (*st*-PMMA) has been investigated in great detail.<sup>94</sup> Despite the intense efforts of several research groups<sup>95,96</sup> in this area the exact mechanism of stereocomplex formation is still under debate.<sup>97</sup> The same type of stereocomplex is formed, independent of the method of preparation and the initial *it* / *st* ratio.<sup>98</sup> This complex comprises a 9/1 double-stranded helix with an asymmetric unit consisting of one *it*-PMMA unit and two *st*-PMMA units (Figure 4).<sup>99,100</sup>

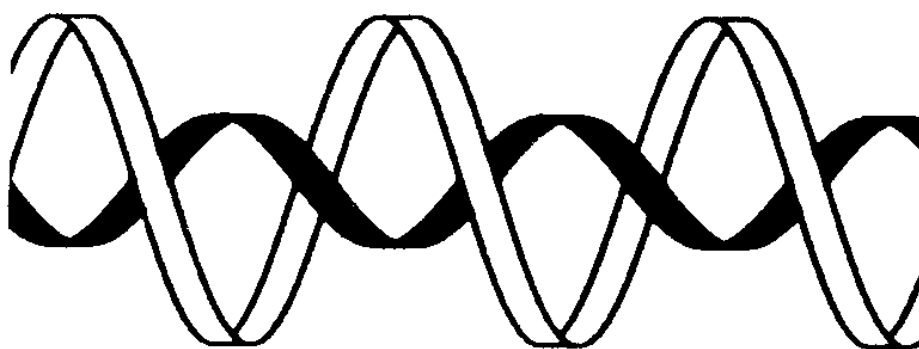


**Figure 4** Schematic representation of the stereocomplex between *it*-PMMA (black ribbon) which is surrounded by *st*-PMMA.

Another type of stereocomplex, *i.e.* a tightly wound 3/1 helix, is formed in the blend when polymers of L-lactic acid (PLLA) and D-lactic acid (PDLA) are mixed.<sup>101,102</sup> Also in solution aggregation of block copolymers containing PLA

segments has been found, however, no studies towards the morphology of the aggregates have been conducted.<sup>103,104</sup>

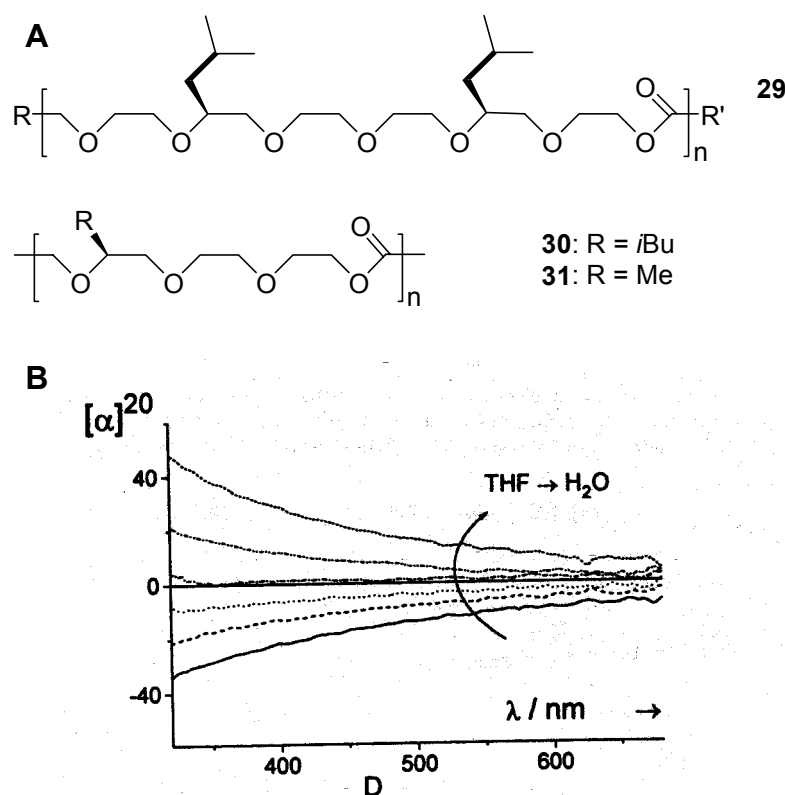
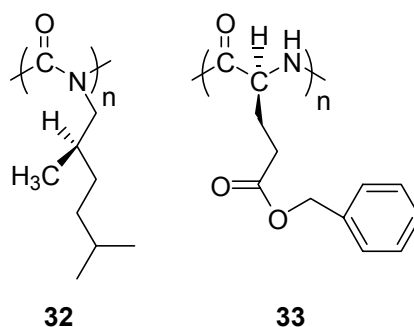


**Figure 5** (A) structures of optically active poly(ethylene oxide) derivatives, (B) ORD spectra of **31** in THF upon increasing the water content.<sup>105</sup>

Meijer and coworkers<sup>105</sup> have reported the aggregation of ribbon-type amphiphilic polymers, based on chiral, substituted poly(ethylene oxides) (PEOs), as synthetic analogues of coiled-coil forming peptides (Figure 5). Polymers **29** – **31** were prepared by ring-opening polymerization of 2-oxo-crown ether monomers or by polycondensation of the corresponding  $\omega$ -hydroxycarboxylic acids.<sup>106</sup> The amphiphilic nature of these poly(ethylene oxides) modified with hydrophobic side chains was confirmed by fluorescence studies, giving critical aggregation constants (cac's) covering a wide range (from 0.002 mg / ml for **29** to 0.15 mg / ml for **31**), depending on the size and repetition frequency of the hydrophobic segments in the polymer chain. The conformation of these macromolecules in solutions comprising different water-THF ratios was studied using ORD spectroscopy.<sup>107</sup> Increasing the water content led to a less negative optical rotation, and in the case of **31** an inversion of the optical rotation was observed (Figure 5B). Based on reference studies in which KSCN was complexed with similar ethylene oxide derivatives, the authors concluded that helical superstructures

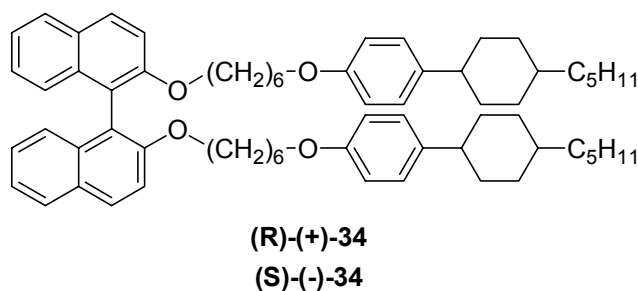
were formed from **29** – **31** upon increasing the water content.<sup>105</sup> TEM studies revealed the formation of large well-defined aggregates, however, details of the hierarchical order in the aggregates could not be unveiled.

Optically active assemblies from chiral substituted  $\pi$ -conjugated polymers can also be regarded as chiral architectures from non-helical polymers. Their formation is, however, beyond the scope of this chapter.<sup>29</sup>



#### 1.4.2 Hierarchical structures from helical polymers

The formation of a nematic liquid crystalline phase, characterized by orientational but not positional molecular order, is often observed for stiff helical macromolecules in solution.<sup>108</sup> Parameters important in describing these structures are the pitch, the radius and the handedness of the helices. In a liquid crystalline state the aggregation of the helices is in some cases accompanied by the formation of a cholesteric phase. The rod-like molecules in this case are no longer oriented parallel, but are twisted with respect to their nearest neighbors. Among others poly((*R*)-2,6-dimethylheptyl isocyanate) (**32**),<sup>109,18</sup> poly(γ-benzyl-α,L-glutamate) (PBLG, **33**),<sup>110,111</sup> and schizophilan<sup>112</sup> (a triple-helical polysaccharide rod) were found to display cholesteric liquid crystalline mesophases in concentrated solutions. The major models describing the transfer of the helical chirality to the cholesteric phase are the *straight-rod*<sup>109</sup> and the *threaded EFJC*<sup>113</sup> models. Both models approach the macromolecular helix as a screw-threaded cylinder, which implies that the aggregation of two of such helices is mainly dependant on the ratio pitch / diameter. The models predict that when this ratio reaches a critical value inversion of the helicity of the resulting superhelix will take place.



An astonishing helical architecture was prepared recently by Akagi et al.<sup>114</sup> They polymerized acetylene in a chiral nematic reaction field. To this end the Ziegler-Natta catalyst  $\text{Ti}(\text{O-n-Bu})_4 / \text{Et}_3\text{Al}$  was dissolved in the stable chiral nematic mesophase obtained by mixing 5 – 14 weight % of (R)- or (S)-**34** with a known nematic liquid crystal, and this medium was subsequently used for the preparation of polyacetylene films. It was found that polymers prepared in the (R)-chiral nematic liquid crystals had counterclockwise (*M*) helical fibrillar morphologies and those prepared in the (S)-phase clockwise (*P*) morphologies (Figure 6A). CD spectra of these films showed a positive Cotton effect for the (*M*) helical fibrils and a negative Cotton effect for the *P* type ones, in the  $\pi$ - $\pi^*$  transition region of the polyacetylene chain. Since the helical pitch of a chiral nematic phase can be controlled by the optical purity or the type of chiral dopant, and the liquid crystalline phase is templating the helicity, it was also possible to produce fibrils with a different helical pitch. An interesting hierarchical transfer of chirality was observed in this case *i.e.* going from the chiral twist in **34**, to the helical polymer and ultimately to the spiral morphology in the microscopic regime.

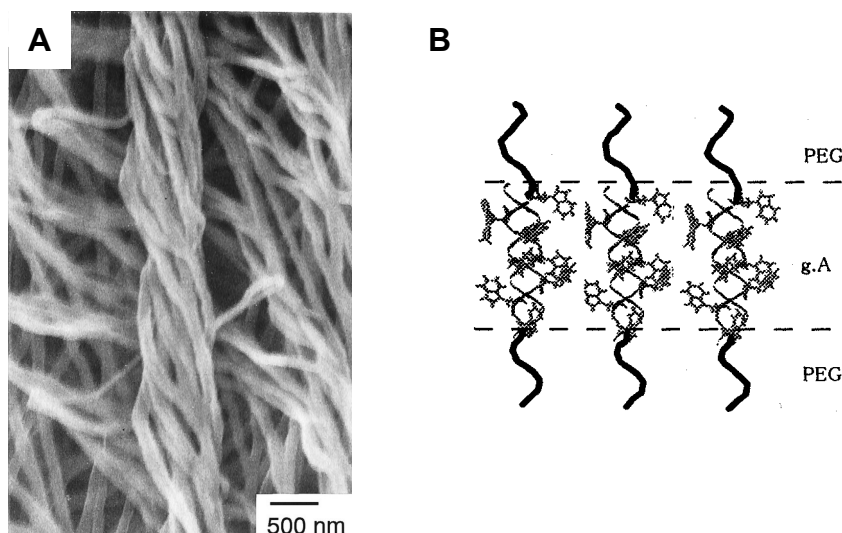
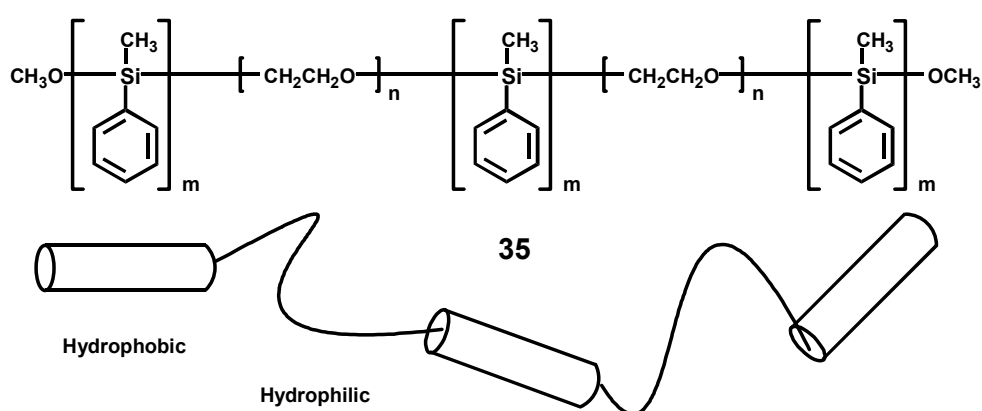


**Figure 6** (A) Scanning electron micrograph of a left-handed helical morphology formed by polyacetylene polymerized in a chiral nematic reaction field.<sup>114</sup> (B) Proposed organization in bilayers formed by a Gramicidin A-poly(ethylene oxide) hybrid.<sup>115</sup>

Hybridization of Gramicidin A, a hydrophobic 15-mer peptide, with a hydrophilic poly(ethylene oxide) (PEO) chain resulted in the formation of an amphiphilic compound as was reported by Kimura et al.<sup>115</sup> Upon dispersion in water these hybrid polymers, in which the degree of polymerization of the PEO segment was 13, gave vesicles with an average diameter of 85 nm. An illustration of the proposed organization of the molecules in the vesicle bilayer is given in Figure 6B. Inclusion experiments confirmed the vesicular nature of the aggregates, while CD measurements supported the presence of the proposed antiparallel double-stranded helix conformation.



The chiral structures discussed above are formed by relatively well-defined macromolecules. Interestingly superhelical structures can also be obtained from rather polydisperse multiblock copolymers, *viz.* of PEO and polymethylphenylsilane (PMPS) (**35**, PDI = 1.6). In a preliminary communication the formation of vesicles was reported in pure water (Figure 7A).<sup>116</sup> In a later paper,<sup>117</sup> it was described that the aggregation behavior of this amphiphilic polymer can be tuned by dispersing it in water / THF mixtures of varying composition. Below water concentrations of 40% (v/v) no aggregates were found. Electron microscopy demonstrated the presence of micellar rods in mixtures containing 40-80% (v/v) water (Figure 7B,C). In solvent mixtures containing more than 80% water helices (Figure 7D)<sup>117</sup> with both left- and right-handed screw pitches were observed. Given the multiblock nature of the polymer and the polydispersity of the PMPS blocks it is unlikely that the helical superstructures arise from preferential aggregation of PMPS segments with identical screw senses. A cooperative process was assumed to occur in which the handedness of the initial PMPS segment(s) determine(s) the handedness of the subsequent PMPS segments assembling

in the same aggregate, such that a chiral architecture is formed by hierarchical assembly of these dynamic helical macromolecules.

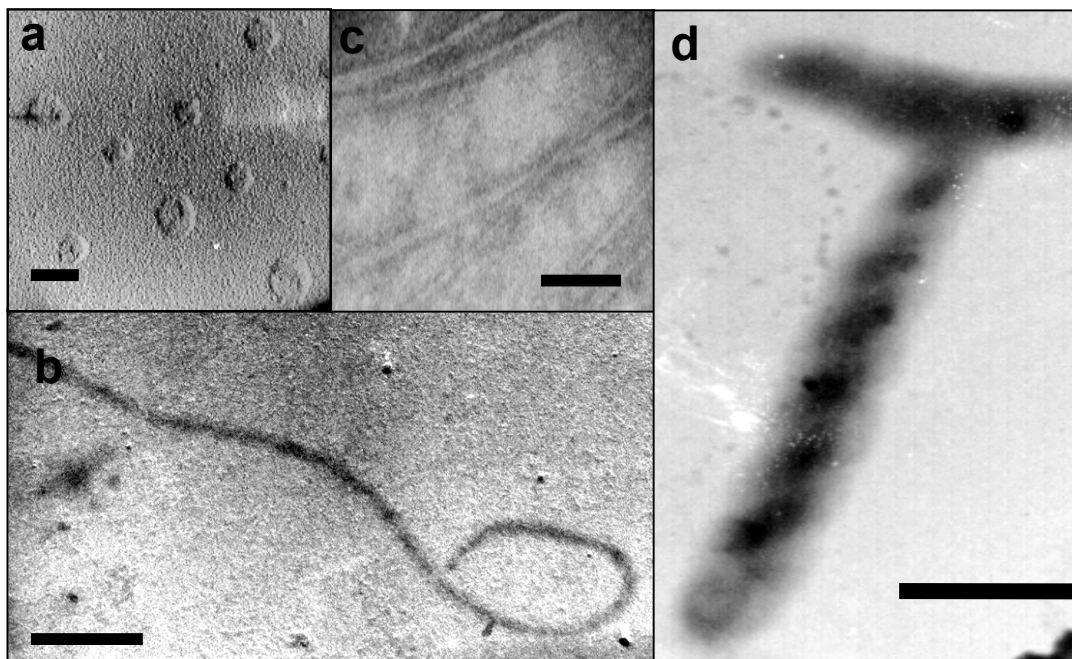


**Figure 7** Transmission electron micrographs showing the formation of (A) vesicles, (B-C) micellar fibers and (D) superhelices from a PEO-PMPS block copolymer 35.<sup>117</sup>

#### 1.4 Aim and Outline of the Thesis

The hierarchical expression of (chiral) information encoded in the molecular building blocks of larger supramolecular assemblies is of increasing interest to numerous researchers.<sup>1-15</sup> For polymeric systems this involves an additional level of organization, viz. the conformational order of the polymer backbone determined by the structural properties of the constituent monomers and in some cases the procedure of polymerization.

The general aim of the research presented in this thesis is to study the hierarchical transfer of (chiral) structural information present in the monomeric building blocks to higher levels of organization in both the resultant polymers and in aggregates formed by these polymers, the latter having dimensions in the nanometer regime. Polymers of isocyanides have been used for this purpose, since these macromolecules have a defined helical conformation and are easy accessible in an optically active form using a nickel catalyst. Moreover these molecules have been extensively studied in our



group in the past.<sup>31,33</sup> Emphasis has been placed on explorative investigations using non-covalent interactions for the conformational fine-tuning of peptide-derived polyisocyanides and on the use of these defined polymers in amphiphilic systems to form defined nanostructures by self-assembly.

The studies presented in this thesis can be divided in two sections; a part describing the structural organization of the polymers, i. e. their intramolecular architecture. Chapters 2 – 4 describe the preparation and properties of homopolymers derived from peptide based isocyanides. The second part outlines the organization between polymers, i. e. the formation of intermolecular architectures. In Chapters 5 and 6 block copolymers containing a polyisocyanide segment and their assembling properties will be discussed .

The synthesis and characterization of dipeptide-derived polyisocyanides is the subject of Chapter 2, in which, using spectroscopic techniques, the presence of hydrogen bonds between polymer side chains of these alanine-alanine and alanine-glycine based macromolecules is shown. Chapter 3 deals with the conformational properties of these polyisocyanodipeptides, in particular the role of the hydrogen bonds. The study of these arrays of hydrogen bonds along the polymeric backbone revealed how these lead to a well defined conformation and provides insight in some unexplained properties of polyisocyanopeptides prepared in the past.<sup>118</sup>

Extension of the side chains in the polyisocyanides from a di- to a tripeptide results in the formation of  $\beta$ -helical polymers; synthetic analogues of natural occurring  $\beta$ -sheet-helices. The synthesis and conformational properties of this polymer will be discussed in Chapter 4, together with the structural persistence of di- and tripeptide-derived polyisocyanides in an aqueous environment.

Using the controlled Ni(II) catalyzed polymerization, block copolymers are accessible having a polyisocyanide segment and a polystyrene block, or a carbosilane dendritic part (Chapter 5 and Chapter 6, respectively). In the former case a superamphiphile is obtained with a hydrophobic polystyrene tail and a charged, hydrophilic helical polyisocyanide headgroup. Under optimized conditions (e.g. pH, ratio hydrophobic/hydrophilic) the chirality of the monomer is, via the secondary structure of the polymer, expressed on the supramolecular level in the form of helical aggregates. Finally, in Chapter 6, the synthesis and aggregation behavior of block copolymers comprising different generations carbosilane dendritic wedges next to the polyisocyanide part is reported. The addition of silver-ions strongly influences the

assembling properties and, ultimately, the aggregates formed by the 3<sup>rd</sup> generation block copolymers act as a template for the formation of silver nanoarrays.

## 1.5 References

- (1) Rowan, A.E.; Nolte, R.J.M. *Angew. Chem. Int. Ed.* **1998**, *37*, 63-68.
- (2) Feiters, M. C.; and Nolte, R. J. M. (2000) in *Advances in Supramolecular Chemistry*, Vol. 6 (Gokel, G. W., Editor), Jai Press Inc., Stamford CT, USA, pp. 41-156. 'Chiral Self-assembled Structures of Biomolecules and Synthetic Analogues'
- (3) (a) Sommerdijk, N.A.J.M.; Buynsters, P.J.J.A.; Pistorius, A.M.A.; Wang, M.; Feiters, M.C.; Nolte, R.J.M.; Zwanenburg, B. *J. Chem. Soc., Chem. Commun.*, **1994**, 1941. (b) *J. Chem. Soc., Chem. Commun.*, **1994** 2739. (c) Sommerdijk, N.A.J.M.; Lambermon, M.H.L.; Feiters, M.C.; Nolte, R.J.M.; Zwanenburg, B. *Chem. Commun.* **1997**, 455. (d) Sommerdijk, N.A.J.M.; Lambermon, M.H.L.; Feiters, M.C.; Nolte, R.J.M. Zwanenburg, B. *Chem. Commun.*, **1997**, 1423. (e) Sommerdijk, N.A.J.M.; Buynsters, P.J.J.A.; Akdemir, H.; Geurts, D.G.; Pistorius, A.M.A.; Feiters, M.C.; Nolte, R.J.M.; Zwanenburg, B. *Chem. Eur. J.*, **1998**, *4*, 127. (f) Buynsters, P.J.J.A.; Feiters, M.C.; Nolte, R.J.M.; Sommerdijk, N.A.J.M.; Zwanenburg, B. *Chem. Commun.*, **2001**, 269-270. (g) Buynsters, P.J.J.A.; Feiters, de Gelder, R.; Ten Holte, P.; M.C.; Nolte, R.J.M.; Pistorius, A.M.A.; Sommerdijk, N.A.J.M.; VerHaegen, A.A.C.; Zwanenburg, B. *J. Mater. Chem.*, **2001**, *11*, 269-277.
- (4) Hafkamp, J.H.; Feiters, M.C.; Nolte, R.J.M. *Angew. Chem.* **1994**, *106*, 1054-1055.
- (5) Schnur, J.M. *Science*, **1993**, *262*, 1669-1676.
- (6) Nakashima, N.; Asakuma, S.; Kunitake, T. *J. Am. Chem. Soc.* **1985**, *116*, 10057-10069
- (7) Frankel, D.A.; O'Brian, D. F. *J. Am. Chem. Soc.* **1994**, *107*, 509-510.
- (8) Fuhrhop, J.-H.; Helfrich, W. *Chem. Rev.* **1993**, 1565-1582.
- (9) Yanagawa, H.; Ogawa, Y.; Furuta, H.; Tsuno, K. *J. Am. Chem. Soc.* **1989**, *111*, 4567-4570.
- (10) (a) Engelkamp, H.; Middelbeek, S.; Nolte, R.J.M.; *Science*, **1999**, *284*, 785-788. (b) Palmans, A.R.A.; Vekemans, J.A.J.M.; Havinga, E.E.; Meijer, E.W. *Angew. Chem. Int. Ed. Engl.* **1997**, *36*, 2648-2651. (c) Gulik-Krzywicki, T.; Fouquey, C.; Lehn, J-M. *Proc. Natl. Acad. Sci.* **1993**, *90*, 163-167. (d) Tachibana, T; Kambara, H. *J. Am. Chem. Soc.* **1965**, *87*, 3015-3016.
- (11) (a) Hafkamp, R.J.H.; Kokke, B.P.A.; Danke, I.M.; Geurts, H.P.M.; Rowan, A.E.; Feiters, M.C.; Nolte, R.J.M. *Chem. Commun.*, **1997**, 545-546 (b) Hanabusa, K. Yamada, M.; Kimura, M.; Shirai, H. *Angew. Chem. Int. Ed. Engl.* **1996**, *35*, 1949-1951 (c) De Loos, M; van Esch, J; Stokroos, I.; Kellog, R.M.; Feringa, B.M. *J. Am. Chem. Soc.* **1997**, *119*, 12675-12676. (d) Van Esch, J.H.; Feringa, B.L. *Angew. Chem., Int. Ed.* **2000**, *39*, 2263-2266.
- (12) Stryer, L. *Biochemistry*, Freeman, New York, **1975**, 4th edition.
- (13) (a) Yang, W.; Chai, X.; Chi, L.; Liu, X.; Cao.; Lu, R.; Jiang, Y.; Tang, X.; Fuchs, H.; Li, T. *Chem. Eur. J.* **1999**, *5*, 1144-1149.
- (14) Reich, Z.; Zaidmann, L.; Gutman, S.B.; Arad, T.; Minski, A. *Biochem.* **1994**, *33*, 14177-14184.
- (15) Hirschberg, J.H.K.K.; Brunsveld, L.; Ramzi, A.; Vekemans, J.A.J.M.; Sijbesma, R.P.; Meijer, E.W. *Nature*, **2000**, *407*, 167-170.
- (16) Novak, B. M.; Goodwin, A. A.; Schlitzer, D.; Patten, T. E.; Deming, T. J. *Polym. Prep.* **1996**, *37*, 446.
- (17) (a) Goodman, M.; Chen S. *Macromolecules* **1970**, *3*, 398; (b) Goodman, M.; Chen S. *Macromolecules* **1971**, *4*, 625.
- (18) Green, M. M.; Peterson, N.C.; Sato, T.; Teramoto, A.; Cook, R.; Lifson, S. *Science* **1995**, *268*, 1861.
- (19) Ciardelli, F.; Lanzillo, S.; Pieroni, O. *Makromol. Chem.* **1967**, *103*, 1.
- (20) Yashima, E.; Maeda, Y.; Okamoto, Y. *Nature* **1999**, *399*, 449.
- (21) (a) Majidi, M.R.; Kane-Maguire, L.A.P.; Wallace, G.G. *Polymer*, **1994**, *35*, 3113. (b) Majidi, M.R.; Kane-Maguire, L.A.P.; Wallace, G.G. *Polymer*, **1995**, *36*, 3597. (c) Majidi, M.R.; Kane-Maguire, L.A.P.; Norris, I.D.; Wallace, G.G. *Polymer*, **1996**, *37*, 359. (d) Majidi, M.R.; Ashraf, S.A.; Kane-Maguire, L.A.P.; Wallace, G.G. *Synth. Met.* **1997**, *84*, 115.
- (22) Havinga, E.E.; Bouman, M.M.; Meijer, E.W.; Pomp, A.; Simenon, M.M.J. *Synth. Met.* **1994**, *66*, 93.
- (23) Fujiki, M., *J. Am. Chem. Soc.* **1996**, *118*, 11345-11346.

- (24) Okamoto, Y.; Suzuki, K.; Ohta, K.; Hatada, K.; Yuki, H. *J. Am. Chem. Soc.* **1979**, *101*, 4763.
- (25) Okamoto, Y.; Nakano, T. *Chem. Rev.* **1994**, *94*, 349.
- (26) Sikorski, P.; Cooper, S. J.; Atkins, E. D. T.; Jaycox, G. D.; Vogl, O. *J. Polym. Sci., Part A: Polym. Chem.* **1998**, *36*, 1855.
- (27) Hatada, K.; Jaycox, G. D.; Vogl, O. *Macromolecular Design of Polymeric Materials. Series: Plastics Engineering*, Hatada, K.; Jaycox, G. D.; Vogl, O. ed.; Marcel Dekker: New York, 1997; Chapter 11, p 181.
- (28) Vogl, O. *J. Polym. Sci., Part A: Polym. Chem.* **2000**, *38*, 2293.
- (29) For extensive overviews on chiral polymers see: a) Pu, L. *Acta Polymer.* **1997**, *48*, 116-141. b) Cornelissen, J. J. L. M.; Rowan, A. E.; Nolte, R. J. M.; Sommerdijk, N. A. J. M. *Chem. Rev.* **2001**, accepted for publication.
- (30) Millich, F. *Chem. Rev.* **1972**, *72*, 101.
- (31) Nolte, R. J. M.; Drenth, W. *New Methods for Polymer Synthesis*, W. J. Mijs ed.; Plenum Press: New York, 1992; Chapter 9, p 273.
- (32) Nolte, R. J. M.; van Beijen, A. J. M.; Drenth, W.; *J. Am. Chem. Soc.* **1972**, *96*, 5932.
- (33) Nolte, R. J. M. *Chem. Soc. Rev.* **1994**, *23*, 11.
- (34) Deming, T. J.; Novak, B. M.; *Macromolecules* **1991**, *24*, 326.
- (35) Deming, T. J.; Novak, B. M.; *Macromolecules* **1991**, *24*, 6043.
- (36) Deming, T. J.; Novak, B. M.; *J. Am. Chem. Soc.* **1993**, *115*, 9101.
- (37) Nolte, R. J. M.; Drenth, W. *Recl. Trav. Chim. Pays-Bas* **1973**, *92*, 788.
- (38) Deming, T. J.; Novak, B. M.; *Macromolecules* **1993**, *26*, 7092.
- (39) Hong, B.; Fox, M. A. *Macromolecules* **1994**, *27*, 5311.
- (40) An intermediate isolated from the polymerization of phenyl isocyanide using NiCl<sub>2</sub> had an intriguing structure but did not give conclusive directions towards the mechanism of polymerization. Euler, W. B.; Huang, J.-T.; Kim, M.; Spencer, L.; Rosen, W. *Chem. Commun.* **1997**, 257.
- (41) Kollmar, C.; Hoffmann R. *J. Am. Chem. Soc.* **1990**, *112*, 8230.
- (42) Cui, C. X.; Kertesz, M. *Chem. Phys. Lett.* **1990**, *169*, 445.
- (43) Huige, C. J. M.; *Ph. D. Thesis*, University of Utrecht, 1985.
- (44) Huige, C. J. M.; Hezemans, A. M. F.; Nolte, R. J. M.; Drenth, W. *Recl. Trav. Chim. Pays-Bas* **1993**, *112*, 33.
- (45) Clericuzio, M.; Alagona, G.; Ghio, C.; Salvadori, P. *J. Am. Chem. Soc.* **1997**, *119*, 1059.
- (46) Pini, D.; Iuliano, A.; Salvadori, P. *Macromolecules* **1992**, *25*, 6059.
- (47) Green, M. M.; Gross, R. A.; Schilling, F.; Zero, K.; Crosby, C., III *Macromolecules* **1988**, *21*, 1839.
- (48) Spencer, L.; Kim, M.; Euler, W. B.; Rosen, W. *J. Am. Chem. Soc.* **1997**, *119*, 8129.
- (49) Spencer, L.; Euler, W. B.; Traficante, D. D.; Kim, M.; Rosen, W. *Magn. Res. Chem.* **1998**, *36*, 398.
- (50) Huang, J.-T.; Sun, J.; Euler, W. B.; Rosen, W. *J. Polym. Sci., Part A: Polym. Chem.* **1997**, *35*, 439.
- (51) Van Beijen, A. J. M.; Nolte, R. J. M.; Drenth, W. *Recl. Trav. Chim. Pays-Bas* **1980**, *99*, 121-123.
- (52) Yamagashi, A.; Tanaka, I.; Tanigushi, M.; Takahashi, M. *J. Chem. Soc., Chem. Commun.* **1994**, 1113.
- (53) a) Kamer, P. C. J.; Nolte, R. J. M.; Drenth, W. *J. Chem. Soc. Chem. Commun.* **1986**, 1789. b) Kamer, P. C. J.; Nolte, R. J. M.; Drenth, W. *J. Am. Chem. Soc.* **1988**, *110*, 6818. c) Deming, T. J.; Novak, B. M.; *J. Am. Chem. Soc.* **1992**, *114*, 4400. d) Deming, T. J.; Novak, B. M.; *J. Am. Chem. Soc.* **1992**, *114*, 7926.
- (54) Kamer, P. C. J.; Cleij, M. C.; Nolte, R. J. M.; Harada, T.; Hezemans, A. M. F.; Drenth, W. *J. Am. Chem. Soc.* **1988**, *110*, 1581.
- (55) Onitsuka, K.; Joh, T.; Takahashi, S. *Angew. Chem.* **1992**, *104*, 893.
- (56) Onitsuka, K.; Yanai, F.; Joh, T.; Takahashi, S. *Organometallics* **1994**, *13*, 3862.
- (57) Recently also the isocyanide polymerization using an alkynyl nickel complex has been reported: Takei, F.; Tung, S.; Yanai, K.; Onitsuka, K.; Takahashi, S. *J. Organomet. Chem.* **1998**, *559*, 91.
- (58) The reversible insertion of aryl isocyanides in a palladium-sulfur bond leading to oligoisocyanides has been reported: Kuniyasu, H.; Sugoh, K.; Su, M. S.; Kurosawa, H. *J. Am. Chem. Soc.* **1997**, *119*, 4669.
- (59) Takai, F.; Yanai, K.; Onitsuka, K.; Takahashi, S. *Angew. Chem. Int. Ed. Engl.* **1996**, *35*, 1554.

- (60) Ohshiro, N.; Shimizu, A.; Okumura, R.; Takei, F.; Onitsuka, K.; Takahashi, S. *Chem. Lett.* **2000**, 786.
- (61) Takei, F.; Yanai, K.; Onitsuka, K.; Takahashi, S. *Chem. Eur. J.* **2000**, 6, 983.
- (62) Takei, F.; Onitsuka, K.; Takahashi, S. *Polymer J.* **1999**, 31, 1029.
- (63) Hasegawa, T.; Kondoh, S.; Matsuura, K.; Kobayashi, K. *Macromolecules* **1999**, 32, 6595.
- (64) Hasegawa, T.; Matsuura, K.; Ariga, K.; Kobayashi, K. *Macromolecules* **2000**, 33, 2772.
- (65) Hong, B.; Fox, M. A. *Can. J. Chem.* **1995**, 73, 2101.
- (66) Kauranen, M.; Verbiest, T.; Boutton, C.; Teerenstra, M. N.; Clays, K.; Schouten, A. J.; Nolte, R. J. M.; Persoons, A. *Science*, **1995**, 270, 966.
- (67) Kauranen, M.; Verbiest, T.; Meijer, E. W.; Havinga, E. E.; Teerenstra, M. N.; Schouten, A. J.; Nolte, R. J. M.; Persoons, A. *Adv. Mater.* **1995**, 7, 641.
- (68) Teerenstra, M. N.; Hagting, Oostergetel, G. T.; Schouten, A. J.; Devillers, M. A. C.; Nolte, R. J. M. *Thin Solid Films* **1994**, 248, 110.
- (69) Teerenstra, M. N.; Klap, R. D.; Bijl, M. J.; Schouten, A. J.; Nolte, R. J. M.; Verbiest, T.; Persoons, A. *Macromolecules* **1996**, 29, 4871.
- (70) Teerenstra, M. N.; Hagting, J. G.; Schouten, A. J.; Nolte, R. J. M.; Kauranen, M.; Verbiest, T.; Persoons, A. *Macromolecules* **1996**, 29, 4876.
- (71) Takei, F.; Onitsuka, K.; Kobayashi, N.; Takahashi, S. *Chem. Lett.* **2000**, 914.
- (72) Bosch, J.; Rovira, C.; Veciana, J.; Castro, C.; Palacio, F. *Synth. Met.* **1993**, 55, 1141.
- (73) Vlietstra, E. J.; Nolte, R. J. M.; Zwikker, J. W.; Drenth, Meijer, E. W. *Macromolecules* **1990**, 23, 946.
- (74) Abdelkader, M.; Drenth, W.; Meijer, E. W. *Chem. Mater.* **1990**, 3, 598.
- (75) Bieglé, A.; Mathis, A.; Galin, J. C. *Macromol. Chem. Phys.* **2000**, 201, 113.
- (76) Grassi, B.; Rempp, S.; Galin, J. C. *Macromol. Chem. Phys.* **1998**, 199, 239.
- (77) Van Walree, C. A.; van der Pol, C. A.; Zwikker, J. W. *Recl. Trav. Chim. Pays-Bas* **1990**, 109, 561.
- (78) Amabilino, D. B.; Ramos, E.; Serrano, J. L.; Sierra, T.; Veciana, J. *J. Am. Chem. Soc.* **1998**, 120, 9126.
- (79) Ramos, E.; Bosch, J.; Serrano, J. L.; Sierra, T.; Veciana, J. *J. Am. Chem. Soc.* **1996**, 118, 4703.
- (80) Similar long-distance chirality transfer has been reported for the polymerization of helicene derived isocyanides. Chen, J. P.; Gao, J. P.; Wang, Z. Y. *Polymer Int.* **1997**, 44, 83.
- (81) Amabilino, D. B.; Ramos, E.; Serrano, J. L.; Veciana, J. *Adv. Mater.* **1998**, 10, 1001.
- (82) Ito, Y.; Ihara, E.; Murakami, M. *J. Am. Chem. Soc.* **1990**, 112, 6446.
- (83) Ito, Y.; Ihara, E.; Murakami, M. *Angew. Chem.* **1992**, 104, 1508.
- (84) Ito, Y.; Kojima, Y.; Murakami, M. *Tetrahedron Lett.* **1993**, 34, 8279.
- (85) Ito, Y.; Ohara, T.; Shima, R.; Suginome, M. *J. Am. Chem. Soc.* **1996**, 118, 9188.
- (86) Ito, Y.; Ihara, E.; Murakami, M.; Sisido, M. *Macromolecules* **1992**, 25, 6810.
- (87) Ito, Y.; Kojima, Y.; Suginome, M.; Murakami, M. *Heterocycles*, **1996**, 42, 597.
- (88) Ito, Y.; Ihara, E.; Uesaka, T.; Murakami, M. *Macromolecules* **1992**, 25, 6711.
- (89) Ito, Y.; Miyake, T.; Ohara, T.; Suginome, M. *Macromolecules* **1998**, 31, 1697.
- (90) Ito, Y.; Miyake, T.; Suginome, M. *Macromolecules* **2000**, 33, 4034.
- (91) Ito, Y.; Kojima, Y.; Murakami, M.; Suginome, M. *Bull. Chem. Soc. Jpn.* **1997**, 70, 2801.
- (92) Ito, Y.; Miyake, T.; Hatano, S.; Shima, R.; Ohara, T.; Suginome, M. *J. Am. Chem. Soc.* **1998**, 120, 11880.
- (93) Liquori, A. M.; Anzuino, G.; Coiro, V. M.; D'Alagni, M.; de Santis, P.; Savino, M. *Nature* **1965**, 206, 358.
- (94) An overview is given in: Mizumoto, T.; Sugimura, N.; Moritani, M.; Sato, Y.; Masuoka *Macromolecules* **2000**, 33, 6757.
- (95) Spevacek, J. *Makromol. Chem., Macromol. Symp.* **1990**, 39, 71.
- (96) Hatada, K.; Kitayama, T.; Ute, K.; Nishiura, T. *Macromol. Symp.* **1998**, 132, 221.
- (97) te Nijenhuis, K.; *Adv. Polym. Sci.* **1997**, 130, 76-81.
- (98) Vorenkamp, E. J.; Bosscher, F.; Challa, G. *Polymer* **1979**, 20, 59.
- (99) Schomaker, E. *PhD Thesis*, State University Groningen, 1988.
- (100) Challa, G. *Integration of Fundamental Polymer Science and Technology – 5*, Lemstra, P. J.; Kleintjes, L. A. ed., Elsevier Applied Science, London, 1991; Vol. 5, p 85.
- (101) For a recent overview see: Spassky, N.; Pluta, C.; Simic, V.; Thiam, M.; Wisniewski, M. *Macromol. Symp.* **1998**, 128, 39.
- (102) Spinu, M.; Gardener, K. H.; *Polym. Mater. Sci. Eng.* **1994**, 74, 19.

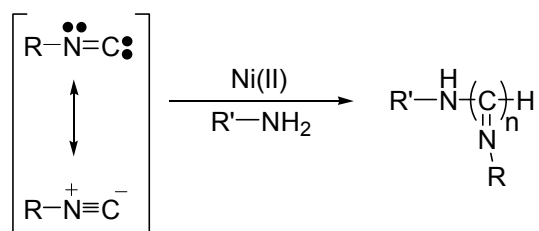
- (103) Stevels, W. M.; Ankone, M. J. K.; Dijkstra, P. J.; Feijen, J. *Macromol. Chem. Phys.* **1995**, *196*, 3687.
- (104) de Jong, S. J.; de Smedt, S. C.; Wahls, M. W. C.; Demeester J.; Kettenes-van den Bosch J. J.; Hennink, W. E. *Macromolecules* **2000**, *33*, 3680.
- (105) Janssen, H. M.; Peeters, E.; van Zundert, M. F.; van Genderen, M. H. P. G.; Meijer, E. W. *Ang. Chem. Int. Ed. Engl.* **1997**, *36*, 122.
- (106) Janssen, H. M.; Peeters, E.; van Zundert, M. F.; van Genderen, M. H. P.; Meijer, E. W. *Macromolecules* **1997**, *30*, 8113.
- (107) Janssen, H. M.; Meijer, E. W. *Macromolecules* **1997**, *30*, 8129.
- (108) Papkov, S. P. *Adv. Polym. Sci.* **1984**, *59*, 75.
- (109) Sato, T.; Sato, Y.; Umemura, Y.; Teramoto, A.; Nagamura, Y.; Wagner, J.; Weng, D.; Okamoto, Y.; Hatada, K.; Green, M.M. *Macromolecules* **1993**, *26*, 4551.
- (110) Lyotropic liquid crystalline behavior of rod-like peptides has been reported for the first time by: Robinson, C.; Ward, J.C. *Nature*, **1957**, *180*, 1183.
- (111) The phase behavior of PBLG has been investigated thoroughly. Wee, E.L.; Miller, W. G. *Nature*, **1990**, *346*, 44.
- (112) Itou, T.; Van, K.; Teramoto, A. *J. Appl. Polym. Sci., Appl. Polym. Symp.* **1985**, *41*, 35.
- (113) Sato, T.; Nakamura, J.; Teramoto, A.; Green, M.M. *Macromolecules*, **1998**, *31*, 1398.
- (114) Akagi, K.; Piao, G.; Kaneko, S.; Sakamaki, K.; Shirakawa, H.; Kyotani, M. *Science*, **1998**, *282*, 1683.
- (115) Kimura, S.; Kim, D.-H.; Sugiyama, J.; Imanishi, Y. *Langmuir*, **1999**, *15*, 4461.
- (116) Holder, S.J.; Hiorns, R.C.; Sommerdijk, N.A.J.M.; Williams, S.J.; Jones, R.G.; Nolte, R.J.M. *Chem. Commun.* **1998**, 1443.
- (117) Sommerdijk, N. A. J. M.; Holder, S. J.; Hiorns, R. C.; Jones, R. G.; Nolte, R. J. M. *Macromolecules* **2000**, *33*, 8289.
- (118) a) Van der Eijk, J. M.; Nolte, R. J. M.; Drenth, W.; Hezemans, A. M. F. *Macromolecules* **1980**, *13*, 1391. b) Visser, H. G. J.; Nolte, R. J. M.; Zwikker, J. W.; Drenth, W. *J. Org. Chem.* **1985**, *50*, 3133. c) Visser, H. G. J.; Nolte, R. J. M.; Zwikker, J. W.; Drenth, W. *J. Org. Chem.* **1985**, *50*, 3138.

# CHAPTER 2

## Synthesis and Characterization of Polyisocyanides Derived from Alanine and Glycine Dipeptides

### 2.1 Introduction

Polyisocyanides can be prepared via a nickel catalyzed polymerization reaction. In these reactions the isocyanides coordinate to the nickel and a nucleophile, such as an amine, initiates the polymerization (Scheme 1).<sup>1</sup> The resulting polymers have the exceptional feature that every carbon atom in the main chain is provided with a substituent, causing severe steric hindrance. This leads to restricted rotation around the carbon-carbon bonds in the polymeric backbone and consequently, due to the ‘merry-go-round’ polymerization mechanism, a helical polymer is obtained. The use of optically active Ni(II) catalysts or enantiopure monomers results in an excess of either left- or right-handed helices, with the possibility to introduce a variety of (functional) side groups.<sup>1</sup> The formed  $4_1$  helices, however, are stable in solution only when bulky side groups are present.

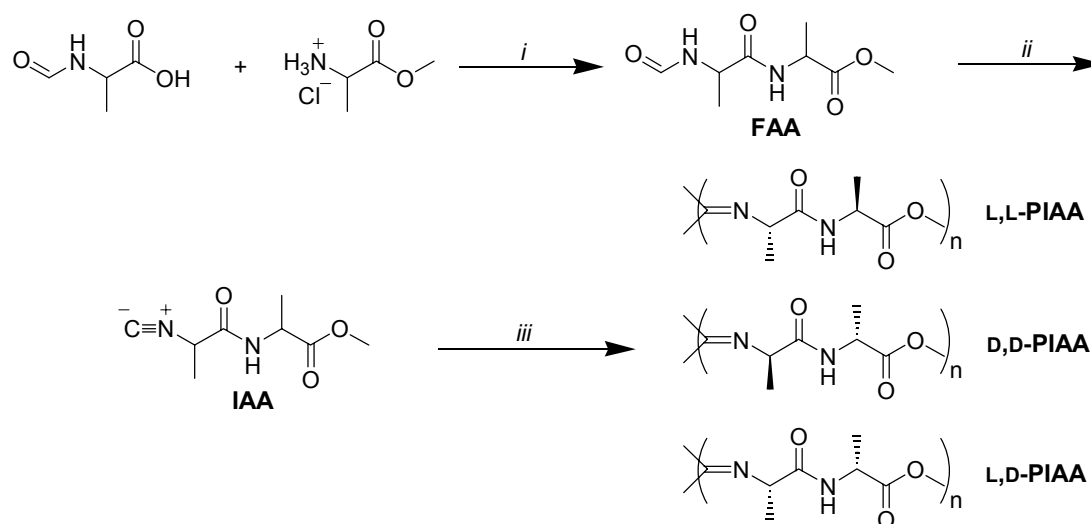


**Scheme 1** Nickel(II) catalyzed polymerization of isocyanides.

Peptide derived polyisocyanides have been reported previously containing serine and histidine residues.<sup>2,3</sup> Here we describe the synthesis of optically active polyisocyanides based on dipeptides of alanine and glycine in which a stable helical conformation is obtained due to the presence of hydrogen bonding interactions between the side chains (Figure 1B).<sup>4</sup>

## 2.2 Results and Discussion

### 2.2.1 Alanine-derived polyisocyanopeptides



**Scheme 2** Synthesis of polyisocyanides derived from alanine based dipeptides. (i)  $Et_3N$ , DCC,  $CH_3CN$ ,  $0\text{ }^\circ\text{C}$ ; (ii) diphosgene, *N*-methyl morpholine,  $CH_2Cl_2$ ,  $-30\text{ }^\circ\text{C}$ ; (iii)  $Ni(ClO_4)_2 \cdot 6H_2O$ ,  $CH_2Cl_2/EtOH$  (117/1 v/v).

**Synthesis.** Alanine-derived polyisocyanopeptides were prepared by a nickel(II) catalyzed isocyanide polymerization as is outlined in Scheme 2. For the preparation of the formamides (FAA), alanine methyl ester was liberated from the HCl-salt using triethylamine in acetonitrile, and was subsequently condensed with *N*-formyl alanine using dicyclohexyl carbodiimide (DCC) as a dehydrating reagent (yields > 75%). Although it is known that *N*-acyl amino acids are sensitive to epimerization when the reactivity of the acid group is enhanced, optically pure diastereomers were obtained via crystallization, as was confirmed by comparing their optical rotations. The isocyanooalanyl-alanine methyl esters (IAA) could be prepared by dehydrating the *N*-formyl moiety using either phosphoryl chloride<sup>5</sup> or diphosgene.<sup>6</sup> The use of the latter

reactant, however, resulted in a more efficient conversion i.e. yields of 60-90% were obtained versus 40-70% in the former case. Polymerization of these isocyanides was achieved by addition of 1/30 equivalents of  $\text{Ni}(\text{ClO}_4)_2 \cdot 6\text{H}_2\text{O}$  to the monomer in  $\text{CH}_2\text{Cl}_2$  solution. The small amount of ethanol required to dissolve the Ni-salt likely also acts as the initiator for the polymerization reaction. The reaction progressed remarkably fast; according to TLC and IR the isocyanide was consumed in less than 5 min. giving the poly(isocyanoalanyl-alanine methyl ester)s (**PIAA**) in good yields ( $\geq 70\%$ ).

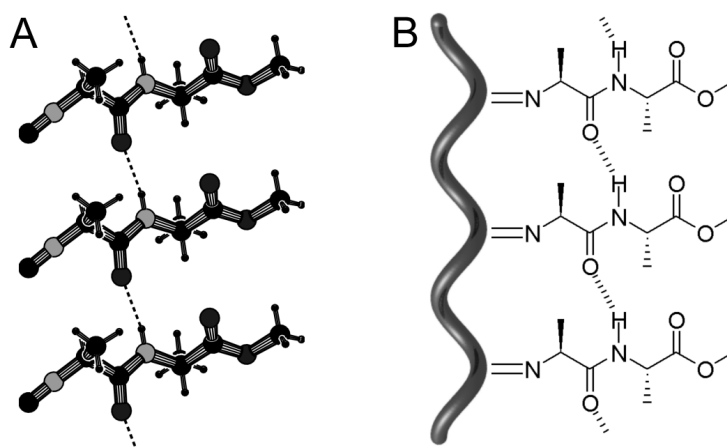


**Figure 1** (A) *PLUTON*<sup>7</sup> drawing of the crystal structure of *L*-isocyanoalanyl-*L*-alanine methyl ester (**L,L-IAA**), showing three molecules and the intramolecular hydrogen bonds. (B) Schematic representation of a hydrogen bonding array along the polymeric backbone based on **L,L-PIAA**.

**Characterization.** The chemical structures of the synthesized formamides and isocyanides were confirmed by spectroscopic techniques. The differences between on one hand the *L,L*- and *D,D*-alanyl-alanine compounds and on the other the *L,D* form were striking. The formamide of the latter was distinctly more hygroscopic and **L,D-IAA** appeared to be unstable in solution in contrast to **L,L**- and **D,D-IAA**. This instability hampered the purification of this isocyanide, however, monomers with satisfactory purity were obtained by repetitive washings.

The conversion of the formamides into the corresponding isocyanides could be monitored conveniently by the disappearance of one of the amide I absorptions in the IR spectrum and the concomitant appearance of the characteristic isocyanide vibration at  $2150\text{ cm}^{-1}$ . For **L,L-IAA** the single crystal X-ray structure was resolved (Figure 1A), confirming the proposed structure and clearly showing the presence of hydrogen bonding arrays in one direction between stacked molecules (see also the Experimental



Section). In the IR spectra of the polymers the isocyanide signal was no longer observed and instead the imine IR absorption ( $\nu = 1617 \text{ cm}^{-1}$ ) indicative of the formation of a polyisocyanide was detected as a shoulder on the amide I vibration. Upon polymerization the amide I vibrations shifted to lower wavenumbers as may be expected when hydrogen bonds are formed between amide groups in side chains  $n$  and  $(n + 4)$ . A selection of relevant solution and solid state IR absorptions present in the monomers and polymers is given in Table 1. In dilute solution the monomers did not display any signs of hydrogen bonding, whereas in the solid state a defined array of hydrogen bonds was formed between the amide groups as is clearly shown in the single crystal X-ray structure of **L,L-IAA**. For the polymers investigated (**D,D-PIAA** is not studied in this respect since it is expected to behave identical to its enantiomer **L,L-PIAA**) the IR spectra showed amide I vibrations and N-H stretch vibrations at wavenumbers that are in agreement with the formation of hydrogen bonds.

**Table 1. Selected IR data indicative of hydrogen bonding<sup>a</sup>**

	Monomer				polymer			
	$\nu_{\text{NH}}$ ( $\text{CDCl}_3$ )	$\nu_{\text{amideI}}$ ( $\text{CDCl}_3$ )	$\nu_{\text{NH}}$ (KBr)	$\nu_{\text{amideI}}$ (KBr)	$\nu_{\text{NH}}$ ( $\text{CDCl}_3$ )	$\nu_{\text{amideI}}$ ( $\text{CDCl}_3$ )	$\nu_{\text{NH}}$ (KBr)	$\nu_{\text{amideI}}$ (KBr)
<b>L,L-IAA</b>	3430 <sup>b</sup>	1688	3279	1669	3265	1657	3276	1657
<b>L,D-IAA</b>	3416	1687	3304	1668	3252	1657	3280	1659
<b>L-IGA</b>	3425 <sup>b</sup>	1689	3306	1659	3285	1654	3293	1654
<b>L-IAG</b>	3436 <sup>b</sup>	1687	3302	1674	3367 3298	1669 <sup>c</sup>	3380 3304	1665 <sup>c</sup>

<sup>a</sup>In  $\text{cm}^{-1}$ . <sup>b</sup>Split signal, average values are given. <sup>c</sup>Broad.

Upon polymerization of the isocyanides <sup>1</sup>H NMR showed broadening of the signals, with only small changes in the chemical shifts ( $\Delta\delta < 0.2 \text{ ppm}$ ), except for the amide NH resonance. For all three stereoisomers of **PIAA** the NH resonance shifted 2.4 ppm downfield, which is in line with the formation of hydrogen bonds between the side chains (Table 2).

The optical rotation of the compounds, expressed per repeat unit, increased by more than an order of magnitude going from the monomers to the polymers (Table 2). Similar results have been observed previously and were attributed to the formation of a helical secondary structure in the resultant polymers.<sup>2,3</sup>

The thermal stability of the **PIAA**'s was investigated using TGA. At approximately 230 °C the polymers started to lose weight, it appeared that **L,D-PIAA** decomposed faster than the other two investigated polymers. In agreement with this result, a lower stability was found for the monomer **L,D-IAA** also. DSC analysis did not show any melting or glass transition in the range from 20 °C to 200 °C for the **PIAA**'s. These observations are in line with the rigid character of these polyisocyanopeptides.

**Table 2. Optical rotation data and selected  $^1\text{H}$  NMR chemical shift displacements**

	optical rotation $[\alpha]^a$		$\Delta\delta_{\text{NH}}^b$
	monomer	polymer	
<b>L,L-PIAA</b>	33.0	338	2.4 <sup>c</sup>
<b>D,D-PIAA</b>	-32.0	-349	2.4 <sup>c</sup>
<b>L,D-PIAA</b>	-5.6	487	2.4
<b>L-PIGA</b>	19.2	196	2.1
<b>L-PIAG</b>	5.7	-32	1.2

<sup>a</sup>In °·dl/g·dm, measured in  $\text{CHCl}_3$ . <sup>b</sup>Chemical shift displacement upon polymerization in ppm, measured in  $\text{CDCl}_3$ . <sup>c</sup>For the polymers the NH signal is split, the average of both  $\Delta\delta$  values is given.

**Solid state NMR.** NMR experiments in the solid state were performed on the alanyl-alanine based polyisocyanopeptides. The complete assignment of the obtained  $^1\text{H}$  MAS and  $^{13}\text{C}$  CP-MAS NMR spectra of isocyanide **L,L-IAA** and the **PIAA** polymers is presented in Table 3, in which for comparison also the solution data of this isocyanide are included. The  $^{13}\text{C}$  CP-MAS NMR spectra of this monomer and the corresponding polymer are given in Figure 2 as an example, for the other investigated polymers similar spectra were obtained. The spectra for this as well as the other polymers investigated showed a remarkable narrow line widths, suggesting a well-defined molecular conformation for all these macromolecules.<sup>8</sup>

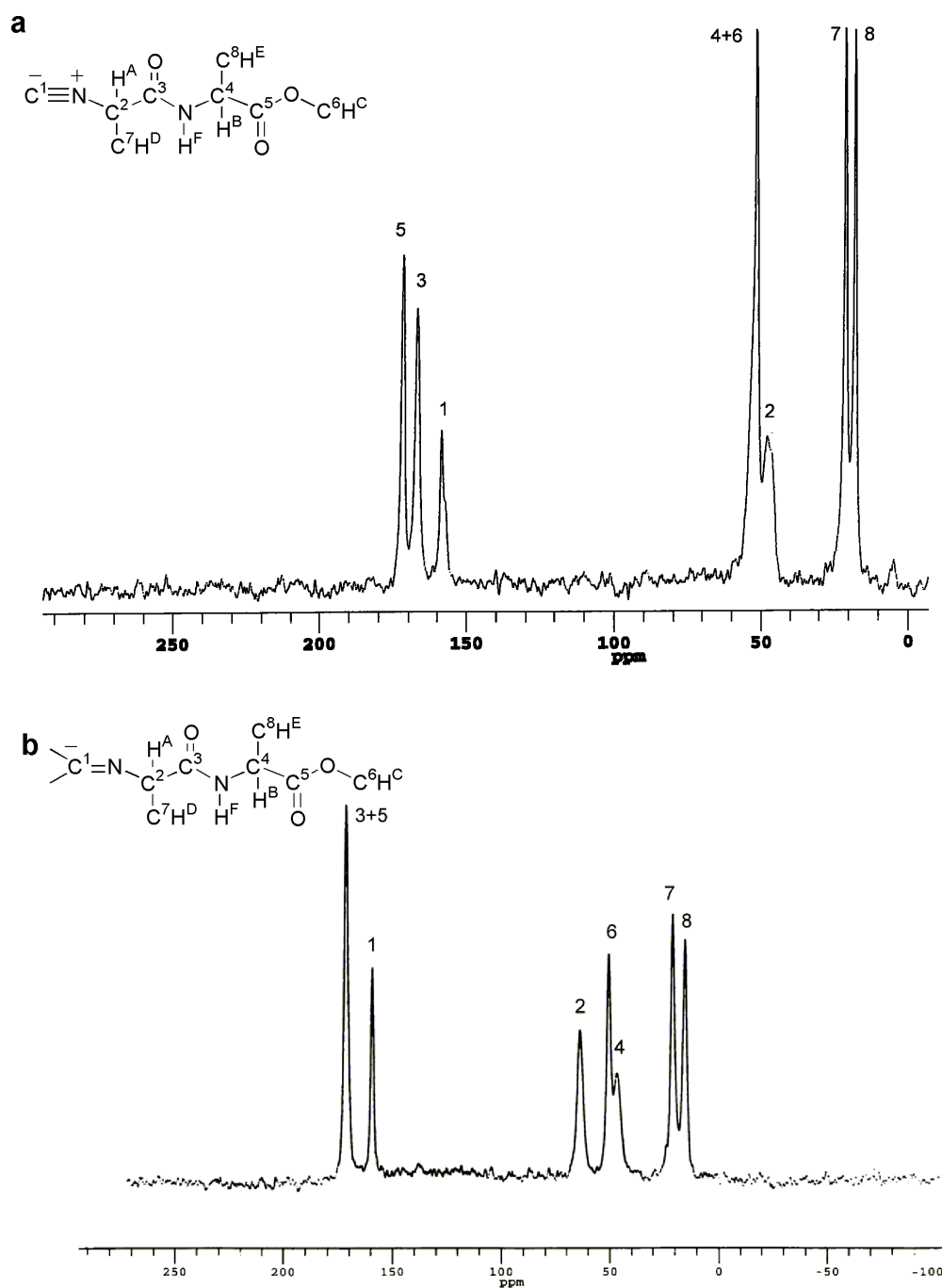


**Figure 2**  $^{13}\text{C}$  CP-MAS NMR spectra and assignment of the peaks of (a) crystalline *L,L*-IAA and (b) *L,L*-PIAA. The structural formulas indicate the labeling of the atoms.

In the  $^1\text{H}$  MAS spectra all signals assigned to the amide protons appeared downfield from 9 ppm, indicating their involvement in hydrogen bonding. Going from *L,L*-IAA in  $\text{CDCl}_3$  solution to the solid state, changes in  $^{13}\text{C}$  chemical shifts assigned to both the amide carbonyl and the  $\alpha$  carbon atoms were observed, in line with those expected for a  $\beta$ -sheet-like stacking.<sup>9</sup> A similar change was observed for this isocyanide going from its monomeric form in solution to the polymer in the solid state. Remarkably, only two

signals were detected in the low field region (155 – 180 ppm) of the  $^{13}\text{C}$  CP MAS NMR spectra although three were expected, corresponding to the backbone imine, the amide carbonyl and the ester carbonyl group. This can be explained either by assuming overlap of two peaks, or by the absence of sufficient cross polarization to obtain a detectable signal from one of the carbon atoms. In  $^{13}\text{C}$  NMR studies on more soluble polyisocyanides the imine carbon atom was assigned to signals found between 160 and

**Table 3. Solid state chemical shifts of L,L-IAA and PIAA's<sup>a</sup>**

	L,L-IAA		L,L-PIAA	D,D-PIAA	L,D-PIAA
	$\text{CDCl}_3$	solid			
$\text{H}_\text{A}+\text{H}_\text{B}$	4.57 4.20	4.6	5.0	4.9	4.6
$\text{H}_\text{C}$	3.77	3.3	3.6	3.5	3.3
$\text{H}_\text{D}+\text{H}_\text{E}$	1.66 1.47	1.1	1.3	1.3	1.2
$\text{H}_\text{F}$	6.91	9.6	9.7	9.6	9.2
$\text{C}_1$	162.0	158.9	160.0	160.1	160.4
$\text{C}_2$	53.9	52.8	64.5	64.1	64.6
$\text{C}_3$	166.3	167.4	171.9	171.9	172.0
$\text{C}_4$	49.2	48.4	47.2	47.2	47.5
$\text{C}_5$	173.2	172.2	171.9	171.9	172.0
$\text{C}_6$	53.4	52.8	51.2	51.2	51.0
$\text{C}_7$	20.3	21.8	21.9	21.9	20.9
$\text{C}_8$	18.7	18.5	16.2	16.2	15.3

<sup>a</sup>In ppm.

165 ppm, and also solution  $^{13}\text{C}$  NMR studies on related homopolymers<sup>10</sup> and block copolymers<sup>11</sup> suggested that the signal at 160 ppm should be attributed to the carbon atoms in the imine backbone. Consequently the peak at  $\delta = 171.9$  ppm originates from one or both of the carbonyl carbon atoms. The overlap of amide and ester carbonyls in solid state  $^{13}\text{C}$  NMR spectra is not uncommon. For example in poly( $\beta$ -benzyl-L-

aspartate) in the  $\beta$ -sheet conformation, the amide and ester carbonyls are also found to have the same chemical shift.<sup>9</sup>

The process of cross polarization was investigated in more detail using the CPWISE puls sequence,<sup>12</sup> this 2D technique gives polarization correlated  $^1\text{H}$ - $^{13}\text{C}$  spins as cross peaks. For atoms  $\text{C}_2$ ,  $\text{C}_4$  and  $\text{C}_{6-8}$  the majority of the polarization originates from the directly connected protons. The cross peaks in the region from 155 to 180 ppm of **D,D-PIAA** are shown as a representative example in Figure 3. In line with the assignment of the signal at 160.0 ppm to the imine carbon atom, cross polarization in this case predominantly takes place with  $\text{H}_A$ , while for the resonances found at 171.9 ppm clearly correlation is present with the protons close to the carbonyl groups. As expected cross peaks between the signals of these carbons and the hydrogen bonded NH protons were found. Finally, direct excited  $^{13}\text{C}$  MAS spectra were found to be in qualitative agreement with the results obtained applying cross polarization. Since for both **L,L-PIAA** and **L,D-PIAA** very similar spectra were obtained, it is improbable that their macromolecular conformation is very different.

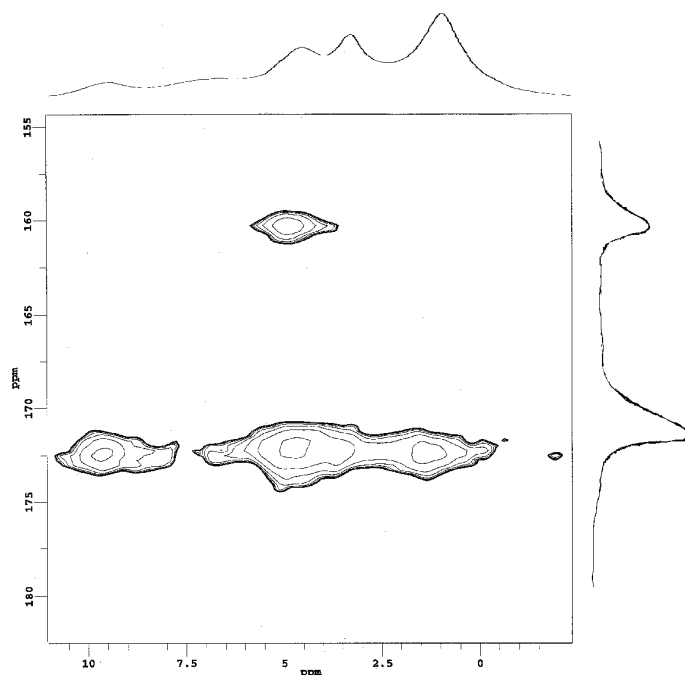


**Figure 3** CPWISE 2D spectrum displaying the  $^{13}\text{C}$  region of 155 – 180 ppm measured for **D,D-PIAA**.

**Molecular weight determination.** As our attempts to determine the absolute molecular weights of the prepared polymers were unsuccessful using GPC and mass spectrometry, and light scattering was hampered due to the broad absorption bands of the

polyisocyanopeptides; we used viscometry to assess the relative molecular weights. The viscosity of a polymer solution is not only dependent on the molecular weight of the solute, but also on its interaction with the solvent and on the macromolecular structure. Therefore only for a specific polymer the viscosity averaged molecular weight ( $M_v$ ) can be determined in an absolute fashion. For this purpose first the Mark-Houwink equation has to be established for this polymer in combination with another technique. This equation has been determined for poly( $\alpha$ -phenyl ethyl isocyanide) by Millich:<sup>13</sup>

$$[\eta] = 3.8 \cdot 10^{-7} M_v^{1.30} \text{ (in toluene, 30 }^\circ\text{C)} \quad \text{eq. (1)}$$

and by van Beijnen et al.<sup>14</sup> for poly(2-octyl isocyanide):

$$[\eta] = 1.4 \cdot 10^{-9} M_v^{1.75} \text{ (in toluene, 30 }^\circ\text{C)} \quad \text{eq. (2)}$$

The intrinsic viscosities of different batches of **L,L-** and **L,D-PIAA** were measured which were all prepared using the same ratio of Ni / monomer (see experimental) and values of  $[\eta] = 1.12 - 2.20$  dl/g were obtained for the former polymer. In the case of **L,D-PIAA** the distribution was even larger, i. e.  $[\eta] = 4.21 - 11.02$  dl/g and for a single batch of **D,D-PIAA** a value of  $[\eta] = 3.31$  dl/g was found. These widespread numbers, resulting from polymers prepared under identical conditions, were a first indication that under these conditions the polymerization reaction did not allow control over the molecular weight.

As a result of the defined rigid conformation, dictated by hydrogen bonds between the side chains, individual macromolecules could be visualized by Atomic Force Microscopy (Figure 4). Due to this rigidity the macromolecules are extended on the surface and their contour lengths can be accurately measured. This approach has been used by Prokhorova *et al*<sup>15</sup> to determine the absolute molecular weight of polymethacrylates and polystyrenes having bulky substituents, and could be applied to our polyisocyanopeptides as well. The lateral width of the polymers was overestimated by a factor 10 due to the AFM tip shape effect,<sup>15</sup> however, the height analysis was in good agreement with the expected macromolecular diameter.<sup>4</sup> For a large number of molecules the contour length was determined, and at the same time the height of the observed features was checked to distinguish between single polymers and overlaying polymer chains. Representative micrographs for **L,L-** and **L,D-PIAA** and the histograms of the length distribution of the investigated polyisocyanopeptides are given in Figure 4. The molecular weight parameters derived from these histograms are summarized in

Table 4. In the analyses the degree of polymerization is derived from the contour length by assuming a  $4_1$  type helix with a helical pitch of 0.46 nm.<sup>4</sup>

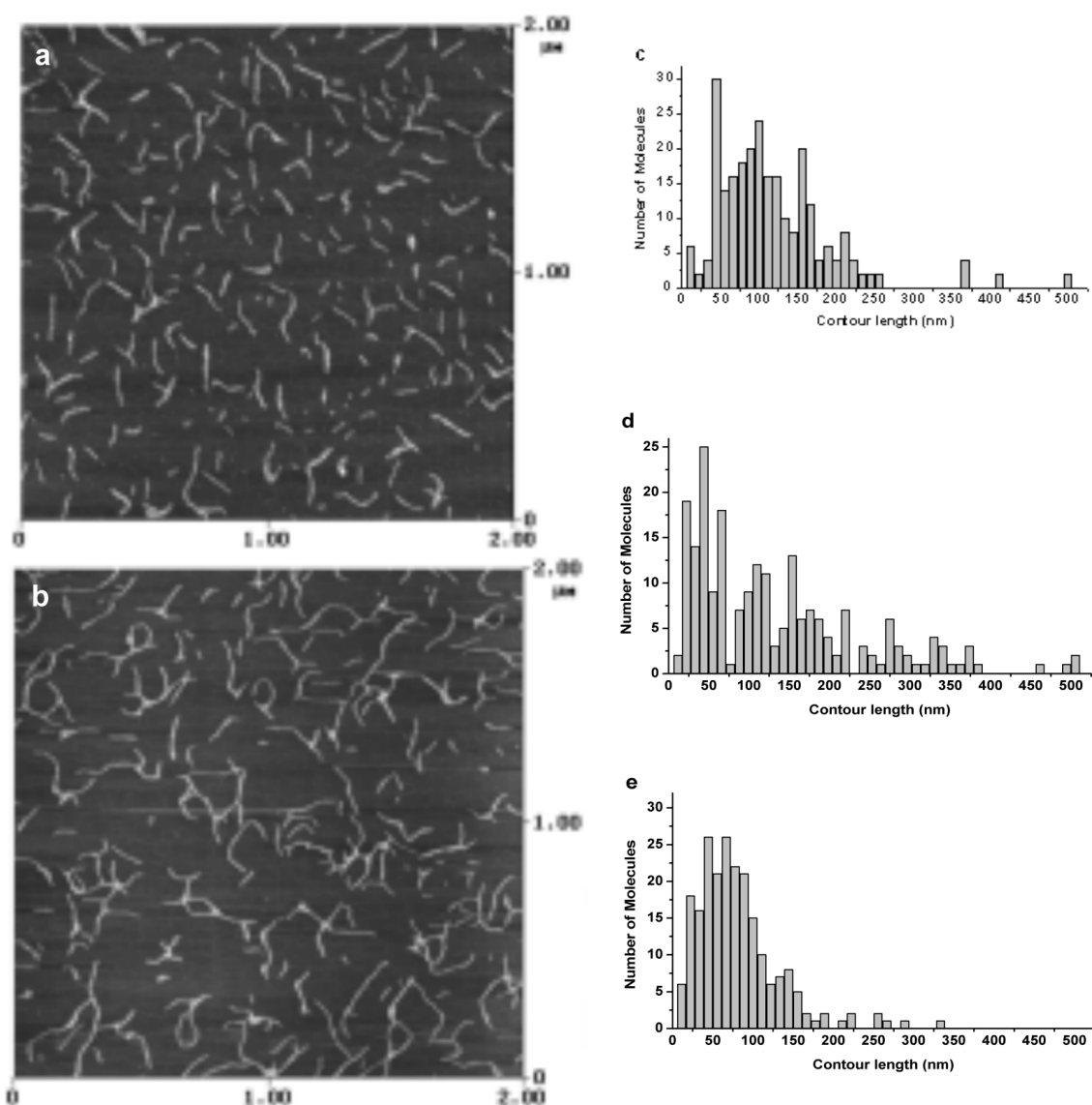


**Figure 3** Atomic force micrographs of (a) *L,L*-PIAA and (b) *L,D*-PIAA. Histograms showing the length distribution as obtained from the AFM images for (c) *L,L*-PIAA, (d) *L,D*-PIAA and (e) *L*-PIGA.

In line with the results from viscosity measurements a significantly higher molecular weight is found for *L,D*-PIAA compared to *L,L*-PIAA. For comparison both the AFM molecular weight data and an estimate of the viscosity averaged molecular weight (based on the two presented Mark-Houwink equations) are included in Table 4. Taking into account the identical polymerization conditions and the fast progressing reaction, the poor control over molecular weight can be explained by assuming a considerably higher rate of propagation compared to initiation. This assumption also

explains the non-linear relation between the degree of polymerization and the monomer to catalyst ratio. The higher molecular weight and PDI found for **L,D-PIAA** point to an even higher rate of propagation for this monomer, which is remarkable regarding the subtle structural difference between this compound and **L,L-PIAA**.

The AFM images suggested also that the higher molecular weight **L,D-PIAA** had a stronger tendency to cluster than **L,L-PIAA**. Aggregation would also explain the extreme high intrinsic viscosity (up to  $[\eta] = 11.02$  dl/g) found for some **L,D-PIAA** batches, and the non-linear relation observed between the viscosity and concentration for these polymers. It is, however, unclear whether this increased propensity to assemble is a result of the higher molecular weight, or from small differences in the molecular structure or from a combination of the two.

**Table 4. Molecular weights of selected polyisocyanopeptides<sup>a</sup>**

	$M_n^b$	$M_w^b$	D	$[\eta]^c$	$M_v^b$	
					eq. (1) <sup>d</sup>	eq. (2) <sup>d</sup>
<b>L,L-PIAA</b>	186	255	1.4	1.33	108	135
<b>D,D-PIAA</b>	n.d. <sup>e</sup>	n.d. <sup>e</sup>	-	3.31	218	227
<b>L,D-PIAA</b>	221	381	1.7	5.26	311	296
<b>L-PIGA</b>	120	196	1.4	n.d. <sup>e</sup>	-	-

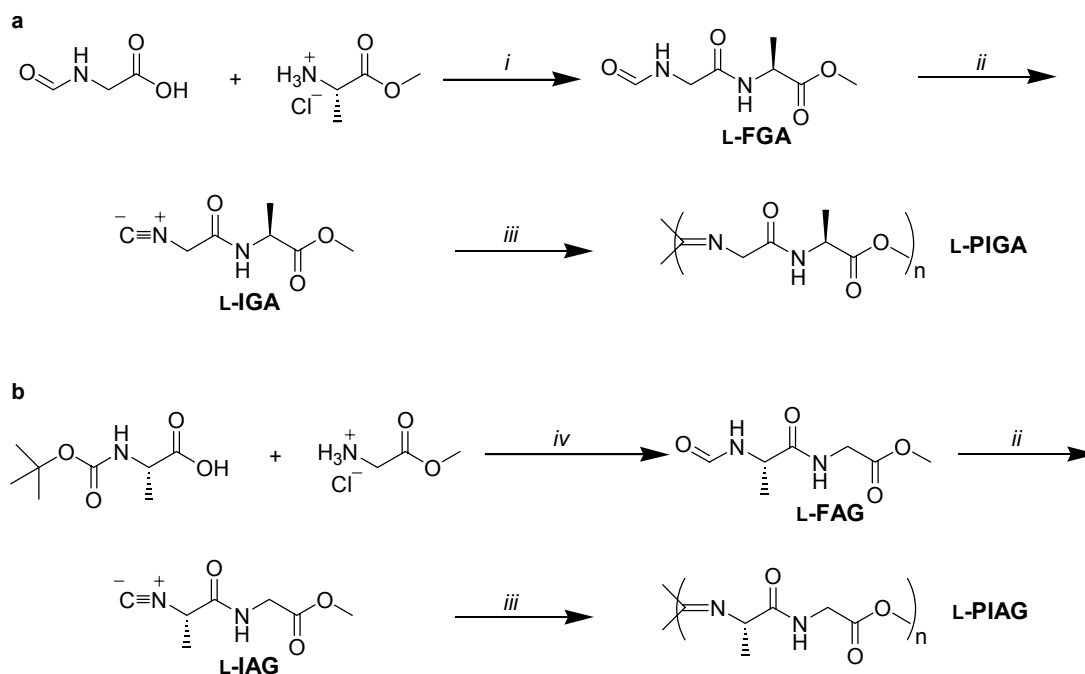
<sup>a</sup>Several batches have been prepared under the same conditions (see above and experimental), the data of polymer batches used in solid state NMR and conformational studies<sup>4</sup> are displayed. <sup>b</sup>In kg/mol. <sup>c</sup>In g/dl measured in CHCl<sub>3</sub>. <sup>d</sup>The number refers to the used Mark-Houwink equation (see text). <sup>e</sup>Not determined.

### 2.2.2 Polyisocyanopeptides based on alanine and glycine

As was demonstrated above the relatively small difference in configuration of **L,L-IAA** and **L,D-IAA** resulted in unexpected differences in the properties of the resultant polymers. To obtain insight in the interactions responsible for these differences, polyisocyanides based on alanyl-glycine and glycyL-alanine have been prepared. In these systems instead of a stereocenter, an achiral methylene group is present, leading to a reduction of the steric interactions and thereby to a smaller preference for a specific side chain conformation.



**Synthesis.** When the achiral amino acid glycine is incorporated in the dipeptides at the C-terminal position (i.e. in the case of **FAG**), special care has to be taken to avoid epimerization, since this would lead to the generation of enantiomers



**Scheme 3** Synthesis of polyisocyanides derived from *L*-alanine and glycine based dipeptides. (i)  $\text{Et}_3\text{N}$ , DCC, DMF/ $\text{CH}_3\text{CN}$  (1/1 v/v), 0 °C; (ii) diphosgene, *N*-methyl morpholine,  $\text{CH}_2\text{Cl}_2$ , -30 °C; (iii)  $\text{Ni}(\text{ClO}_4)_2 \cdot 6\text{H}_2\text{O}$ ,  $\text{CH}_2\text{Cl}_2/\text{EtOH}$  (117/1 v/v); (iv) 1:  $\text{Et}_3\text{N}$ , DCC, DMF/ $\text{CH}_3\text{CN}$  (1/1 v/v), 0 °C; 2: HCl, EtOAc; 3:  $\text{HCO}_2\text{C}_2\text{H}_5$ ,  $\text{HCO}_2\text{Na}$ , reflux.

rather than diastereomers and hence purification would be more laborious. For the synthesis of *N*-formyl-*L*-glycyl-alanine methyl ester (**L-FGA**) a similar route as for **FAA** was followed (Scheme 3a). In order to synthesize **FAG**, glycine methyl ester was reacted with Boc-*L*-alanine (Scheme 3b), since these carbamates are less sensitive to epimerization. The Boc protecting group was removed by dissolving the dipeptide in HCl-saturated ethyl acetate. Subsequent formylation was achieved by refluxing the HCl-salt of the dipeptide in a mixture of ethyl formate and sodium formate, in which the last compound acted as a base in the deprotonation of the ammonium group. When at least 4 equivalents of sodium formate were used the amine was quantitatively converted into the formamide. In the presence of a lower concentration of base a variety of products was formed, including the unreacted ammonium salt and compounds in which the amide group was formylated. Both **FGA** and **FAG** were converted into the

corresponding isocyanides using the diphosgene route and polymerized in a manner similar to the one used for the alanine dipeptide monomers. A striking observation was the significantly lower rate of polymerization observed for **L-IAG**, *i. e.* more than 2 hrs. were needed for this reaction to be completed compared to less than 5 min. for all other polyisocyanopeptides reported here.

**Characterization.** The characteristic infrared properties of **L-IGA** and the resulting polymer were comparable to those observed for the **IAA**'s (Table 1). For **L-PIAG** two N-H stretching vibrations were observed in  $\text{CHCl}_3$  at 3367 and 3298  $\text{cm}^{-1}$  which were assigned to the amide group in a full hydrogen bond and to one in a partly hydrogen bonded state, respectively. A similar feature was observed for the amide I vibration, although the splitting in this case was relatively small so only a broadening of the resultant peak was observed.

Also in the case of **L-PIGA** the optical rotation was an order of magnitude higher than the one found for the monomer (Table 2), suggesting that again a helical secondary structure is formed. Almost no amplification of chirality was observed upon polymerization of **L-IAG**, indicating that the only partly formed hydrogen bonds are insufficient to secure the helical structure of the polymer.<sup>4</sup>

The shift of the NH resonances found in the solution  $^1\text{H}$  NMR spectra for **L-PIGA** matched with the complete participation of all amide groups in side chain hydrogen bonding. The only partial formation of the hydrogen bonding arrays in the case of **L-PIAG** as mentioned above is indeed reflected in a significant smaller  $\Delta\delta_{\text{NH}}$  value. The DSC analysis of **L-PIGA** indicated no transitions in the region of 20 °C to 200 °C, in line with the observations for **PIAA**.

**Molecular weight determination.** The molecular weight characteristics of **L-PIGA** as determined by AFM are given in Table 4 and Figure 4e. For **L-PIAG** this technique was impracticable for the determination of the molecular weight due to the lack of rigidity in this polymer. The degree of polymerization of **L-PIGA** is similar to that of **L-PIAA**, suggesting that for the formation of these polyisocyanopeptides by Ni(II) catalysis similar rates of polymerization apply, regardless of the different steric requirements of the side group next to the isocyanide moiety. In these polymerization reactions the nickel is acting as a template to bring the monomeric isocyanides together.<sup>1</sup> The propagation step requires only a slight rearrangement of the bonds to form the polymer. The creation of

hydrogen bonds between monomers, complexed to the metal center, and the side chains of the growing polymer chain, can provide a similar pre-organizing effect.<sup>4</sup> This would explain the rapid formation of these polyisocyanopeptides, as well as the pronounced effect of subtle changes in the side chain configuration on the polymer properties. Since these Ni(II) catalyzed isocyanide polymerization reactions are kinetically controlled,<sup>1</sup> a monomer which fits in precisely with the hydrogen bonding pattern and experiences the least unfavorable steric interactions, will be inserted in the growing chain faster than other monomers. The extent to which the former type of monomer is incorporated faster in the polymer chain determines the regularity of the resultant macromolecules.

### 2.3 Conclusions

Starting from glycine and both enantiomers of alanine different combinations of optically pure dipeptides containing isocyanide functionalities have been prepared. Using a Ni(II)-based polymerization catalyst, polyisocyanopeptides were formed in which intramolecular hydrogen bonds are present presumably between side chains  $n$  and  $(n + 4)$ ,<sup>4</sup> as was indicated by infrared and <sup>1</sup>H NMR spectroscopy. The differences between **L,L-PIAA** and **L,D-PIAA** can be explained by assuming that in the latter polymer less unfavorable steric interactions are present between the side chains.<sup>4</sup> It is proposed that in the case of **L-IGA** the chiral bias to create an excess of one particular helix type is provided by the remote alanine unit, which is remarkable. The Ni(II) center organizes the isocyanide functionalities and consequently the monomer behaves similar to **L,L-IAA**. For **L-IAG** the pre-organizing capacity of the alanine-group is diminished, which again is remarkable giving rise to a polymer in which hydrogen bonds between the side chains are only partially present. The increased rotational freedom of the glycine segment compared to an alanine one might account for this difference.

The sharpness of the signals in the solid state <sup>13</sup>C NMR spectra supports the presence of a well-defined macromolecular conformation.<sup>8</sup> A detailed conformational analysis and the role the hydrogen bonds play will be discussed in Chapter 3.<sup>4</sup> As a result of the rigidity of the polyisocyanopeptides these macromolecules could be visualized with AFM. This allowed us to determine the absolute molecular weights, something that was not possible using more conventional techniques. Pre-organization

of the monomers can possibly explain the high rate of propagation and the regular structure of the obtained polyisocyanopeptides.

## 2.4 Experimental Section

### 2.4.1 General methods and materials

Dichloromethane was distilled from  $\text{CaH}_2$  (under atmospheric pressure), *N*-methyl morpholine and triethylamine were distilled under reduced pressure from sodium and  $\text{CaH}_2$ , respectively. All other chemicals were commercial products and were used as received. Flash chromatography was performed using silica gel (0.035-0.075 mm) purchased from Acros and TLC analyses on silica 60  $\text{F}_{254}$  coated glass either from Merck or Acros. Compounds were visualized with  $\text{I}_2$ -vapour or  $\text{Cl}_2/\text{TDM}$ .  $^1\text{H}$  NMR spectra were recorded on Bruker AC-100, Bruker WM-200 and Bruker AC-300 instruments at 297 K,  $^{13}\text{C}$  NMR spectra were acquired on a Bruker AC-300 spectrometer. Chemical shifts are reported in ppm relative to tetramethylsilane ( $\delta = 0.00$  ppm) as an internal standard. FT-Infrared spectra were recorded on a Bio-Rad FTS 25 instrument (resolution  $2\text{ cm}^{-1}$ ), melting points were measured using a Büchi capillary melting point apparatus or a Jeneval THMS 600 microscope equipped with a Linkam 92 temperature control unit and are reported uncorrected. Mass spectrometry (FAB, EI) was performed on a VG 7070E instrument; for FAB-MS 3-nitrobenzyl alcohol was used as a matrix. Elemental analyses were determined on a Carlo Erba 1180 instrument. DSC and TGA measurements were performed on a Perkin Elmer DSC 7 (10  $^\circ\text{C}/\text{min.}$ ) and a Perkin Elmer TGA 7 (20  $^\circ\text{C}/\text{min.}$ ) respectively. Optical rotations were measured on a Perkin Elmer 241 polarimeter. Solution viscosities were determined in chloroform (Biosolve P.A.) with Ubbelohde microviscometers with a suspended level bulb of different capillary tube diameters in a Schott CT-1650 thermostatted bath at 20.00 $^\circ\text{C}$ .

**Solid State NMR.**  $^{13}\text{C}$  CP MAS measurements were performed on a Chemagnetics CMX-600 instrument (carbon frequency 150 MHz, proton frequency 600 MHz), using the Hartmann-Hahn puls sequence<sup>16</sup> with  $\tau_{\text{mix}} = 2$  ms, a delay of 2 s and a proton pulse of 2.60  $\mu\text{s}$ , the spinning frequency was 23 kHz. Direct excited  $^1\text{H}$  and  $^{13}\text{C}$  NMR spectra were measured on the same instrument and on a Bruker DMX-300 spectrometer operating at 300 and 75 MHz for proton and carbon respectively. Spectra were recorded using single pulse excitation, and high proton decoupling in the case of  $^{13}\text{C}$ .

**Atomic Force Microscopy.** Imaging was carried out on a Nanoscope III from Digital Instruments operating in the tapping mode at room temperature. Samples were prepared by spin coating (1800 rpm) a 0.01 g/l polymer solution on freshly cleaved mica. It appeared useful to slightly heat the mica just before and after spin coating, to improve the quality of the samples. It was assumed that the overestimation of the length of the polymers, because of the tip shape, was equal to the overestimation of the width.

**Table 5. Crystal data and data collection parameters for L,L-PIAA**

parameters	L,L-PIAA
crystal colour	transparent colorless
crystal shape	irregular thin needle
crystal size [mm]	0.84 x 0.07 x 0.04
empirical formula	C <sub>8</sub> H <sub>12</sub> N <sub>2</sub> O <sub>3</sub>
M <sub>w</sub>	184.20
T [K]	293(2)
crystal system	orthorhombic
space group	P 2 <sub>1</sub> 2 <sub>1</sub> 2 <sub>1</sub>
unit cell dimensions	a [Å] = 4.7281(6), α = 90° b [Å] = 9.202(2), β = 90° c [Å] = 23.792(4), γ = 90°
range [°]	16.941 < θ < 22.865
Volume [Å <sup>3</sup> ]	1035.1(3)
Z	4
calculated density [Mg/m <sup>3</sup> ]	1.182
absorption coefficient [mm <sup>-1</sup> ]	0.767
F(000)	392
θ range for data collection [°]	3.72 to 70.09
index ranges	-5 ≤ h ≤ 0 0 ≤ k ≤ 11 -29 ≤ l ≤ 29
reflections collected / unique	2335 / 1972
R(int)	0.0338
reflections observed [I <sub>o</sub> > 2σ(I <sub>o</sub> )]	1067
Range of relative transm. factors	1.020 / 0.978
data / restraints / parameters	1972 / 0 / 134
goodness-of-fit on F <sup>2</sup>	1.033
SHELXL-97 weight parameters	0.073000 0.016400
R indices (all data)	R1 = 0.1289, wR2 = 0.1662
final R indices [I > 2σ(I)]	R1 = 0.0632, wR2 = 0.1378
largest diff. peak and hole [Å <sup>3</sup> ]	0.155 and -0.178

#### 2.4.2 Single crystal X-ray resolution of L,L-IAA.

Crystals of L,L-PIAA suitable for X-ray diffraction studies were obtained from diethyl ether by slow evaporation of the solvent. A single crystal was mounted in air on a glass fiber. Intensity data were collected at room temperature. An Enraf-Nonius CAD4 single-crystal diffractometer was used, Cu-Kα

radiation,  $\theta$ - $2\theta$  scan mode. Unit cell dimensions were determined from the angular setting of 15 reflections. Intensity data were corrected for Lorentz and polarization effects. Semi-empirical absorption correction ( $\psi$ -scans)<sup>17</sup> was applied. The structure was solved by the program CRUNCH<sup>18</sup> and was refined with standard methods (refinement against  $F^2$  of all reflections with SHELXL97<sup>19</sup>) with anisotropic parameters for the nonhydrogen atoms. The hydrogen atoms of the methyl groups were refined as rigid rotors with idealized  $sp^3$  hybridization and a C-H bond length of 0.97 Å to match maximum electron density in a difference fourier map. All other hydrogen atoms were initially placed at calculated positions and were freely refined subsequently. A structure determination summary is given in Table 5 and PLUTON<sup>7</sup> drawings of the molecular structure are shown in Figure 1B (stacking of the molecules) and Figure 4 (relative) arrangement of the stacks).

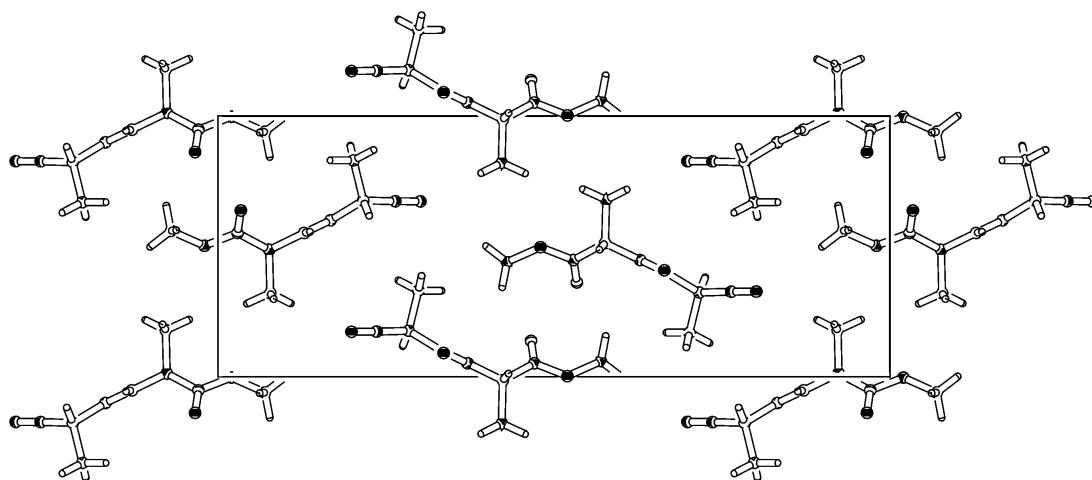


**Figure 4** PLUTON<sup>7</sup> drawing of the crystal structure of *L,L*-PIAA displaying the arrangement of hydrogen bonded stacks of molecules. The unit cell along the *b*- and *c*-axes is indicated.

### 2.4.3 Compounds.

*N*-Formyl-L-alanine, *N*-formyl-D-alanine,<sup>3</sup> *N*-Formyl-glycine,<sup>20</sup> and D-alanine methyl ester<sup>21</sup> were prepared as reported previously.

***N*-Formyl-L-alanyl-L-alanine methyl ester (*L,L*-FAA).** L-Alanine methyl ester hydrochloride (21.5 g, 0.15 mol) was dissolved in 575 mL acetonitrile. Upon cooling in an ice bath, 21 mL triethylamine and subsequently 18 g (0.15 mol) *N*-formyl-L-alanine were added. The reaction mixture was slightly heated until a clear solution was obtained, the ice bath was replaced and 34.8 g (0.17 mol) dicyclohexyl carbodiimide was added. After stirring for 3 hrs the precipitate formed (dicyclohexyl urea) was filtered off and the solvent was evaporated. The white product was brought into 800 mL ethyl acetate, triethyl ammonium chloride was filtered off and the filtrate was washed with 40 mL water. The organic layer was dried using  $MgSO_4$  and evaporated to dryness, the product was recrystallized from ethanol/diisopropyl ether resulting in 23.2 g (82%) of white needle-like crystals. Mp: 105-107 °C.  $[\alpha]_D^{25}$  ( $CH_2Cl_2$  *c* 1) = -52.5°.

$^1\text{H}$  NMR ( $\delta$  ppm, DMSO- $\text{D}_6$ , 300 MHz): 8.38 (d, 1H, NH,  $J = 6.8$  Hz), 8.24 (d, 1H, NH,  $J = 7.5$  Hz), 7.95 (s, 1H, HCO), 4.38 (m, 1H, CH), 4.25 (m, 1H, CH), 3.60 (s, 3H,  $\text{OCH}_3$ ), 1.27 (d, 3H,  $\text{CH}_3$ ,  $J = 7.3$  Hz), 1.19 (d, 3H,  $\text{CH}_3$ ,  $J = 7.0$  Hz).  $^{13}\text{C}$  NMR ( $\delta$  ppm, DMSO- $\text{D}_6$ , 75 MHz):  $\delta = 173.1$ , 172.0 (C=O), 160.8 (HC=O), 52.1 (CH), 47.7 ( $\text{OCH}_3$ ), 45.7 (CH), 18.7, 17.0 ( $\text{CH}_3$ ). FT-IR ( $\text{cm}^{-1}$ , KBr): 3297 (NH), 1757 (C=O ester), 1652, 1637 (amide I), 1549, 1534 (amide II). FAB-MS:  $m/z = 203$  [ $\text{M}+\text{H}$ ] $^+$ . El. Anal. Calcd. for  $\text{C}_8\text{H}_{14}\text{N}_2\text{O}_4$ : C, 47.52; H, 6.98; N, 13.85. Found: C, 47.84; H, 7.10; N, 13.49.

***N*-Formyl-*D*-alanyl-*D*-alanine methyl ester (**D,D-FAA**).** Starting from *D*-alanine methyl ester and *N*-formyl-*D*-alanine, following the same procedure as for **L,L-FAA**, **D,D-FAA** was obtained as a white crystalline product (yield 79%). Mp: 108 °C.  $[\alpha]_{\text{D}}$  ( $\text{CH}_2\text{Cl}_2$   $c$  0.6) = 53.1°.  $^1\text{H}$  NMR ( $\delta$  ppm, DMSO- $\text{D}_6$ , 300 MHz): 8.39 (d, 1H, NH,  $J = 6.8$  Hz), 8.24 (d, 1H, NH,  $J = 7.3$  Hz), 7.96 (s, 1H, HCO), 4.39 (m, 1H, CH), 4.26 (m, 1H, CH), 3.61 (s, 3H,  $\text{OCH}_3$ ), 1.27 (d, 3H,  $\text{CH}_3$ ,  $J = 7.3$  Hz), 1.19 (d, 3H,  $\text{CH}_3$ ,  $J = 7.0$  Hz).  $^{13}\text{C}$  NMR ( $\delta$  ppm, DMSO- $\text{D}_6$ , 75 MHz):  $\delta = 173.0$ , 171.9 (C=O), 160.7 (HC=O), 51.9 (CH), 47.6 ( $\text{OCH}_3$ ), 46.3 (CH), 18.4, 16.8 ( $\text{CH}_3$ ). FT-IR ( $\text{cm}^{-1}$ , KBr): 3296 (NH), 1757 (C=O ester), 1651, 1637 (amide I), 1549, 1534 (amide II). FAB-MS:  $m/z = 203$  [ $\text{M}+\text{H}$ ] $^+$ . El. Anal. Calcd. for  $\text{C}_8\text{H}_{14}\text{N}_2\text{O}_4$ : C, 47.52; H, 6.98; N, 13.85. Found: C, 47.35 ; H, 6.94; N, 13.57.

***N*-Formyl-*L*-alanyl-*D*-alanine methyl ester (**L,D-FAA**).** Starting from *D*-alanine methyl ester and *N*-formyl-*L*-alanine, following the same procedure as for **L,L-FAA**, **L,D-FAA** was obtained as a white crystalline product (yield 75%). Mp: 88-92 °C.  $[\alpha]_{\text{D}}$  ( $\text{CH}_2\text{Cl}_2$   $c$  0.5) = -49.0°.  $^1\text{H}$  NMR ( $\delta$  ppm, DMSO- $\text{D}_6$ , 300 MHz): 8.41 (d, 1H, NH,  $J = 6.7$  Hz), 8.24 (d, 1H, NH,  $J = 7.3$  Hz), 7.96 (s, 1H, HCO), 4.40 (m, 1H, CH), 4.24 (m, 1H, CH), 3.60 (s, 3H,  $\text{OCH}_3$ ), 1.27 (d, 3H,  $\text{CH}_3$ ,  $J = 7.1$  Hz), 1.18 (d, 3H,  $\text{CH}_3$ ,  $J = 7.1$  Hz).  $^{13}\text{C}$  NMR ( $\delta$  ppm, DMSO- $\text{D}_6$ , 75 MHz): 173.2, 172.0 (C=O), 160.8 (HC=O), 52.1 (CH), 47.8 ( $\text{OCH}_3$ ), 46.6 (CH), 19.0, 17.2 ( $\text{CH}_3$ ). FT-IR ( $\text{cm}^{-1}$ , KBr): 3318 (NH), 1747 (C=O ester), 1662, 1631 (amide I), 1556, 1515 (amide II). FAB-MS:  $m/z = 203$  [ $\text{M}+\text{H}$ ] $^+$ . El. Anal. Calcd. for  $\text{C}_8\text{H}_{14}\text{N}_2\text{O}_4 \cdot \frac{1}{2}\text{H}_2\text{O}$ : C, 45.49; H, 7.16; N, 13.26. found: C, 45.64; H, 6.98; N, 12.87.

***N*-Formyl-glycyl-*L*-alanine methyl ester (**L-FGA**).** In 250 mL acetonitrile/DMF (1:1 v/v) were dissolved 6.75 g (0.05 mol) *L*-alanine methyl ester, 5 g triethylamine and 5 g (0.05 mol) *N*-formyl-glycine by gentle heating. The reaction mixture was cooled in an ice bath, 11.3 g (0.055 mol) dicyclohexyl carbodiimide was added and stirred for 3 hrs. The formed precipitate was removed by filtration and the solution concentrated in vacuo. The resulting yellow oil was redissolved in 300 mL ethyl acetate and the residual triethyl ammonium chloride was filtered off. Washing the organic layer with 25 mL water, drying ( $\text{Na}_2\text{SO}_4$ ) and subsequent evaporation gave **L-FGA** in 63% yield. Due to the intense color of the product no reliable optical rotation could be obtained.  $^1\text{H}$  NMR ( $\delta$  ppm,  $\text{CDCl}_3$ , 300 MHz): 8.23 (s, 1H, HCO), 8.02 (br, 1H, NH), 7.49 (br, 1H, NH), 4.48 (qn, 1H, CH,  $J = 7.2$  Hz), 4.29 (d, 2H,  $\text{CH}_2$ ,  $J = 5.7$  Hz), 3.67 (s, 3H,  $\text{OCH}_3$ ), 1.32 (d, 3H,  $\text{CH}_3$ ,  $J = 7.2$  Hz).  $^{13}\text{C}$  NMR ( $\delta$  ppm,  $\text{CDCl}_3$ , 75 MHz): 173.9 (C=O), 169.2 (C=O), 162.8 (HC=O), 53.0 (CH), 49.6 ( $\text{OCH}_3$ ), 41.8 ( $\text{CH}_2$ ), 18.2 ( $\text{CH}_3$ ). EI-MS:  $m/z = 188$  [ $\text{M}$ ] $^+$ , 129 [ $\text{M} - \text{CO}_2\text{CH}_3$ ] $^+$ . Because of the volatile nature of this compound no elemental analyses were determined.

***N*-Formyl-L-alanyl-glycine methyl ester (L-FAG).** Glycine methyl ester (3.15 g, 0.025 mol) and 3 g triethylamine were dissolved in 125 mL acetonitrile/DMF (1:1 v/v) by gentle heating. The solution was cooled in ice and first 4.73 g (0.025 mol) *tert*-butoxycarbonyl-L-alanine and then 5.67 g dicyclohexyl carbodiimide (0.0275 mol) were added, after which the solution was stirred for 16 hrs. The precipitated dicyclohexyl urea was filtered off and the solvents were removed in vacuo. The white residue was redissolved in 250 mL ethyl acetate. The resulting suspension was filtered and the clear filtrate was washed subsequently with an aqueous 10 % (w/w) sodium bicarbonate solution (2 × 20 mL), an aqueous 10% (w/w) citric acid solution (2 × 20 mL), brine (20 mL) and water (20 mL). After drying with Na<sub>2</sub>SO<sub>4</sub> and evaporation of the solvent, the *tert*-butoxycarbonyl protecting group was removed by dissolving the dipeptide in HCl-saturated ethyl acetate. According to TLC (eluent: acetone/CHCl<sub>3</sub>, 1:1, v/v) the starting material was completely consumed after stirring for 10 min. The solvent was evacuated and the excess of HCl was removed by dissolving the product in *tert*-butanol and subsequent evaporation. The resulting L-alanyl-glycine methyl ester HCl salt (3 g, 0.015 mol, 61%) was formylated without further characterization by refluxing in 300 mL ethyl formate in the presence of 4.2 g (0.06 mol) sodium formate for 4 hrs. The volatile parts of the reaction mixture were evaporated and the product was extracted from the residual solid using CH<sub>2</sub>Cl<sub>2</sub> (1 × 75 mL, 2 × 25 mL). Evaporation of the combined CH<sub>2</sub>Cl<sub>2</sub> parts and recrystallization of the product from CH<sub>2</sub>Cl<sub>2</sub>/petroleum-ether (40-60) resulted in 2.7 g (0.014 mol, 96 %) white crystalline **L-FAG**. Overall yield: 58 %. Mp: 112 °C. [ $\alpha$ ]<sub>D</sub> (DMF *c* 2) = -29.1°. <sup>1</sup>H NMR ( $\delta$  ppm, DMSO-D<sub>6</sub>, 300 MHz): 8.40 (t, 1H, NH, *J* = 5.7 Hz), 8.30 (d, 1H, NH, *J* = 7.7 Hz), 7.96 (s, 1H, HCO), 4.38 (m, 1H, CH), 3.82 (dd, 2H, CH, *J* = 5.7 Hz, *J* = 2.8 Hz), 3.61 (s, 3H, OCH<sub>3</sub>), 1.20 (d, 3H, CH<sub>3</sub>, *J* = 7.1 Hz). <sup>13</sup>C NMR ( $\delta$  ppm, DMSO-D<sub>6</sub>, 75 MHz): 172, 170 (C=O), 160.6 (HC=O), 51.7 (CH), 46.4 (OCH<sub>3</sub>), 40.5 (CH<sub>2</sub>), 18.5 (CH<sub>3</sub>). FT-IR (cm<sup>-1</sup>, KBr): 3305 (NH), 1744 (C=O ester), 1657, 1633 (amide I), 1563, 1518 (amide II). EI-MS: *m/z* = 188 [M]<sup>+</sup>, 129 [M - CO<sub>2</sub>CH<sub>3</sub>]<sup>+</sup>. El. Anal. Calcd. for C<sub>7</sub>H<sub>12</sub>N<sub>2</sub>O<sub>4</sub>: C, 44.68; H, 6.43; N, 14.89. Found: C, 44.65; H, 6.46; N, 14.82.

**L-Isocyanoalanyl-L-alanine methyl ester (L,L-IAA).** Under a N<sub>2</sub> atmosphere **L,L-FAA** (9.39 g, 46.5 mmol) was dissolved in 250 ml CH<sub>2</sub>Cl<sub>2</sub>, N-methyl morpholine (10.9 mL, 98.9 mmol) was added and this solution was cooled to -30 °C using acetone/CO<sub>2</sub>. Over a period of 1 h., 2.8 mL (23.2 mmol) diphosgene in 50 mL CH<sub>2</sub>Cl<sub>2</sub> was added dropwise maintaining T = -30 °C. The solution was stirred for an additional 10 min at this temperature and brought to 0 °C. An ice-cold saturated aqueous sodium bicarbonate solution (45 mL) was added and the mixture was stirred vigorously for 5 min. The organic part was separated, extracted once with 25 mL water and dried using Na<sub>2</sub>SO<sub>4</sub>. The solvent was evaporated resulting in a yellow/orange crystalline product. This product was washed with diisopropyl ether until the filtrate was colorless and recrystallized from diethyl ether, yielding **L,L-IAA** in 80% as white needle-like crystals. Mp: 87 °C. [ $\alpha$ ]<sub>D</sub> (CHCl<sub>3</sub>, *c* 0.5) = +33.0°. <sup>1</sup>H NMR ( $\delta$  ppm, CDCl<sub>3</sub>, 300 MHz): 6.91 (br, 1H, NH), 4.57 (m, 1H, NHCHCH<sub>3</sub>), 4.20 (q, 1H, CHCH<sub>3</sub>, *J* = 7.08 Hz), 3.77 (s, 3H, OCH<sub>3</sub>), 1.66 (d, 3H, CHCH<sub>3</sub>, *J* = 7.08 Hz), 1.47 (d, 3H, NHCHCH<sub>3</sub>, *J* = 7.20 Hz). <sup>13</sup>C NMR ( $\delta$  ppm, CDCl<sub>3</sub>, 75 MHz): 173.2, 166.3 (C=O), 162.0 (CN), 53.9 (CH), 53.4 (OCH<sub>3</sub>), 49.2 (CH), 20.3, 18.7 (CH<sub>3</sub>). FT-IR (cm<sup>-1</sup>, KBr): 3279 (NH), 2158 + 2147 (CN), 1743 (C=O ester), 1669 (amide I), 1559 (amide II). EI-MS: *m/z* = 184 [M]<sup>+</sup>,



153 [M - OCH<sub>3</sub>]<sup>+</sup>, 125 [M - CO<sub>2</sub>CH<sub>3</sub>]<sup>+</sup>, 102 [M - CH(CH<sub>3</sub>)CO<sub>2</sub>CH<sub>3</sub>]<sup>+</sup>. El. Anal. Calcd. for C<sub>8</sub>H<sub>12</sub>N<sub>2</sub>O<sub>3</sub>: C, 52.17; H, 6.57; N, 15.21. Found: C, 52.28; H, 6.57; N, 14.96.

**D-Isocyanoalanyl-D-alanine methyl ester (D,D-IAA).** Starting from **D,D-FAA** this compound was synthesized as described for **L,L-IAA**. Due to the instable nature of the product a large quantity of the product was lost during the recrystallization process (yield < 10%). Mp: 84 °C. [α]<sub>D</sub> (CHCl<sub>3</sub>, c 0.5) = -32.0°. <sup>1</sup>H NMR (δ ppm, CDCl<sub>3</sub>, 300 MHz): δ = 6.90 (br, 1H, NH), 4.57 (m, 1H, NHCH<sub>2</sub>CH<sub>3</sub>), 4.26 (q, 1H, CH<sub>2</sub>CH<sub>3</sub>, J = 7.08 Hz), 3.79 (s, 3H, OCH<sub>3</sub>), 1.67 (d, 3H, CHCH<sub>3</sub>, J = 7.08 Hz), 1.48 (d, 3H, NHCHCH<sub>3</sub>, J = 7.19 Hz). <sup>13</sup>C NMR (δ ppm, CDCl<sub>3</sub>, 75 MHz): 173.2, 166.3 (C=O), 162.1 (CN), 53.9 (CH), 53.4 (OCH<sub>3</sub>), 49.2 (CH), 20.3, 18.7 (CH<sub>3</sub>). FT-IR (cm<sup>-1</sup>, KBr): ν = 3279 (NH), 2159 + 2148 (CN), 1743 (C=O ester), 1669 (amide I), 1569 (amide II). EI-MS: m/z = 184 [M]<sup>+</sup>, 153 [M - OCH<sub>3</sub>]<sup>+</sup>, 125 [M - CO<sub>2</sub>CH<sub>3</sub>]<sup>+</sup>, 102 [M - CH(CH<sub>3</sub>)CO<sub>2</sub>CH<sub>3</sub>]<sup>+</sup>. El. Anal. Calcd. for C<sub>8</sub>H<sub>12</sub>N<sub>2</sub>O<sub>3</sub>: C, 52.17; H, 6.57; N, 15.21. Found: C, 52.34; H, 6.45; N, 15.21.

**L-Isocyanoalanyl-D-alanine methyl ester (L,D-IAA).** Using the same procedure as for **L,L-IAA**, **L,D-IAA** was obtained in 60 % yield. Due to the instability of this isocyanide in solution purification by recrystallization was not possible, however, after repeated washing with diisopropyl ether the desired product was obtained with satisfactory purity. Mp: 98 °C (dec.). [α]<sub>D</sub> (CHCl<sub>3</sub>, c 1.5) = -5.6°. <sup>1</sup>H NMR (δ ppm, CDCl<sub>3</sub>, 300 MHz): 6.97 (br, 1H, NH), 4.57 (m, 1H, NHCH<sub>2</sub>CH<sub>3</sub>), 4.29 (q, 1H, CH<sub>2</sub>CH<sub>3</sub>, J = 7.09 Hz), 3.77 (s, 3H, OCH<sub>3</sub>), 1.67 (d, 3H, CHCH<sub>3</sub>, J = 7.09 Hz), 1.48 (d, 3H, NHCHCH<sub>3</sub>, J = 7.19 Hz). <sup>13</sup>C NMR (δ ppm, CDCl<sub>3</sub>, 75 MHz): 173.1, 166.4 (C=O), 162 (CN), 54.0 (CH), 53.4 (OCH<sub>3</sub>), 49.1 (CH), 20.3, 18.6 (CH<sub>3</sub>). FT-IR (cm<sup>-1</sup>, KBr): 3304 (NH), 2156 + 2144 (CN), 1757 (C=O ester), 1668 (amide I), 1560 (amide II). EI-MS: m/z = 184 [M]<sup>+</sup>, 153 [M - OCH<sub>3</sub>]<sup>+</sup>, 125 [M - CO<sub>2</sub>CH<sub>3</sub>]<sup>+</sup>, 102 [M - CH(CH<sub>3</sub>)CO<sub>2</sub>CH<sub>3</sub>]<sup>+</sup>. El. Anal. Calcd. for C<sub>8</sub>H<sub>12</sub>N<sub>2</sub>O<sub>3</sub>: C, 52.17; H, 6.57; N, 15.21. Found: C, 51.93; H, 6.67; N, 14.75.

**Isocyanoglycyl-L-alanine methyl ester (L-IGA).** Following the same procedure as for **L,L-IAA**, **L-IGA** was obtained from 0.6 g (3.20 mmol) **L-FGA** as a white crystalline material in 76 % yield. Mp: 61 °C. [α]<sub>D</sub> (CHCl<sub>3</sub>, c 0.3) = 19.2°. <sup>1</sup>H NMR (δ ppm, CDCl<sub>3</sub>, 300 MHz): 6.94 (br, 1H, NH), 4.61 (qn, 1H, CH, J = 7.2 Hz), 4.20 (s, 2H, CH<sub>2</sub>), 3.79 (s, 3H, OCH<sub>3</sub>), 1.46 (d, 3H, CH<sub>3</sub>, J = 7.2 Hz). <sup>13</sup>C NMR (δ ppm, CDCl<sub>3</sub>, 75 MHz): 173.1, 166.4 (C=O), 162.6 (CN), 53.5 (OCH<sub>3</sub>), 49.2 (CH), 45.8 (CH<sub>2</sub>), 18.8 (CH<sub>3</sub>). FT-IR (cm<sup>-1</sup>, KBr): 3306 (NH), 2164 (CN), 1740 (C=O ester), 1659 (amide I), 1560 (amide II). EI-MS: m/z = 170 [M]<sup>+</sup>, 111 [M - CO<sub>2</sub>CH<sub>3</sub>]<sup>+</sup>. El. Anal. Calcd. for C<sub>7</sub>H<sub>10</sub>N<sub>2</sub>O<sub>3</sub>: C, 49.41; H, 5.92; N, 16.46. Found: C, 49.15; H, 5.77; N, 16.12.

**L-Isocyanoalanyl-glycine methyl ester (L-IAG).** Starting from 105 mg (0.56 mmol) **L-FAG**, **L-IAG** was prepared following a similar procedure as for **L,L-IAA**, with the exception that in this case the product was purified using column chromatography (eluent: acetone/CHCl<sub>3</sub> 1:4 v/v) and subsequently recrystallized. Yield 58 mg (0.34 mmol, 61 %) of sticky white crystals. Mp: 68 - 71 °C. [α]<sub>D</sub> (CH<sub>2</sub>Cl<sub>2</sub>, c 0.4) = 5.7°. <sup>1</sup>H NMR (δ ppm, CDCl<sub>3</sub>, 300 MHz): 6.95 (br, 1H, NH), 4.31 (q, 1H, CH, J = 7.2 Hz), 4.08 (d, 2H, CH<sub>2</sub>, J = 5.3 Hz), 3.80 (s, 3H, OCH<sub>3</sub>), 1.67 (d, 3H, CH<sub>3</sub>, J = 7.2 Hz). <sup>13</sup>C NMR (δ ppm, CDCl<sub>3</sub>, 75

MHz): 170.1, 166.3 (C=O), 162.0 (CN), 53.9 (CH), 53.3 (OCH<sub>3</sub>), 42.1 (CH<sub>2</sub>), 20.4 (CH<sub>3</sub>). FT-IR (cm<sup>-1</sup>, KBr): 3302 (NH), 2158 (CN), 1748 (C=O ester), 1674 (amide I), 1564 (amide II).

**Poly(L-isocyanoalanyl-L-alanine methyl ester) (L,L-PIAA).** To 0.26 g (1.41 mmol) L-isocyanoalanyl-L-alanine methyl ester (**L,L-IAA**) in 13 ml CH<sub>2</sub>Cl<sub>2</sub> was added, while stirring, 17.5 mg (0.048 mmol) Ni(ClO<sub>4</sub>)<sub>2</sub>·(H<sub>2</sub>O)<sub>6</sub> in 13.4 ml CH<sub>2</sub>Cl<sub>2</sub> and 0.14 ml ethanol (abs.). The solution turned red/brown immediately and IR showed complete consumption of the isocyanide in a few min. After 5 min. the solvents were evaporated and the resulting glassy solid was redissolved in a minimal amount of CHCl<sub>3</sub>. The polymer was precipitated by dropping this solution in 50 ml of methanol/water (3/1 v/v) under vigorous stirring. The product was filtered off and washed with methanol/water (3/1) until the filtrate remained colorless and than once with methanol. Drying in vacuo gave the polymer in 88% yield as an off-white powder.  $[\alpha]_D$  (CHCl<sub>3</sub>, *c* 0.34) = +338°. <sup>1</sup>H NMR (δ ppm, CDCl<sub>3</sub>, 300 MHz): 9.45 (br, 1H, NH), 9.18 (br, 1H, NH), 5.4 – 4.0 (br, 2H, CH), 3.63 (s, 3H, OCH<sub>3</sub>), 3.60 (s, 3H, OCH<sub>3</sub>), 1.8 – 1.1 (br, 6H, CH<sub>3</sub>). FT-IR (cm<sup>-1</sup>, KBr): 3276 (NH), 1752 (C=O ester), 1657 (amide I), 1618 (C=N), 1530 (amide II). El. Anal. Calcd. for C<sub>8</sub>H<sub>12</sub>N<sub>2</sub>O<sub>3</sub>: C, 52.17; H, 6.57; N, 15.21. Found: C, 52.20; H, 6.60; N, 14.94.

**Poly(D-isocyanoalanyl-D-alanine methyl ester) (D,D-PIAA).** This polymer was prepared under identical conditions as **L,L-PIAA** from D-isocyanoalanyl-D-alanine methyl ester (**D,D-IAA**), resulting in an off-white powder (yield 70 %).  $[\alpha]_D$  (CHCl<sub>3</sub>, *c* 0.24) = -349°. <sup>1</sup>H NMR (δ ppm, CDCl<sub>3</sub>, 300 MHz): 9.44 (br, 1H, NH), 9.16 (br, 1H, NH), 5.5 – 4.0 (br, 2H, CH), 3.63 (s, 3H, OCH<sub>3</sub>), 3.59 (s, 3H, OCH<sub>3</sub>), 1.8 – 1.0 (br, 6H, CH<sub>3</sub>). FT-IR (cm<sup>-1</sup>, KBr): 3275 (NH), 1752 (C=O ester), 1656 (amide I), 1617 (C=N), 1531 (amide II). El. Anal. Calcd. for C<sub>8</sub>H<sub>12</sub>N<sub>2</sub>O<sub>3</sub>: C, 52.17; H, 6.57; N, 15.21. Found: C, 52.12; H, 6.59; N, 14.90.

**Poly(L-isocyanoalanyl-D-alanine methyl ester) (L,D-PIAA).** This polymer was prepared under identical conditions as **L,L-PIAA** from L-isocyanoalanyl-D-alanine methyl ester (**L,D-IAA**), resulting in an off-white fibrous film (yield 87 %).  $[\alpha]_D$  (CHCl<sub>3</sub>, *c* 0.58) = 487°. <sup>1</sup>H NMR (δ ppm, CDCl<sub>3</sub>, 300 MHz): 9.4 (br, 1H, NH), 5.6 – 4.2 (br, 2H, CH), 3.6 (s, 3H, OCH<sub>3</sub>), 1.9 – 0.9 (br, 6H, CH<sub>3</sub>). FT-IR (cm<sup>-1</sup>, KBr): 3280 (NH), 1752 (C=O ester), 1659 (amide I), 1618 (C=N), 1530 (amide II). El. Anal. Calcd. for C<sub>8</sub>H<sub>12</sub>N<sub>2</sub>O<sub>3</sub>: C, 52.17; H, 6.57; N, 15.21. Found: C, 51.91; H, 6.51; N, 14.72.

**Poly(isocyanoglycyl-L-alanine methyl ester) (L -PIGA).** Using the same conditions as for the polymerization of **L,L-IAA**, **L-PIGA** was prepared from 101 mg (0.6 mmol) **L-IGA** in 85% yield.  $[\alpha]_D$  (CHCl<sub>3</sub>, *c* 0.08) = +196°. <sup>1</sup>H NMR (δ ppm, CDCl<sub>3</sub>, 300 MHz): 9.1 (br, 1H, NH), 4.8 – 3.9 (br, 1H, CH), 3.7 (s, 3H, OCH<sub>3</sub>), 3.7 – 3.4 (br, 2H, CH<sub>2</sub>), 1.9 – 1.0 (br, 3H, CH<sub>3</sub>). FT-IR (cm<sup>-1</sup>, KBr): 3293 (NH), 1751 (C=O ester), 1654 (amide I), 1616 (C=N), 1538 (amide II).

**Poly(L-isocyanoalanyl-glycine methyl ester) (L-PIAG).** Using the same conditions as for the polymerization of **L,L-IAA**, **L-PIAG** was prepared from 28 mg (0.16 mmol) **L-IAG** in 73% yield.  $[\alpha]_D$  (CHCl<sub>3</sub>, *c* 0.02) = -32°. <sup>1</sup>H NMR (δ ppm, CDCl<sub>3</sub>, 300 MHz): 8.2 (br, 1H, NH), 4.6 – 3.8 (br, 1H, CH),

3.7 (s, 3H, OCH<sub>3</sub>), 3.7 – 3.4 (br, 2H, CH<sub>2</sub>), 1.8 – 1.1 (br, 3H, CH<sub>3</sub>). FT-IR (cm<sup>-1</sup>, KBr): 3380, 3304 (NH), 1755 (C=O ester), 1665 (amide I), 1619 (C=N), 1530 (amide II).

## 2.5 References and Notes

- 1 Nolte, R. J. M. *Chem. Soc. Rev.* **1994**, 23, 11.
- 2 Van der Eijk, J. M., Nolte, R. J. M., Drenth, W., Hezemans, A. M. F. *Macromolecules* **1980**, 13, 1391.
- 3 Visser, H. G. J., Nolte, R. J. M., Zwikker, J. W., Drenth, W. *J. Org. Chem.* **1985**, 50, 3138.
- 4 a) Cornelissen, J. J. L. M.; Donners, J. J. J. M.; de Gelder, R.; Graswinckel, W. S.; Rowan, A. E.; Sommerdijk, N. A. J. M.; Nolte, R. J. M. *Science* **2001**, 293, 676. b) Chapter 3 of this thesis.
- 5 Ugi, I. In *Isonitrile Chemistry*; Academic Press: New York, 1971.
- 6 Skorna, G., Ugi, I. *Angew. Chem.* **1977**, 89, 267.
- 7 Spek, A. L. *PLUTON. A program for plotting molecular and crystal structures*. University of Utrecht, Utrecht, the Netherlands, 1995.
- 8 Green, M. M., Gross, R. A., Schilling, F. C., Zero, K., Crosby III, C. *Macromolecules* **1988**, 21, 1839.
- 9 Ando, I., Kuroki, S. In *Encyclopedia of Nuclear Magnetic Resonance*, Volume 3; J. Wiley & Sons Ltd.; Chichester, 1996, pp 4458.
- 10 Vlietstra, E. J., Nolte, R. J. M., Zwikker, J. W., Drenth, W., Jansen, R. H. A. M. *Recl. Trav. Chim. Pays-Bas* **1982**, 101, 183.
- 11 Cornelissen, J. J. L. M., Fischer, M., Sommerdijk, N. A. J. M., Nolte, R. J. M. *Science* **1998**, 280, 1427.
- 12 Schmidt-Rohr, K.; Clauss, J.; Spiess, H. W. *Macromolecules* **1992**, 25, 3273.
- 13 Millich, F. *J. Polym. Sci. Macromol. Rev.* **1980**, 15, 207.
- 14 van Beijen, A. J. M., Nolte, R. J. M., Drenth, W., Hezemans, A. M. F., van de Coolwijk, P. J. F. M. *Macromolecules* **1980**, 13, 1386.
- 15 Prokhorova, S. A., Sheiko, S. S., Möller, M., Ahn, C.-H., Percec, V. *Macromol. Rapid Commun.* **1998**, 19, 359.
- 16 Burum, D. P. In *Encyclopedia of Nuclear Magnetic Resonance*, Volume 3; J. Wiley & Sons Ltd.; Chichester, 1996, pp 1535.
- 17 North, A.C.T.; Philips, D.C.; Mathews, F.S. *Acta Crystallogr.* **1968**, A24, 351.
- 18 Gelder, R. de; Graaff, R.A.G. de; Schenk, H. *Acta Crystallogr.* **1993**, A49, 287.
- 19 Sheldrick, G.M. SHELXL-97. Program for the refinement of crystal structures; University of Göttingen: Germany, 1997.
- 20 Sheenan, J. C., Yang, D.-D. H., *J. Am. Chem. Soc.* **1958**, 80, 1154.
- 21 Brenner, M., Huber, W., *Helv. Chim. Acta*, **1953**, 26, 1109.

# CHAPTER 3

## Conformational Analysis of Dipeptide Derived Polyisocyanides

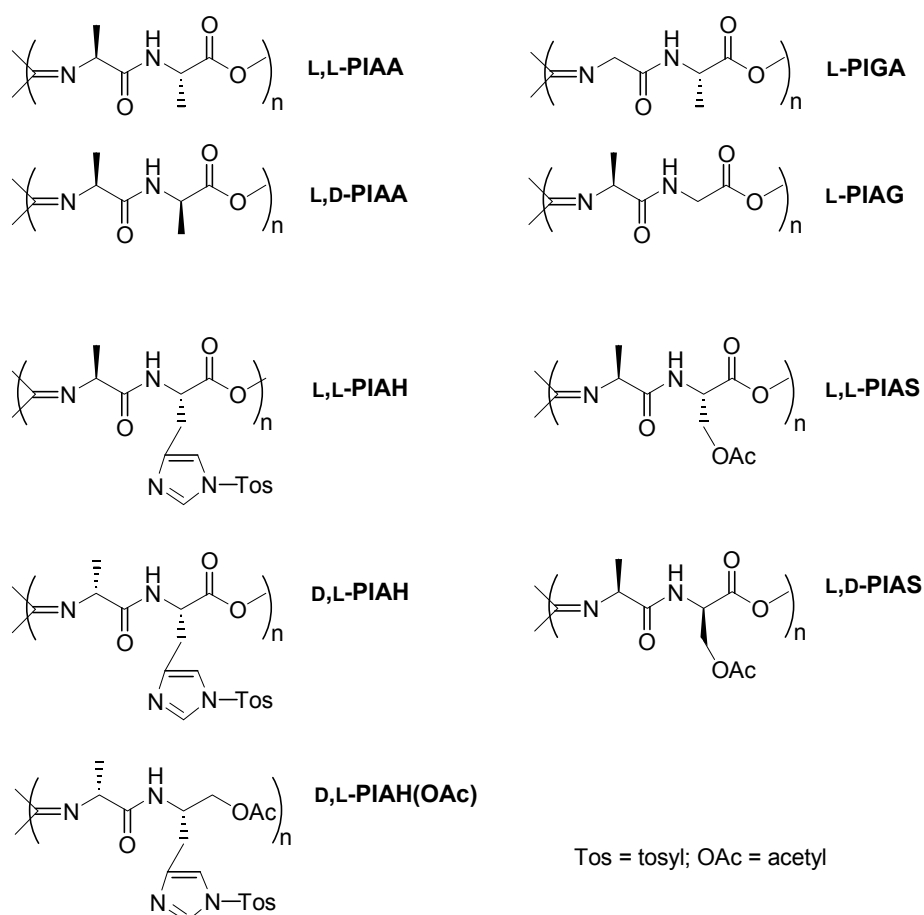
### 3.1 Introduction

The function of biopolymers, such as proteins, RNA and DNA, is strongly related to their folding patterns. Similar correlations between the physical properties of macromolecules and the conformations of their macromolecular chains have been found in the field of synthetic polymers.<sup>1</sup> One of the important structural motifs in biomacromolecules is the helical architecture which recently has also gained considerable interest in relation to the controlled structuring of synthetic macromolecules, e.g. polymers of isocyanides and isocyanates.<sup>2</sup>

Based on molecular models Millich proposed a  $4_1$  helical conformation for the main chain in polyisocyanides.<sup>3</sup> Experimental evidence for this structure was first provided by Nolte and Drenth; using chromatography they were able to resolve the polymer of achiral *tert.*-butyl isocyanide into the two optical antipodes.<sup>4</sup> The optical activity in this case is solely originating from the conformation of the polyisocyanide backbone, which was stable even at elevated temperatures. By applying Ni(II) as a catalyst a vast amount of polyisocyanides was prepared, utilizing different approaches to create an excess of either left- or right-handed helices.<sup>5</sup>

The conformation of polyisocyanides with sterically less demanding side chains than present in poly(*tert.*-butyl isocyanide), however, is still under debate. Computational studies<sup>6</sup> have indicated that the  $4_1$  helix, in particular when bulky substituents are present, is the most favorable conformation. More recently this conformation was recognized as a local minimum, whereas the so-called *syndio*

conformation was considered to be the absolute minimum.<sup>7</sup> Experimental investigations towards the conformation of polyisocyanides are limited. Green and coworkers<sup>8</sup> showed that sterically unencumbered polyisocyanides have a limited persistence length of  $\sim 3$  nm. In the case of polyphenylisocyanide a combination of GPC, light scattering and X-ray diffraction revealed that the native polyisocyanide has rigid rod character, but that the polymer slowly precipitates from solution as a random coil. These data suggest that the helix inversion barrier in polyphenylisocyanide is not sufficiently high to create a stable helical conformation at room temperature, and that as a result of the *merry-go-round mechanism*<sup>5</sup> the  $4_1$  helix is initially formed as the kinetic product.<sup>9</sup>



In many biopolymers a combination of (non-covalent) interactions is required to maintain a stable secondary structure in solution. In the field of helical polymers examples of the combined use of such interactions are rare and in the reported cases mainly steric interactions have been used to realize a high helix inversion barrier. In this Chapter conformational studies on polyisocyanides derived from alanine-alanine and alanine-glycine based dipeptides<sup>10</sup> are reported. Attention is focussed on the

formation of well-defined hydrogen bonded arrays between the side chains to stabilize the helix structure of the polymers. Polyisocyanopeptides derived from alanine-serine<sup>11</sup> and alanine-histidine<sup>12,13</sup> have been prepared in the past but the precise structures of these polymers were not elucidated. In this Chapter the properties of these polymers are revisited in the light of the possible formation of extended arrays of hydrogen bonds.

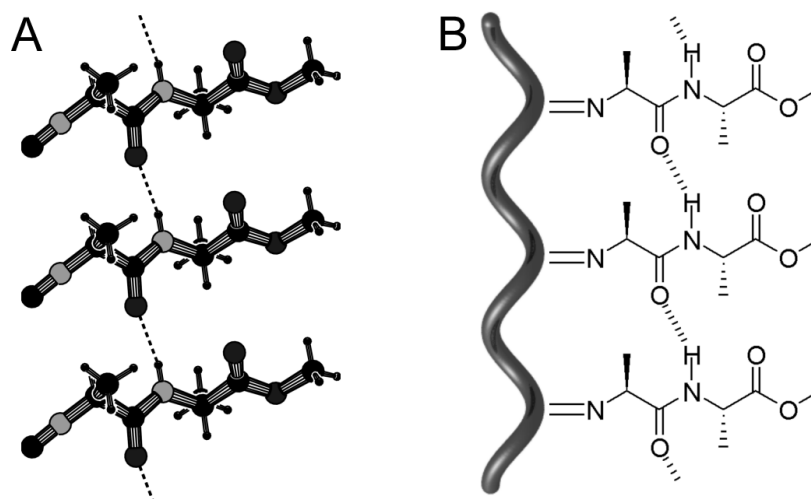


**Figure 1** (A) Single crystal X-ray structure of *L,L*-IAA showing three stacked molecules and the intramolecular hydrogen bonds. (B) Schematic representation of the hydrogen bonding arrays between the side chains in *L,L*-PIAA.

## 3.2 Results and Discussion

### 3.2.1 Side chain hydrogen bonding

The conformational properties of polyisocyanides reported to date are largely determined by steric interactions between usually bulky side groups.<sup>5</sup> In the case of the polymers derived from L-alanyl-L-alanine (*L,L*-PIAA) and glycyl-L-alanine (*L*-PIGA) and L-alanyl-glycine (*L*-PIAG) dipeptides, NMR and IR spectroscopic investigations indicated that hydrogen bonds are present between the amide groups in the side chains.<sup>10</sup> The single crystal X-ray structure of L-isocyanoalanyl-L-alanine methyl ester (*L,L*-IAA) was used as a reference point in these studies (Figure 1).<sup>10</sup> For this monomer the presence of the hydrogen bonding array resulted in a characteristic N-H stretching vibration in the solid state IR spectrum ( $\nu_{\text{NH}} = 3279 \text{ cm}^{-1}$ ), whereas no hydrogen bonding was observed in chloroform solution. The IR spectra of the polymers all

showed N-H stretching vibrations in the range of 3260 to 3300  $\text{cm}^{-1}$ , both in solution and in the solid state, implying that they possess a structure in which the side chains have a hydrogen bonding arrangement similar to that found in the crystal structure of **L,L-IAA** and that this arrangement is preserved in solution. Further confirmation of the presence of hydrogen bonds came from  $^1\text{H}$  NMR spectra. All the resonances assigned to the amide protons of the isocyanopeptides were significantly shifted downfield by 1.5 – 2.5 ppm upon polymerization, indicative of very strong hydrogen bonding.<sup>10</sup> In neither the IR nor the NMR spectra any signals were detected corresponding to amide groups not participating in hydrogen bonds.

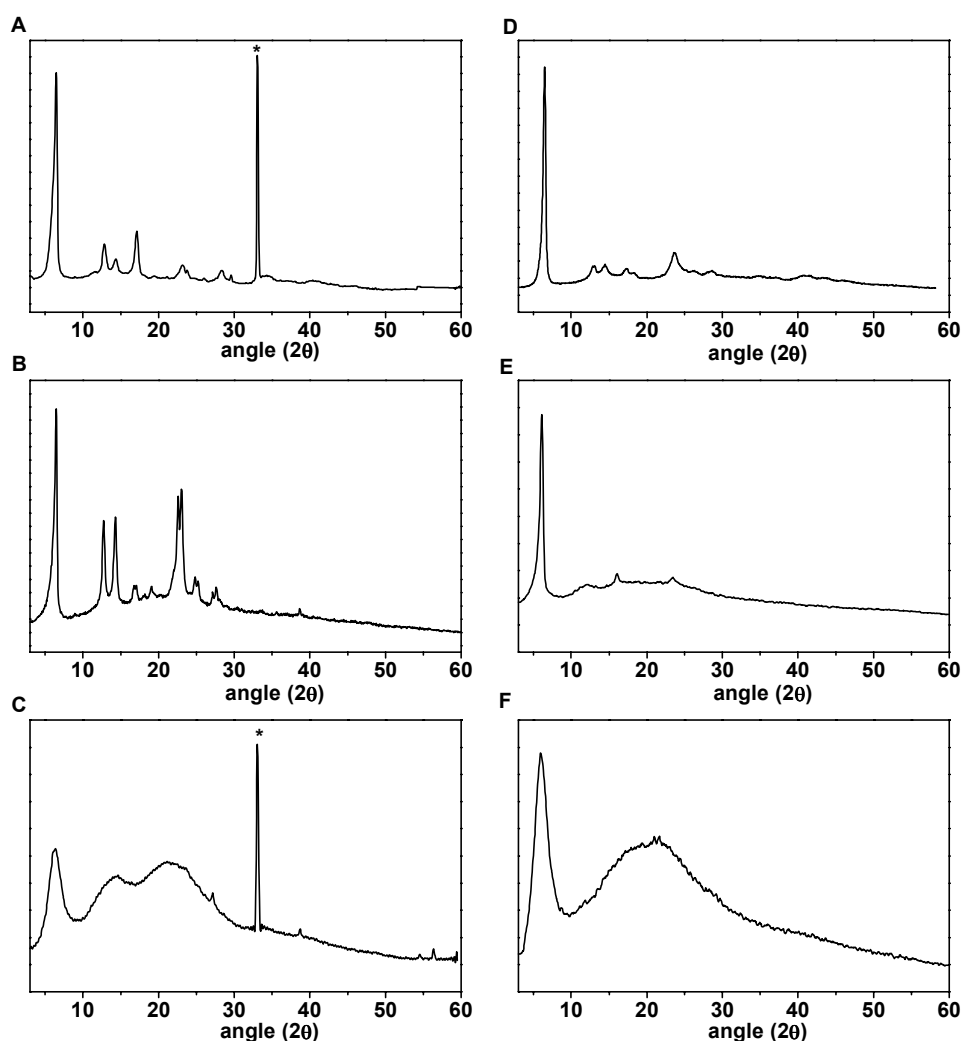


**Figure 2** Powder X-ray diffraction patterns of (A) *L,L*-PIAA as cast film; (B) *L,L*-PIAA as powder; (C) *L,L*-PIAA as cast film after treatment with TFA; (D) *L,D*-PIAA as cast film; (E) *L*-PIGA as cast film; (F) *L*-PIGA as cast film after heating the polymer at 60 °C during 1 hour in  $\text{CHCl}_3$ .

**Powder X-ray diffraction measurements.** The dimensions of the macromolecular rods in the solid state were determined by powder X-ray diffraction (PXRD); **L,L-PIAA**, **L,D-PIAA** and **L-PIGA** were investigated as representative models for the polyisocyanopeptides discussed in this chapter. Diffraction patterns displaying sharp signals were observed (Figure 2),<sup>9</sup> which point to a regular crystallization of well-defined macromolecular rods.<sup>14</sup> Local ordering of the rods and the presence of solvent molecules possibly explain the observed differences in intensities and widths of some signals when the samples were measured as a powder or as a cast film from  $\text{CHCl}_3$  solution. Diameters were calculated from the diffraction patterns obtained from both types of specimen. Several crystallographic descriptions can be distinguished based on the organization of the polymeric rods. The measured reflections gave the best fit with an orthorhombic arrangement of the polymers (see Experimental Section), from which the macromolecular diameters could be derived. These diameters amounted to 15.9 Å for both **L,L-PIAA** and **L,D-PIAA** and 16.6 Å for **L-PIGA**.

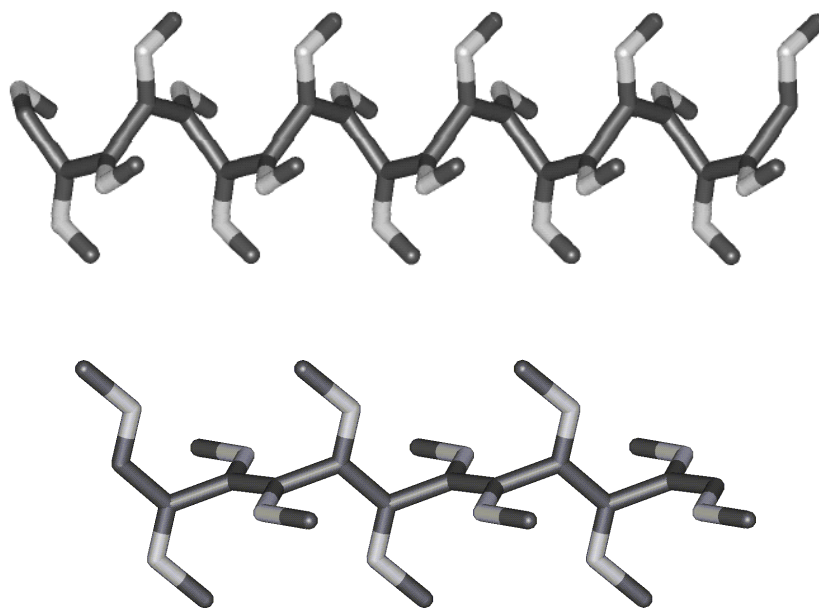


**Figure 3** Modeled structures of the  $4_1$  helical conformation of a 20 residue polyisocyanide (top) and the syndio conformation of a 12 residue polyisocyanide.

**Model calculations.** Two different macromolecular conformations have been proposed for polyisocyanides,<sup>5</sup> the  $4_1$  helix<sup>3-6</sup> and the so-called *syndio* conformation. Clericuzio *et al.*<sup>7</sup> calculated that the latter conformation is thermodynamically more favorable. In the *syndio* conformation two adjacent imine groups are in one plane, which makes an angle



of  $\sim 90^\circ$  with the plane of the next two imines (Figure 3). For both the  $4_1$  helix and the *syndio* structure model calculations were carried out to determine the distance between the side chains that are more or less on top of each other. The spacing between the amide groups in the crystal structure of **L,L-IAA** is 4.728 Å (Figure 1A). Calculations on the *syndio* model revealed an average spacing between side chains  $n$  and  $(n + 4)$  of 5.5 Å, which is too large for the formation of defined hydrogen bonds. Decreasing this distance is difficult to achieve without losing the *syndio* conformation: the adjacent imine groups are in conjugation and, therefore, have to retain at an N-C-C-N dihedral angle close to  $180^\circ$ .

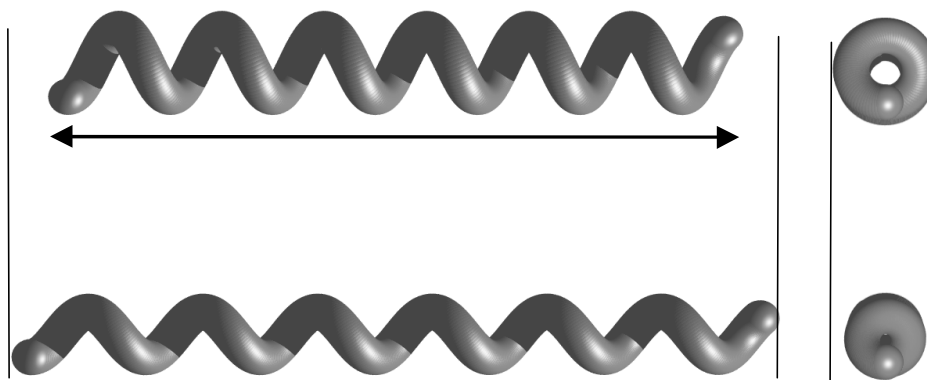


**Figure 4** Schematic representation of the relationship between the relative length and the diameter of a helical system.

In the case of the  $4_1$  helix for both **L,L-PIAA** and **L,D-PIAA** a pitch of 4.2 Å was calculated, in good agreement with previous reports.<sup>5,6</sup> This distance, however, is significantly smaller than the optimal span for hydrogen bond formation between the amide groups in side chains  $n$  and  $(n + 4)$ . The  $4_1$  helical conformation, however, can be regarded as a spring. Extension or compression of this ‘polymeric spring’, elongates or shortens the polymer backbone and consequently narrows or widens its diameter (Figure 4). Applying this procedure to **L,L-PIAA** and **L,D-PIAA** resulted for both polymers in macromolecular rods with a calculated diameter of 15.8 - 15.9 Å, a helical pitch of 4.6 Å, and an average spacing between the side chains  $n$  and  $(n + 4)$  of 4.7 Å. These calculated diameters are in excellent agreement with those determined experimentally using PXRD (i.e. 15.9 Å, see above). Strictly speaking the polymer no

longer has a  $4_1$  helical conformation, but a  $39_{10}$  helix is obtained in this way. For simplicity, however, in the following sections we will refer to this model as the (extended)  $4_1$  helix. Using basis sets for **L,L-PIAA** and **L,D-PIAA** the diameter of **L-PIGA** was calculated to be 16.3 – 16.5 Å; a value of 16.6 Å was determined by PXRD (see above).

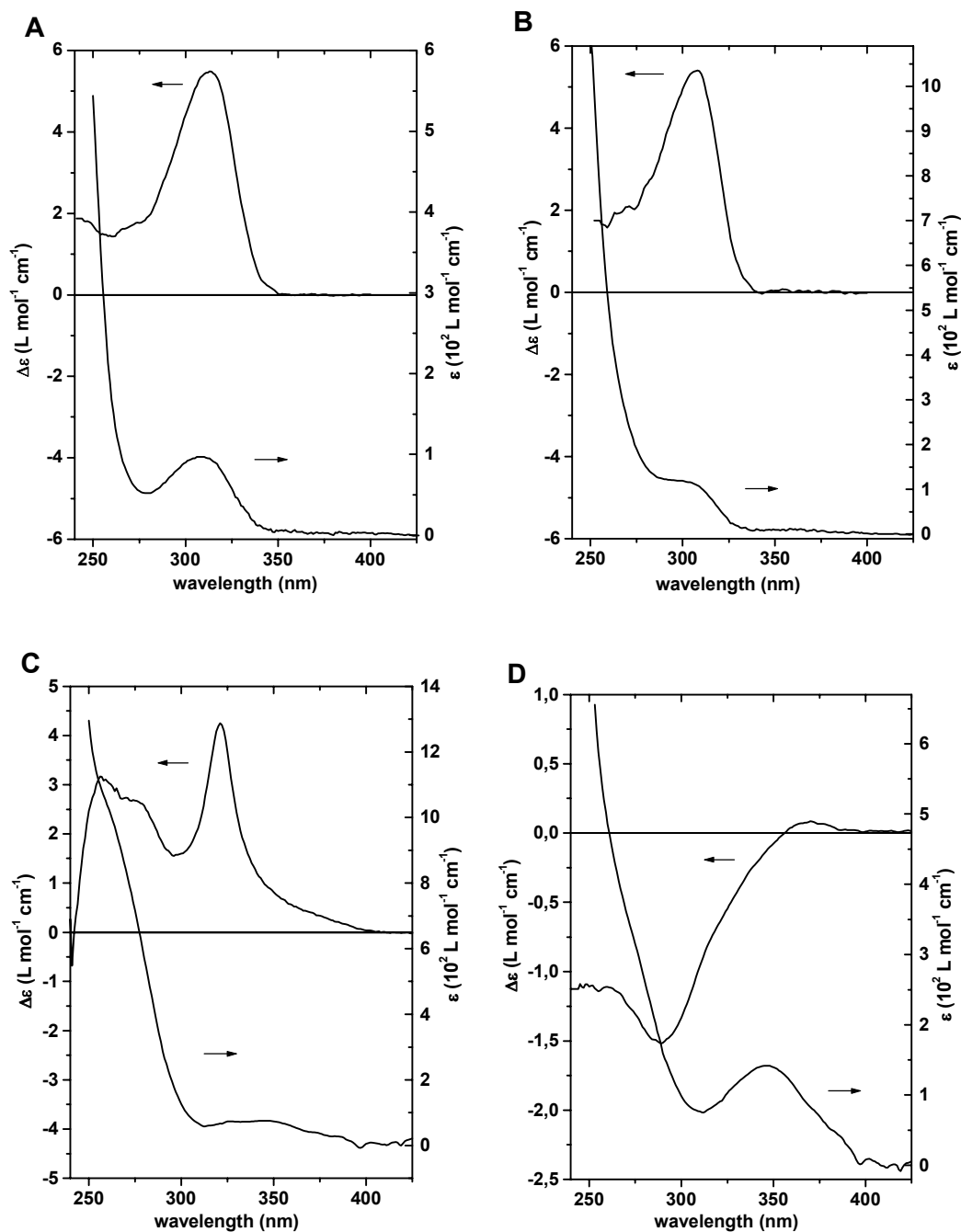


**Figure 5** CD and UV/vis spectra in  $\text{CHCl}_3$  of (A) **L,L-PIAA**, (B) **L,D-PIAA**, (C) **L-PIGA** and (D) **L-PIAG**.

**Circular dichroism spectroscopy.** From the IR and  $^1\text{H}$  NMR spectroscopic investigations it was concluded that the hydrogen bonding arrangement of the side chains in the polymers is preserved in solution (*see above*).<sup>10</sup> It is therefore expected that the helical conformation of the polyisocyanopeptides in the solid state can be translated directly to the properties of the polymers in solution. Because optically pure monomers were used, an excess of one particular helix type was obtained, which allowed CD spectroscopic<sup>15</sup> structural investigations to be carried out, monitoring the  $n\text{-}\pi^*$  transitions of the backbone imine functions residing in the wavelength range from 250 to 350 nm. UV/vis spectra and the corresponding CD spectra of the polyisocyanopeptides discussed in this Chapter as well as spectra taken from the literature<sup>11-13</sup> are displayed in Figures 5 and 6. Two types of CD spectra can be distinguished: (i) spectra displaying a single strong Cotton effect centered around 315 nm and (ii) spectra featuring a couplet with a smaller intensity. It appears that the former type is observed for the polyisocyanodipeptides in which the hydrogen bonding arrays between side chains  $n$  and  $(n + 4)$  are present, *i. e.* **L-PIGA**, **L,L-** and **L,D-PIAA**. In the case of **L-PIAG** which has no well-defined hydrogen bonding arrays, the second type of spectrum is observed. Also in the case of the polyisocyanodipeptides previously reported in the literature this division into two classes can be probably made.

The differences between the spectra reported here and the ones obtained for aliphatic polyisocyanides either experimentally<sup>5</sup> by or calculations<sup>7,15</sup> can be attributed to an effect of the side chains on the  $n\text{-}\pi^*$  transitions of the  $\text{C}=\text{N}$  chromophores. The well-defined arrangement of the amide groups as a result of the hydrogen bonding arrays, is tentatively regarded as being the major component of this effect of the side chains. Due to the hydrogen bonds the amide carbonyls in a particular array all point in the same direction (Figure 1). This will locally result in the formation of a large permanent dipole, which will strongly influence the  $n\text{-}\pi^*$  transitions of the nearby imine groups. Although the electronic transitions of the amide functionalities cannot be directly seen because they are masked by the solvent, the ordering of these amides is reflected in the imine  $n\text{-}\pi^*$  transitions. This opens the possibility to study these hydrogen bonding arrays by using the imine groups as ‘spectator’ groups.

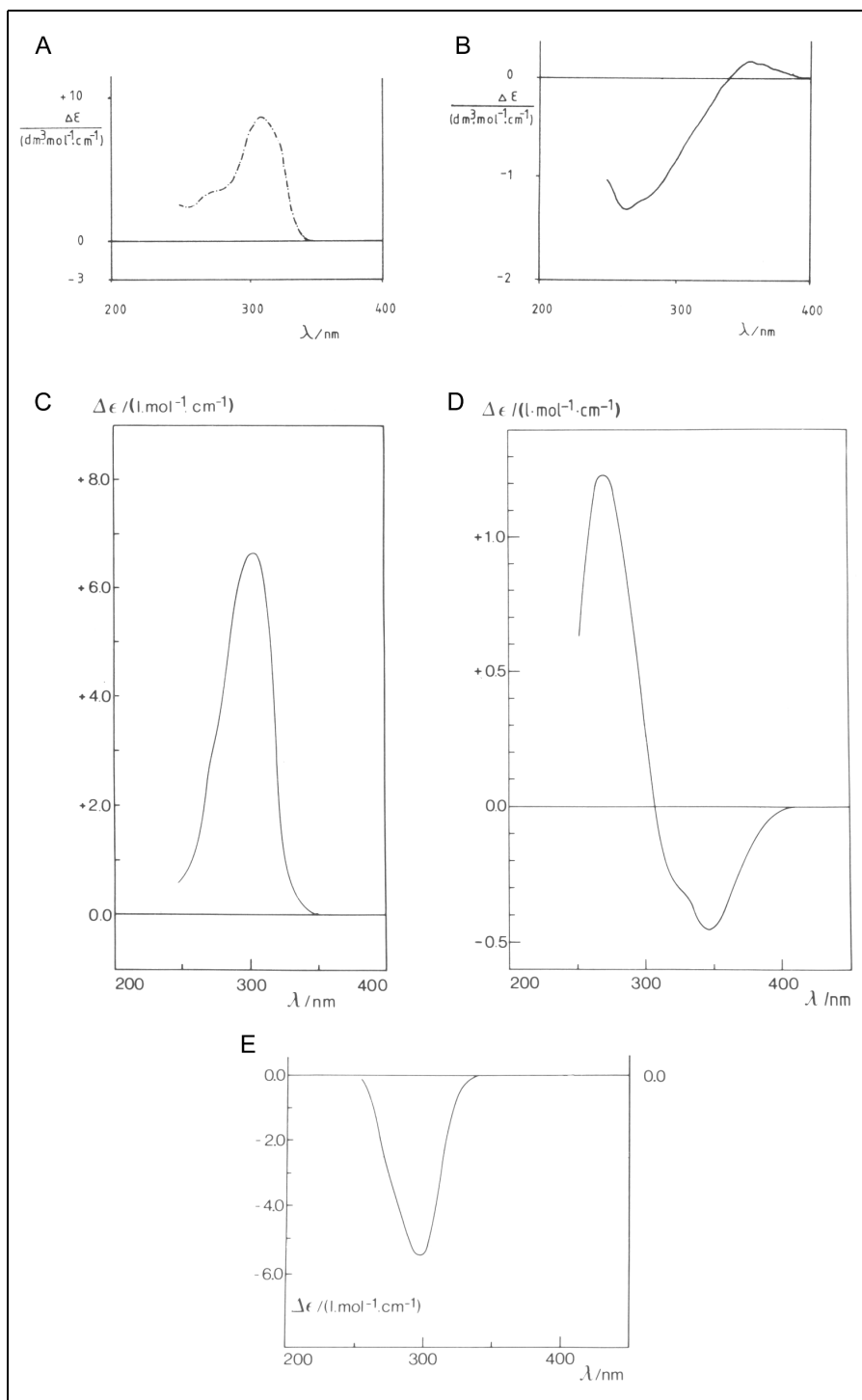


**Figure 6** CD spectra of (A) poly(L-isocyanoalanyl-L-serine methyl ester) (**L,L-PIAS**),<sup>12</sup> (B) **L,D-PIAS**,<sup>12</sup> (C) poly(L-isocyanoalanyl-L-histidine methyl ester) (**L,L-PIAH**),<sup>11</sup> (D) **D,L-PIAH**,<sup>11</sup> (E) poly(L-isocyanoalanyl-L-O-acetyl histidinol) (**D,L-PIAH(OAc)**).<sup>13</sup> For the measuring conditions see the references cited.

### 3.2.2 Unfolding of the secondary structure

It should be possible to disrupt the well-defined hydrogen bonding arrays in the polyisocyanopeptides in a manner analogous to the denaturation of proteins. This would lead to a distinct change in the secondary structure and properties of these polymers.

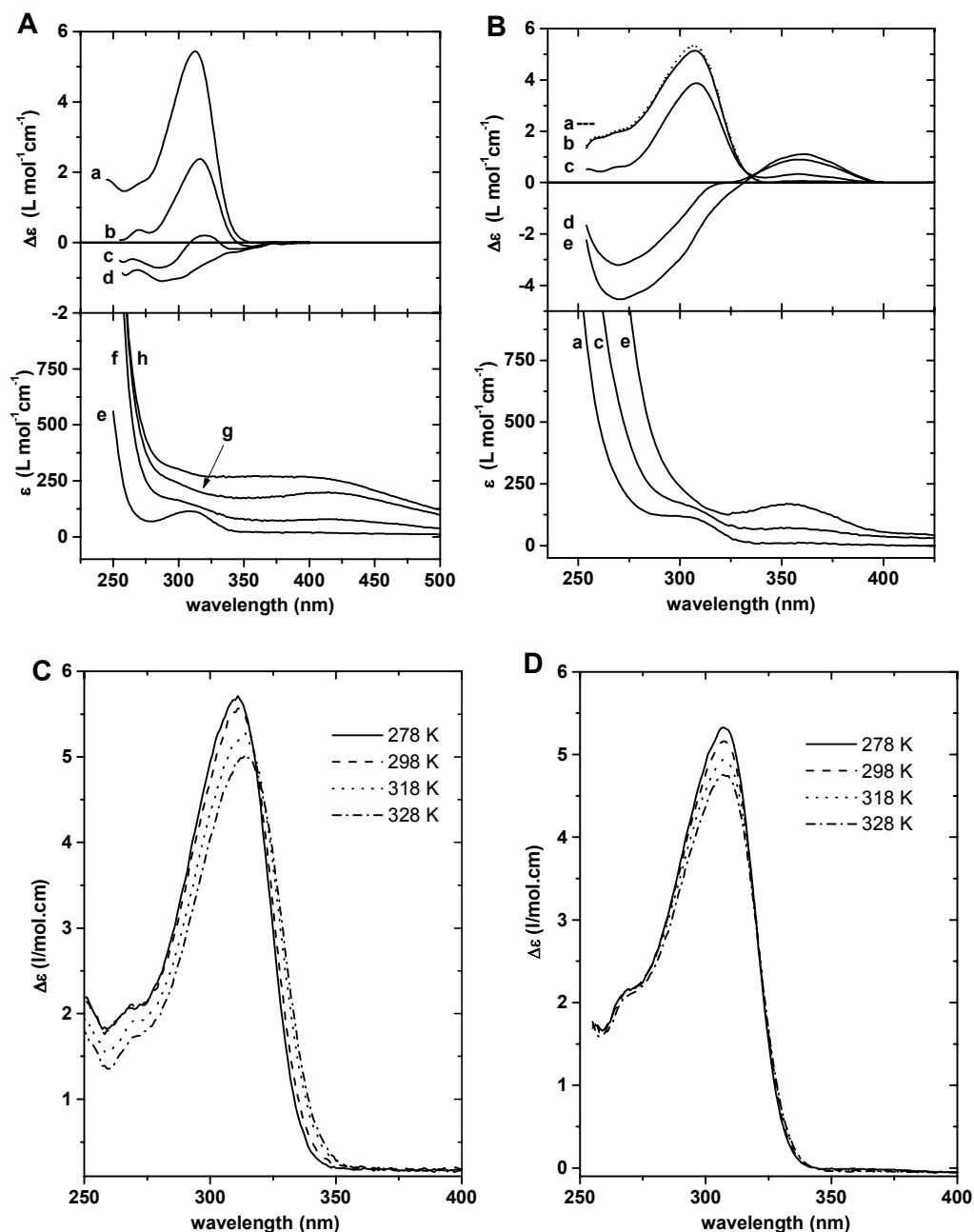


**Figure 7** (A) Change in the CD and UV/vis spectra upon the addition of 18.2 % (v/v) TFA to L,L-PIAA. CD spectra: a, before addition; b, 1 min. after addition; c, idem after 6 min.; d, idem after 17 min. UV/vis spectra: e, before addition; f, 3 min. after addition; g, idem after 14 min.; h, idem after 35 min. (B) Change in the CD and UV/vis spectra of L,D-PIAA upon the addition of a, 0%; b, 2.2%; c, 6.3%; d, 10.0%; e, 13.5% TFA. (C) CD spectra of L,L-PIAA at different temperatures. (D) Idem for L,D-PIAA.

**Circular dichroism spectroscopy.** Since the well-defined hydrogen bonding arrays between side chains  $n$  and  $(n + 4)$  in the polymers are reflected in the intense Cotton effects observed in the CD spectra, their disruption could be monitored using this technique. The strength of hydrogen bonds in solution is strongly dependant on the type of solvent and usually decreases with increasing temperature. The effect of changing these two parameters was investigated for **L,L-** and **L,D-PIAA** and for **L-PIGA** using CD spectroscopy.

Initially hydrogen bonding solvents like MeOH and DMSO were added to a solution of **PIAA** in  $\text{CHCl}_3$ , which did not lead to any noticeable change in the CD spectra. It appeared that strong acids such as trifluoroacetic acid (TFA) or HCl are needed to break the hydrogen bonding array. In Figure 7 the effects of TFA and temperature on the UV/vis and CD spectra of the studied **PIAA**'s are displayed. In the case of **L,L-PIAA** the addition of an excess of acid led to a decrease of the strong Cotton effect at 312 nm eventually resulting in a weak negative signal. In the case of **L,D-PIAA**, the decrease in the CD intensity was so fast that no intermediate state could be detected. Stepwise addition of smaller amounts of acid allowed the recording of the intermediate spectra (Figure 7b), showing that the strong signal at 307 nm vanished and 2 new signals appeared, *viz.* a positive peak with  $\Delta\epsilon_{\text{max}} = 361$  nm and a negative signal having  $\Delta\epsilon_{\text{max}} = 275$  nm. Also in the UV/vis spectra significant changes were observed; for **L,L-PIAA** the band at 308 nm broadened and shifted to longer wavelengths. In the IR spectrum the acidification was accompanied by a small shift of the amide NH vibration to higher wavenumbers ( $\Delta\nu = 23 \text{ cm}^{-1}$ ) and the appearance of a shoulder at  $\nu = 3395 \text{ cm}^{-1}$ , clearly pointing to a weakened or less defined hydrogen bonding pattern between the amide groups in the side chains. Compared to **L,L-PIAA**, **L,D-PIAA** responded differently in the UV/vis spectra upon the addition of acid; a similar red-shift was observed, but, the absorption remained narrow. The structural changes induced by TFA on **L-PIGA** were so fast even in the presence of small amounts of acid, that it was impossible to obtain reproducible intermediate spectra. The ultimate spectrum showed no Cotton effect at all.

The disruption of the hydrogen bonding arrays between the polymeric side chains apparently strongly influences the helical structure of the macromolecular backbone. When the stabilization by the hydrogen bonds is no longer present, the

rotation around the carbon-carbon bonds in the polymeric backbone is only hindered by the steric bulk of the side groups, in particular those close to the imine groups. For **L,L-PIAA** without the presence of the hydrogen bonding arrays similar structural properties can be expected as found for poly(L-isocyanoalanine ethyl ester). Indeed the CD spectrum of the latter polymer displays a high similarity with that of acidified **L,L-PIAA**.<sup>15</sup> The same resemblance is observed between these spectra and the CD spectrum of **L-PIAG** (Figure 5D), for which no defined array of hydrogen bonds was found (see Chapter 2).<sup>10</sup> The absence of this array in **L-PIAG** was further confirmed by the lack of any observable change in the chiroptical properties of this polymer upon the addition of TFA. We may conclude that small differences in the side chain configuration leads to large differences with respect to the ease of disruption of the hydrogen bonds. Compared to **L,L-PIAA**, **L,D-PIAA** displayed stronger CD signals in the presence of acid and a relatively narrow band in the UV/vis spectrum was found, pointing to a more regular structure. The presence of an isodichroic point at 335 nm (Figure 7b) reveals a transition between two discrete conformations when this polyisocyanodipeptide is treated with TFA. The absence of a large substituent next to the imine moiety in **L-PIGA** creates a helix inversion barrier which is sufficiently low to allow reversal and equilibration of the helical senses once hydrogen bonds are no longer present, ultimately resulting in the complete loss of the optical activity.

In addition to protonation of the amide groups and the subsequent disruption of the hydrogen bonding pattern, also the imine groups can be protonated. This reversible process<sup>16</sup> was invoked by Kamer *et al.*<sup>17</sup> to explain the coincidence of <sup>1</sup>H NMR signals of poly(4-methoxyphenyl isocyanide) which were different because of *syn-anti* isomerism. The changes in the chiroptical properties of the polyisocyanopeptides described here are not likely the result of protonation of the imines. First, the changes induced by acid in the CD and UV/vis spectra were irreversible upon neutralization of the solution with base and second, similar structural changes were found for **L,L-** and **L,D-PIAA** when the temperature was increased (Figure 7C and D). In the case of **L-PIGA** the intensity of the Cotton band at 309 nm decreased significantly faster when compared to the lowering of the same bands in the **PIAA**'s (Figure 8A). The absence of sterically demanding groups next to the imine groups in the polymeric backbone of this polymer (*see above*) explains this effect. After heating the polymer for one hour at 60 °C in CHCl<sub>3</sub> IR studies revealed that hydrogen bonds were only partially left, which is comparable to the situation found for **L-PIAG**.<sup>10</sup> The relation between  $\epsilon$  and  $\Delta\epsilon$  as a

function of the temperature is plotted in Figure 8B. The observed non-linear relationships indicate that the unwinding of the helical backbone is a co-operative process, which as expected was irreversible. For the **PIAA**'s partial reversibility was found when the temperature was lowered after it had been raised first stepwise to 55 °C, confirming the expected higher helix inversion barrier of these polymers compared to **L-PIAG**. The breaking of the hydrogen bonds in **PIAA** does not necessarily lead to unfolding of the helical backbone, however, for entropic reasons the well-defined starting situation will not be regained. In line with absence of hydrogen bonding arrays no temperature effect was observed for **L-PIAG**.

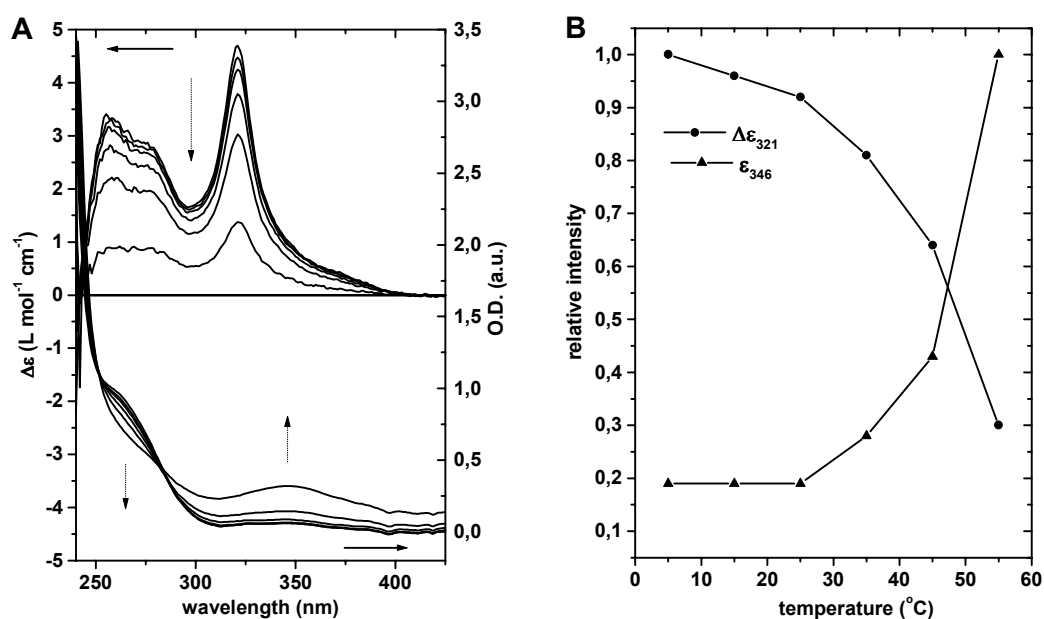


**Figure 8** CD and UV/vis spectra of **L-PIGA** upon increasing the temperature (A); arrows indicate the direction of the changes. Relative intensity of selected CD and UV/vis bands as a function of temperature (B).

**Powder X-ray diffraction measurements.** The changes in the macromolecular conformations of the polyisocyanopeptides induced by the disruption of the hydrogen bonding arrays along the polymeric backbone, were studied by PXRD for **L,L-PIAA** and **L-PIGA**. Whereas for the polymers with hydrogen bonds between their side chains relatively sharp reflections were observed in the diffraction patterns, only broad signals were found for the polyisocyanopeptides without these arrays (Figure 2C and F). In the case of **L,L-PIAA** treatment of the polymer with TFA resulted in a different macromolecular conformation as was indicated by CD spectroscopy and a reduced order in the solid state packing of the macromolecules. From the reflections observed in



the diffraction pattern of this sample (Figure 2C) a diameter of 16.3 Å can be calculated for the rods in a presumably hexagonal ordering. As a direct consequence of the lack of bulky substituents close to the polymer backbone in **L-PIGA**, the hydrogen bonds in this polymer can be disrupted by thermal treatment. The diffraction pattern of a sample which had been heated in CHCl<sub>3</sub> for 1 hour at 60 °C displayed broad reflections which could be attributed to macromolecules in a hexagonal arrangement having diameters of 17.2 Å. Despite the low helix inversion barrier proposed for **L-PIGA** still some ordering was found in this polymer after thermal treatment, although no optical activity was observed. In line with the proposed ‘polymeric spring’ model (Figure 3), the diameters of both **L,L-PIAA** and **L-PIGA** increase when the hydrogen bonds become disrupted.

The results presented above indicate that the macromolecular ordering in the polyisocyanodipeptides studied here is substantially reduced when the hydrogen bonds are disrupted. However, still an organization of stiff macromolecules appears to be present when the obtained PXRD patterns are compared with those reported for poly(phenyl isocyanide) by Huang et al.<sup>9</sup> and for rigid rod polyphenylene by Gin<sup>18</sup>. The conformational properties of the polyisocyanopeptides without the hydrogen bonding arrays are determined by steric interactions between the side groups only,<sup>6a</sup> likely leading to a reduction in the persistence length of the polymers.<sup>8</sup>

### 3.2.3 Determination of the helix sense

The atropisomerism present in polyisocyanides gives rise to a helical conformation of the polymeric backbone, and by various methods<sup>5</sup> an excess of either left-handed (*M*) or right-handed (*P*) polymers can be obtained. The determination of the screw sense of polyisocyanides has been the subject of intense research efforts by van Beijnen *et al.*<sup>15,19,20</sup> Assuming that the helix sense is kinetically controlled, - *i. e.* the ratio between left- and right-handed helices is determined by the relative activation energies of the possible transition states- a procedure was proposed to predict the screw direction of the polymers.<sup>15</sup> In this procedure the relative steric requirements of the substituents on the carbon atom next to the isocyanide functionality are considered as well as the possible interactions of these substituents with the nickel center. In later studies this concept was successfully applied to explain the formation of *P* helices from the polymerization of achiral isocyanides using (S)-(-)- $\alpha$ -phenyl ethylamine as the initiator.<sup>21</sup> For poly(L-isocyanoalanine ethyl ester) van Beijnen predicted a *P*-screw based on steric parameters, whereas the opposite helicity was proposed for **L,L-PIAH** although this

proposition is probably incorrect.<sup>22</sup> The occurrence of more than one configuration of the initiating Ni(II) complex, however, makes the above procedure a delicate one. It appears that when a chiral carbon atom is present next to the isocyanide moiety the asymmetric substitution of this atom exercises a dominant influence on the ultimate screw sense of the polymer in this kinetic model. The same is true if the screw sense would be thermodynamically controlled as proposed by Huige.<sup>6c</sup> Calculations on oligomeric compounds performed by him and recently by us (*see above*) revealed that *P* helices have a lower overall energy when the chiral side groups close to the backbone are in the S-configuration.

Based on CD calculations using Tinoco's exciton theory<sup>19</sup> and De Voe's polarizability theory<sup>6c</sup> it was found that a Z-shaped (negative) couplet in the  $n-\pi^*$  transitions of the imine chromophores of poly(*tert.*-butyl isocyanide), corresponds to a right-handed helical conformation and that a S-shaped (positive) couplet corresponds to a left-handed conformation. Simulation of the CD spectrum of poly(L-isocyanoalanine ethyl ester) resulted in a negative couplet superimposed on a negative symmetrical Cotton effect, leading to the assignment of a *P* helical structure to this polymer.<sup>15</sup> The CD spectra of the polyisocyanodipeptides without or with disrupted hydrogen bonding arrays, *viz.* **L-PIAG** (Figure 5C) and **L,L-PIAA** after treatment with TFA (Figure 7A), resemble the spectrum measured for poly(L-isocyanoalanine ethyl ester).<sup>15</sup> The above results suggest that a right-handed helical polymer is obtained upon polymerization of L-alanine derived polyisocyanides. A direct relation between the experimental CD spectra and the theoretically predicted ones is, however, difficult to make, in particular since side chain contributions to the  $n-\pi^*$  transitions of the imines appear to have a dominant effect on the CD spectra. It should be noted that the interpretation of the CD spectra by van Beijnen has been questioned by Clericuzio *et al.*<sup>9</sup> They pointed out that the utilized exciton theory is not directly applicable to a  $n-\pi^*$  transition. These transitions have a large magnetic dipole contribution which has also to be included in the CD calculations, as is done when using the dynamic ( $\mu-m$ ) coupling mechanism. Employing this latter approach to polyisocyanides indicated, however, that the assignment of the absolute conformation to poly(*tert.*-butyl isocyanide) as done by van Beijnen was correct.<sup>9</sup>

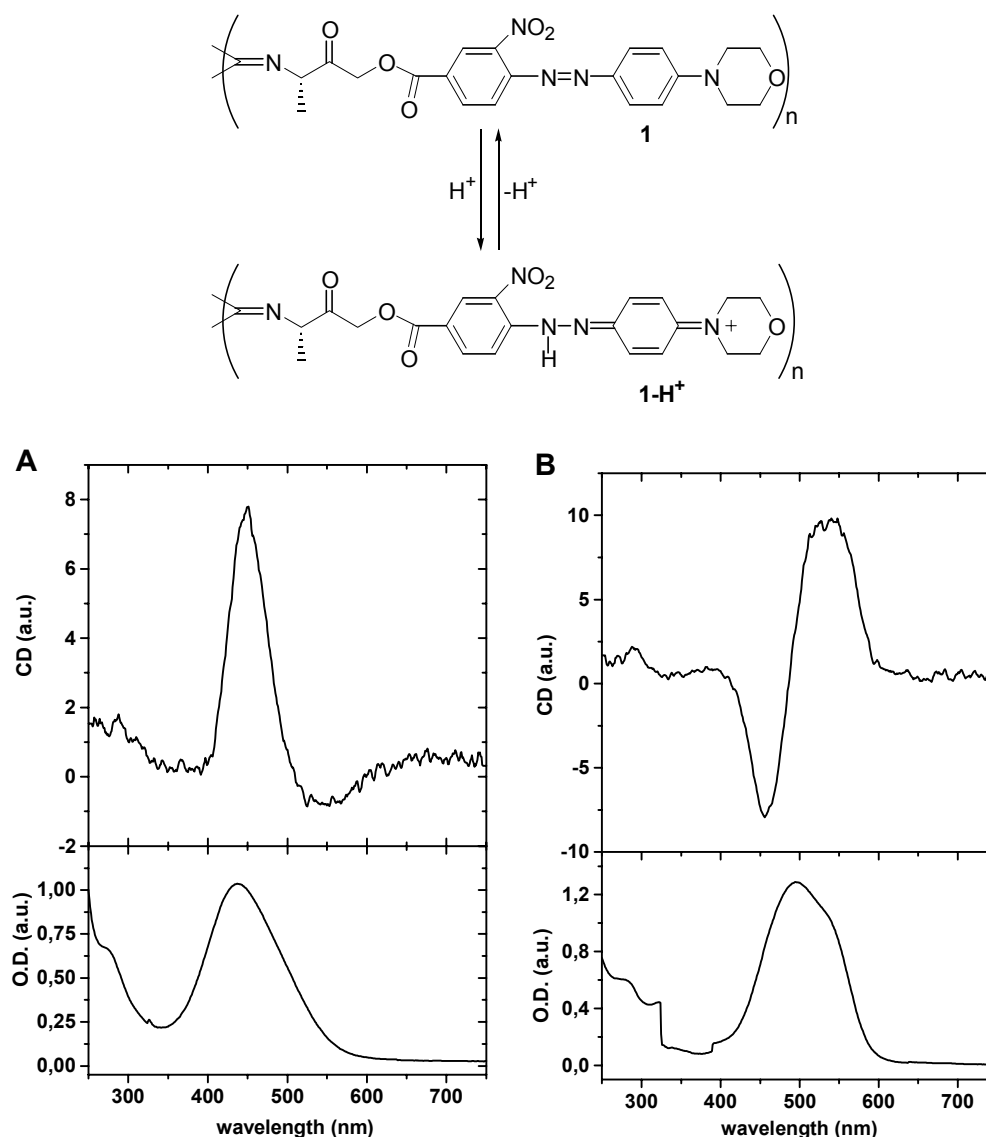


**Figure 9** CD and UV/vis spectra of polyisocyanide **1** in CHCl<sub>3</sub> (A) and of **(1-H<sup>+</sup>)** CHCl<sub>3</sub> (TFA was used as the acide) (B).

To verify our hypothesis that L-alanine derived polyisocyanides form a right-handed helix, the chiroptical properties of polymer **1** were investigated. This polyisocyanide was prepared from L-alaninol and a diazo compound and was originally designed to the study the non-linear optical properties of this macomolecule in relation to the helical organization of the chromophores.<sup>23</sup> The UV/vis and CD spectra of **1** and of this compound in its protonated form (**1-H<sup>+</sup>**) are presented in Figure 9. For both polymer systems it was assumed that no direct electronic interaction was present between the polyisocyanide backbone and the chromophores. Neutral **1** gave a broad absorption in the UV/vis spectrum with  $\lambda_{\text{max}} = 439$  nm and a positive Cotton effect at the corresponding wavelength (Figure 9A). Upon acidification of **1** a different quinoid-

like chromophore<sup>24</sup> is formed. Addition of TFA led to a step-wise protonation, the conversion between the two distinct forms being indicated by the appearance of an isosbestic point at  $\lambda = 453$  nm in the UV/vis spectra (not shown). For **1-H<sup>+</sup>** eventually a signal with  $\lambda_{\text{max}} = 495$  nm and a shoulder at  $\lambda = 539$  nm was found in the UV/vis spectrum. The CD spectrum showed a distinct bisignate signal pointing to exciton coupling of the chromophores absorbing at  $\lambda_{\text{max}} = 495$  nm. For the absorption present as a shoulder a positive CD signal was observed, partly overlapping with the positive couplet.<sup>25</sup> From the sign of this exciton couplet, which corresponds to a  $\pi$ - $\pi^*$  transition a right-handed organization of the chromophores can be derived.<sup>26</sup> Given the short distance between these chromophores and the polyisocyanide backbone, a right-handed screw sense is therefore deduced from this geometry and tentatively translated to all L-alanine based polyisocyanides.

**Table 1. Selected properties of dipeptide derived polyisocyanides**

Compound	[ $\alpha$ ] <sup>a</sup>		$\Delta\epsilon$ ( $\lambda$ ) <sup>b</sup>	Screw sense	[ $\eta$ ] <sup>c</sup>	$t_{\text{pol}}$ <sup>d</sup>	H-bonds
	Monomer	Polymer					
<b>L,L-PIAA<sup>e</sup></b>	33	338	5.6 (313)	<i>P</i>	1.33	< 5	yes
<b>L,D-PIAA<sup>e</sup></b>	-5.6	487	5.8 (307)	<i>P</i>	5.26	< 5	yes
<b>L-PIGA<sup>e</sup></b>	19.2	196	5.1 (321)	<i>P</i>	n.d. <sup>i</sup>	< 5	yes
<b>L-PIAG<sup>e</sup></b>	5.7	-32	-1.5 (290)	<i>P</i>	n.d. <sup>i</sup>	>120	no
<b>L,L-PIAH<sup>f</sup></b>	164	580	6.5 (304)	<i>P</i>	1.04	~240 <sup>k</sup>	yes
<b>D,L-PIAH<sup>f</sup></b>	75	-700	-0.45 (345) 1.22 (270)	<i>M</i>	insol. <sup>j</sup>	~240 <sup>k</sup>	no
<b>L,L-PIAS<sup>g</sup></b>	-58.1	205	8.6 (310)	<i>P</i>	4.1	< 30	yes
<b>L,D-PIAS<sup>g</sup></b>	-12.0	-33	0.17 (355) -1.3 (263)	<i>P</i>	0.35	240	no
<b>D,L-PIAH(OAc)<sup>f</sup></b>	14	-610	-5.5 (300)	<i>M</i>	0.33	~240 <sup>k</sup>	yes/ no <sup>l</sup>
<b>L-PIA<sup>h</sup></b>	16.7	-280	-0.5 (300)	<i>P</i>	0.44	7200 <sup>k</sup>	no

<sup>a</sup>In °·dl/g·dl; for concentrations and solvent see refs cited. <sup>b</sup>In l/mol·cm, maximal values at the indicated wavelength. <sup>c</sup>In dl/g; for conditions see refs cited. <sup>d</sup>In min., reaction time for complete consumption of the monomer. <sup>e</sup>See ref. 10. <sup>f</sup>See ref. 13. <sup>g</sup>See ref. 12. <sup>h</sup>Poly(L-isocynoalanyl ethyl ester), see ref. 15. <sup>i</sup>Not determined. <sup>j</sup>Not measured due to low solubility. <sup>k</sup>No exact reaction time was determined; after the indicated period the isocyanide was no longer detected. <sup>l</sup>Hydrogen bonds are expected based on the CD data which is, however, in contrast with the low viscosity.

Selected properties of the polyisocyanodipeptides discussed in this Chapter are summarized in Table 1. When hydrogen bonds are present (e.g. **L,L-PIAA**, **L,D-PIAA** and **L-PIGA**) a positive optical rotation and a strong positive Cotton effect around  $\lambda = 315$  nm are attributed to a right-handed (*P*) helix. Taking the difference between polymers with and without hydrogen bonds into account, this assignment is consistent with other polyisocyanopeptides prepared in the past in which the presence of hydrogen bonds is reflected in the high viscosities and the short polymerization times.<sup>11-13</sup> For the polyisocyanides where no hydrogen bonding arrays are found the optical rotations and the intensities in the CD spectra are significantly smaller (Table 1). These polyisocyanides resemble the properties of poly(L-isocyanoalanyl ethyl ester) (**L-PIA**). As expected opposite chiroptical properties are observed for the macromolecules for which a *M*-type helix is assumed.

### 3.2.4 Effects of side chain configuration

From the data presented in Table 1 it can be concluded that subtle variances in the monomer side chain configuration lead to important differences in the properties of the resultant polymers. For example, in **L,L-PIAS** the existing data point to the presence of a hydrogen bonding array along the polymeric backbone, while no indication for such an arrangement is found in **L,D-PIAS**. The same relationship appears to exist in the case of **L,L-PIAH** and **D,L-PIAH**. Remarkably, however, both **L,L-PIAA** and **L,D-PIAA** contain hydrogen bonding arrays. In the latter polymer the disruption of the hydrogen bonds between side chains *n* and (*n* + 4) results in significant differences in the CD spectra (*see above*). The CD spectrum of acidified **L,D-PIAA** has, in turn, a similar shape as the spectrum measured for **L,D-PIAS** (see Figures 6 and 7).

Based on the kinetic control of the Ni(II) catalyzed polymerization reaction and the differences in polymerization time between polymers that form a hydrogen bonding array and polymers that do not (Table 1), a kind of preorganization of the monomers and the growing chain must be present to explain the observed differences.<sup>10</sup> A monomer that fits precisely into the hydrogen bonding array of the growing chain will be incorporated faster than a monomer that has a poor fit. This match of growing chain and incoming monomer may be the result of both steric and configurational factors and will be reflected in the rate of polymerization and the properties of the resultant polymers. For **L,D-PIAS** and **D,L-PIAH** the lack of hydrogen bonds parallel to the helix

axis can be explained by unfavorable steric interactions between the side chains or by the fact that the hydrogen bonding functionalities in serine and histidine prefer to form other types of hydrogen bonds in these cases. Since in **L,D-PIAA** the hydrogen bonding arrays are formed, the latter explanation seems to be more likely. On the other hand in **L-PIAG** no well-defined hydrogen bonding arrays were found, indicating that the bulkiness of the side groups in the second amino acid (and the related rotational freedom within the monomer) does play a role. A combination of the two factors is probably closest to the actual situation, however, more experiments are required to verify this.

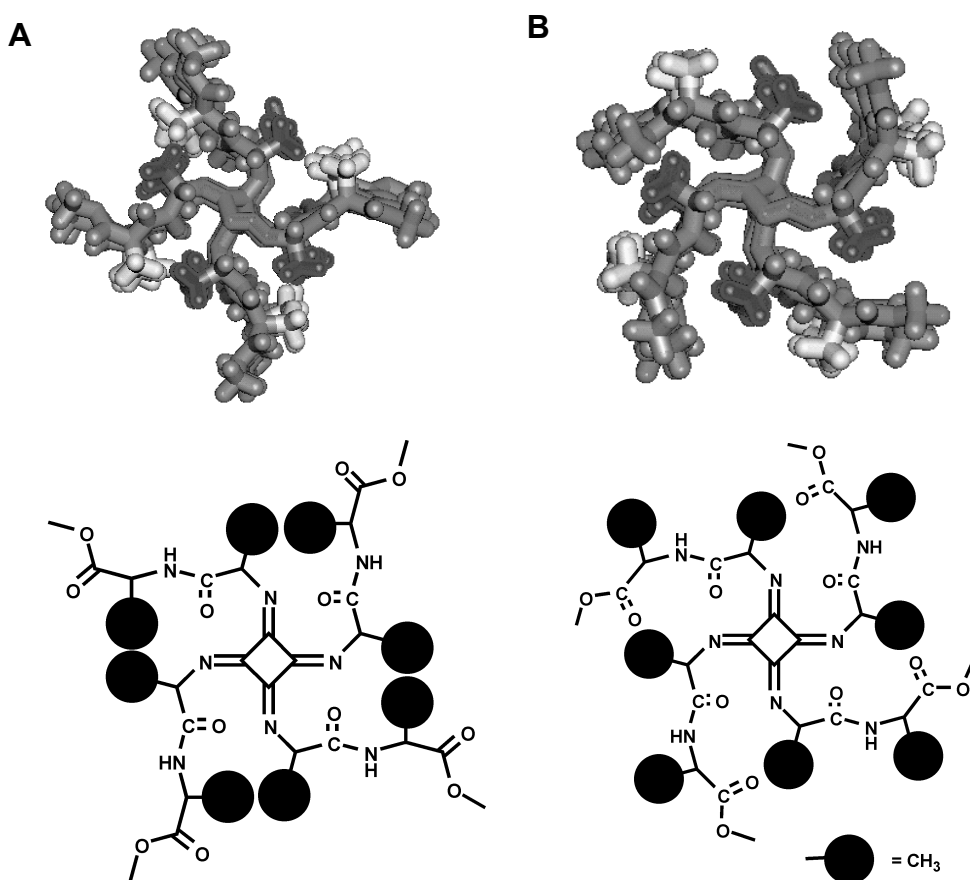


**Figure 10** Calculated molecular models of (A) **L,L-PIAA** and (B) **L,D-PIAA** revealing the different configurations of the side chains. In black: schematic drawings showing the difference in steric interactions resulting from the change in side chain configuration.

Molecular modeling calculations revealed that the polymer derived from **L,D-PIAA** is more stable than the polymer derived from **L,L-PIAA**. In the latter case the methyl group of the second alanine unit is in van der Waals contact with the methyl group of the first alanine entity of the next repeating unit, thereby leading to an

unfavorable steric interaction. In the case of **L,D-PIAA** this methyl group and the proton in the second alanine function are interchanged and this interaction is then absent (Figure 10). We found that L-isocyanoalanyl-D-alanine methyl ester (**L,D-IAA**) can be polymerized with acid, that is without the templating effect of the nickel(II) catalyst.<sup>27</sup> The formation of **L,D-PIAA** was evident from IR spectroscopy (Figure 11). Under the applied conditions (see experimental) **L,L-PIAA** did not show any sign of polymerization. The **L,D-PIAA** isolated from this acid catalyzed polymerization gave CD spectra which were very similar to those of the polymer prepared using a nickel catalyst, but due to the high viscosity of the sample and the low solubility of the formed product no quantitative comparison was possible. The fact that **L,D-PIAA** can be polymerized with acid and **L,L-PIAA** can not supports the idea that the polymer derived from the former monomer is more stable than that from the latter monomer, in line with the above mentioned calculations.

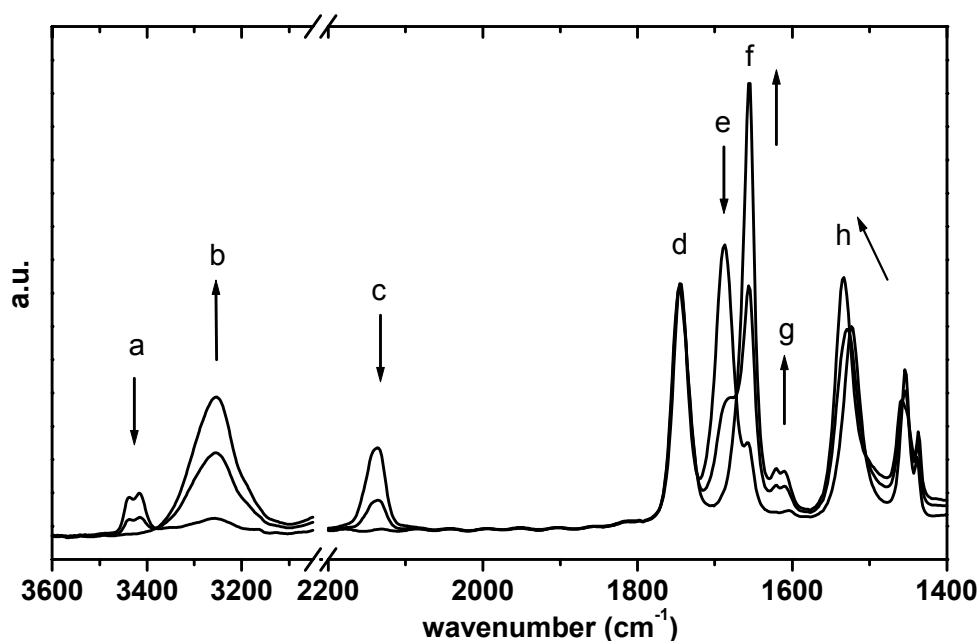


**Figure 11** IR spectra of the progressing acid catalyzed polymerization of **L,D-PIAA**. Arrows indicate the direction of change; a, NH non-hydrogen bonded; b, NH hydrogen bonded; c, CN isocyanide; d, C=O ester; e, amideI non-hydrogen bonded; f, amideI hydrogen bonded; g, C=N imine; h, amideII.

### 3.2.5 Lyotropic liquid crystalline behaviour

The formation of a nematic liquid crystalline (LC) phase, characterized by orientational order of the molecules, is often observed for rigid macromolecules in solution.<sup>28</sup> For

one-handed helical polymers with a sufficiently long persistence length the aggregation of the polymer molecules is in some case accompanied by the formation of a cholesteric phase. In this phase the rod-like macromolecules are no longer oriented parallel, but twisted with respect to their nearest neighbors.<sup>29</sup> For polyisocyanides the number of reported lyotropic LC phases are very limited; poly(octyl isocyanide)<sup>16</sup> was shown to form a nematic phase in  $\text{CHCl}_3$  and poly( $\alpha$ -phenyl ethyl isocyanide)<sup>3</sup> was proposed to give a cholesteric mesophase. Since the polyisocyanides reported in this chapter have a very well-defined macromolecular structure and possibly a long persistence length, the formation of lyotropic LC phases was investigated for **L,L-** and **L,D-PIAA**.



**Figure 12** Optical micrograph between crossed polarizers of a 10% w/w solution of **L,L-PIAA** in  $\text{CHCl}_3$ .

Indeed in a concentrated (above 10 % w/w) solution of **L,L-PIAA** in  $\text{CHCl}_3$  a LC phase was formed, as was indicated by the birefringence of this solution visualized between crossed polarizers (Figure 12). The observed characteristic fingerprint texture points to a cholesteric arrangement of the macromolecules,<sup>30</sup> in which the distance between the observed stripes corresponds to the cholesteric pitch. The alignment of the polymers proceeded slowly since it was found that the pitch gradually decreased with time: it amounted to 17  $\mu\text{m}$  24 hours after sample preparation and eventually became 9.2  $\mu\text{m}$  after 40 hours standing (solution was 10% w/w). Upon the formation of a cholesteric phase a drastic effect on the optical rotation of the solution is expected.<sup>30</sup> While for **L,L-PIAA** in diluted solution the optical rotation amounted to  $[\alpha]_D = 338^\circ$ ,<sup>10</sup>



for the LC phase with a pitch of 17  $\mu\text{m}$   $[\alpha]_{\text{D}} = -44,000^{\circ}$  and for the LC phase with a pitch of 9.2  $\mu\text{m}$  even  $[\alpha]_{\text{D}} = -72,000^{\circ}$ , in line with a left-handed cholesteric arrangement of the macromolecules.

A lyotropic LC phase was also observed for **L,D-PIAA**, however, the observed texture appeared less well-defined after 40 hours standing. Similar to the observations for **L,L-PIAA** the fingerprint texture was slowly formed. Due to the higher viscosity of the solution and the tendency to gelate the process was so slow that only small domains with a cholesteric texture were visible after 3 days, hampering further investigations. The polymer samples that had been treated with acid to disrupt the hydrogen bonding arrays did not show any sign of a lyotropic LC phase. Neither was any increase in the specific optical rotation found upon increasing the polymer concentration. These polyisocyanodipeptide samples apparently no longer have the high degree of organization and long persistence length required for the formation of a lyotropic LC phase.

### 3.3 Conclusions

Polyisocyanides derived from dipeptides have, depending on the configuration of the side chains, a highly defined conformation induced by hydrogen bonding arrays formed between amide functionalities in the polymer side chains. From the absence of any detectable signals of non-hydrogen bonded amide groups and the excellent correlation between observed and calculated macromolecular diameters, an extended  $4_1$  helical conformation is proposed for these polymers in which hydrogen bonds are present between side chains  $n$  and  $(n + 4)$ . The way the side chains are organized in the polyisocyanopeptides is comparable to the hydrogen bonding patterns found in parallel  $\beta$ -sheet structures in Nature. Similar to the denaturation of proteins, disruption of the hydrogen bonds by increasing the temperature or by treatment of the polymers with strong acid leads to a less well-defined macromolecular conformation.

In the case of **L,L-** and **L,D-PIAA** the helix inversion barrier is large, which is caused by a combined effect of the sterically demanding substituents and the stabilization by the hydrogen bonds. For these polymers LC properties were observed which support the idea that these macromolecules have a well-defined structure.

The presence of hydrogen bonding arrays along the polymeric backbone is reflected in the intense Cotton effects that are present around 315 nm in the CD spectra. This technique therefore is a powerful tool to study the conformation of the macromolecules. Indeed, upon disruption of the hydrogen bonds drastic changes in the CD spectra are found. By comparing the properties of the present polymers with those reported in the literature<sup>15</sup> and with the properties of a chromophore containing model compound tentatively a right-handed helical geometry is proposed for the L-alanine derived polyisocyanides. Since the Ni(II) catalyzed polymerization of isocyanides is a kinetically controlled process it is likely that all polymers grown from L-alanine-based monomers have the same stereochemistry. Based on this kinetic control and the observed properties of the polymers e.g. short polymerization time, high intrinsic viscosity, and intense Cotton effects it is proposed that the L-alanine derived peptide monomers fit better in the developing polymer helix than monomers having different configurational properties, because they can form internal hydrogen bonding arrays.<sup>31</sup> As a result of the combination of steric interactions and hydrogen bonding, subtle differences in side chain configuration can have a pronounced effect on the formation of the polymers as was demonstrated for **L,D-PIAA**, which can be formed even without the help of nickel(II) ions, *i.e.* by H<sup>+</sup> catalysis.

The accessibility of a large number of natural and unnatural amino acids opens the possibility to design and synthesize a wide array of well-defined polyisocyanopeptides and related block copolymers. The  $\beta$ -sheet-like arrangement of the side groups provides a stable and robust scaffold to which a variety of functional groups can be attached such as metal catalyst<sup>32</sup> or non-linear optical chromophores.<sup>23</sup>

## 3.4 Experimental Section

### 3.4.1 General methods and materials

All chemicals were commercial products and were used as received. <sup>1</sup>H NMR spectra were recorded on Bruker AC-100, Bruker WM-200, and Bruker AC-300 instruments at 297 K. Chemical shifts are reported in ppm relative to tetramethylsilane ( $\delta = 0.00$  ppm) as an internal standard. FT-Infrared spectra were recorded on a Bio-Rad FTS 25 instrument. UV/Vis spectra were measured on a Varian Cary 50 conc spectrophotometer and CD spectra on a JASCO 810 instrument. X-ray powder diffractograms were collected on a Philips PW1710 diffractometer equipped with a Cu LFF X-ray tube operating at 40 kV and

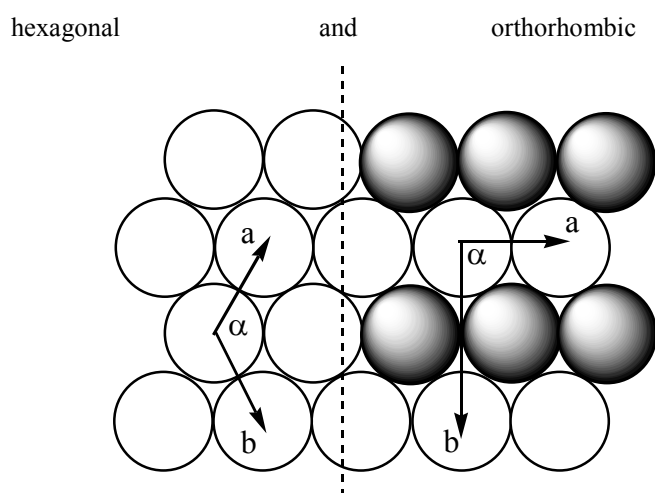
55 mA. Samples were measured on a silicon wafer between 3 and 60°, using a step width of 0.05°. Optical micrographs between cross polarizers were obtained on a Jeneval THMS 600 microscope.

### 3.4.2 CD spectroscopy

CD spectra were measured at ambient temperature in  $\text{CHCl}_3$ . Spectra of the samples to which acid was added were recorded in 8/1 (v/v)  $\text{CHCl}_3/\text{MeOH}$  to prevent precipitation of the polymers. During the temperature dependent measurements after each interval the solution was equilibrated for 10 min.

### 3.4.3 Powder X-ray diffraction

Two models were considered for the description of the arrangement of the polyisocyanodipeptides discussed here, viz.:



In an orthorhombic arrangement the macromolecules are packed in an identical fashion as in the hexagonal arrangement. Only the molecules in different layers are inequivalent. This inequivalency results in a doubling of the unit cell in one direction, which in the case of the polyisocyanopeptides can probably be attributed to alternating directions of the stacking of the hydrogen bonds between the side chain amide groups, *i. e.* helices pointing in and outward of the plane of the paper. The following mathematical descriptions can be derived.

In the hexagonal case:

$$|a| = |b| \text{ and } \alpha = 120^\circ$$

from these:

$$d_{hk} = \sqrt{3}a / 2\sqrt{(h^2 + hk + k^2)}$$

and the macromolecular diameter (d):

$$d = |a|$$

In the orthorhombic case:

$$|b| = \sqrt{3}|a| \text{ and } \alpha = 90^\circ$$

$$d_{hk} = a / \sqrt{(h^2 + (k/3)^2)}$$

$$d = |a|$$

Occasionally the experimental data points to a distortion of the ideal unit cells as described above. For example when in the orthorhombic lattice the angle  $\alpha \neq 90^\circ$  a triclinic unit cell is formed, described by a different set of vectors. This triclinic arrangement is found in an oriented film of poly( $\alpha$ -phenyl ethyl isocyanide) using electron diffraction.<sup>33</sup> Also in the orthorhombic lattice it is possible that the relation between  $|a|$  and  $|b|$  deviates from the model situation, in such cases:

$$d_{hk} = 1 / \sqrt{(h^2/a^2 + k^2/b^2)} \text{ and the macromolecular diameter (d):} \quad d = |a|$$

As a representative example the indexation of the peaks observed in PXR diffractogram of **L,L-PIAA** measured as a powder (Figure 2B) is given.

$d_{\text{obs}}$ (Å)	$d_{\text{calc}}$ (Å)	$hkl$ (orth) a = 15.9 Å b = 29.5 Å
13.72	14.02	110
9.92	9.84	030
6.95	7.01	220
6.20	6.19	230
5.31	5.31	300
5.18	5.23	310
4.89	4.92	060
4.66	4.67	330
3.93	3.95	410 / 350
3.85	3.85	420
3.59	3.59	180
3.52	3.51	440

### 3.4.4 Synthesis

The polymers **PIAA**, **PIGA** and **PIAG** were synthesized as described in Chapter 2 of this thesis.<sup>10</sup> The polymerization of **L,D-IAA** by acid was performed by dissolving the monomer in  $\text{CHCl}_3$  containing a trace amount of HCl. The final concentration of monomer was between 1 and 5 mM.

## 3.5 References and Notes

- 1 Bovey, F. A.; Winslow, F. H. ed. *Macromolecules. An introduction to polymer science*. Academic Press, Inc. San Diego, 1979.
- 2 a) Rowan, A.E.; Nolte, R.J.M. *Angew. Chem. Int. Ed.* **1998**, *37*, 63-68. b) Okamoto, Y.; Nakano, T. *Chem. Rev.* **1994**, *94*, 349. c) Cornelissen, J. J. L. M.; Rowan, A. E.; Nolte, R. J. M.; Sommerdijk, N. A. J. M. *Chem. Rev.* **2001**, submitted.

- 3 Millich, F. *Chem. Rev.* **1972**, *72*, 101.
- 4 a) Nolte, R. J. M.; van Beijen, A. J. M.; Drenth, W. *J. Am. Chem. Soc.* **1972**, *96*, 5932. b) van  
Beijnen, A. J. M.; Nolte, R. J. M.; Drenth, W. *Recl. Trav. Chim. Pays-Bas*, **1980**, *90*, 121.
- 5 Nolte, R. J. M. *Chem. Soc. Rev.* **1994**, *23*, 11.
- 6 a) Kollmar, C.; Hoffmann R. *J. Am. Chem. Soc.* **1990**, *112*, 8230. b) Cui, C. X.; Kertesz, M  
*Chem. Phys. Lett.* **1990**, *169*, 445. c) Huige, C. J. M.; *Ph. D. Thesis*, University of Utrecht, 1985.  
d) Huige, C. J. M.; Hezemans, A. M. F.; Nolte, R. J. M.; Drenth, W. *Recl. Trav. Chim. Pays-Bas*  
**1993**, *112*, 33.
- 7 Clericuzio, M.; Alagona, G.; Ghio, G.; Salvadori, P. *J. Am. Chem. Soc.* **1997**, *119*, 1059.
- 8 Green, M. M.; Gross, R. A.; Schilling, F. C.; Zero, K.; Crosby III, C. *Macromolecules* **1988**, *21*,  
1839.
- 9 Huang, J.-T.; Sun, J.; Euler, W. B.; Rosen, W. *J. Polym. Sci., Part A: Polym. Chem.* **1997**, *35*,  
439.
- 10 a) Cornelissen, J. J. L. M.; Graswinckel, W. S.; Adams, P. J. H. M.; Nachtegaal, G.; Kentgens,  
A.; Sommerdijk, N. A. J. M.; Nolte R. J. M. submitted for publication. b) Chapter 2 of this  
thesis.
- 11 van der Eijk, J. M.; Nolte, R. J. M.; Drenth, W.; Hezemans, A. M. F. *Macromolecules* **1980**, *13*,  
1391.
- 12 Visser, H. G. J.; Nolte, R. J. M.; Zwikker, J. W.; Drenth, W. *J. Org. Chem.* **1985**, *50*, 3138.
- 13 van der Eijk, J. M. *Ph.D.Thesis*, University of Utrecht, The Netherlands, 1980.
- 14 Ballauf, M. *Angew. Chem.* **1989**, *101*, 261.
- 15 van Beijen, A. J. M.; Nolte, R. J. M.; Naaktgeboren, A. J.; Zwikker, J. W.; Drenth, W.  
*Macromolecules* **1983**, *16*, 1679.
- 16 Aharoni, S. M. *J. Polym. Sci: Polym. Phys. Ed.* **1979**, *17*, 683.
- 17 Kamer, P. C. J.; Drenth, W.; Nolte, R. J. M. *Polym. Prep.* **1989**, *30*, 418.
- 18 Gin, D. L.; Conticello, V. P.; Grubbs, R. H. *J. Am. Chem. Soc.* **1994**, *116*, 10507.
- 19 van Beijnen, A. J. M.; Nolte, R. J. M.; Drenth, W.; Hezemans, A. M. F. *Tetrahedron* **1976**, *32*,  
2017.
- 20 van Beijnen, A. J. M.; Nolte, R. J. M.; Zwikker, J. W.; Drenth, W. *J. Mol. Catal.* **1978**, *4*, 427.
- 21 a) Kamer, P. C. J.; Nolte, R. J. M.; Drenth, W. *J. Chem. Soc. Chem. Commun.* **1986**, 1789. b)  
Kamer, P. C. J.; Nolte, R. J. M.; Drenth, W. *J. Am. Chem. Soc.* **1988**, *110*, 6818.
- 22 van Beijnen, A. J. M. *Ph.D.Thesis*, University of Utrecht, The Netherlands, 1980.
- 23 Kauranen, M.; Verbiest, T.; Boutton, C.; Teerenstra, M. N.; Clays, K.; Schouten, A. J.; Nolte, R.  
J. M.; Persoons, A. *Science* **1995**, *270*, 966.
- 24 Ueno, A. et al. *Nature* **1992**, *356*, 136 and references cited.
- 25 A detailed discussion on the chiroptical properties of **1** and **1+H<sup>+</sup>** will be presented elsewhere.
- 26 Harada N.; Nakanishi, K. *Circular Dichroism Spectroscopy. Exciton Coupling in Organic  
Stereochemistry*; Oxford University Press: Oxford, 1983.
- 27 This acid catalyzed isocyanide polymerization is only applicable to a limited number of  
monomers, see: Saegusa, T.; Taka-Ishi, N.; Ito, Y. *J. Org. Chem.* **1969**, *34*, 4040.
- 28 Papkov, S. P. *Adv. Polym. Sci.* **1984**, *59*, 75.
- 29 Well studied compounds in this respect are the polyisocyanates: a) Green, M. M.; Peterson,  
N.C.; Sato, T.; Teramoto, A.; Cook, R.; Lifson, S. *Science* **1995**, *268*, 1861. b) Sato, T.; Sato, Y.;  
Umemura, Y.; Teramoto, A.; Nagamura, Y.; Wagner, J.; Weng, D.; Okamoto, Y.; Hatada, K.;  
Green, M.M. *Macromolecules* **1993**, *26*, 4551.
- 30 Collings, P. J.; Hird, M. *Introduction to liquid crystals. Chemistry and physics*, Taylor & Francis  
Ltd, London, 1997.
- 31 A similar relation was recognized by Visser et al. although no relation with hydrogen bond  
formation was found at that time, see ref. 12.
- 32 Knapen, J. W. J. et al. *Nature* **1994**, *372*, 659.
- 33 Kiamco, E. A. *Ph.D.Thesis*, University of Missouri-Kansas City, U.S.A. 1975.

# CHAPTER 4

## $\beta$ -Helical Polymers from Isocyanopeptides

### 4.1 Introduction

The two principal structural elements found in proteins are the  $\alpha$ -helix and the  $\beta$ -sheet.<sup>1</sup> In 1993 a new structural motif was discovered, the so-called  $\beta$ -helix<sup>2</sup> which was first observed in the bacterial enzyme *pectate lyase* and later in several other proteins.<sup>3,4,5</sup> The  $\beta$ -helical architecture is constructed from polypeptides that are coiled into a large helix, formed by stacks of  $\beta$ -sheets separated by loops.  $\beta$ -Sheet helices are present in the fibrous form of thranstyretin which plays an important role in BSE and Creutzfeldt-Jacob diseases, type II diabetes, and Alzheimer's disease.<sup>3</sup> They are also the crucial structural elements in insect anti-freeze proteins which depress solution freezing points by ice-growth inhibition.<sup>5</sup> Here we report on synthetic analogues of  $\beta$ -helices which are formed by polymerization of isocyanopeptides.<sup>6</sup> Unlike the so-called foldamers,<sup>7</sup> in which the backbone conformation (folding) of a well-defined oligomer is controlled by secondary interactions, the peptide derived polymers contain a helical backbone which acts as a director<sup>8</sup> for the  $\beta$ -sheet-like arrangement of the peptide strands (Figure 1). The  $\beta$ -sheet arrays of hydrogen bonds are present not only in organic solvent but even persist in water, highlighting the efficiency of the helical backbone in organizing the peptide side chains.

Polymers of isocyanides are prepared<sup>6</sup> by a nickel(II) catalyzed reaction and can adopt a  $\sim 4_1$  (four repeats per turn) helical conformation depending on their side chains. When bulky side groups are present (e.g. as in poly(*tert*-butylisocyanide)) the helices

are stable,<sup>9</sup> however, in the case of less sterically demanding side chains,<sup>10,11</sup> e.g. as in

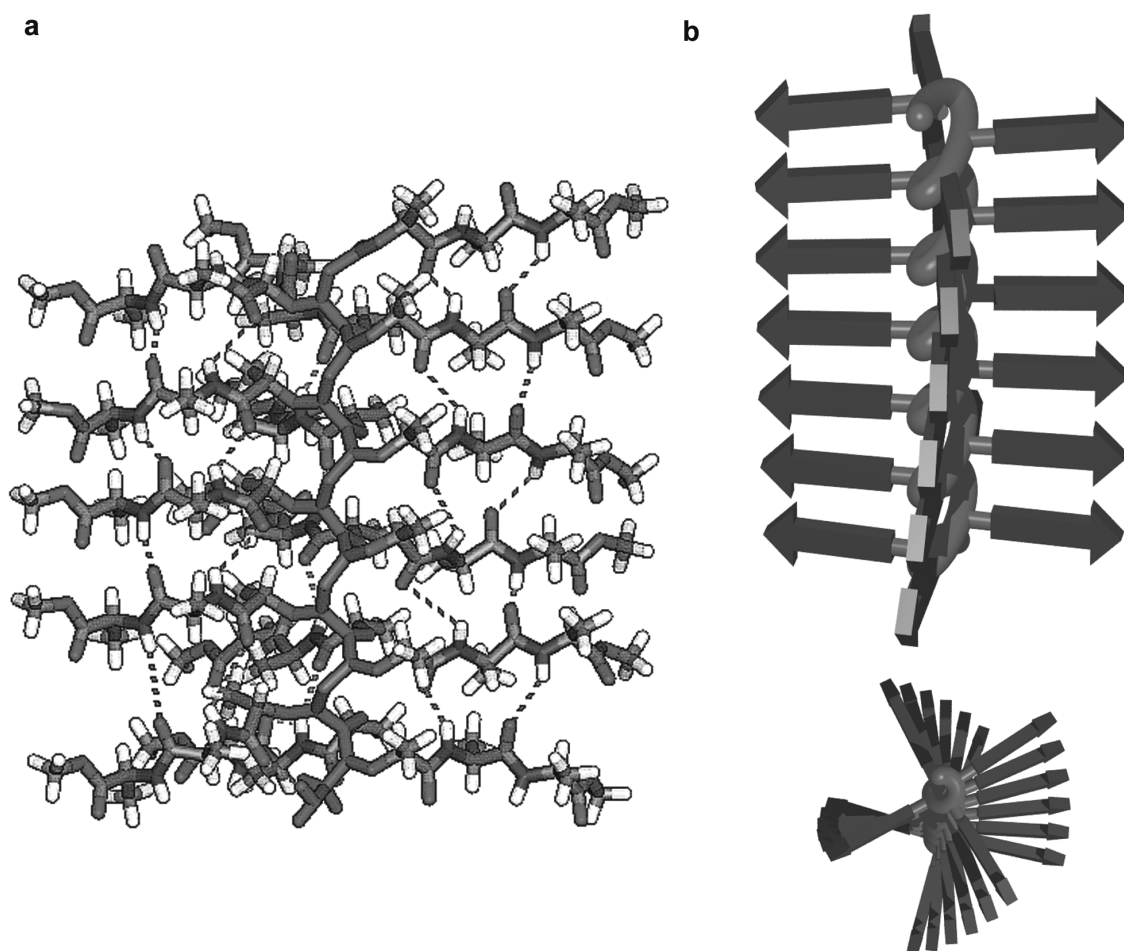
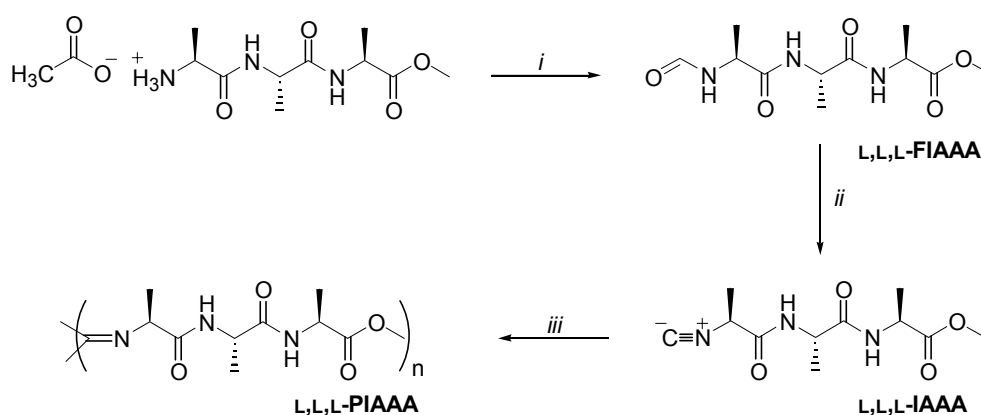


**Figure 1** (a) Calculated structure of a 24 residue long *L,L,L*-PIAAA chain; the dashed lines indicate the hydrogen bonds. One strand of the side chains (the one towards the viewer) is not displayed to give a clearer view on the polymeric back bone. (b) Schematic model showing the helical back bone and the  $\beta$ -strands. Top: side view highlighting the stacked arrangement of the  $\beta$ -strands. Bottom: top view.

poly(phenylisocyanide) the helical backbone slowly uncoils upon standing in solution.<sup>12</sup> The helix sense of the backbone can be controlled by using either optically active monomers, or a chiral catalyst.<sup>13</sup> Enantiopure isocyanides can be obtained easily from amino acids and peptides.<sup>14,15</sup> In the previous chapter it has been shown that in polymers of isocyanopeptides an array of hydrogen bonds between the amide groups in parallel side chains along the helical backbone is present. Each side chain in these polyisocyanopeptides can be regarded as an individual  $\beta$ -strand, and the overall arrangement of the side chains leads to a helical  $\beta$ -sheet-like organization. If a tripeptide-derived isocyanide, i.e. *L*-isocyanoalanyl-*L*-alanine-*L*-alanine methyl ester, *L,L,L*-IAAA is used, the  $\beta$ -strand will be extended with an extra amino acid. In the first

part of this chapter the synthesis and properties of this polyisocyanotriptide (**L,L,L-PIAAA**) are described. In the second part the  $\beta$ -helical organization of the deprotected side chains of this polymer in water will be discussed and compared with the organization of the side chains in the dipeptide derived polyisocyanides **L,L-** and **L,D-PIAA**.



**Scheme 1** Synthesis of polyisocyanotriptide **L,L,L-PIAAA**. (i)  $\text{HCO}_2\text{C}_2\text{H}_5$ , reflux; (ii)  $\text{SOCl}_2$ , DMF; (iii)  $\text{Ni}(\text{ClO}_4)_2 \cdot 6\text{H}_2\text{O}$ ,  $\text{CH}_2\text{Cl}_2/\text{EtOH}$  (117/1 v/v).

## 4.2 Results and Discussion

### 4.2.1 Synthesis and characterization of **L,L,L-PIAAA**

The synthesis of tripeptide based polyisocyanide **L,L,L-PIAAA** is depicted in Scheme 1. Starting from  $\text{CH}_3\text{COOH} \cdot \text{H}_2\text{N-L-Ala-L-Ala-L-Ala-OMe}$  the formamide (**L,L,L-FIAAA**) was obtained by refluxing a suspension of the tripeptide in ethyl formate. In contrast to the procedures for the formylation of ammonium chloride salts,<sup>16</sup> no base was needed in this case to obtain **L,L,L-FIAAA** in quantitative yield. The low solubility of the formamide in chlorinated solvents, which are required for the dehydration of the *N*-formyl group using phosphoryl chloride or disphosgene,<sup>17</sup> prevented the use of these procedures. Employing a Vilsmeier-Haack type chloroiminium ion as the reagent, this dehydration reaction could be performed in DMF (a moderate solvent for **L,L,L-FIAAA**) following a procedure developed by Walborski and Niznik<sup>18</sup> which gave the desired isocyanide (**L,L,L-IAAA**) in low yields (10 – 13%). This monomer was polymerized in  $\text{CH}_2\text{Cl}_2$  using 1/30 equivalents of  $\text{Ni}(\text{ClO}_4)_2 \cdot 6\text{H}_2\text{O}$  as a catalyst; according to TLC this



reaction was complete in less than 10 min. giving the polyisocyanotriptide in ~ 70% yield.

**Table 1. Selected data of L,L,L-IAAA and L,L,L-PIAAA**

	monomer		polymer	
	CDCl <sub>3</sub>	KBr	CDCl <sub>3</sub>	KBr
$\nu_{\text{NH}}^{\text{a}}$	3420 <sup>b</sup>	3315 3285	3290 3260	3300 3267
$\nu_{\text{amideI}}^{\text{a}}$	1675	1647	1648	1651
$\nu_{\text{amideII}}^{\text{a}}$	1511	1549	1536	1537
$\delta_{\text{NH}}^{\text{c}}$		7.04 6.38		9.5 7.8
$[\alpha]^{\text{d}}$		2.4		188
Mol. weight	255 g/mol <sup>e</sup>		290 kg/mol PDI = 1.6 <sup>f</sup>	

<sup>a</sup>In cm<sup>-1</sup>. <sup>b</sup>In a non-hydrogen bonded state only one signal is observed for both NH vibrations. <sup>c</sup>In ppm, measured in CDCl<sub>3</sub>. <sup>d</sup>In °·dl/g·dm, see experimental for measuring conditions. <sup>e</sup>Determined by EI-MS.

<sup>f</sup>Determined by AFM

The formamide and isocyanide were identified using spectroscopic techniques, and also the formation of the polymer was apparent from IR and <sup>1</sup>H NMR spectroscopy. Selected spectral data for both the monomer and polymer are presented in Table 1. From the shifts of the amide vibrations in the IR spectra, the formation of hydrogen bonds between both amide functionalities present in each side chain is evident. Going from the monomer to the polymer both in solution and in the solid state, a significant shift of  $\Delta\nu_{\text{NH}} = 120 - 160 \text{ cm}^{-1}$  in the NH stretching vibrations of the polymer was found, indicating that during polymerization hydrogen bonds are formed (Figure 2). As expected also the polymer amide I and amide II vibrations were shifted compared to those present in the monomers.<sup>16</sup> In the <sup>1</sup>H NMR spectra of the monomer and the polymer the NH resonances appeared as well-resolved signals exhibiting a displacement of the chemical shift of  $\Delta\delta = 2.4 - 1.5 \text{ ppm}$  upon polymerization, which is in line with the formation of hydrogen bonds between the side chains (Table 1). For both amide groups relatively sharp signals were observed and no sign of non-hydrogen bonded amide functionalities could be detected.

The optical rotation, expressed per repeat unit, increased substantially going from the monomer to the polymer. This is attributed to the formation of a helical secondary macromolecular structure as was found for different polyisocyanopeptides reported previously.<sup>14-16,19</sup> The individual macromolecules of **L,L,L-PIAAA** could be visualized by Atomic Force Microscopy (AFM), pointing to a rigid conformation as a result of the hydrogen bonds between the side chains. Measuring the contour length of the polymers permitted the determination of the molecular weights<sup>20</sup> (Table 1) as has also been done for the dipeptide derived polyisocyanides.<sup>16</sup>

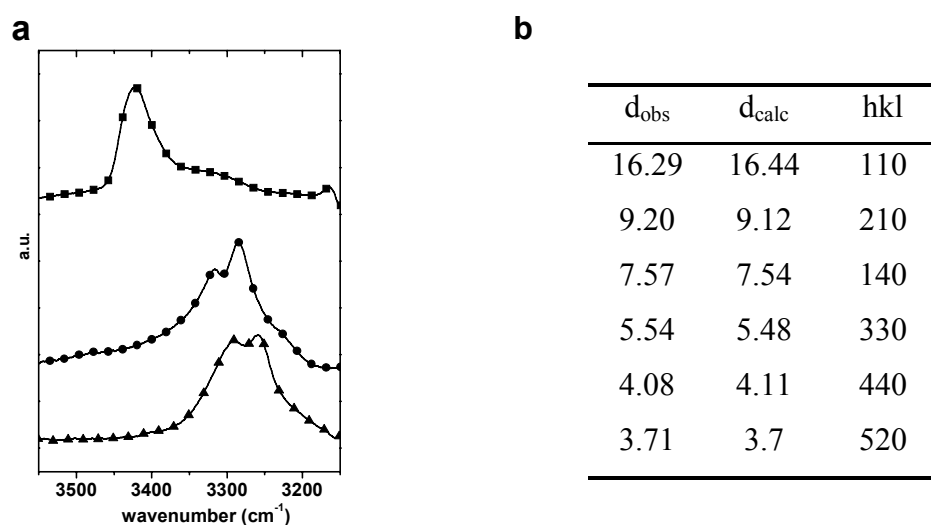


**Figure 2** (a) IR spectra of the NH stretching vibrations of **L,L,L-IAAA** in  $\text{CHCl}_3$  (squares) and **L,L,L-PIAAA** in  $\text{KBr}$  (circles) and  $\text{CHCl}_3$  (triangles). (b) Indexation of the reflections found in the PXR D based on an orthorhombic lattice with  $a = 19.0 \text{ \AA}$  and  $b = 32.9 \text{ \AA}$ .

#### 4.2.2 Conformational analysis of **L,L,L-PIAAA**

Using the parameters obtained for the alanine based dipeptide derived polyisocyanides as input (see Chapter 3), the macromolecular structure of **L,L,L-PIAAA** was calculated (Figure 1a). The most favorable geometry was an extended  $4_1$  helix, having a pitch of  $4.6 \text{ \AA}$  and a diameter of  $18.9 - 19.2 \text{ \AA}$ , which results in a distance between side chains  $n$  and  $(n + 4)$  of  $4.7 \text{ \AA}$ .

From Powder X-Ray Diffraction (PXR D) performed on a sample cast from  $\text{CHCl}_3$  solution a macromolecular diameter of  $19.0 \text{ \AA}$  was obtained, in good agreement with the calculated values. The obtained diffraction pattern displayed sharp signals, comparable to those observed for the related polyisocyanodipeptides, which could be assigned to an orthorhombic ordering of the macromolecules. The defined PXR D

pattern obtained for this polyisocyanotripeptide in combination with the spectroscopic results which indicated that all amide functionalities are involved in hydrogen bonding, points to a defined arrangement of the polymer side chains.<sup>21</sup> As a direct consequence the  $^1\text{H}$  NMR spectra of the former polyisocyanopeptide were better resolved than those of the dipeptide polymers, allowing the study of the side chain arrangement by NOE spectroscopy. In Figure 3a the NOESY spectrum of **L,L,L-PIAAA** is displayed. Figure 3b shows contacts that originate from the organization within the macromolecules, since these contacts were not found in a comparable sample of the monomer. The  $\alpha$  proton ( $\text{H}^1$ ) of the first alanine residue of the side chain  $n$  exhibits a NOE with the first amide proton ( $\text{H}^3$ ) and the  $\alpha$  proton ( $\text{H}^4$ ) of the second alanine unit of a side chain in the next turn. In addition, NOE effects are also observed between  $\text{H}^6$  and  $\text{H}^7$  and the methyl ester protons ( $\text{H}^9$ ). Calculations in combination with the PXRD data clearly showed that such contacts are only possible between stacked side chains in an  $n / (n + 4)$   $\beta$ -sheet-like organization (Figure 1).

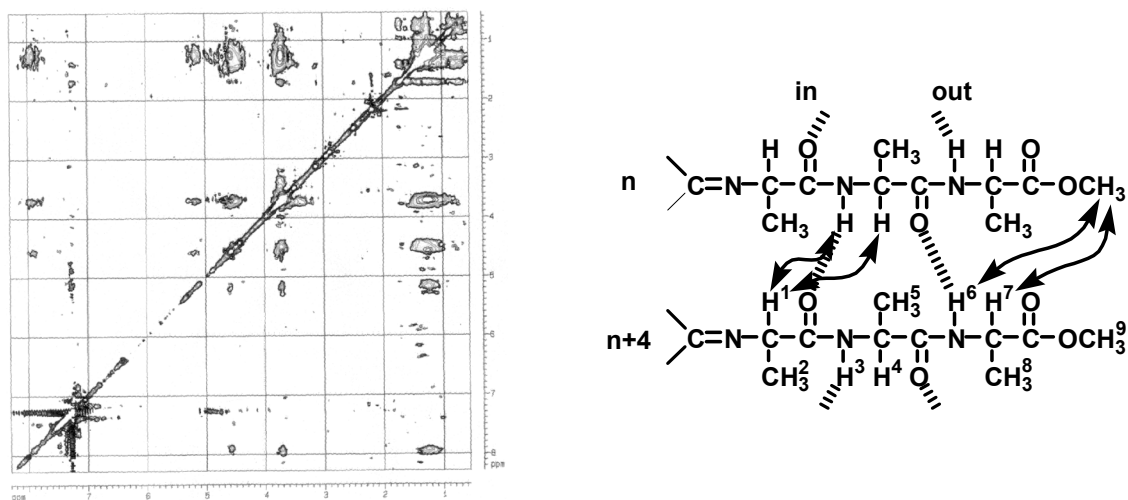


**Figure 3** (left) 2D NOE spectrum of **L,L,L-PIAAA** in  $\text{CDCl}_3$ . (right) Interactions found between side chains  $n$  and  $n + 4$ , which are stacked above each other.

Since **L,L,L-PIAAA** was built from an optically pure monomer an excess of either left- or right-handed  $\beta$ -helical polymers was expected. Therefore CD spectroscopy was used to further investigate this compound. In line with the results obtained for other polyisocyanopeptides having a defined hydrogen bonding array along the polymeric back bone, a strong positive Cotton effect was measured centered at 321 nm where the  $n\text{-}\pi^*$  transitions of the imine functions occur (Figure 4). This Cotton

effect corresponded to a shoulder on a larger absorption band in the UV/vis spectra.<sup>15</sup> Extrapolation of this similarity, taking into account the (*S*)-configuration of the L-alanine unit closest to the polymeric backbone, allowed the assignment of a *P* type helix to **L,L,L-PIAAA**.<sup>21</sup> The observed value of  $\Delta\epsilon_{\max} = 2.5$  l/mol·cm was approximately half the intensity of the values found for the polyisocyanodipeptides ( $\Delta\epsilon_{\max} = 5.1 - 5.8$  l/mol·cm). The alignment of the amide carbonyls due to the hydrogen bonding arrays in the side chains and the effect of this on the resulting permanent dipole may explain this difference. In the dipeptide polymers, only a single amide group is present in each side chain and the individual contributions of the amide groups will add up to form this permanent dipole. The tripeptide also contains a second amide function, which is likely to point in the opposite direction when compared to the first one<sup>3</sup> and therewith reduces the magnitude of the permanent dipole originating from the hydrogen bonding arrays. Since the presence of this dipole was used to tentatively explain the relatively strong Cotton effects around 315 nm observed for polyisocyanopeptides having hydrogen bonding arrays along the polymeric backbone (see Chapter 3), a decrease in the magnitude of this dipole is expected to result in less intense CD effects at this wavelength.

**Disruption of the hydrogen bonding arrays.** Similar to the denaturation of proteins the hydrogen bonding patterns in **L,L,L-PIAAA** could be disturbed by the addition of strong acid (trifluoroacetic acid, TFA) or by increasing the temperature. The intense Cotton effects in the CD spectra reflect the defined hydrogen bonding arrays so the disruption processes could be followed by monitoring the changes in the CD spectra. In Figure 4a the effect of acid on the CD spectra of **L,L,L-PIAAA** is shown; upon the addition of TFA the 321 nm CD band gradually decreased and a new band centered around 360 nm appeared with an isodichroic point at 345 nm. These results indicate that the breaking of the hydrogen bonds leads to a slow transition of one discrete conformation into another. Identical changes in the CD spectra of **L,L,L-PIAAA** were found when the temperature of the sample was increased (Figure 4b), indicating that these co-operative processes indeed are the result of the breaking of the hydrogen bonds and not from protonation of the polymer. Initial variable temperature (VT) <sup>1</sup>H NMR experiments showed that only the outer one of the two hydrogen bonding arrays ( $\delta = 7.8$

ppm, Table 1; Figure 3b) became disrupted, whilst the inner one remained initially unchanged.

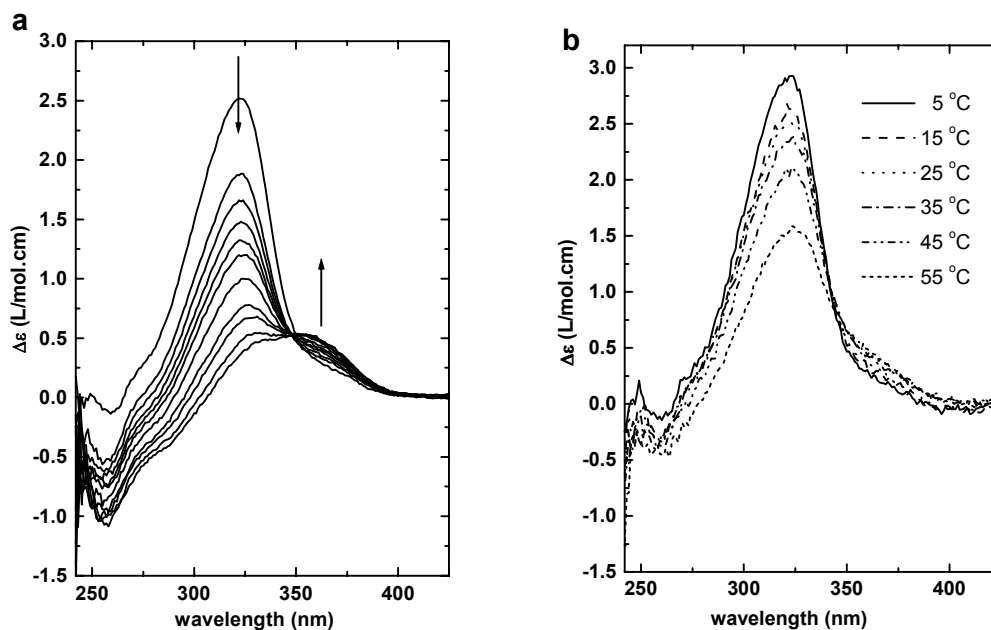


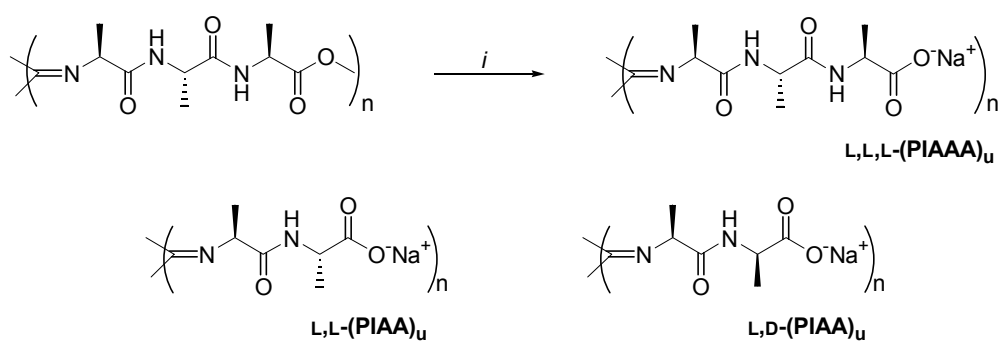
**Figure 4** CD spectra of *L,L,L*-PIAAA upon disruption of the hydrogen bonding arrays, (a) by addition of 0.2 ml TFA to a 0.22 mg/ml (0.85 mM expressed per repeat unit) polymer solution, a spectrum was recorded every 2.5 min.; (b) by increasing the temperature.

For some of the investigated polyisocyanodipeptides having hydrogen bonding arrays along the polymeric backbone a cholesteric lyotropic liquid crystalline mesophase was found at high concentrations in chloroform solutions ( $> 10\%$  w/w).<sup>21</sup> Also in the case of the tripeptide derived polyisocyanide such a mesophase was observed. The characteristic fingerprint texture was slowly formed when a solution of the polymer was placed between crossed polarizers. Also the optical rotation changed sign at high concentration and increased an order of magnitude compared to the one measured for the polymer in dilute solution. When, however, a sample in which the hydrogen bonds were disrupted was investigated no such LC behavior was observed.

#### 4.2.3 Retention of the $\beta$ -helical architecture in an aqueous environment

The folding of peptides in water is dictated by a well-defined set of secondary interactions involving hydrogen bonds, van der Waals interactions, and hydrophobic effects. It has been notoriously difficult to achieve well-defined conformations of

synthetic oligomers and polymers stabilized by hydrogen bonds in aqueous solution.<sup>7,22</sup> To investigate whether the present  $\beta$ -helical polymer would retain its structure in aqueous solution the methyl ester functions in the side chains were removed with base to yield a water soluble polyisocyanopeptide (Scheme 2).



**Scheme 2** Hydrolysis of the polyisocyanopeptides to the water soluble sodium salts. (i) NaOH, H<sub>2</sub>O, 2 days.

**Table 2. Selected IR and <sup>1</sup>H NMR data of hydrolyzed polymers**

	$\nu_{\text{NH}}^a$	$\nu_{\text{amideI}}^a$	$\nu_{\text{amideII}}^a$	$\delta_{\text{NH}}^b$ [T <sub>1/2</sub> ] <sup>c</sup>
<b>L,L-(PIAA)<sub>u</sub></b>	3288 <sup>d</sup>	1647	1537	8.8 <sup>e</sup> [>24]
<b>L,D-(PIAA)<sub>u</sub></b>	3304 <sup>d</sup>	1647	1527	8.3 [>24]
<b>L,L,L-(PIAAA)<sub>u</sub></b>	3305 <sup>d</sup>	1653	1528	8.2 [>18] <sup>f</sup>

<sup>a</sup>In cm<sup>-1</sup>. <sup>b</sup>In ppm. <sup>c</sup>Estimated half-life time for H/D exchange in hours.

<sup>d</sup>Appearing as a shoulder on a larger peak. <sup>e</sup>Split signals average values are given.

<sup>f</sup>After 48 hours a residual broad NH signal remained which we attribute to the non-exchanging inner amide protons. All measurements were performed at room temperature.

For comparison the unprotected polyisocyanodipeptides **L,L-** and **L,D-(PIAA)<sub>u</sub>** were also prepared and studied. No significant shifts in the positions of the amide I and II absorption bands were observed after the treatment of **L,L,L-(PIAAA)<sub>u</sub>** with aqueous base (Table 2), indicating that the amide hydrogen bonds between the side chains remain intact. Strong evidence for the retention of the hydrogen bonds in aqueous solution came from <sup>1</sup>H NMR experiments. The exchange of the NH protons for deuterium in D<sub>2</sub>O was slow as expected for protons participating in hydrogen bonds

(Table 2).<sup>23</sup> VT <sup>1</sup>H NMR spectroscopy further confirmed the presence of such hydrogen bonds; a shift of the NH resonances towards higher field was observed in D<sub>2</sub>O upon increasing the temperature. NOESY experiments (conc. ~ 40 mM expressed per repeat unit) indicated that several protons in the side chains were in close proximity. However, due to the high viscosity of even dilute solutions, and the resulting anisotropy of the sample, no definite assignments of inter and intra side chain contacts could be made.

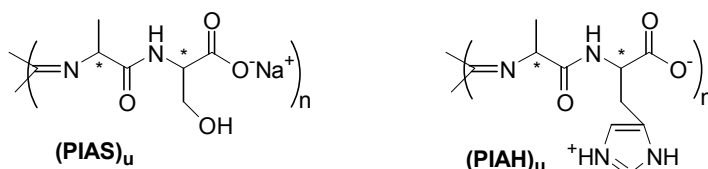


**Table 3** pK<sub>a</sub> values of polyisocyanodipeptides and model compounds

	pK <sub>a</sub> (COOH)	pK <sub>a</sub> (ImH <sup>+</sup> )
L,L-(PIAA) <sub>u</sub>	5.6	
L,D-(PIAA) <sub>u</sub>	5.9	
L,L-(PIAS) <sub>u</sub> <sup>a</sup>	5.2	
L,D-(PIAS) <sub>u</sub> <sup>a</sup>	4.9	
L,L-(PIAH) <sub>u</sub> <sup>b</sup>	2.9	9.4
D,L-(PIAH) <sub>u</sub> <sup>b</sup>	2.3	8.4
poly(histidine) <sup>b</sup>	-	5.9
histidine <sup>b</sup>	1.8	6.0

<sup>a</sup>Taken from ref.15. <sup>b</sup>Taken from ref. 14.

The pK<sub>a</sub> values of the carboxylic acid groups in the polyisocyanides L,L- and L,D-(PIAA)<sub>u</sub> were determined by titrating the acidified samples (aq. HCl) with NaOH. The obtained values were compared with those reported previously for other polyisocyanodipeptides (Table 3). It is noticed that the pK<sub>a</sub>'s of the (PIAA)<sub>u</sub>'s are substantially higher than those of the constituent amino acids, a phenomenon also observed for (PIAS)<sub>u</sub> and (PIAH)<sub>u</sub>. The close packing of the charged groups and the possible interactions between these functionalities can explain these increased values, which are correlated to the defined arrangement of the side chains. Indeed, for polymers not having the β-sheet-like hydrogen bonding arrays in organic solvents (i.e. L,D-PIAS

and **D,L-PIAH**)<sup>21</sup> the corresponding water soluble macromolecules display  $pK_a$  values that are closer to the ones observed for the amino acids than the  $pK_a$  values found for the water soluble polyisocyanodipeptides that do have this hydrogen bonding arrangement. Because the  $\beta$ -sheet-like hydrogen bonding arrays are formed with the help of the directing nickel catalyst, the presence or absence of these arrays is determined during the polymerization process. This is expected not to change during conversion to the water-soluble equivalents.

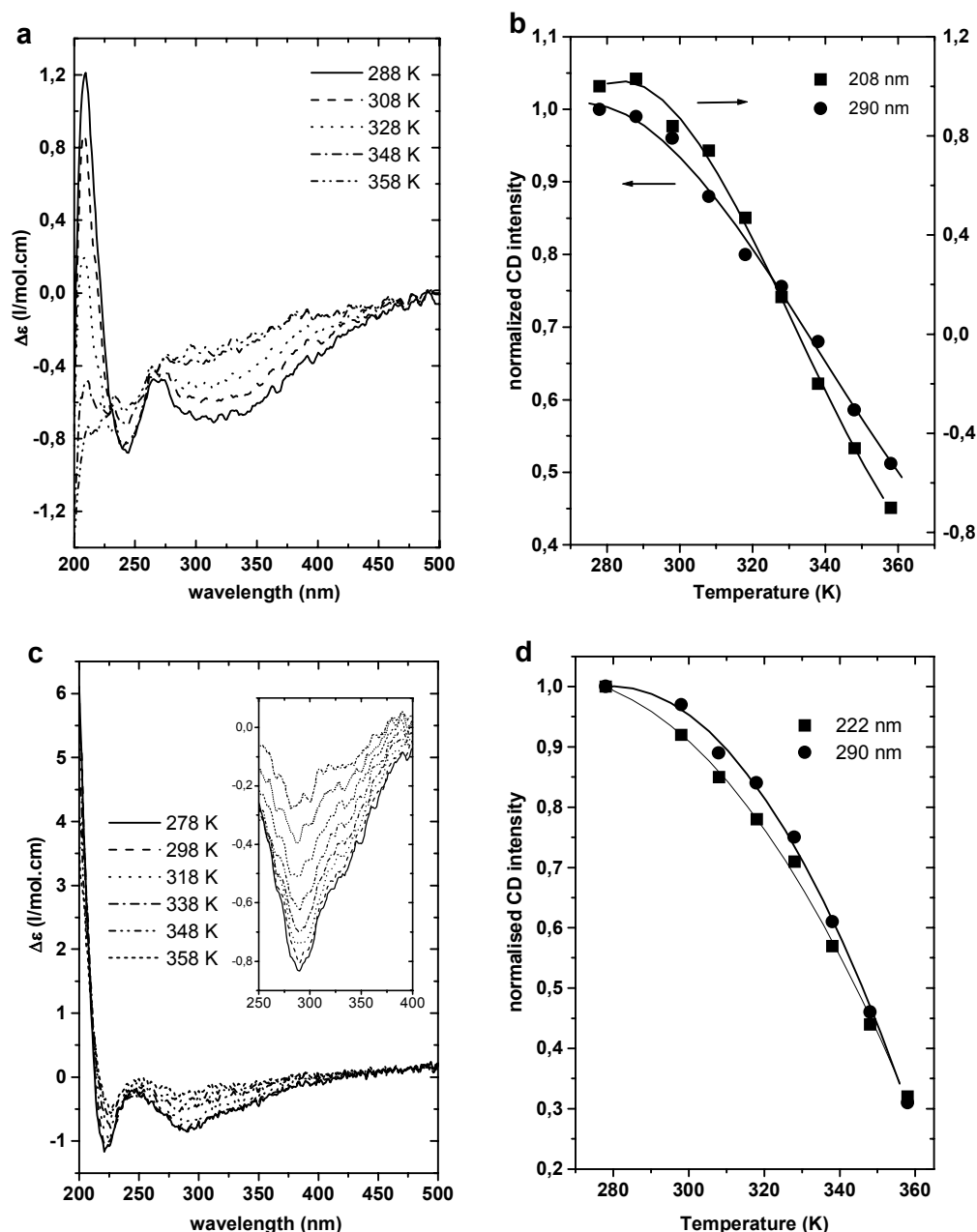


**Figure 5** CD spectra at different temperatures in water for (a)  $L,L$ -(PIAA)<sub>u</sub> and (b) the normalized decrease in  $\Delta\epsilon$  as function of temperature, (c) and (d) *idem* for  $L,D$ -(PIAA)



CD spectroscopy was also used to investigate the structural properties of the  $\beta$ -helical polymers in water. The broader spectral window available in this solvent, as compared to  $\text{CHCl}_3$  which was used for the protected macromolecules, also enabled the amide region of the polyisocyanopeptides to be studied. A negative CD signal was found due to the imine  $n\text{-}\pi^*$  transitions residing between 260 nm and 400 nm (Figures 5 and 6), for both  $L,L$ - and  $L,D$ - $(\text{PIAA})_n$  as well as for  $L,L,L$ - $(\text{PIAAA})_n$ . The CD-bands in the region between 200 nm and 260 nm could be assigned to the amide groups present in the side chains and, as expected, these bands were different for the three polymers investigated.

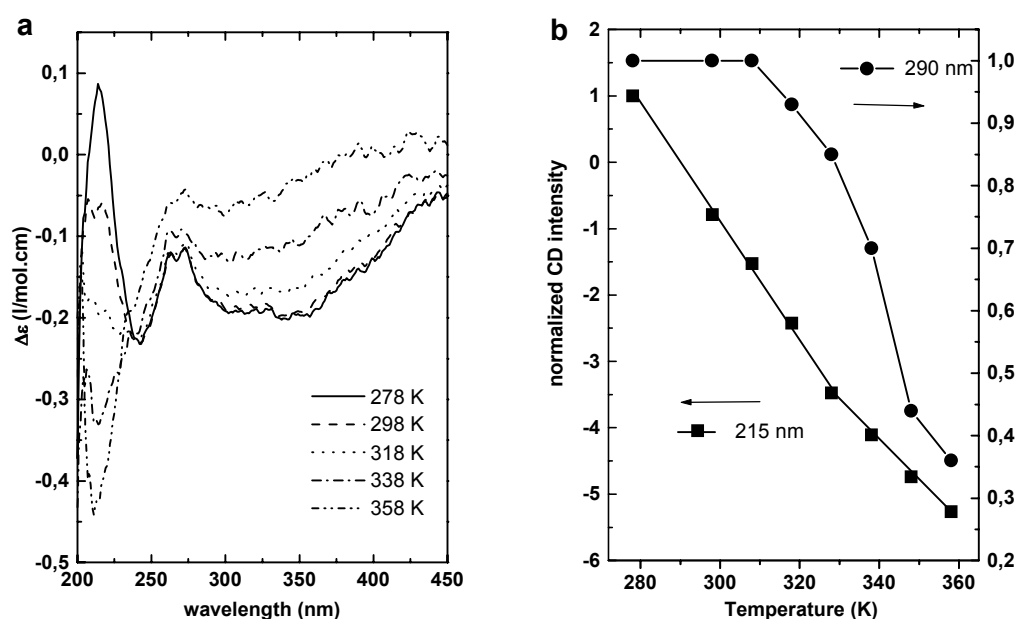
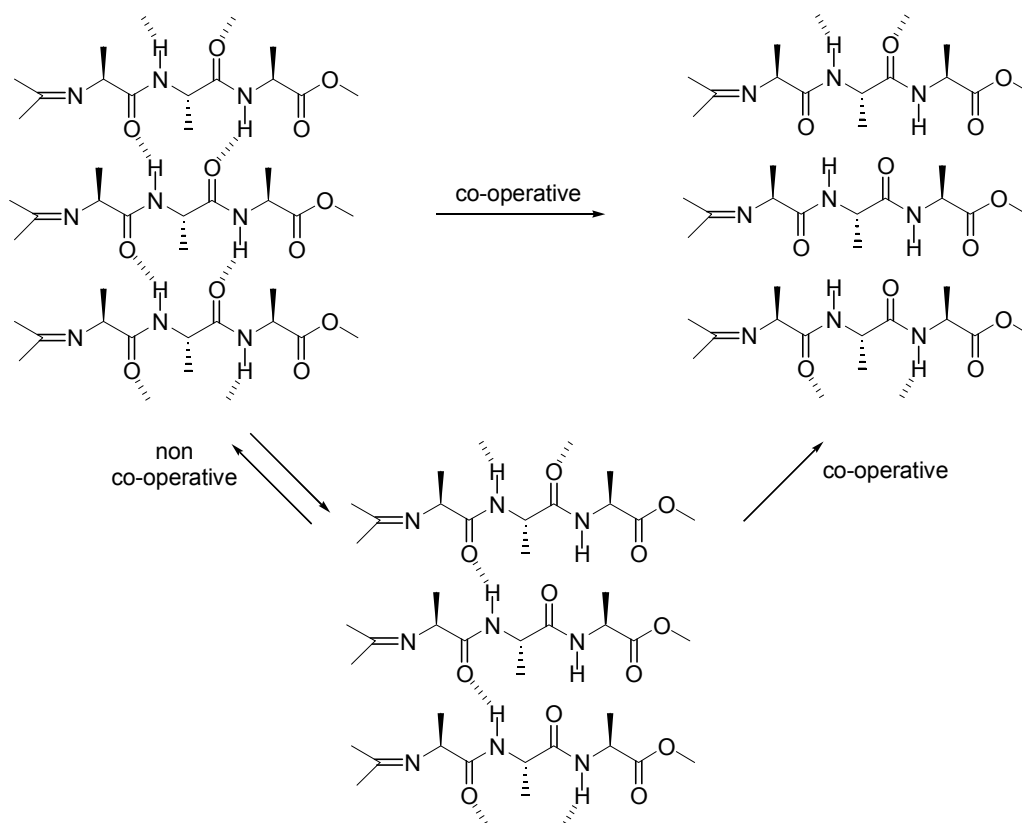


**Figure 6** CD spectra at different temperatures in water for (a)  $L,L,L$ - $(\text{PIAAA})_n$  and (b) the normalized decrease in  $\Delta\epsilon$  as function of temperature.

VT CD experiments showed that high structural order is present at room temperature and below, but that this order is lost at elevated temperatures. Dilution studies indicated that the observed CD effects are not the result of aggregation, but are inherent to the macromolecular architecture. The observed non-linear decrease in intensity in the imine region was attributed to the co-operative unwinding of the helical backbone for all  $\beta$ -helical polymers investigated (Figures 5 and 6). This unfolding of the polyisocyanopeptides was found to be irreversible as in the case of proteins, i.e. once unfolded the helical geometry was not recovered and only local order of the side chains was regained. This feature can be understood from the mechanism of the polymerisation reaction. During polymerisation the isocyanide monomers are knitted together by a

series of consecutive insertion reactions which take place in a circular manner around a square planar nickel centre. One rotation around the nickel adds one turn to the helix, in a ‘merry-go-round’ like fashion.<sup>6</sup> The resulting polymer is the kinetically-controlled product of the reaction. After unwinding by thermal treatment it would be difficult entropically for the polyisocyanopeptide chains to refold into the original  $\beta$ -helical



**Scheme 3** Different pathways of hydrogen bond breaking, it is unlikely that these processes can be regarded separately.

structure without the help of the directing nickel template. The observed changes in the spectra in the amide region during the VT experiments also supported the co-operative unwinding of the polymer chains upon increasing temperature. After cooling to 298 K ca. 20% of the original intensity was recovered showing that the helix cannot completely refold into its native state. The behavior was more complex in the case of the tripeptide polymer. The decrease in the amide CD band appeared to be linear with increasing temperature in contrast to the S-shaped curve observed for the CD band of the imines (Figure 6b). It has been previously proposed that the formation and disruption of hydrogen bonds in  $\beta$ -sheets is a complex process which proceeds co-operatively in a direction perpendicular to the strand,<sup>24</sup> but it may not be co-operative

along the strand direction (Scheme 3). It is possible that in the tripeptide polymer a similar dual mechanism is operative: a non-cooperative one on initial heating, and a co-operative one on further heating, leading to the observed VT curve at 215 nm. The curve at 290 nm clearly reveals that the unwinding of the helix is an overall co-operative process, linked to the breaking of the inner hydrogen bonded array.

### 4.3 Conclusions

An optically pure isocyanide derived from an L-alanine based tripeptide has been prepared via a procedure carried out in DMF. This monomer was subsequently polymerized using a Ni(II) catalyst yielding a polymer in which well-defined arrays of intramolecular hydrogen bonds are present between side chains  $n$  and  $(n + 4)$ . Both amide functionalities present in each side chain are involved in this hydrogen bonding pattern resulting in a highly defined macromolecular geometry.

The helical backbone of this polyisocyanopeptide acts as a highly efficient scaffold for the organization of  $\beta$ -strands. For dipeptide derived polymers discussed in Chapter 3 and for the polyisocyanotripeptide reported here it was shown that in organic solvents a well-defined  $\beta$ -sheet-like organization of the side chains is present. Studies in water revealed that for the polymers studied in this chapter these hydrogen bonds persist in this solvent, while the co-operative unfolding upon increasing temperature confirms the higher structural order present in the macromolecules.

These remarkably defined and rigid, high molecular weight polymers can be considered as structural and functional mimics of naturally occurring  $\beta$ -sheet-helices. The co-operative behavior of the hydrogen bonding network in these peptide polymers in combination with the availability of numerous (un)natural amino acids, allows their architecture and ultimately their properties to be finely tuned. Applications of these macromolecules as scaffolds for the organization of functional groups, for example as templates for directing crystal growth as is currently under investigation,<sup>25</sup> can be foreseen.

## 4.4 Experimental Section

### 4.4.1 General methods and materials

Dichloromethane was distilled from CaH<sub>2</sub> (under atmospheric pressure), thionyl chloride and DMF (after stirring for 7 days on CaO) were distilled under reduced pressure. All other chemicals were commercial products and were used as received. Flash chromatography was performed using silica gel (0.035-0.075 mm) purchased from Acros and TLC analyses on silica 60 F<sub>254</sub> coated glass either from Merck or Acros. Compounds were visualized with I<sub>2</sub>-vapour or Cl<sub>2</sub>/TDM. <sup>1</sup>H NMR spectra were recorded Bruker WM-500 and Bruker AC-300 instruments at 297 K, <sup>13</sup>C NMR spectra were acquired on a Bruker AC-300 spectrometer. Chemical shifts are reported in ppm relative to tetramethylsilane (δ = 0.00 ppm) as an internal standard. FT-Infrared spectra were recorded on a Bio-Rad FTS 25 instrument (resolution 2 cm<sup>-1</sup>), melting points were measured using a Büchi capillary melting point apparatus or a Jeneval THMS 600 microscope equipped with a Linkam 92 temperature control unit and are reported uncorrected. Mass spectrometry (EI) was performed on a VG 7070E instrument, elemental analyses were determined on a Carlo Erba 1180 instrument. Optical rotations were measured on a Perkin Elmer 241 polarimeter. UV/Vis spectra were measured on a Varian Cary 50 conc spectrophotometer and CD spectra on a JASCO 810 instrument. X-ray powder diffractograms were collected on a Philips PW1710 diffractometer equipped with a Cu LFF X-ray tube operating at 40 kV and 55 mA. Samples were measured on a silicon wafer between 3 and 60°, using a step width of 0.05°. Optical micrographs between cross polarizers were obtained on a Jeneval THMS 600 microscope.

**Atomic Force Microscopy.** Imaging was carried out on a Nanoscope III from Digital Instruments operating in the tapping mode at room temperature. The sample was prepared by spin coating (1800 rpm) a 0.01 g/l polymer solution on freshly cleaved mica. It appeared useful to slightly heat the mica just before and after spin coating, to improve the quality of the samples. It was assumed that the overestimation of the length of the polymers, because of the tip shape, was equal to the overestimation of the width.

**CD spectroscopy.** CD spectra were recorded at ambient concentration either in CHCl<sub>3</sub> or water (Milli-Q). During the temperature dependent measurements after each interval the solution was equilibrated for 10 min.

### 4.4.2 Synthesis.

CH<sub>3</sub>COOH·H<sub>2</sub>N-L-Ala-L-Ala-L-AlaOMe was a commercially available product. The synthesis of L,L- and L,D-PIAA has been described in Chapter 2 of this thesis.<sup>16</sup>

**N-formyl-L-alanyl-L-alanyl-L-alanine methyl ester (L,L,L-FAAA).** A suspension of 1.4 g (4.6 mmol) CH<sub>3</sub>COOH·H<sub>2</sub>N-L-alanyl-L-alanyl-L-alanine methyl ester in 100 ml ethyl formate was refluxed for 14 hrs. and subsequently evaporated to dryness. The resulting white powder was washed twice with diisopropyl

ether and dried in vacuo, yield 1.25 g (100 %). Mp: 218-219 °C (dec).  $[\alpha]_D$  (CHCl<sub>3</sub>/MeOH 5/2 *c* 0.2) = -99.2°. <sup>1</sup>H NMR (δ, DMSO-D<sub>6</sub>, 300 MHz): 8.22 (m, 2H, NH), 8.04 (d, 1H, NH, *J* = 7.5 Hz), 7.96 (s, 1H, HCO), 4.40-4.19 (m, 3H, CH), 3.60 (s, 3H, OCH<sub>3</sub>), 1.26 (d, 3H, CH<sub>3</sub>, *J* = 7.3 Hz), 1.20 (d, 3H, CH<sub>3</sub>, *J* = 7.6 Hz), 1.17 (d, 3H, CH<sub>3</sub>, *J* = 7.6 Hz). <sup>13</sup>C NMR (δ, DMSO-D<sub>6</sub>, 75 MHz): δ = 173.2, 172.3, 171.6 (C=O), 160.9 (HC=O), 52.1, 47.9 (CH), 47.7 (OCH<sub>3</sub>), 46.8 (CH), 18.7, 18.3, 17.0 (CH<sub>3</sub>). FT-IR (cm<sup>-1</sup>, KBr): 3299, 3264 (NH), 1755 (C=O ester), 1666, 1633 (amide I), 1552, 1535 (amide II). EI-MS: *m/z* = 274 [M+H]<sup>+</sup>, El. Anal. Calcd. for C<sub>11</sub>H<sub>19</sub>N<sub>3</sub>O<sub>5</sub>: C, 48.34 %; H, 7.01 %; N, 15.38 %. Found: C, 48.46 %; H, 7.05 %; N, 15.11 %.

**L-Isocyanoalanyl-L-alanyl-L-alanine methyl ester (L,L,L-IAAA).** In 37 ml freshly distilled DMF was dissolved 0.75 g (2.7 mmol) FAAA by gentle heating. The solution was cooled to -60 °C and slowly a solution of 1.15 ml (16.2 mmol, 6 eq.) SOCl<sub>2</sub> in 6 ml DMF was added, while keeping the temperature at -60 °C. After the addition was complete the cooling bath was removed and the solution was allowed to warm to -35 °C. The bath was replaced and while keeping the temperature below -45 °C, 3.33 g Na<sub>2</sub>CO<sub>3</sub> was added. The resulting red suspension was vigorously stirred for 15 min after which the cooling bath was replaced by an ice bath. After stirring for 4 hrs at 0 °C the reaction mixture was stirred at room temperature for another 16 hrs., diluted with 35 ml CH<sub>2</sub>Cl<sub>2</sub> and quickly washed with 40 ml of iccold water. The aqueous layer was subsequently extracted three times with 25 ml CH<sub>2</sub>Cl<sub>2</sub>. The combined organic fractions were dried using Mg<sub>2</sub>SO<sub>4</sub> and evaporated to dryness. The resulting reddish oil was subjected to column chromatography (eluent: CHCl<sub>3</sub>/acetone 1/1 v/v) resulting in a slightly contaminated isocyanide. Recrystallization from CHCl<sub>3</sub>/diisopropyl ether (1/10) gave the pure compound as a yellow/white powder (yield 94 mg, 13.4 %) Mp: 161 °C (dec).  $[\alpha]_D$  (CDCl<sub>3</sub> *c* 0.3) = 2.4°. <sup>1</sup>H NMR (δ, CDCl<sub>3</sub>, 300 MHz): 7.06 (br, 1H, NH), 6.33 (br, 1H, NH), 4.55 (qn, 1H, CH, *J* = 7.3 Hz), 4.44 (qn, 1H, CH, *J* = 7.0 Hz), 4.27 (q, 1H, CN-CH(CH<sub>3</sub>), *J* = 7.1 Hz), 3.77 (s, 3H, OCH<sub>3</sub>), 1.66 (d, 3H, CN-CH(CH<sub>3</sub>), *J* = 7.1 Hz), 1.45 (d, 3H, CH<sub>3</sub>, *J* = 7.3 Hz), 1.43 (d, 3H, CH<sub>3</sub>, *J* = 7.0 Hz). <sup>13</sup>C NMR (δ, CDCl<sub>3</sub>, 75 MHz): 173.2, 171.4, 166.5 (C=O), 162.2 (CN), 54.1 ((CN-CH(CH<sub>3</sub>)), 53.4 (OCH<sub>3</sub>), 49.9 (CH), 49.0 (CH), 23.6 (CN-CH(CH<sub>3</sub>)), 19.1, 19.0 (CH<sub>3</sub>). FT-IR (cm<sup>-1</sup>, KBr): 3315, 3285 (NH), 2151 (CN), 1747 (C=O ester), 1647 (amide I), 1549 (amide II). EI-MS: *m/z* = 255 [M]<sup>+</sup>, 196 [M - CO<sub>2</sub>CH<sub>3</sub>]<sup>+</sup>, 153 [M - NHCH(CH<sub>3</sub>)CO<sub>2</sub>CH<sub>3</sub>]<sup>+</sup>, 126 [M - CONHCH(CH<sub>3</sub>)CO<sub>2</sub>CH<sub>3</sub>]<sup>+</sup>. El. Anal. Calcd. for C<sub>11</sub>H<sub>17</sub>N<sub>3</sub>O<sub>4</sub>: C, 51.76 %; H, 6.71 %; N, 16.46 %. Found: C, 52.03 %; H, 6.76 %; N, 16.14 %.

**Poly(L-isocyanoalanyl-L-alanyl-L-alanine methyl ester) (L,L,L-PIAAA).** To 60 mg (0.24 mmol) L-isocyanoalanyl-L-alanyl-L-alanine methyl ester (L,L,L-IAAA) in 5 ml CH<sub>2</sub>Cl<sub>2</sub> was added, while stirring, 3.0 mg (0.01 mmol) Ni(ClO<sub>4</sub>)<sub>2</sub>·(H<sub>2</sub>O)<sub>6</sub> in 2.28 ml CH<sub>2</sub>Cl<sub>2</sub> and 0.02 ml ethanol (abs.). The solution turned red/brown immediately and IR showed complete consumption of the isocyanide in a few min. After 5 min the solvents were evaporated and the resulting glassy solid was redissolved in a minimal amount of CHCl<sub>3</sub>. The polymer was precipitated by dropping this solution in 10 ml of methanol/water (3/1 v/v) under vigorous stirring. The product was filtered off and washed with methanol/water (3/1 v/v) until the filtrate remained colorless and than once with methanol. Drying in vacuo gave the polymer as a slightly yellow powder in 72% yield.  $[\alpha]_D$  (CHCl<sub>3</sub>, *c* 0.22) = +188°. <sup>1</sup>H NMR (δ ppm, CDCl<sub>3</sub>, 300 MHz): 9.5 (br,

1H, NH), 7.8 (br, 1H, NH), 5.4 – 4.9 (br, 1H, CH), 4.9 – 4.0 (br, 2H, CH), 3.7 (s, 3H, OCH<sub>3</sub>), 2.2 – 1.4 (br, 3H, CH<sub>3</sub>), 1.4 – 0.9 (br, 6H, CH<sub>3</sub>). FT-IR (cm<sup>-1</sup>, KBr): 3300, 3276 (NH), 1749 (C=O ester), 1651 (amide I), 1537 (amide II), the imine stretching vibration was obscured by the amide I.

**Hydrolysis of the polyisocyanopeptides.** The general procedure for the formation of the water soluble polyisocyanopeptides consisted of stirring the polymer sample (5 mg/ml) in aqueous 0.5 N NaOH at a maximum temperature of 40 °C until a clear solution was obtained.

**Poly(L-isocyanalanyl-L-alanyl-L-alanine) (L,L,L-(PIAAA)<sub>n</sub>).** <sup>1</sup>H NMR ( $\delta$  ppm, D<sub>2</sub>O, 300 MHz): 8.2 (br, 1H, NH), 5.2 – 4.0 (br, 3H, CH), 2.2 – 1.1 (br, 9H, CH<sub>3</sub>). FT-IR (cm<sup>-1</sup>, KBr): 3550-3200 (OH, H<sub>2</sub>O), 3305 (NH), 1653 (amide I), 1600 (C=O carboxylate), 1528 (amide II).

**Poly(L-isocyanalanyl-L-alanine) (L,L-(PIAA)<sub>n</sub>).** <sup>1</sup>H NMR ( $\delta$  ppm, D<sub>2</sub>O, 300 MHz): 8.8 (br, 1H, NH), 5.4 – 4.1 (br, 2H, CH), 1.9 – 1.1 (br, 6H, CH<sub>3</sub>). FT-IR (cm<sup>-1</sup>, KBr): 3550-3200 (OH, H<sub>2</sub>O), 3288 (NH), 1647 (amide I), 1601 (C=O carboxylate), 1537 (amide II).

**Poly(L-isocyanalanyl-L-alanine) (L,L-(PIAA)<sub>n</sub>).** <sup>1</sup>H NMR ( $\delta$  ppm, D<sub>2</sub>O, 300 MHz): 8.3 (br, 1H, NH), 5.3 – 4.1 (br, 2H, CH), 1.9 – 1.1 (br, 6H, CH<sub>3</sub>). FT-IR (cm<sup>-1</sup>, KBr): 3550-3200 (OH, H<sub>2</sub>O), 3304 (NH), 1647 (amide I), 1600 (C=O carboxylate), 1527 (amide II).

#### 4.5 References and Notes

1. Pauling, L., Corey, R. B. & Branson, H.R. *Proc. Natl. Acad. Sci. U.S.A.* **37**, 205-211 (1951).
2. Pauling, L. & Corey, R. B. *Proc. Natl. Acad. Sci. U.S.A.* **37**, 729-740 (1951).
3. Yoder, M.D., Keen, N.T. & Jurnak F. *Science* **260**, 1503-1507 (1993).
4. Branden, C. & Tooze, J. *Introduction to Protein Structure*, 2nd ed. (Garland Publishing Inc., New York, 1999).
5. Steinbacher, S. *et al. Science* **265**, 383-386 (1994).
6. Liou, Y.-C., Tocilj, A., Davies, P. L. & Jia, Z. *Nature* **406**, 322-324 (2000) and references cited.
7. Nolte, R. J. M. *Chem. Soc. Rev.* **23**, 11-19 (1994).
8. Gellman, S. H. *Acc. Chem. Res.* **31**, 173-180 (1998) and references cited.
9. Nowick, J. S. *Acc. Chem. Res.* **32**, 287-296 (1999) and references cited.
10. Nolte, R. J. M., Van Beijen, A. J. M. & Drenth, W. *J. Am. Chem. Soc.* **96**, 5932-5933, (1972).
11. Van Beijen, A. J. M. Nolte, R. J. M. & Drenth, W. *Recl. Trav. Chim. Pays-Bas* **99**, 121-123 (1980).
12. Clericuzio, M., Alagona, G., Ghio, G. & Salvadori, P. *J. Am. Chem. Soc.* **119**, 1059-1071 (1997).
13. Green, M. M., Gross, R. A., Schilling, F. C., Zero, K. & Crosby III, C. *Macromolecules* **21**, 1839-1846 (1988).
14. Huang, J.-T., Sun, J., Euler, W. B. & Rosen, W. *J. Polym. Sci., Part A: Polym. Chem.* **35**, 439-446 (1997).
15. Kamer, P. C. J., Nolte, R. J. M. & Drenth, W. *J. Am. Chem. Soc.* **110**, 6818-6825 (1988).
16. Deming, T. J. & Novak, B. M. *J. Am. Chem. Soc.* **114**, 7926-7927 (1992).
17. van der Eijk, J. M., Nolte, R. J. M., Drenth, W. & Hezemans, A. M. F. *Macromolecules* **13**, 1391-1397 (1980).
18. Visser, H. G. J., Nolte, R. J. M., Zwikker, J. W. & Drenth, W. *J. Org. Chem.*, **50**, 3133-3137 (1985).
19. Visser, H. G. J., Nolte, R. J. M., Zwikker, J. W. & Drenth, W. *J. Org. Chem.*, **50**, 3138-3143 (1985).

16. Cornelissen, J. J. L. M., Graswinckel, W. S., Adams, P. J. H. M., Nachtegaal, G., Kentgens, A., Sommerdijk, N. A. J. M., Nolte, R. J. M. submitted for publication. b) Chapter 2 of this thesis.
17. Skorna, G. & Ugi, I. *Angew. Chem.* **89**, 267-268 (1977).
18. Walborsky, H. M., Niznik, G. E. *J. Org. Chem.* **37**, 187 (1972).
19. a) Cornelissen, J. J. L. M., Donners, J. J. J. M., de Gelder, R., Graswinckel, W. S., Rowan, A. E., Sommerdijk, N. A. J. M., Nolte, R. J. M. *Science*, **293**, 676-680 (2001). b) Chapter 3 of this thesis.
20. Prokhorova, S. A., Sheiko, S. S., Möller, M., Ahn, C.-H., Percec, V. *Macromol. Rapid Commun.* **19**, 359 (1998).
21. Chapter 3 of this thesis.
22. a) Tsang, K. Y., Diaz, H., Graciani, H. & Kelly, J. W. *J. Am. Chem. Soc.* **116**, 3988-4005 (1994). b) Hirschberg, J. H. K. K. *et al. Nature* **407**, 167-170 (2000). c) Seebach, D., Jacobi, A., Rueping, M., Gademann, K., Ernst, M. & Jaun B. *Helv. Chim. Act.* **83**, 2115-2140 (2000). d) Baumeister, B. & Matile, S. *Chem. Commun.* 913-914 (2000).
23. Nesloney, C. L. & Kelly, J. W. *J. Am. Chem. Soc.* **118**, 5836-5845 (1996).
24. a) Schenk, H. L. & Gellman, S. H. *J. Am. Chem. Soc.* **120**, 4869-4870 (1998). b) Griffiths-Jones, S. R. & Searle, M. S. *J. Am. Chem. Soc.* **122**, 8350-8356 (2000).
25. Donners, J. J. J. M. *et al.* manuscript in preparation.

# CHAPTER 5

## Helical Superstructures from Polystyrene-Polyisocyanodipeptide Block Copolymers

### 5.1 Introduction

Chirality may be used as a tool to assemble molecules and macromolecules into larger structures with dissymmetric, for example helical shapes. Interesting applications for these chiral architectures can be foreseen in the fields of materials science and catalysis.<sup>1,2</sup> It is well known that amphiphilic compounds with low molecular weights, such as phospholipids, but also amino acid, nucleic acid and carbohydrate derivatives can form a variety of chiral superstructures in water.<sup>3</sup> Amphiphilic diblock copolymers in an aqueous environment also can assemble into various nanosized morphologies,<sup>4</sup> depending on the structure of the block copolymer<sup>5,6</sup> or the presence of inorganic salts.<sup>7</sup> These types of block copolymers may be referred to as superamphiphiles, since they resemble the traditional surfactants in shape but differ in size. Only a limited number of examples of amphiphilic block copolymers which generate chiral nanosized architectures in water are known.<sup>8</sup> In this chapter the formation of such dissymmetric architectures from chiral superamphiphiles consisting of a block copolymer of styrene and an optically active isocyanodipeptide is described.

Polymers of isocyanides can adopt helical structures depending on their side chains. These helical structures are stable when monomers with bulky side groups are used<sup>9</sup> or when the macromolecular conformation is stabilized by hydrogen bonding interactions between the side chains.<sup>10,11</sup> The use of an optically active isocyanide monomer or a chiral Ni(II) catalyst can control the helix sense of a polyisocyanide molecule.<sup>9</sup> The charged block copolymers presented in this Chapter have a helical



polyisocyanide headgroup (Figure 1), of which the helix type is determined by the monomer used. Upon dispersal in water, these macromolecules self-assemble to form different types of supramolecular structures, including super-helices.

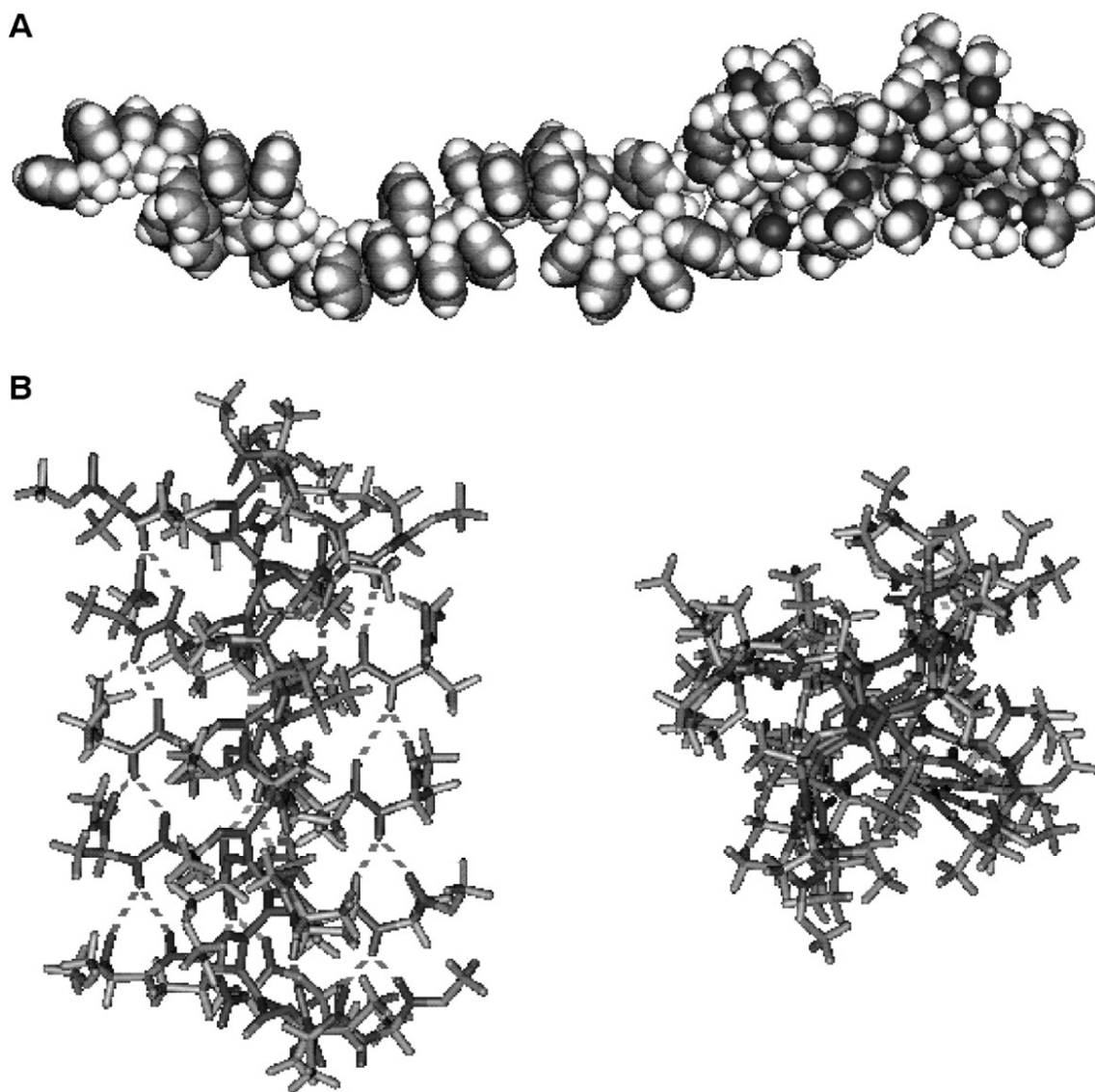


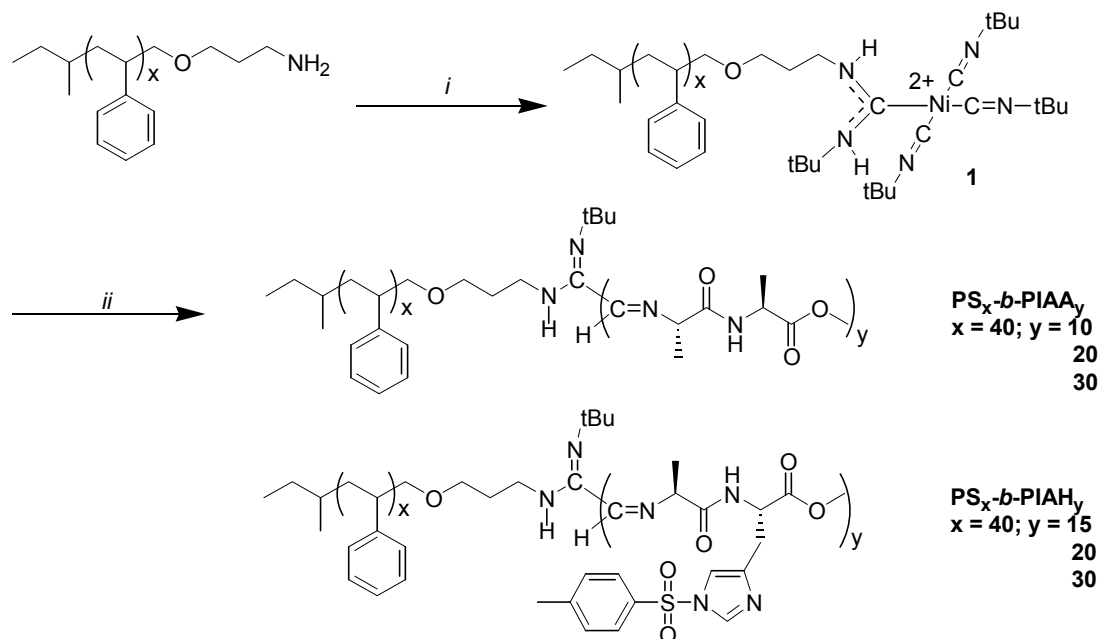
**Figure 1** (A) Computer generated representation of PS-b-PIAA. (B) Right-handed helical backbone of PIAA. (Left) Side view; dashed lines depict hydrogen bonds. (Right) Top view.

## 5.2 Results and Discussion

### 5.2.1 Synthesis and characterization

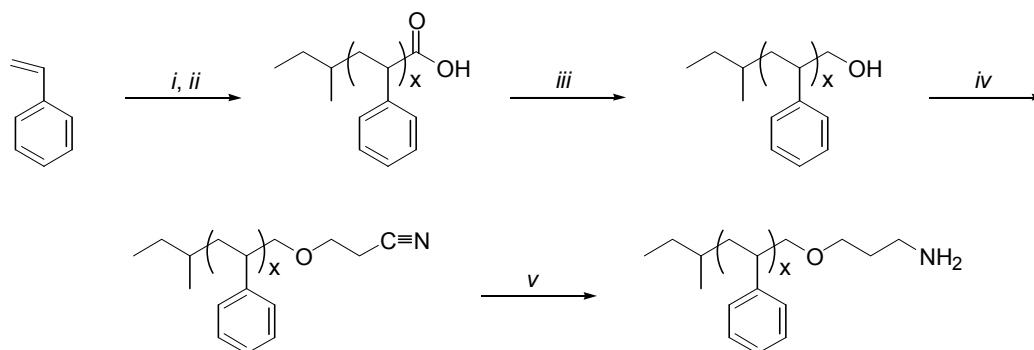
Block copolymers were prepared by polymerizing the isocyanopeptides using a Ni(II) catalyst and amino terminated polystyrene as the initiator (Scheme 1). Both alanine-

alanine<sup>10</sup> and alanine-histidine<sup>12</sup> derived monomeric isocyanides were prepared according to known procedures.



**Scheme 1** Synthesis of block copolymers containing different polyisocyanopeptide segments. (i) 1 eq.  $\text{Ni}(\text{CN-tBu})_4(\text{ClO}_4)_2$ ,  $\text{CH}_2\text{Cl}_2$ ; (ii)  $y$  eq. *L*-isocyanoalanyl-*L*-alanine methyl ester or *L*-isocyanoalanyl-*N*(*Im*)-tosyl-*L*-histidine methyl ester,  $\text{CH}_2\text{Cl}_2$ .

**Amine end-capped polystyrene.** Amino functionalized polystyrene was prepared following an indirect amination route (Scheme 2) developed by van Hest *et al.*<sup>13,14</sup> using a multigram polymerization set-up. The resulting  $\text{PS}_{40}\text{-CO}_2\text{H}$  ( $M_n = 4160$  g/mol;  $D =$



**Scheme 2** Synthesis of amine end-capped polystyrene. (i)  $1/x$  *sec.*-butyl lithium, cyclohexane (ii)  $\text{CO}_2$ , THF, (iii)  $\text{LiAlH}_4$ , THF, (iv) acrylonitril, phase transfer catalyst, NaOH, toluene, water, (v)  $\text{H}_2$ , Raney/Co (or Raney/Ni),  $\text{NH}_3$ , toluene, MeOH, (or:  $\text{BH}_3\cdot\text{THF}$ , THF).

1.05) was reduced to PS<sub>40</sub>-OH and subsequently modified with a cyano functionality, employing a Michael-type cyanoethylation step with acrylonitrile. The Raney/Ni catalyzed hydrogenation of the generated PS<sub>40</sub>-CN gave the desired PS<sub>40</sub>-NH<sub>2</sub> in 50 – 70% yield. After work-up the product could be separated from the starting material by straightforward column chromatography. A more convenient route towards PS-NH<sub>2</sub> appeared to be the use of BH<sub>3</sub>·THF as a reducing agent resulting in the quantitative conversion of PS-CN.<sup>15</sup>

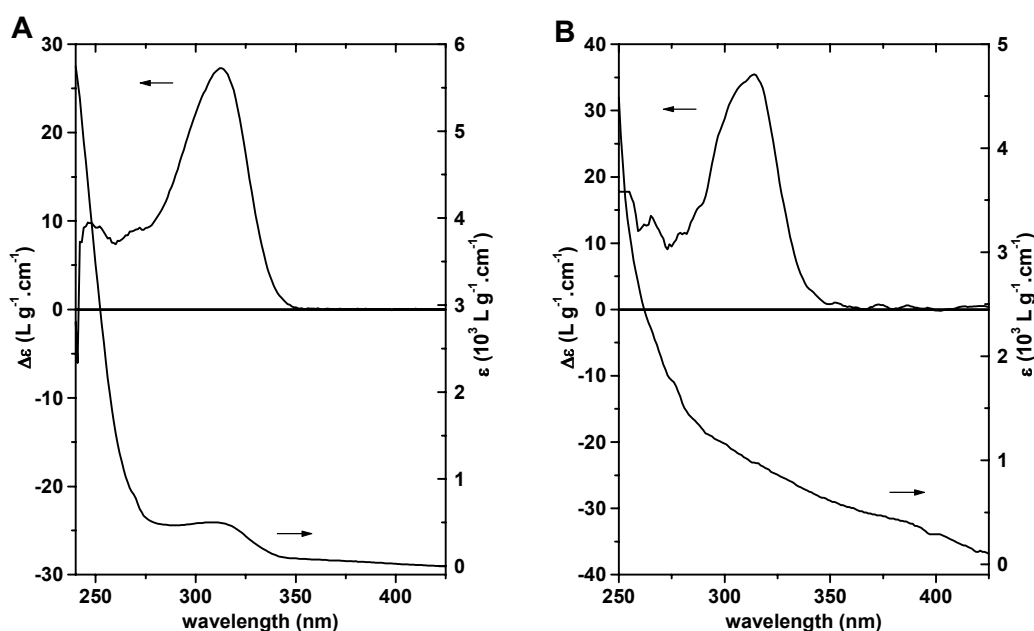


**Figure 2** CD and UV/vis spectra of (A) PS<sub>40</sub>-b-PIAA<sub>20</sub> and (B) PS<sub>40</sub>-b-PIAH<sub>20</sub> both recorded in CHCl<sub>3</sub> at ambient concentration.

**Macromolecular catalyst.** The macromolecular nickel complex **1** in Scheme 1 was prepared by nucleophilic attack of the amine end-capped polystyrene (PS<sub>40</sub>-NH<sub>2</sub>) on the stable complex Ni(II)(CN-tBu)<sub>4</sub>(ClO<sub>4</sub>)<sub>2</sub>.<sup>16</sup> In CH<sub>2</sub>Cl<sub>2</sub>, a good solvent for polystyrene, this reaction took place remarkably easy given the introduced steric bulk. Upon addition of the amine to the slightly yellow suspension of the Ni(II) complex in CH<sub>2</sub>Cl<sub>2</sub>, immediately a clear orange solution was formed which turned back to yellow after a few minutes, in line with observations reported by Kamer *et al.*<sup>17</sup> using  $\alpha$ -phenylmethyl amine as an initiator. Indeed TLC showed complete consumption of PS-NH<sub>2</sub>, and in the <sup>13</sup>C NMR and IR spectra of the obtained product signals characteristic for the desired carbene-like polymerization catalyst **1** ( $\delta = 179$  ppm, N-C-N;  $\delta = 121$  ppm, Ni-C=N and  $\nu = 2256$  &  $2223$  cm<sup>-1</sup>, C=N;  $\nu = 1575$  cm<sup>-1</sup>, N-C-N) were observed. Contrary to the

results previously reported,<sup>9,17</sup> in this case only a single conformation of the catalyst was observed. This can be explained by taking into account the steric congestion imposed by the polymer chain and the possible favorable interactions between the polystyrene phenyl groups and the nickel(II) center as described by Kamer *et al.*<sup>17</sup>

**Table 1. Optical rotations and glass transition temperatures.**

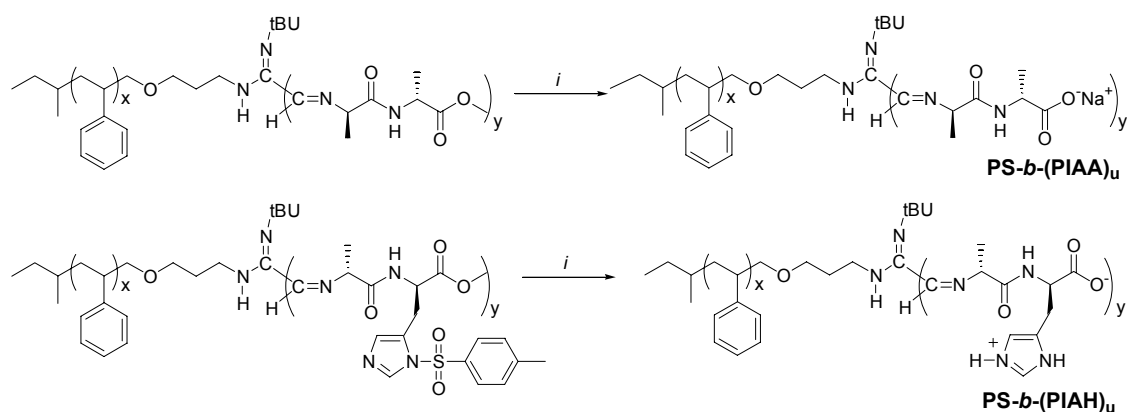
polymer	$[\alpha]$ (c) <sup>a</sup>	T <sub>g</sub> (in °C) <sup>b</sup>
PS <sub>40</sub> -NH <sub>2</sub>	-	67.2
PIAA	338 (0.34)	>200
PS <sub>40</sub> - <i>b</i> -PIAA <sub>10</sub>	105 (0.08)	67.2
PS <sub>40</sub> - <i>b</i> -PIAA <sub>20</sub>	151 (0.06)	68.0
PS <sub>40</sub> - <i>b</i> -PIAA <sub>30</sub>	184 (0.05)	69.4
PIAH	420 (0.35)	n.d.
PS <sub>40</sub> - <i>b</i> -PIAH <sub>15</sub>	190 (0.06)	67.6
PS <sub>40</sub> - <i>b</i> -PIAH <sub>20</sub>	205 (0.06)	72.0
PS <sub>40</sub> - <i>b</i> -PIAH <sub>30</sub>	282 (0.05)	80.0

<sup>a</sup>In °·dl/g·dm, measured in CHCl<sub>3</sub>. <sup>b</sup>Scan rate 10°C/min.

**Block copolymers.** When the dipeptide-based isocyanides were added to a solution of the catalyst, the polymerization commenced due to the rapid exchange of isocyanides on the nickel center. This yielded the desired block copolymers in moderate to good yields (60-85%). In their protected form (*i.e.* as methyl esters), these macromolecules were soluble in common organic solvents and could be conveniently characterized by NMR spectroscopy. The molecular weights could be determined by comparing the integrated peak areas in the <sup>1</sup>H NMR spectra. In this way a series of poly(styrene)-*block*-poly(L-isocyanoalanyl-L-alanine methyl ester) (PS<sub>x</sub>-*b*-PIAA<sub>y</sub>) and poly(styrene)-*block*-poly(L-isocyanoalanyl-*N*(Im)-tosyl-L-histidine methyl ester) (PS<sub>x</sub>-*b*-PIAH<sub>y</sub>) block copolymers were prepared, in which x was 40 in all cases and y varied from 10 to 30 (Scheme 1). By comparing the spectral characteristics of the isocyanide segments in the block copolymers with those of the homopolymers L,L-PIAA and L,L-PIAH it was concluded that a similar conformation was present in the two cases.<sup>11</sup> From the relatively strong Cotton effects centered around 312 nm observed in both cases, a right-handed helix was proposed for the block copolymers studied (Figure 2). As a result of the stabilizing hydrogen bonds between the side chains *n* and (*n* + 4) the rigid helix has a pitch of 4.6

Å. A diameter of 15.8 Å for PIAA has been found (see Chapter 3) and for PIAH an estimate based on molecular models gives 20 Å. The optical rotation data of the block copolymers and those of model compounds are displayed in Table 1. As expected the observed magnitudes of these rotations are related to the weight fraction of the polyisocyanopeptide segment in the block copolymers.

Thermal analysis of block copolymers with short ( $n = 10, 15$ ) polyisocyanide segments revealed  $T_g$ 's (Table 1) which were very close ( $67.2 - 67.6$  °C) to that of the parent PS-NH<sub>2</sub>, *viz.* 67.2 °C. Only for PS<sub>40</sub>-*b*-PIAH the increase of the polyisocyanide block length led to a significant increase of the  $T_g$ . For PS<sub>40</sub>-*b*-PIAA only a marginal rise in the  $T_g$  was observed upon extending the length of the polyisocyanide segment to 30 repeat units. This suggests that the PIAA segments have a poorer miscibility with the polystyrene blocks compared to the PIAH segments.



**Scheme 3** Formation of the chiral charged polystyrene-polyisocyanopeptide superamphiphiles. (i) NaOH, toluene, H<sub>2</sub>O.

Saponification of the ester functions of PS-*b*-PIAA by treatment with a mixture of 1.0 molar aqueous NaOH and toluene (1:1 v/v) resulted in a superamphiphile (PS-*b*-(PIAA)<sub>u</sub>), *i.e.* an amphiphilic diblock copolymer consisting of two well defined component blocks, with a negatively charged helical headgroup. Hydrolysis of PS-*b*-PIAH gave a superamphiphile with a zwitterionic headgroup (superamphiphile (PS-*b*-(PIAH)<sub>u</sub>, Scheme 3). The deprotected block copolymers were separated from the excess of NaOH by ultrafiltration; subsequent lyophilization yielded spongy brown solids. These conversions could be conveniently monitored using infrared spectroscopy, which showed the disappearance of the ester vibrations at 1747 cm<sup>-1</sup> and the concomitant appearance of new absorptions around 1600 cm<sup>-1</sup> (Figure 3).

The CD spectra of block copolymer dispersions in water displayed significant Cotton effects. However, scattering resulting from aggregation of the macromolecules prevented a quantitative analysis of the spectra. Aggregate formation also hampered the potentiometric determination of the ionization state of the carboxylic acid and imidazole functions. It was assumed, therefore, that the ionization states of the amphiphilic block copolymers were similar to those of the respective homopolymers. The  $pK_a$  of the carboxylic acid groups in  $(PIAA)_u$  was determined to be 5.6. The  $pK_a$  values of  $(PIAH)_u$  have been determined earlier,<sup>18</sup> amounting to 3.1 for the carboxylate groups and 9.1 for the imidazole groups, resulting in an isoelectric point of 5.4.

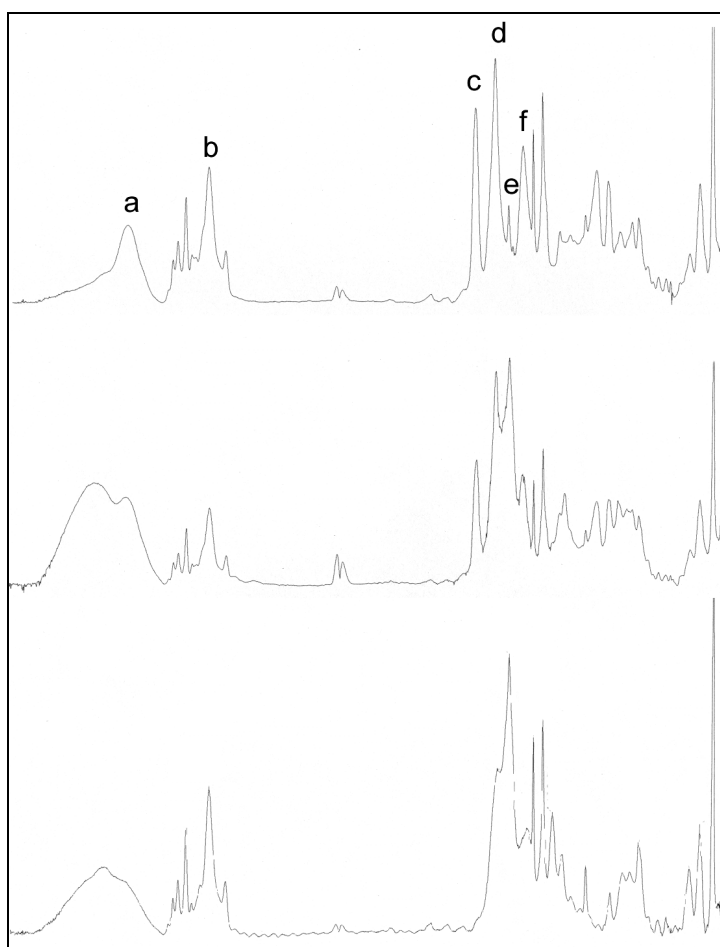


**Figure 3** IR spectra of  $PS_{40}\text{-}b\text{-}(PIAA)_{u,20}$  recorded during hydrolysis of the methyl ester functions, after 10 min. (top), 1 day (middle) and 2 days (bottom). Indices: a, amide NH; b, CH; c, ester C=O; d, amide I; e, C=C and carboxylate C=O; f, amide II. The amide vibrations (a, d and f) remained at the same position during hydrolysis indicating that the hydrogen bonds between these groups stay intact (see Experimental Section for peak positions).

### 5.2.2 Aggregation behaviour

The aggregation behaviour of the different polystyrene-polyisocyanopeptide block copolymers was studied, mainly by TEM and AFM.

**Effect of pH.** Aggregates of  $\text{PS}_{40}\text{-}b\text{-(PIAA)}_u$  and  $\text{PS}_{40}\text{-}b\text{-(PIAH)}_u$  were prepared by sonicating a 0.1 % w/w dispersion in water of  $\text{pH} = 7$  for 1 hour at  $70\text{ }^\circ\text{C}$ . At this pH no distinct morphologies were observed for  $\text{PS}_{40}\text{-}b\text{-(PIAA)}_{u,20}$ , while  $\text{PS}_{40}\text{-}b\text{-(PIAH)}_{u,20}$  showed micellar aggregates. Dispersions were then prepared in a sodium acetate buffer of  $\text{pH} = 5.6$  (equal to the  $\text{pK}_a$  value of the block copolymer), in order to generate attractive interactions between the rod-like headgroups. At this pH approximately half of the available acid residues of  $\text{PS-}b\text{-(PIAA)}_u$  is expected to be protonated, thereby optimizing the possible formation of intermolecular hydrogen bonds. Rod-like aggregates with a diameter of 12 nm were observed (Figure 4A) for this compound. In the case of  $\text{PS}_{40}\text{-}b\text{-(PIAH)}_{u,20}$ , the main part of the polyisocyanide block is expected to be zwitterionic at  $\text{pH} = 5.6$ , minimizing the repulsive electrostatic interactions between the highly charged macromolecules. This resulted in rod-like structures (not shown) identical to those found for  $\text{PS}_{40}\text{-}b\text{-(PIAA)}_{u,20}$ . The rods were assumed to be micellar aggregates consisting of a polystyrene core with a diameter of 8 nm, and a corona of polyisocyanide blocks with a thickness of approximately 2 nm as was estimated from the length of the constituting segments (Figure 4B). When more diluted dispersions were prepared less rod-like assemblies were observed, instead an increasing amount of spherical micelles was found. Based on the dimensions of the block copolymers one can calculate that a single rod of  $1\text{ }\mu\text{m}$  length contains approximately 6000 macromolecules. TEM and AFM analysis of aggregates deposited on Formvar and mica, respectively, showed that the rod-like aggregates possessed a zigzag structure (Figure 4A and 4C). The zigzag morphology showed a remarkable resemblance with the pattern observed for annealed thin films of block copolymers of styrene and hexyl isocyanate,<sup>19</sup> which was attributed to a smectic like organization of these macromolecules. The repeating zigzag arrangement of the micellar rods, observed for the superamphiphiles discussed here, suggested that similar interactions play a role in this case.

For both superamphiphiles investigated besides the defined aggregates discussed above also a substantial amount of material with undefined morphology was observed on the microscope grids. Based a rough visual estimation the relative amount of aggregates is 50 – 70%, improving this quantity is therefore desirable.

**Counter ions.** It is known that the addition of ions can influence the self-assembly of both traditional surfactants and amphiphilic block copolymers. Changing the cation of the buffer (from sodium acetate to potassium acetate or to ammonium acetate) at

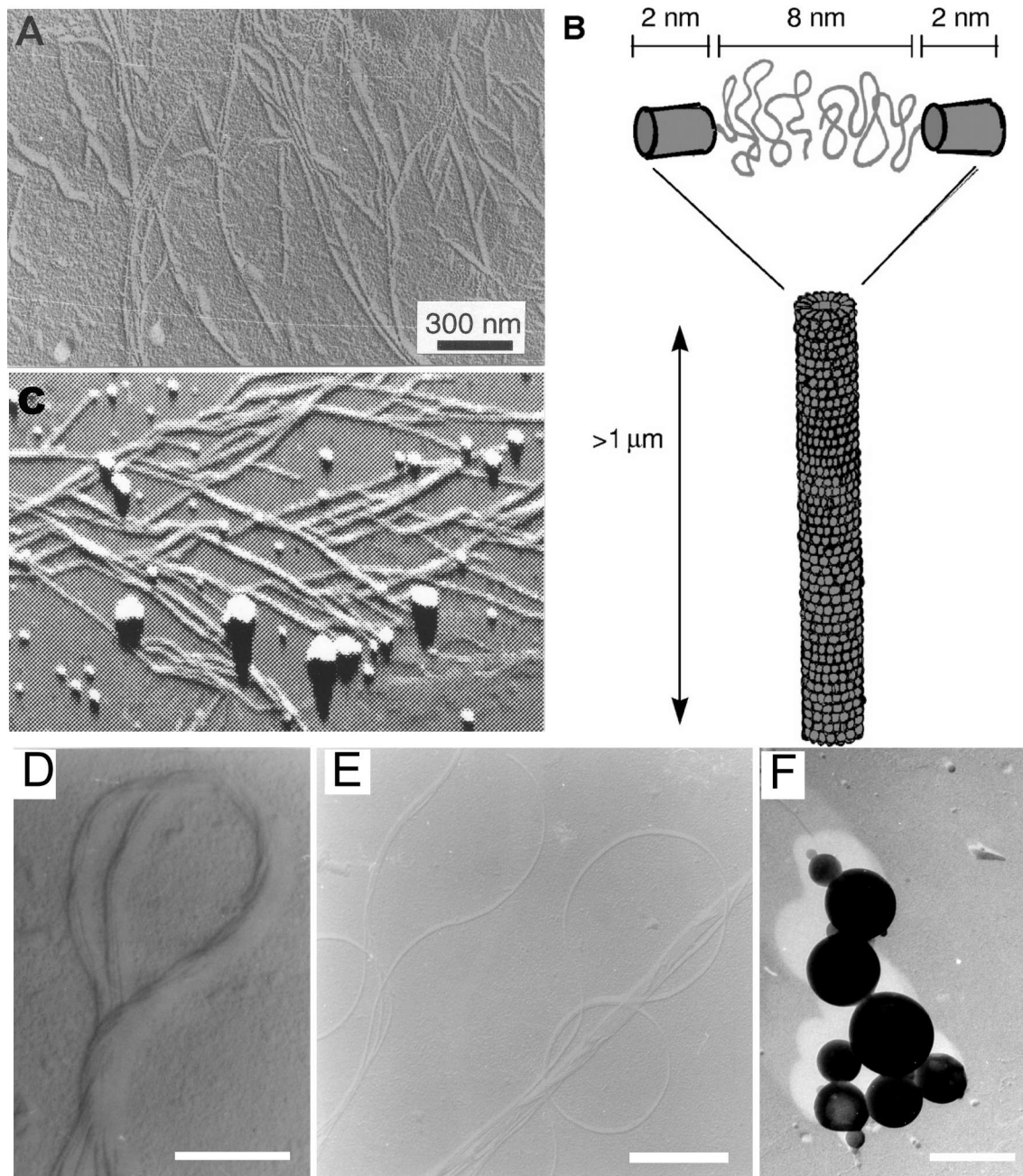


**Figure 4** TEM images and a schematic representation of micellar rods formed by  $PS_{40}\text{-}b\text{-}(PIAA)_{u,20}$  in an aqueous NaOAc buffer of  $pH = 5.6$ , (A) TEM, bar = 300 nm; (B) schematic representation; (C) Atomic force micrograph. (D bar = 250 nm, E bar = 350 nm) Micellar rods formed by  $PS_{40}\text{-}b\text{-}(PIAH)_{u,20}$  in an aqueous Na citrate buffer of  $pH = 5.6$ . (F) Spherical aggregates formed by  $PS_{40}\text{-}b\text{-}(PIAA)_{u,20}$  when dispersed from DMF in an aqueous NaOAc buffer of  $pH = 5.6$ , bar = 200 nm.



identical pH did not affect the morphology of the micellar rods formed by PS<sub>40</sub>-*b*-(PIAA)<sub>u,20</sub> and PS<sub>40</sub>-*b*-(PIAH)<sub>u,20</sub>. When the anion of the buffer, however, was changed from sodium acetate to sodium tartrate and then to sodium citrate (all pH = 5.6) the micellar rods from PS<sub>40</sub>-*b*-(PIAH)<sub>u,20</sub> became increasingly more flexible (Figure 4D). Although the more flexible fibers incidentally intertwined (Figure 4E), no transfer of the chirality from the macromolecular helix to the level of the generated aggregates was observed. In contrast, PS<sub>40</sub>-*b*-(PIAA)<sub>u,20</sub> did not respond to the change of anions in the buffer solution, suggesting that a direct interaction of these anions is present with the zwitterionic polyisocyanopeptide headgroups of PS<sub>40</sub>-*b*-(PIAH)<sub>u,20</sub>. A possible explanation for these observations is a decrease of the phase boundary tension present between polystyrene and polyisocyanide rich domains in the assemblies. This tension is expected to be linked to the interaction of the rigid part of the block copolymers with the increasingly larger anions. More experiments are, however, needed to verify this hypothesis.

**Method of dispersion.** It has been found by Eisenberg and coworkers<sup>4a</sup> that the procedure by which amphiphilic block copolymers are dispersed in water has a pronounced effect on the aggregate morphologies that are formed. To study whether the morphology of the chiral superamphiphiles could be controlled and in particular if it was possible to obtain quantitative formation of well defined aggregates, the block copolymers were dispersed in aqueous buffer starting from a common solvent for both segments.

DMF was found to be a common solvent for both the polystyrene and the hydrolyzed polyisocyanopeptide blocks. To a solution of 5 mg PS<sub>40</sub>-*b*-(PIAA)<sub>u,20</sub> in 1 ml DMF, 9 ml of a 1 mM NaOAc (pH = 5.6) was added dropwise while vigorously stirring. The organic solvent was subsequently removed by using an ultrafiltration membrane (cut-off 10,000 D) applying 10 concentration / redispersion cycles with 5 ml aliquots of buffer. The resulting suspension was investigated with TEM, which showed the formation of spherical aggregates with diameters ranging from 100 nm to over 350 nm and with a minor amount of micelles (Figure 4F). The size of the formed spheres and the transparent interior observed in some cases (Figure 4F, bottom left corner) are in line with a vesicle-like structure. Care has to be taken, however, in distinguishing these vesicular aggregates from spherical latex particles. These were for example

formed in a control experiment in dispersing PS<sub>40</sub>-NH<sub>2</sub> from DMF in pure water and consequently no definite conclusions can be drawn considering the structure of the spherical aggregates.

In a qualitative experiment buffer was slowly added to a DMF solution of PS<sub>40</sub>-*b*-(PIAA)<sub>u,20</sub>, which was subsequently filtered to remove any undissolved material. The CD spectra (Figure 5) of the fully hydrolyzed PS<sub>40</sub>-*b*-(PIAA)<sub>u,20</sub> in DMF and in a (1:1) DMF / water mixture, resembled the spectra obtained for PIAA in CHCl<sub>3</sub>.<sup>11</sup> In contrast the CD spectra recorded for (PIAA)<sub>u</sub> in water displayed a negative signal, which is believed to be the result of the polarity of the medium (see Chapter 4). From the Cotton effects observed for the block copolymer at water contents >98% (Figure 5) it followed that clustering of the optically active polyisocyanopeptide segments occurred, leading to the formation of chiral aggregates, although no expression of chirality in the aggregate morphologies was observed by electron microscopy.

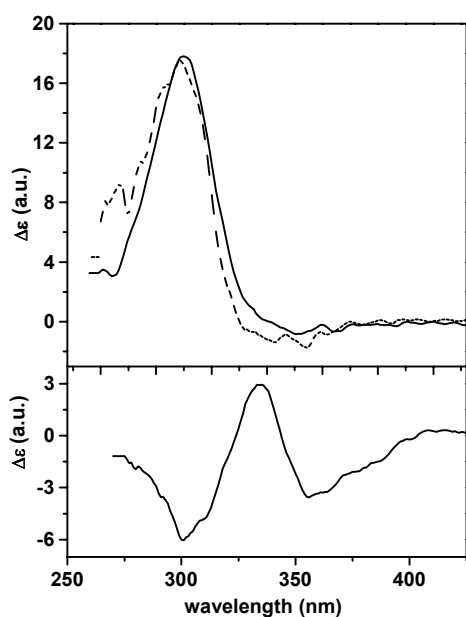


**Figure 5** CD spectra of PS<sub>40</sub>-*b*-(PIAA)<sub>u,20</sub> in DMF (top, straight line), in water/DMF (1/1 v/v) (top, dashed line) and in water/DMF (>98/2 v/v) (bottom).

**Temperature.** Since the  $T_g$  of the block copolymers studied is well above room temperature (Table 1) the formed aggregates will be kinetically trapped already at low water contents.<sup>4a</sup> Aggregates were therefore prepared by sonication at 70 °C. DSC analysis of a 0.1% w/w dispersion of PS<sub>40</sub>-*b*-(PIAA)<sub>u,20</sub> in buffer displayed an endothermic peak at 68 °C, the temperature at which the glass transition of the protected block copolymer PS<sub>40</sub>-*b*-PIAA<sub>20</sub> was found. The finding of this peak suggests that the macromolecular chains gain mobility in a cooperative fashion and therefore some

comparison with the melting of the paraffinic tails in aggregates formed by phospholipids can be made. When this superamphiphile was dispersed from DMF the majority of the material was present as spheres (*see above*). However, after applying sonicating for 1 hour at 70 °C a large amount of micellar rods next to these spheres were also observed, suggesting that this type of morphology is thermodynamically more favorable for PS<sub>40</sub>-*b*-(PIAA)<sub>u,20</sub>, at least at this elevated temperature.

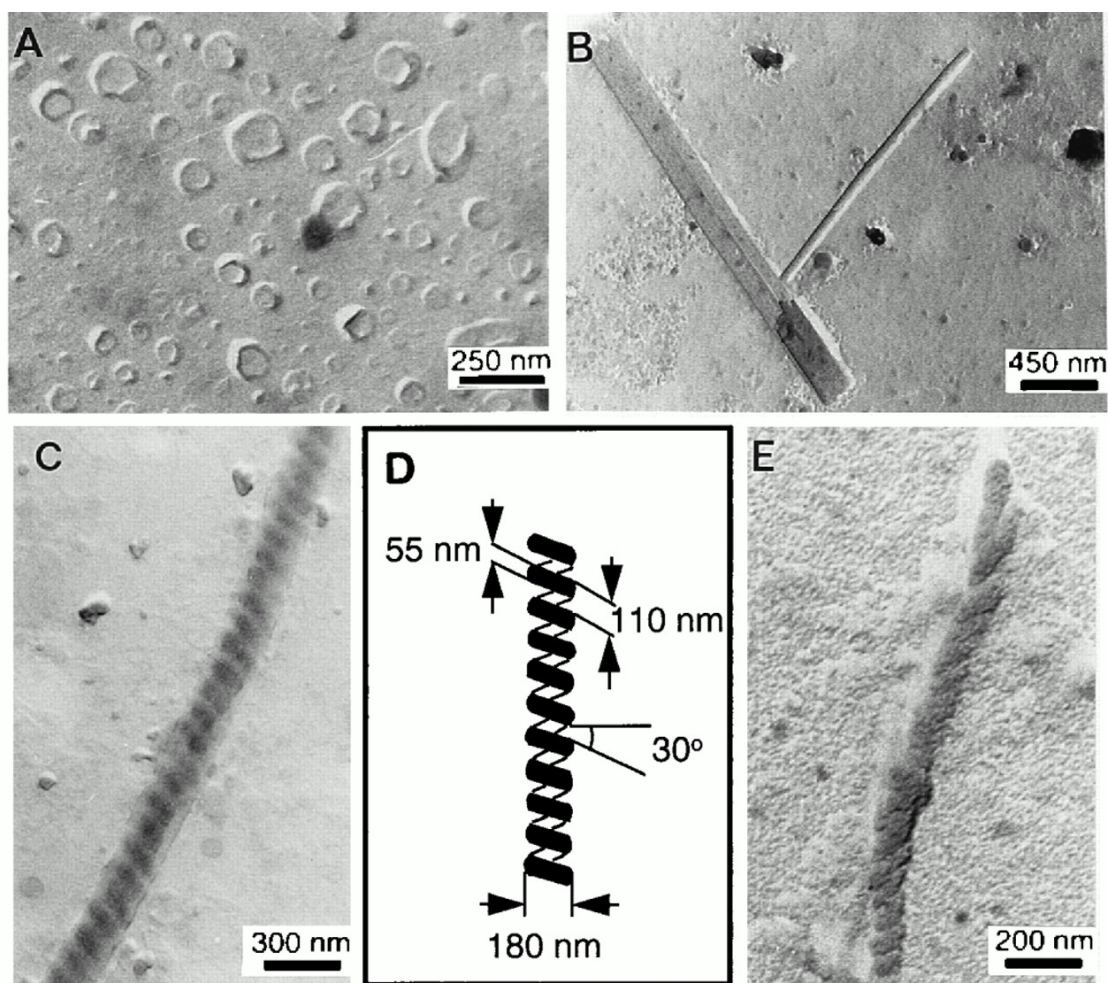


**Figure 6** TEM images of morphologies formed by PS<sub>40</sub>-*b*-(PIAA)<sub>u,10</sub> in a NaOAc buffer at pH = 5.6 (0.2 mM). (A) collapsed vesicles. (B) Bilayer filaments. (C) Left-handed superhelix. (D) Schematic representation of the helix in (C). (E) Right-handed helical aggregate formed by PS<sub>40</sub>-*b*-(PIAH)<sub>u,15</sub> in a NaOAc buffer of pH = 5.6 (0.2 mM).

**Block copolymer structure.** The effect of the polyisocyanide block length on the aggregation behavior of PS<sub>40</sub>-*b*-(PIAA)<sub>u,y</sub> and PS<sub>40</sub>-*b*-(PIAH)<sub>u,y</sub> was investigated in a sodium acetate buffer of pH = 5.6. Rod-like micellar aggregates were observed for both systems when  $y = 20$  (*see above*), whereas dispersions of block copolymers with  $y = 30$

showed no distinct morphologies. When  $\text{PS}_{40}\text{-}b\text{-}(\text{PIAA})_{u,10}$  was dispersed in buffer by sonication at 70 °C, a variety of bilayer type structures were observed. In addition to collapsed vesicles (with diameters ranging from 50 to 200 nm and a bilayer thickness of ~16 nm, Figure 6A) and bilayer fragments (Figure 6B), left-handed superhelices were also formed (Figure 6C). These super coils had diameters of 180 nm and a pitch of 110 nm (Figure 6D). Upon dispersion  $\text{PS}_{40}\text{-}b\text{-}(\text{PIAH})_{u,15}$  also formed helical superstructures (Figure 6E), however, this superhelix was right-handed and had a diameter of 28 nm and a pitch of 19 nm. These dimensions are considerably smaller than those observed for  $\text{PS}_{40}\text{-}b\text{-}(\text{PIAA})_{u,10}$ . In the case of  $\text{PS}_{40}\text{-}b\text{-}(\text{PIAH})_{u,15}$ , one helix turn corresponds to the diameter of the micellar rods (12 nm, *see above*), and thus we propose that for this block copolymer the helical superstructure is composed of coiled rods. In the case of  $\text{PS}_{40}\text{-}b\text{-}(\text{PIAA})_{u,10}$ , no clues as to the hierarchy of the assembly process can be given at this moment. Direct transfer of molecular chirality to a dissymmetric supramolecular structure is the most widely accepted route towards the formation of these types of aggregates.<sup>20</sup> The spontaneous breaking of achiral symmetry<sup>21</sup> or anisotropy in the interfacial energy<sup>22</sup> are other mechanisms for the formation of chiral superstructures, in the latter case this results in an irregular helical pitch. For the chiral superamphiphiles discussed here a regular helical structure is found. The CD experiments in water indicate that the macromolecular helices are arranged in a dissymmetric geometry with a preference for one particular handedness. Although a direct relation between formed superhelices and the polyisocyanide helix is difficult to establish, based on the CD measurements the spontaneous breaking of symmetry appears unlikely. A mechanism in which the chiral information present in the amino acids is transferred in a hierarchical fashion to the helical conformation of the macromolecules and eventually to the chiral aggregates formed in water seems therefore reasonable. However, the mechanism of formation of the helical superstructure is apparently different for  $\text{PS}_{40}\text{-}b\text{-}(\text{PIAA})_{u,10}$  and  $\text{PS}_{40}\text{-}b\text{-}(\text{PIAH})_{u,15}$ . This may be attributed to dissimilarity in the polyisocyanide structure (anionic versus zwitterionic) and or the difference in the length of the polyisocyanide block.<sup>6</sup>

### 5.3 Conclusions

Using the Ni(II) catalyzed polymerization of isocyanopeptides with amine terminated polystyrene as an initiator, block copolymers have been prepared containing a helical

polyisocyanide segment. These copolymers can be converted to chiral superamphiphiles which form a variety of morphologies upon dispersal in water. Since these polymers with a permanent and precisely defined helical structure allow the generation of well-defined chiral superstructures, it is the contention that this class of macromolecules are interesting reference compounds toward a better understanding of the principles underlying the generation of functional polymeric materials with higher structural order from synthetic building blocks with a known secondary structure. These insights are important for the development of materials with, for example, liquid-crystalline or non-linear optical properties.

## 5.4 Experimental Section

### 5.4.1 General methods and materials

Dichloromethane was distilled from  $\text{CaH}_2$  and THF from sodium, all other chemicals were commercial products and were used as received. TLC analyses were performed on silica 60 F<sub>254</sub> coated glass either from Merck or Acros, compounds were visualized using UV light, with I<sub>2</sub>-vapour or Cl<sub>2</sub>/TDM. <sup>1</sup>H NMR spectra were recorded on Bruker AC-100, Bruker WM-200 and Bruker AC-300 instruments at 297 K, <sup>13</sup>C NMR spectra were measured on a Bruker AC-300 machine, all chemical shifts are reported in ppm relative to tetramethylsilane ( $\delta = 0.00$  ppm) as an internal standard. FT-Infrared spectra were recorded on a Bio-Rad FTS 25 instrument, DSC was performed on a Perkin Elmer DSC 7 (10 °C/min.). Optical rotations were measured on a Perkin Elmer 241 polarimeter. CD spectra were recorded on Jasco J600 and Jasco J810 instruments. GPC analyses were performed on a Plgel (5  $\mu\text{m}$ , 500 Å, 300 × 7.5 mm<sup>2</sup>) column using chloroform as the eluens and were calibrated against polystyrene standards.

**Sample preparation.** In a typical procedure, 1 mg superamphiphile was dispersed in 1 ml buffer solution by sonication at 70 °C in a bath-type sonicator. Diluted samples were obtained by dispersing 0.1, 0.2 or 0.5 mg compound in the same buffer volume. Samples from DMF were prepared by dissolving 5 mg polymer in 1 ml DMF in a flask placed in a thermostatted water bath, subsequently 9 ml buffer was added in a controlled fashion using a peristaltic pump. The organic solvent was removed from the dispersion by repeated ultrafiltration (see text).

**Microscopy.** TEM was performed on a Philips EM 210 microscope at an acceleration voltage of 60 kV. For AFM a Nanoscope III from Digital Instruments was used operating in the tapping mode at room temperature. Samples for TEM were deposited from the aqueous dispersions onto copper grids coated with a thin film of polyvinyl formaldehyde plastid (Formvar). Water was evaporated during a period of 1 to 10 min. at atmospheric pressure. The remaining water was drained off, and the grids were shadowed

with platinum at an angle of 45°. In an analogous manner samples for AFM were prepared on freshly cleaved mica, without the application of any shadowing or staining technique.

## 5.4.2 Compounds

The monomers isocyno-L-alanyl-L-alanine methyl ester and L-isocynoalanyl-*N*(Im)-tosyl-L-histidine methyl ester were prepared as previously reported.<sup>10,12</sup>

**Polystyrenes.** Following the same procedure and set-up as reported by van Hest<sup>13,14</sup> several batches PS-CO<sub>2</sub>H with variable degrees of polymerization were prepared (Table 2). TLC analyses indicated that after work-up the product consisted of PS-CO<sub>2</sub>H and the dimeric product (PS)<sub>2</sub>CO.

**Table 2. Molecular weight data and degree of functionalization of CO<sub>2</sub> end-capped polystyrenes**

	M <sub>n</sub> (g/mol) <sup>a</sup>	M <sub>w</sub> (g/mol) <sup>a</sup>	D <sup>a</sup>	CO <sub>2</sub> H funct. <sup>a,b</sup>	overall yield
PS <sub>29</sub> -CO <sub>2</sub> H	2960	3170	1.07	82%	89%
PS <sub>37</sub> -CO <sub>2</sub> H	3870	4103	1.06	93%	95%
PS <sub>40</sub> -CO <sub>2</sub> H	4170	4400	1.05	90%	98%
PS <sub>51</sub> -CO <sub>2</sub> H	5310	5612	1.06	94%	94%
PS <sub>89</sub> -CO <sub>2</sub> H	9190	9960	1.08	91%	92%
PS <sub>95</sub> -CO <sub>2</sub> H	9821	10200	1.06	89%	94%

<sup>a</sup>determined by GPC, <sup>b</sup>in weight/weight

The other polystyrene derivatives (PS-OH, PS-CN and PS-NH<sub>2</sub>) were prepared following analogous procedures as previously reported and had similar spectral characteristics.<sup>13,14</sup>

**Catalyst 1:** To a well-stirred suspension of 41 mg (0.07 mmol) Ni(CN-tBu)<sub>4</sub>(ClO<sub>4</sub>)<sub>2</sub> in 5 ml CH<sub>2</sub>Cl<sub>2</sub> under a N<sub>2</sub> blanket, was added 300 mg (0.07 mmol) PS-NH<sub>2</sub>. The clear yellow solution was stirred for an additional 15 min. after which the solvent was evaporated, resulting in a slightly yellow amorphous powder (yield 100%). <sup>1</sup>H NMR (CDCl<sub>3</sub>): δ = 0.58-1.22 (*Bu*-(CH<sub>2</sub>-CHPh)<sub>x</sub>), 1.22 – 1.8 (CH<sub>2</sub>-CHPh)<sub>x</sub>, 1.45 (NHC(CH<sub>3</sub>), 1.57 (CH<sub>3</sub>), 1.8 – 2.4 ((CH<sub>2</sub>-CHPh)<sub>x</sub>), 2.9 – 3.3 (CH<sub>2</sub>-O-CH<sub>2</sub> + CH<sub>2</sub>-O-CH<sub>2</sub>), 3.7 (CH<sub>2</sub>CH<sub>2</sub>NH), 6.3 – 7.3 ((CH<sub>2</sub>-CHPh)<sub>x</sub>), 8.0 (CH<sub>2</sub>CH<sub>2</sub>NH) ppm. <sup>13</sup>C NMR (CDCl<sub>3</sub>): δ = 13.9 (CH<sub>3</sub>-CH<sub>2</sub>-CH(CH<sub>3</sub>)-(CH<sub>2</sub>-CHPh)<sub>x</sub>), 22.3 (CH<sub>3</sub>-CH<sub>2</sub>-CH(CH<sub>3</sub>)-(CH<sub>2</sub>-CHPh)<sub>x</sub>), 26.9 (CH<sub>2</sub>-O-CH<sub>2</sub>-CH<sub>2</sub>-CH<sub>2</sub>-NH), 28.2 (br, CH<sub>3</sub>-CH<sub>2</sub>-CH(CH<sub>3</sub>)-(CH<sub>2</sub>-CHPh)<sub>x</sub>), 29.5 ((CH<sub>3</sub>)CNH), 30.3 ((CH<sub>3</sub>)CN), 31.7 (CH<sub>3</sub>-CH<sub>2</sub>-CH(CH<sub>3</sub>)-(CH<sub>2</sub>-CHPh)<sub>x</sub>), 40 – 46 (br, (CH<sub>2</sub>-CHPh)<sub>x</sub>), 40.7 (br, (CH<sub>2</sub>-CHPh)<sub>x</sub>), 54.9 (CH<sub>2</sub>-O-CH<sub>2</sub>-CH<sub>2</sub>-CH<sub>2</sub>-NH), 61.2 (C(CH<sub>3</sub>)), 68 (br, CH<sub>2</sub>-O-CH<sub>2</sub>-CH<sub>2</sub>-CH<sub>2</sub>-NH), 75 (br, CH<sub>2</sub>-O-CH<sub>2</sub>-CH<sub>2</sub>-CH<sub>2</sub>-NH), 124 – 127 (br, (CH<sub>2</sub>-CHPh<sub>para</sub>)<sub>x</sub>), 123 (br, Ni-C=N) 127 – 129.5 (br, (CH<sub>2</sub>-CHPh<sub>ortho+meta</sub>)<sub>x</sub>), 145-146.5 (br, (CH<sub>2</sub>-CHPh<sub>ipso</sub>)<sub>x</sub>), 178 (NCN) ppm; IR (KBr): ν = 3284 (NH), 3060, 3025, 2923, 2849 (CH), 2253 + 2226 (C=N), 1601 (C-C ar), 1575 (N-C-N), 1493, 1452 (C-C ar), 1097 (ClO<sub>4</sub>) cm<sup>-1</sup>. UV/Vis (CH<sub>2</sub>Cl<sub>2</sub>): λ (ε) 250 (10900), 257 (12300), 289 (4100).

**Block copolymer synthesis.** Block copolymers were prepared by dissolving 65 mg (13  $\mu\text{mol}$ ) **1** in 5 ml  $\text{CH}_2\text{Cl}_2$  and subsequent addition of  $y$  equivalents of the desired isocyanopeptide. After stirring for 1 hour the solutions were poured in 150 ml  $\text{H}_2\text{O}/\text{MeOH}$  (5/1 v/v), on a rotary evaporator the majority of the  $\text{CH}_2\text{Cl}_2$  was removed and the resulting yellow/brown product was filtered off, washed with methanol and dried in vacuo (yields 55 – 95%).

**PS<sub>x</sub>-b-PIAA<sub>y</sub>.**  $^1\text{H}$  NMR ( $\text{CDCl}_3$ ):  $\delta = 0.73 - 1.22$  ( $\text{Bu}-(\text{CH}_2-\text{CHPh})_x$ ),  $1.22 - 1.75$  ( $\text{CH}_2-\text{CHPh})_x + (\text{CN}-\text{CH}(\text{CH}_3)-\text{CONH}-\text{CH}(\text{CH}_3)-\text{CO}_2\text{CH}_3)_y$ ,  $1.75 - 2.35$  ( $(\text{CH}_2-\text{CHPh})_x$ ),  $3.42 - 3.90$  ( $\text{CN}-\text{CH}(\text{CH}_3)-\text{CONH}-\text{CH}(\text{CH}_3)-\text{CO}_2\text{CH}_3)_y$ ,  $3.90 - 4.88$  ( $(\text{CN}-\text{CH}(\text{CH}_3)-\text{CONH}-\text{CH}(\text{CH}_3)-\text{CO}_2\text{CH}_3)_y$ ),  $6.28 - 7.25$  ( $(\text{CH}_2-\text{CHPh})_x$ ) ppm.  $^{13}\text{C}$  NMR ( $\text{CDCl}_3$ ):  $\delta = 14$  ( $\text{CH}_3-\text{CH}_2-\text{CH}(\text{CH}_3)-(\text{CH}_2-\text{CHPh})_x$ ),  $15 - 19.5$  (br, ( $\text{CN}-\text{CH}(\text{CH}_3)-\text{CONH}-\text{CH}(\text{CH}_3)-\text{CO}_2\text{CH}_3)_y$ ),  $20 - 24.5$  (br, ( $\text{CN}-\text{CH}(\text{CH}_3)-\text{CONH}-\text{CH}(\text{CH}_3)-\text{CO}_2\text{CH}_3)_y$ ),  $22.5$  ( $\text{CH}_3-\text{CH}_2-\text{CH}(\text{CH}_3)-(\text{CH}_2-\text{CHPh})_x$ ),  $27$  ( $\text{CH}_3-\text{CH}_2-\text{CH}(\text{CH}_3)-(\text{CH}_2-\text{CHPh})_x$ ),  $30$  ( $\text{C}=\text{N}-\text{C}(\text{CH}_3)$ ),  $32$  ( $\text{CH}_3-\text{CH}_2-\text{CH}(\text{CH}_3)-(\text{CH}_2-\text{CHPh})_x$ ),  $33.5 - 39.5$  (br,  $\text{CH}_2-\text{O}-\text{CH}_2-\text{CH}_2-\text{CH}_2-\text{NH}_2$ ),  $40 - 46$  (br, ( $\text{CH}_2-\text{CHPh})_x$ ),  $40.5$  (br, ( $\text{CH}_2-\text{CHPh})_x$ ),  $46.5 - 48$  (br, ( $\text{CN}-\text{CH}(\text{CH}_3)-\text{CONH}-\text{CH}(\text{CH}_3)-\text{CO}_2\text{CH}_3)_y$ ),  $49 - 51$  (br, ( $\text{CN}-\text{CH}(\text{CH}_3)-\text{CONH}-\text{CH}(\text{CH}_3)-\text{CO}_2\text{CH}_3)_y$ ),  $61 - 64$  (br, ( $\text{CN}-\text{CH}(\text{CH}_3)-\text{CONH}-\text{CH}(\text{CH}_3)-\text{CO}_2\text{CH}_3)_y$ ),  $68$  (br,  $\text{CH}_2-\text{O}-\text{CH}_2-\text{CH}_2-\text{CH}_2-\text{NH}_2$ )  $74$  (br,  $\text{CH}_2-\text{O}-\text{CH}_2-\text{CH}_2-\text{CH}_2-\text{NH}_2$ ),  $124 - 127$  (br, ( $\text{CH}_2-\text{CHPh}_{\text{para}}$ )<sub>x</sub>),  $127 - 129.5$  (br, ( $\text{CH}_2-\text{CHPh}_{\text{ortho+meta}}$ )<sub>x</sub>),  $145 - 146.5$  (br, ( $\text{CH}_2-\text{CHPh}_{\text{ipso}}$ )<sub>x</sub>),  $160 - 165$  (br, ( $\text{CN}-\text{CH}(\text{CH}_3)-\text{CONH}-\text{CH}(\text{CH}_3)-\text{CO}_2\text{CH}_3)_y$ ),  $171 - 174$  (br, ( $\text{CN}-\text{CH}(\text{CH}_3)-\text{CONH}-\text{CH}(\text{CH}_3)-\text{CO}_2\text{CH}_3)_y$ ) ppm. IR (KBr):  $\nu = 3270$  (NH),  $3060$ ,  $3025$ ,  $2923$ ,  $2849$  (CH),  $1749$  ( $\text{C}=\text{O}$  ester),  $1601$  (C-C ar),  $1657$  (amide I),  $1532$  (amide II),  $1493$ ,  $1452$  (C-C ar)  $\text{cm}^{-1}$ .

**PS<sub>x</sub>-b-PIAH<sub>y</sub>.**  $^1\text{H}$  NMR ( $\text{CDCl}_3$ ):  $\delta = 0.6 - 1.2$  ( $\text{Bu}-(\text{CH}_2-\text{CHPh})_x$ ),  $1.2 - 1.6$  ( $\text{CH}_2-\text{CHPh})_x + (\text{CN}-\text{CH}(\text{CH}_3)-\text{CONH}-\text{CH}(\text{CH}_2\text{Im})-\text{CO}_2\text{CH}_3)_y$ ,  $1.6 - 2.2$  ( $(\text{CH}_2-\text{CHPh})_x$ ),  $2.2 - 2.5$  ( $\text{PhCH}_3$ ),  $2.6 - 3.8$  ( $\text{CN}-\text{CH}(\text{CH}_3)-\text{CONH}-\text{CH}(\text{CH}_2\text{Im})-\text{CO}_2\text{CH}_3)_y$ ,  $4.2 - 5.3$  ( $(\text{CN}-\text{CH}(\text{CH}_3)-\text{CONH}-\text{CH}(\text{CH}_2\text{Im})-\text{CO}_2\text{CH}_3)_y$ ),  $6.2 - 7.2$  ( $(\text{CH}_2-\text{CHPh})_x$ ),  $7.2 - 7.6$  ( $\text{ToS}$ ),  $7.6 - 8.2$  ( $\text{Im}$ ) ppm.  $^{13}\text{C}$  NMR ( $\text{CDCl}_3$ ):  $\delta = 14$  ( $\text{CH}_3-\text{CH}_2-\text{CH}(\text{CH}_3)-(\text{CH}_2-\text{CHPh})_x$ ),  $20 - 24$  (br, ( $\text{CN}-\text{CH}(\text{CH}_3)-\text{CONH}-\text{CH}(\text{CH}_2\text{Im})-\text{CO}_2\text{CH}_3)_y$ ),  $22.5$  ( $\text{CH}_3-\text{CH}_2-\text{CH}(\text{CH}_3)-(\text{CH}_2-\text{CHPh})_x$ ),  $26.4$  ( $\text{CH}_3-\text{CH}_2-\text{CH}(\text{CH}_3)-(\text{CH}_2-\text{CHPh})_x$ ),  $28$  ( $\text{PhCH}_3$ ),  $29 - 33$  (br, ( $\text{CN}-\text{CH}(\text{CH}_3)-\text{CONH}-\text{CH}(\text{CH}_2\text{Im})-\text{CO}_2\text{CH}_3)_y$ ),  $31$  ( $\text{C}=\text{N}-\text{C}(\text{CH}_3)$ ),  $32$  ( $\text{CH}_3-\text{CH}_2-\text{CH}(\text{CH}_3)-(\text{CH}_2-\text{CHPh})_x$ ),  $33.5 - 39.5$  (br,  $\text{CH}_2-\text{O}-\text{CH}_2-\text{CH}_2-\text{CH}_2-\text{NH}_2$ ),  $40 - 46$  (br, ( $\text{CH}_2-\text{CHPh})_x$ ),  $40.5$  (br, ( $\text{CH}_2-\text{CHPh})_x$ ),  $49 - 56$  (br, ( $\text{CN}-\text{CH}(\text{CH}_3)-\text{CONH}-\text{CH}(\text{CH}_2\text{Im})-\text{CO}_2\text{CH}_3)_y + (\text{CN}-\text{CH}(\text{CH}_3)-\text{CONH}-\text{CH}(\text{CH}_2\text{Im})-\text{CO}_2\text{CH}_3)_y$ ),  $61 - 64$  (br, ( $\text{CN}-\text{CH}(\text{CH}_3)-\text{CONH}-\text{CH}(\text{CH}_2\text{Im})-\text{CO}_2\text{CH}_3)_y$ ),  $68$  (br,  $\text{CH}_2-\text{O}-\text{CH}_2-\text{CH}_2-\text{CH}_2-\text{NH}_2$ )  $74$  (br,  $\text{CH}_2-\text{O}-\text{CH}_2-\text{CH}_2-\text{CH}_2-\text{NH}_2$ ),  $113 - 117$  ( $\text{Im}_{\text{meta}}$ ),  $124 - 127$  (br, ( $\text{CH}_2-\text{CHPh}_{\text{para}}$ )<sub>x</sub>),  $127 - 129.5$ ,  $130 - 132$  (br, ( $\text{CH}_2-\text{CHPh}_{\text{ortho+meta}}$ )<sub>x</sub> +  $\text{ToS}_{\text{ortho+meta}}$ ),  $134 - 137$  ( $\text{Im}_{\text{ortho}}$ ),  $138 - 143$  ( $\text{Im}_{\text{ipso}}$ ),  $145 - 146.5$  (br, ( $\text{CH}_2-\text{CHPh}_{\text{ipso}}$ )<sub>x</sub> +  $\text{ToS}_{\text{ipso}}$ ),  $160 - 165$  (br, ( $\text{CN}-\text{CH}(\text{CH}_3)-\text{CONH}-\text{CH}(\text{CH}_3)-\text{CO}_2\text{CH}_3)_y$ ),  $171 - 174$  (br, ( $\text{CN}-\text{CH}(\text{CH}_3)-\text{CONH}-\text{CH}(\text{CH}_2\text{Im})-\text{CO}_2\text{CH}_3)_y$ ) ppm. IR (KBr):  $\nu = 3260$  (NH),  $3024$ ,  $2925$ ,  $2851$  (CH),  $1745$  ( $\text{C}=\text{O}$  ester),  $1598$  (C-C ar),  $1659$  (amide I),  $1529$  (amide II),  $1493$ ,  $1452$ ,  $1375$ ,  $1171$  (C-C ar)  $\text{cm}^{-1}$ .

## 5.5 References and Notes

- 1 S. I. Stupp V. LeBonheur, K. Walker, L. S. Li, K. E. Huggins, M. Keser, A. Amstutz *Science* **276**, 384 (1997).
- 2 'Frontiers in Materials Science' special section in *Science* **277**, 1213 (1997).
- 3 Phospholipid derived surfactants: J. M. Schnur, *Science* **262**, 1669 (1993) and references therein; N. A. J. M. Sommerdijk et al., *J. Chem. Soc. Chem. Commun.* 1941 (1994); N. A. J. M. Sommerdijk, M. H. L. Lambermon, M. C. Feiters, R. J. M. Nolte, B. Zwanenburg, *Chem. Commun.* 1423 (1997). Amino acid derived surfactants: N. Nakashima, S. Asakuma, T. Kunitake, *J. Am. Chem. Soc.* **107**, 509 (1985); T. Kunitake and N. Yamada, *J. Chem. Soc. Chem. Commun.*, 655 (1986); T. Kunitake, J.-M. Kim, Y. Ishikawa, *J. Chem. Soc. Perkin Trans.* **2**, 885 (1991); N. A. J. M. Sommerdijk, M. H. L. Lambermon, M. C. Feiters, R. J. M. Nolte, B. Zwanenburg, *Chem. Commun.*, 455 (1997). Nucleic acid derived surfactants: H. Yanagawa, Y. Ogawa, H. Furuta, K. Tsuno, *Chem. Lett.*, 269 (1988); H. Yanagawa, Y. Ogawa, H. Furuta, K. Tsuno, *J. Am. Chem. Soc.* **114**, 3414 (1989). Carbohydrate based surfactants: J. H. Fuhrhop, W. Helfrich, *Chem. Rev.* **93**, 1565 (1993) and references therein; R. J. H. Hafkamp, M. C. Feiters, R. J. M. Nolte, *Angew. Chem.* **106**, 1054 (1994).
- 4 H. Shen, L. Zhang and A. Eisenberg, *J. Am. Chem. Soc.* **121**, 2728 (1999).
- 5 J. C. M. van Hest, D. A. P. Delnoye, M. W. P. L. Baars, M. H. P. van Genderen, E. W. Meijer, *Science* **268**, 1592 (1995).
- 6 L. Zhang and A. Eisenberg, *Science* **268**, 1728 (1995).
- 7 L. Zhang, K. Yu, A. Eisenberg, *Science* **272**, 1777 (1996).
- 8 N. A. J. M. Sommerdijk, S. J. Holder, R. C. Hiorns, R. G. Jones, R. J. M. Nolte, *Macromolecules*, **33**, 8289 (2000).
- 9 R. J. M. Nolte, *Chem. Soc. Rev.*, **23**, 11 (1994).
- 10 a) J. J. L. M. Cornelissen, W. S. Graswinckel, P. J. H. M. Adams, G. Nachtegaal, A. Kentgens, N. A. J. M. Sommerdijk, R. J. M. Nolte submitted for publication. b) Chapter 2 of this thesis.
- 11 a) J. J. L. M. Cornelissen, J. J. J. M. Donners, R. de Gelder, W. S. Graswinckel, A. E. Rowan, N. A. J. M. Sommerdijk, R. J. M. Nolte *Science*, **293**, 676 (2001). b) Chapter 3 of this thesis.
- 12 J. M. van der Eijk, R. J. M. Nolte, W. Drenth, A. M. F. Hezemans, *Macromolecules* **13**, 1391 (1980)
- 13 Different batches CO<sub>2</sub> end-capped polystyrene (M<sub>n</sub> ranges from 3000 – 10,000 g/mol) could be prepared conveniently and with efficiencies comparable with those reported; J. C. M. van Hest, *Ph.D. Thesis*, Eindhoven University of Technology, (1996).
- 14 J. C. M. van Hest, Delnoye, D. A. P., M. W. P. L. Baars, C. Elissen-Roman, M. H. P. van Genderen, E. W. Meijer *Chem. Eur. J.* **12**, 1616 (1996).
- 15 P. van Rijnsbergen, unpublished results.
- 16 R. W. Stephany and W. Drenth, *Recl. Trav. Chim. Pays-Bas* **91**, 1453 (1972).
- 17 P. C. J. Kamer, R. J. M. Nolte, W. Drenth, *J. Chem. Soc. Chem. Commun.*, 1789 (1986); P. C. J. Kamer, R. J. M. Nolte, W. Drenth, *J. Am. Chem. Soc.* **110**, 6818 (1988).
- 18 H. G. J. Visser, R. J. M. Nolte, J. W. Zwikker, W. Drenth, *J. Org. Chem.* **17**, 3139 (1985).
- 19 J. T. Chen, E. L. Thomas, C. K. Ober, G.-P. Mao, *Science* **273**, 343 (1996).
- 20 J. M. Schnur, B. R. Ratna, J. V. Selinger, A. Singh, G. Jyothi, K. R. K. Easwaran, *Science* **264**, 945 (1994).
- 21 B. N. Thomas, C. M. Lindemann, N. A. Clark, *Phys. Rev. E* **59**, 3040 (1999).
- 22 J. van Esch, F. Schoonbeek, M. de Loos, H. Kooijman, A. L. Spek, R. M. Kellogg, B. L. Feringa *Chem. Eur. J.* **5**, 937 (1999).





# CHAPTER 6

## Block Copolymers based on Polyisocyanopeptides and Carbosilane Dendrimers

### 6.1 Introduction

The control over block copolymer morphologies is of great importance for fine-tuning the performance of structural and functional polymers and the preparation of nanoscale devices. Aggregation and microphase separation of block copolymer systems has yielded a variety of morphologies both in the bulk phase and in solution.<sup>1-8</sup> The phase behavior of block copolymers is determined by differences in polarity but also by incompatibilities in conformational flexibility and in volume filling characteristics of the component blocks.<sup>2,3</sup> Recently, highly ordered structures have been obtained from block copolymers combining branched and linear blocks,<sup>4</sup> as well as from block copolymers comprising both rigid and flexible polymer segments.<sup>5,6,7,8</sup>

In previous work the generation of helical superstructures from rod-coil block copolymers combining a hydrophobic polystyrene tail with a charged helical polyisocyanopeptide headgroup was reported.<sup>8</sup> Polymers of isocyanides adopt a helical backbone conformation due to steric interactions between the side chains. The polymerization of isocyanides is catalyzed by Ni(II) complexes in which a nucleophile, such as an amine, acts as the initiator.<sup>9</sup> In the present case we applied carbosilane dendritic wedges<sup>10</sup> of different generations as initiators of the polymerization reaction which resulted in block copolymers containing a unique combination of structural elements, *i.e.* a flexible, bulky and apolar dendritic carbosilane segment and a rigid, helical rod-like polyisocyanide block (Figure 1). Here we report on the self-assembling behavior of these block copolymers, in particular those derived from the 3<sup>rd</sup> generation dendrimers which in the presence of Ag<sup>+</sup> ions from metallic nano-arrays.

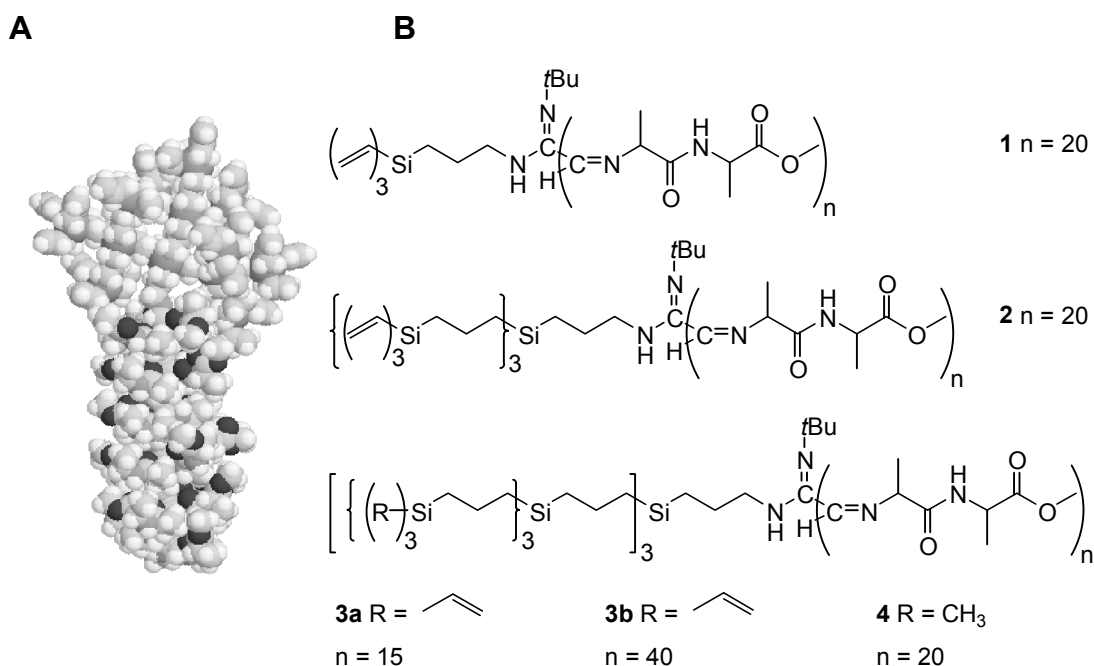


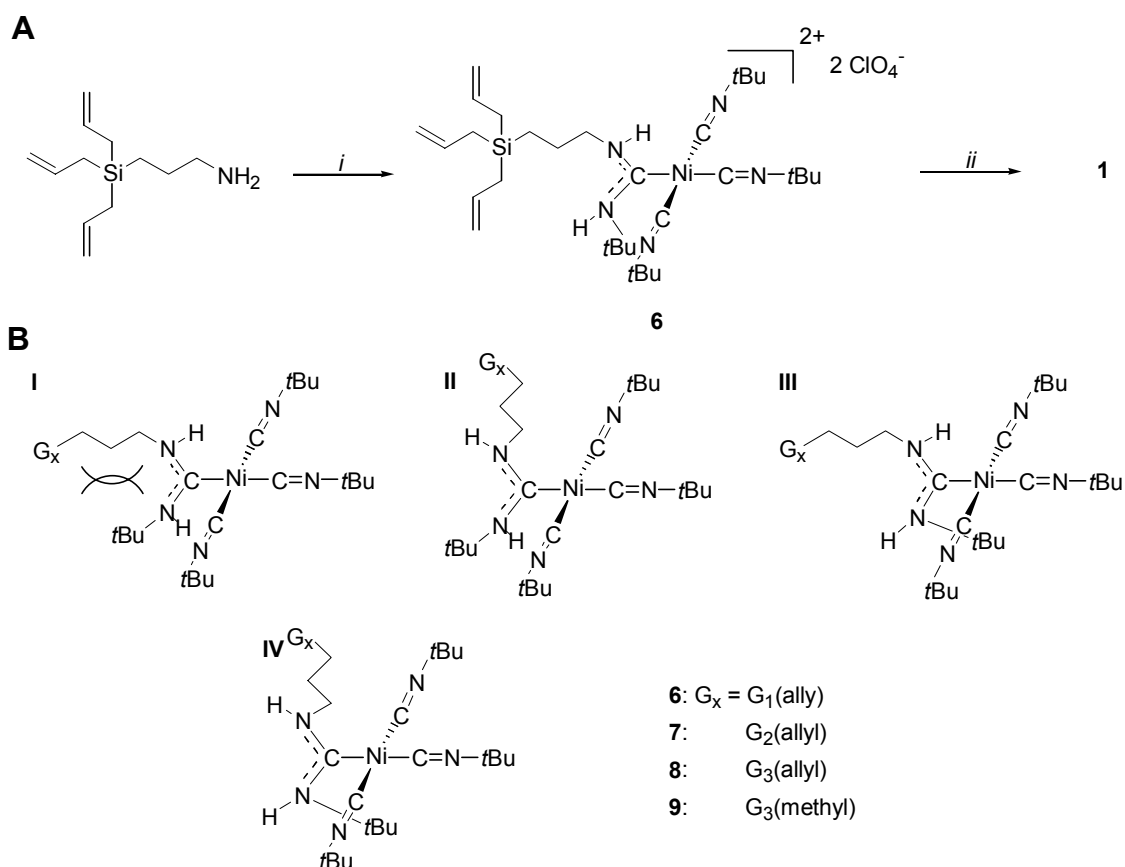
**Figure 1** (A) Computer generated representation of a carbosilane dendrimer-isocyanopeptide block copolymer (**3a**). (B) Synthesized block copolymers based on carbosilane dendritic wedges and polyisocyanopeptides.

## 6.2 Results and Discussion

### 6.2.1 Synthesis and characterization

Carbosilane dendritic wedges were prepared according to the divergent approach with an amine group at the focal point.<sup>10</sup> The nucleophilic wedges, ranging from generation 1 to 3, were reacted with the stable complex  $\text{Ni}(\text{C}=\text{N}-t\text{Bu})_4(\text{ClO}_4)_2$  (**5**) to form the carbene polymerization catalysts (**6** – **9**).<sup>11</sup> The desired block copolymers were obtained by addition of L-isocyanoalanyl-L-alanine methyl ester<sup>12</sup> to these Ni(II) complexes in  $\text{CH}_2\text{Cl}_2$  (Scheme 1). These carbene like catalysts are sufficiently stable to isolate and study them by UV/Vis, IR and NMR spectroscopy, as will be discussed using complex **6** as a model. Both the starting complex **5** and the catalysts **6** - **9** have a square planar arrangement of the ligands and as a consequence approximately the same UV/Vis spectra were found. In the IR spectra the changes were more pronounced: due to the change in symmetry around the nickel center the C=N stretching frequency splits. In **5** a single sharp peak was observed at  $\nu = 2254 \text{ cm}^{-1}$ , whereas in **6** a broader signal at  $\nu = 2228 \text{ cm}^{-1}$  with a shoulder at  $\nu = 2254 \text{ cm}^{-1}$  was found. The presence of a secondary

amine was indicated by the appearance of a vibration at  $\nu = 3294 \text{ cm}^{-1}$  and the signal at  $\nu = 1587 \text{ cm}^{-1}$  with a shoulder at  $\nu = 1544 \text{ cm}^{-1}$  was assigned to the carbene like N-C=N stretching vibration.<sup>11</sup> The broadening of some signals, but in particular the shoulder on this last peak indicates the presence of more than one conformation for **6** and its equivalents **7** – **9**. As a result of the double bond character in the N-C-N moiety free rotation around the C-N bond is unlikely, leading to the presence of multiple conformations which was confirmed by NMR spectroscopy.



**Scheme 1** (A) Synthesis of block copolymers initiated by a first generation carbosilane dendritic wedge with allyl end groups. (i) 1 eq.  $\text{Ni}(\text{CN-tBu})_4(\text{ClO}_4)_2$ ,  $\text{CH}_2\text{Cl}_2$ ; (ii) 20 eq. *L*-isocyanoalanyl-*L*-alanine methyl ester,  $\text{CH}_2\text{Cl}_2$ . (B) Possible conformations and numbering of carbosilane derived carbene like polymerization catalysts.

Both  $^1\text{H}$  and  $^{13}\text{C}$  NMR indicated two major conformations for complex **6** and a trace of a third one. From peak integration and selective saturation experiments the presence of all signals in the NMR spectra could be explained, and the ratio of the two dominant conformations was determined to be 5:2. Based on molecular models

conformation **I** (Scheme 1) was found to be unlikely because of severe steric hindrance between the substituents on the carbene like carbon. In **IV** this strain is somewhat released since these side groups point away from the nickel plain. It is therefore tentatively concluded that conformation **IV** corresponds to the trace amount observed in the  $^1\text{H}$  NMR spectra and that the major conformations are **II** and **III**. The chemical shifts found for  $\text{H}_\text{A}$  and  $\text{H}_\text{B}$  ( $\delta_\text{A} = 8.08$  ppm and  $\delta_\text{B} = 7.00$  ppm for one case and  $\delta_\text{A} = 6.84$  ppm  $\delta_\text{B} = 7.95$  ppm for the other) were in line with an *anti* like organization of the substituents on the N-C-N moiety. In the case of a *syn* type structure a relatively smaller

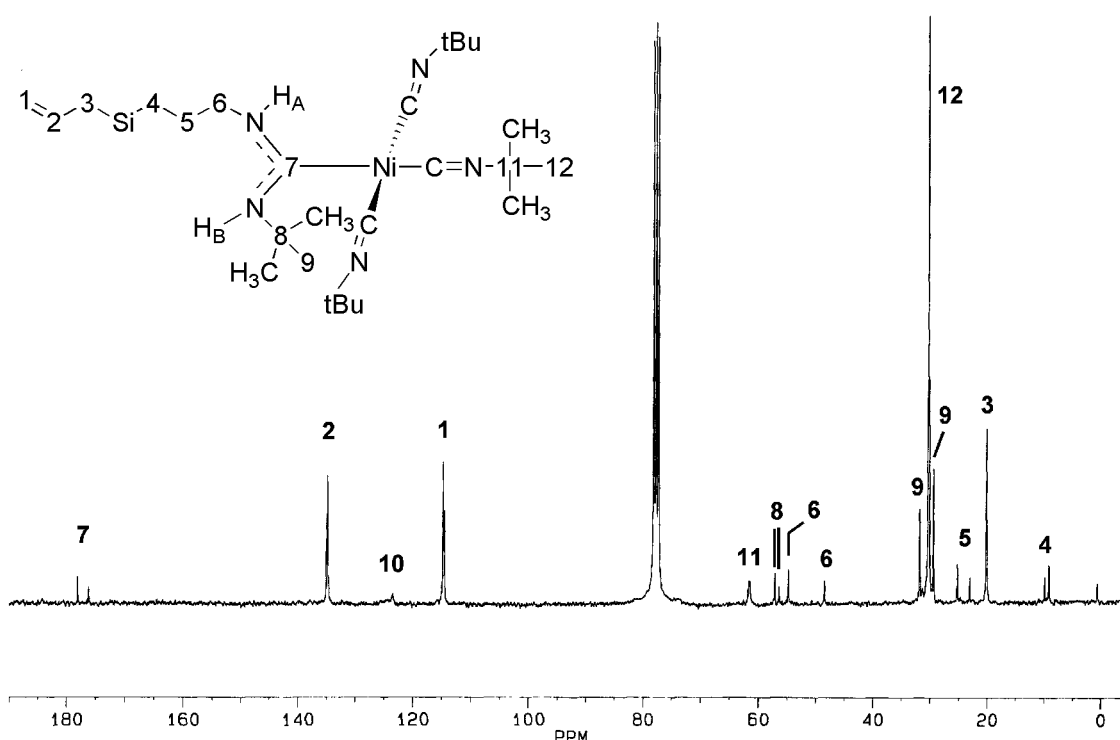


**Figure 2**  $^{13}\text{C}$  NMR spectrum of **6** and assignment of the signals. For some of the signals the doubling is present but not indicated.

difference between both protons is expected, because they will be present in a similar chemical environment (indeed for **IV**  $\delta_\text{A} = 7.48$  ppm and  $\delta_\text{B} = 7.80$  ppm were measured). In line with two different conformations of catalyst **6** for every carbon (except  $\text{C}_3$ ) the signals in the  $^{13}\text{C}$  NMR were doubled (Figure 2). The obtained data did not allow a conclusive assignment of the observed signals to a certain structure. Identification of the different conformations, however, is an important issue as each catalyst might have a different initiating efficiency, *i. e.* a different rate of initiation (*see below*).

The addition of a calculated amount of the dipeptide derived isocyanide to the highly soluble polymerization catalysts **6** – **9** resulted in the block copolymers **1** – **4** which after precipitation were isolated as amorphous powders. Infrared spectroscopy showed fast consumption of the monomers (< 15 min.) and the spectra of the resultant polymers displayed vibrations that could be assigned to characteristic groups of both the polyisocyanide part and the carbosilane dendrimer. Similar features were found in the  $^1\text{H}$  NMR spectra; integration of the signals revealed the ratio between the carbosilane and the polyisocyanopeptide segments in each of the block copolymers synthesized (Figure 1). Further evidence for the formation of block copolymers was obtained from  $^{13}\text{C}$  NMR and size exclusion chromatography. Calibrated against polystyrene samples, molecular weights larger than  $10^3$  g/mol were found and the dendritic initiators were no longer present. In all cases a bimodal molecular weight distribution was found. This was attributed to some aggregation of the macromolecules in the eluent; indeed, varying the concentrations of the samples led to different ratios of the two peaks. The absence of initiator and the linear correlation found between the ratios catalyst/monomer and dendrimer/polyisocyanide as was determined by  $^1\text{H}$  NMR, suggested that the catalysts with different conformations all initiate the isocyanide polymerization reaction. It should be noted, however, that no distribution of the molecular weights could be determined and therefore care has to be taken with regard to this suggestion. No glass transition nor a melting transition could be observed between 225 K and 475 K for the macromolecules described in this Chapter.

Whereas the homopolymer of the L-Ala-L-Ala-derived polyisocyanide is sparingly soluble in chlorinated solvents only,<sup>12</sup> the block copolymers showed enhanced solubility with increasing generation of the dendritic part. For example, **3a** is soluble in a variety of solvents ranging from MeOH to hexane. All block copolymers showed similar UV/Vis and CD spectra with a strong Cotton effect centered around 3125 nm, indicative of the helical organization of the polyisocyanide backbone (Figure 3). The increased solubility of polymers **3a** and **4** allowed the detection of CD bands which are otherwise masked by the solvent (Figure 3A). The strong bisignate signal found in the region 210 – 260 nm, which is attributed to transitions in the amide functionalities, was not observed for the monomer measured at a comparable concentrations. This is in line with a high level of organization of these functions, as is expected for the  $\beta$ -sheet-like organization of the side chains in these polyisocyanopeptides.<sup>13</sup>

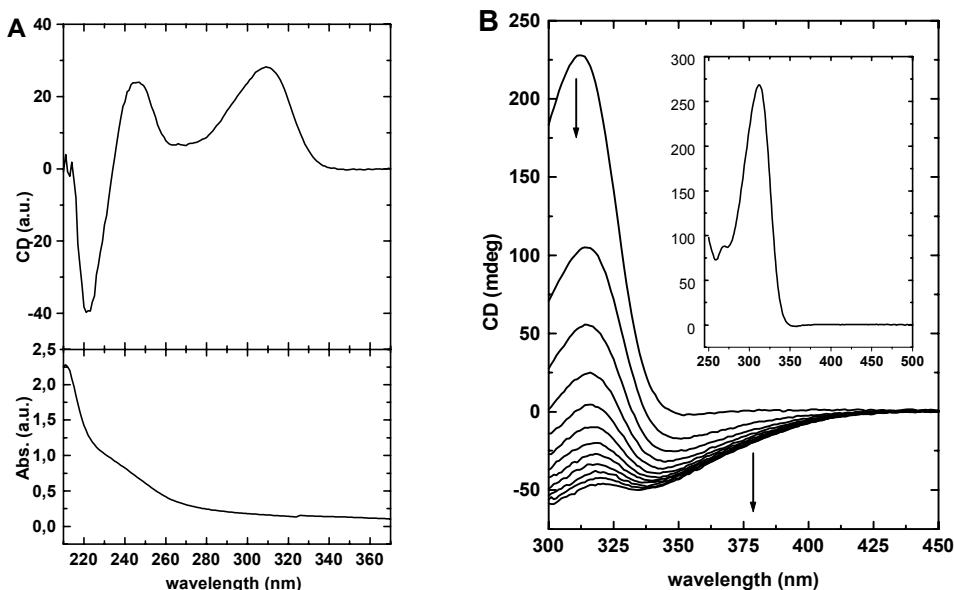


**Figure 3** CD and UV/Vis spectra of **3a** in MeOH (**A**). CD spectra of **4** monitored in time upon addition of silver ions. Spectra were recorded with intervals of 2 min. after the addition of a 10  $\mu$ L aliquot of a 0.3 M solution of  $\text{AgBF}_4$  in acetone to 1.5 ml of a solution containing 0.3 g/L of **4** in chloroform. Inset shows the CD spectrum of **4** in pure chloroform (**B**).

### 6.2.2 Self-assembling properties

Initial studies on the first and second generation systems (block copolymers **1** and **2** respectively), showed that these these block copolymers displayed physical properties which were rather similar to those of the constituent homopolymer. The self-organizing properties of the block copolymers **3** and **4** were different and were studied in more detail.

Dynamic light scattering (DLS) revealed that in  $\text{CHCl}_3$  at concentrations larger than 0.5 % (w/w) two types of structures were present: one type with a diameter of ~6 nm (likely micellar in nature based on the size of the block copolymers and the expected size of the formed assemblies) and a second one with a hydrodynamic diameter of approximately 90 nm. TEM analysis of these dispersions did not demonstrate the formation of well-defined aggregates, only amorphous material was observed. In the solid state, X-ray powder diffraction studies displayed sharp reflections which could be related to a pseudo hexagonal organization of the polyisocyanopeptide blocks, similar as found for the homopolymer.<sup>13</sup> The observation of the same type of organization found for the rod-like segments in both the block copolymers and the homopolymers in the solid state points to the presence of (at least partial) phase separated domains of the

component segments. No detailed investigations have been conducted, however, to further substantiate this. Subsequent experiments were aimed at finding out how ordered assemblies could be obtained in solution. To this end it was tried to produce block copolymers with less compatible component segments, which would give rise to a more developed phase behavior.

First the methyl ester functions in the isocyanide part of **3a** were hydrolyzed to carboxylate groups with base. The complete removal of the ester groups was confirmed by IR spectroscopy. Surprisingly the modified block copolymer was soluble in water and as a result no (well defined) aggregates were formed. The second attempt involved the modification of the dendritic parts of the block copolymers investigated. Oxidation of the allyl functionalities to the corresponding epoxides would provide a synthetic handle to introduce a variety of (functional) groups. The use of either mCPBA or  $\text{Ni}(\text{acac})_2 / \text{O}_2$  as oxidants did not result in the detectable formation of the desired epoxides.

### 6.2.3 Effect of $\text{Ag}^+$ ions on the self-assembling properties

In a third approach to increase the incompatibility of the component blocks and to create an organic / inorganic hybrid polymer, complexation of metal ions targeting the allyl-periphery of the  $\text{G}_3$ -dendritic part of **3** was investigated. We chose to complex soft  $\text{Ag}^+$  ions to the allyl functions, however, it appeared from initial experiments that these ions preferentially complexed to the hard peptide donors present in the polyisocyanide segments. This was indicated by CD spectroscopy (Figure 3B, *see below*) in combination with FT-IR spectroscopy, *i.e.* a broadening of the  $\text{C}=\text{O}$  resonances in the IR spectrum was observed and a shift to lower wavenumbers (*viz.* from  $1657$  to  $1651\text{cm}^{-1}$  and from  $1751$  to  $1743\text{cm}^{-1}$ ) of the amide I and the ester carbonyl vibrations. These results imply that it does not make any difference whether **3** or **4** is used in the present experiments. The polyisocyanide segments dominate the (binding) properties of the systems.

Polymeric silver complexes were subsequently prepared by adding  $\text{AgBF}_4$  in acetone to a solution of the block copolymers **3** and **4** in  $\text{CHCl}_3$ . With the help of CD spectroscopy the complexation of the silver ions was monitored. The strong Cotton effect originally present at  $312\text{ nm}$  slowly decreased in intensity and a new broad band with a negative sign was formed (Figure 3B). Addition of pure acetone (0-25 % v/v) to



a solution of **3** or **4** in  $\text{CHCl}_3$  did not lead to any change in the shape or sign of the

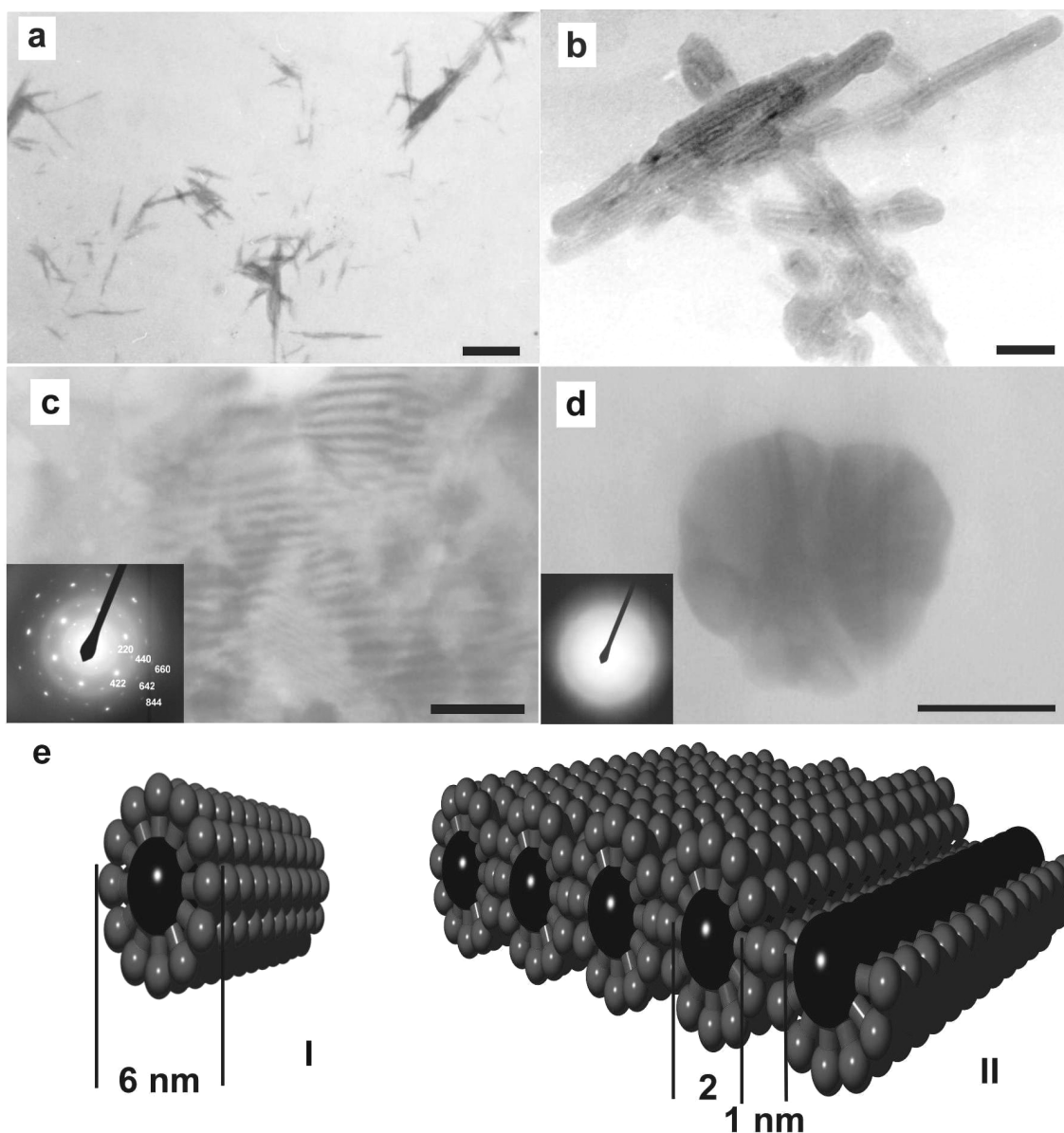


**Figure 4** (a) Transmission electron micrograph of a chloroform solution containing **3a** and 50 equivalents of  $\text{AgBF}_4$  displaying nanoarrays of block copolymers and silver (bar = 150 nm); (b) Enlargement of the structures in (a), showing nanoarrays of block copolymers and silver (bar = 100 nm). (c) Transmission electron micrograph of a chloroform solution containing **4** and 40 equivalents of  $\text{AgBF}_4$  displaying nanoarrays of block copolymers and silver; bar = 20 nm [inset: electron diffraction pattern of the area shown in (c)]. (d) Idem of **3b** and 40 equivalents of  $\text{AgBF}_4$  (bar = 50 nm) [inset: electron diffraction pattern of the area shown in (d)]. (e) Schematic representation of the proposed molecular organization of the block copolymers (I) in the presence of  $\text{Ag}^+$  and (II) deposited on a carbon coated microscope grid. The indicated dimensions are derived from DLS (I) and the electron micrographs (II).

Cotton effects indicating that the observed effects are not due to the presence of acetone. DLS revealed that the complexation of silver ions was accompanied with the formation of larger structures in solution. Upon addition of  $\text{AgBF}_4$  in acetone to a  $\text{CHCl}_3$  solution of **4**, the hydrodynamic diameters of the assemblies rapidly increased from  $\sim 90$  nm to values larger than  $1 \mu\text{m}$ . The use of lower concentrations of silver-ions led to a reduction in both the growth rate and in the ultimate size of the observed structures.

The obtained aggregates were deposited from pure  $\text{CHCl}_3$  (see Experimental) on carbon coated microscopy grids and were studied using TEM which revealed the presence of well-defined silver-containing patterns of nano-sized dimensions. For both **3a** and **4** similar patterns of alternating light and dark stripes were observed (Figure 4b and c). When the length of the polyisocyanide segment in the copolymers was increased (e.g. as in **3b**) differently shaped aggregates with a less defined interior fine-structure were found (Figure 4d). According to Electron Dispersive Spectroscopy (EDS) the aggregates had an elemental composition consistent with silver complexes of the block copolymers.

The formation of the defined nano-sized patterns by **3a** and **4** can be explained by assuming that initially micellar fibers are present which cluster by the addition of  $\text{Ag}^+$ . The periphery of the fibers is thought to consist of the flexible dendritic segments, whereas their cores contain the silver-binding polyisocyanopeptide blocks (Figure 4b and e). The deposition of these clustered fibers on the surface of the microscope grid while maintaining the fibrous organization over longer distances, would then lead to the formation of striped patterns which consist of alternating purely organic and silver-containing nanodomains (Figure 4e).

The effect of the complexation of  $\text{Ag}^+$  ions on the aggregation behavior of the block copolymers was also studied at the air-water interface in a Langmuir trough. In Figure 5 the monolayer isotherms of **3b** and **4** in the absence and presence of  $\text{AgNO}_3$  in the subphase are depicted. The onset of the isotherms resemble in shape the isotherms obtained for the corresponding homopolymers.<sup>14</sup> A quantitative comparison, however, is difficult since the homopolymers and copolymers display large differences in molecular weights and structural composition. The lift-off area for block copolymer **3** was found to be much larger than that of block copolymer **4**, which is in line with longer block length of the polyisocyanide segment in the former polymer. For both **3**

and **4** it was found that the presence of silver resulted in an increase in the molecular area, while the pressure characteristics remained virtually the same. Apparently complexation of the  $\text{Ag}^+$  ions to the polyisocyanide part leads to an increased molecular radius without having a substantial effect on the conformation of this segment. The binding of these ions enhances the clustering of the block copolymers as was clear from the decompression curves. Homopolymers of the isocyanide give highly reversible isotherms on compression and decompression,<sup>14</sup> but for the block copolymers on pure water significant hysteresis was observed and finally when  $\text{AgNO}_3$  was present a steep decrease in pressure was found upon decompression of the monolayer. Monitoring the compression and decompression processes by Brewster angle microscopy (BAM) revealed that in the former case a featureless dense film was formed. Decompression led to the breaking of the film into large solid domains.

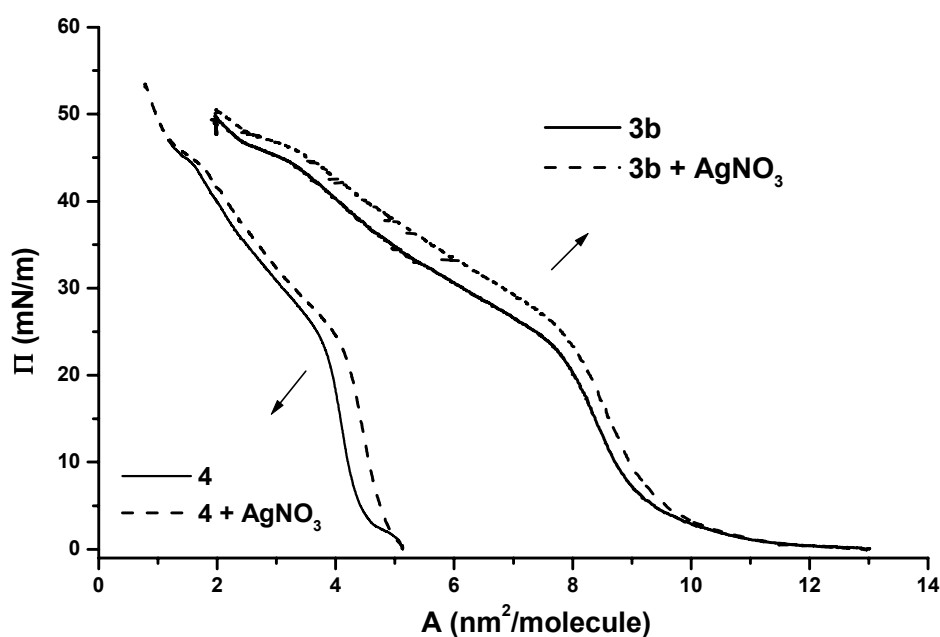


**Figure 5** Pressure-area isotherms of **3b** and **4** on the air-water interface both in the absence and presence of  $\text{AgNO}_3$ .

An enhancement of contrast in the fine structure was observed when the assemblies were irradiated with the electron beam during visualization in the TEM. This suggests that during exposure the  $\text{Ag}^+$  ions are reduced to metallic silver,<sup>15</sup> which was confirmed by selected area electron diffraction experiments (Figure 3c and d, insets). Interestingly, this experiment also revealed that in the case of **3a** and **4** the reduction

predominantly leads to [111] oriented silver-crystals. When, however, block copolymers containing a larger polyisocyanide segment (i.e. **3b**) were used, the silver present in the aggregates had polycrystalline character (Figure 3d, inset). This indicates that the assemblies formed by the block copolymers have a substantial influence on the type of silver nanopatterns that is formed. The silver present in the polyisocyanide segment crystallizes, which results in the formation of silver arrays. In the case of **3a** these arrays had a diameter of less than 2 nm and lengths longer than 80 nm. When the ratio dendrimer/polyisocyanide was smaller, e.g. as in **3b**, the formed aggregates were less well defined and therefore had a diminished capacity of directing the precise location of the silver ions. As a result less well defined silver structures were generated. This control by small changes in the block copolymer composition opens the possibility of using the phase behavior of these systems to direct the formation of metallic precipitates.<sup>16</sup> The unprecedented formation of predominantly [111] oriented silver arrays is remarkable and at this moment not completely understood.

### 6.3 Conclusions

Using the Ni(II) catalyzed polymerization of isocyanides, novel block copolymers can be prepared starting from amine-functionalized carbosilane dendrimers. The combination of two conformationally highly inequivalent blocks in these copolymers leads to aggregate formation in organic solutions which is strongly affected by the presence of silver salts. It is been demonstrated that these block copolymers respond to the addition of silver ions by the generation of nanowires consisting of [111] oriented crystalline silver.<sup>17</sup> This process offers interesting possibilities for the generation of conducting nanoscopic architectures.

## 6.4 Experimental Section

### 6.4.1 General methods and materials

Dichloromethane was distilled from CaH<sub>2</sub>, all other chemicals were commercial products and were used as received. Flash chromatography was performed over silica gel (0.035-0.075 mm) purchased from Acros and TLC analyses on silica 60 F<sub>254</sub> coated glass either from Merck or Acros. Compounds were visualized with I<sub>2</sub>-vapour or Cl<sub>2</sub>/tetramethyldiaminophenylmethane (TDM). <sup>1</sup>H NMR spectra were recorded on Bruker AC-100, Bruker WM-200 and Bruker AC-300 instruments at 297 K. <sup>13</sup>C NMR

spectra were measured on a Bruker AC-300 machine. All chemical shifts are reported in ppm relative to tetramethylsilane ( $\delta = 0.00$  ppm) as an internal standard. FT-Infrared spectra were recorded on a Bio-Rad FTS 25 instrument and DSC measurements were performed on a Perkin Elmer DSC 7 instrument (10 °C/min.). UV/Vis spectra were measured on a Varian Cary 50 conc spectrophotometer and CD spectra on a JASCO 810 instrument. Transmission electron microscopy was performed on Philips EM210 and JEOL JEM 2000 FX operating at 60 kV and 120 kV, respectively. X-ray powder diffractograms were collected on a Philips PW1710 diffractometer equipped with a Cu LFF X-ray tube operating at 40 kV and 55 mA. Samples were measured on a silicon wafer between 3 and 60°, using a step width of 0.05°.

**Monolayer experiments.** Pressure-area isotherms were recorded on a thermostatted (20 °C), home-built trough (140 × 210 mm). The surface pressure was measured using Wilhelmy plates mounted on a Trans-Tek transducer (Connecticut, U.S.A.). The surface of the monolayers was studied with a Brewster angle microscope (NFT BAM-1), equipped with a 10 mW He-Ne laser (632.8 nm) having a spot diameter of 0.68 mm. Reflections were detected using a CCD camera. The subphase consisted of water (Milli-Q) or a 1 mM AgNO<sub>3</sub> solution; 15 – 20  $\mu$ l of a 1.2 mg/ml polymer solution was spread on the surface, allowed to evaporate for 30 min, and the monolayer was subsequently compressed with a rate of 1.1 cm<sup>2</sup>/min.

**Transmission electron microscopy.** A drop of a dispersion of a copolymer in CHCl<sub>3</sub> was placed on a carbon coated microscope grid, after the solvent had evaporated the specimen was examined without shadowing or staining. The Ag<sup>+</sup> complexes of the block copolymers were prepared by adding a calculated amount of AgBF<sub>4</sub> in acetone to a polymer solution in CHCl<sub>3</sub>. The solvent was evaporated and the complexes were redissolved in CHCl<sub>3</sub>. All experiments were carried out under careful exclusion of light. See text for the characterization of the silver complexes.

**Dynamic light scattering.** Measurements were performed on a home built equipment in the group of prof. M. Schmidt, Institut für Physikalische Chemie der Universität Mainz, Mainz, Germany. Samples were prepared by dissolving 50.6 mg of **4** in 5 ml of CHCl<sub>3</sub>. The solutions were filtered over a 1  $\mu$ m pore size filter. The effect of Ag<sup>+</sup> ions was monitored by adding AgBF<sub>4</sub> solutions in acetone with concentrations ranging from 0.1 – 0.02 M. The final acetone/CHCl<sub>3</sub> ratio was 1/20 v/v.

## 6.4.2 Compounds

Carbosilane dendritic wedges prepared following procedures described in ref. 10, were kindly donated by Dr. J.N.H. Reek (University of Amsterdam). L-Isocyanoalanyl-L-alanine methyl ester was prepared as described in Chapter 2 of this thesis.

**General synthesis of the block copolymers.** The Ni(II) carbene complexes (**6** – **9**) were prepared by dissolving 0.15 mmol of the amine functionalized carbosilane dendritic wedges in 2 ml of CH<sub>2</sub>Cl<sub>2</sub>. This solution was subsequently added to a well-stirred suspension of 3 mM Ni(CN-*t*Bu)<sub>4</sub>(ClO<sub>4</sub>)<sub>2</sub> (**5**)<sup>11a</sup> in CH<sub>2</sub>Cl<sub>2</sub>. After 15 min. the solvent was evaporated and the oily products were redissolved in a known amount of CH<sub>2</sub>Cl<sub>2</sub>. The block copolymers were prepared by adding a calculated volume of the Ni(II)

carbene solution, corresponding to the desired Ni/isocyanide ratio to an isocyanide solution in CH<sub>2</sub>Cl<sub>2</sub>. The reaction mixture was stirred for 30 min. after which IR showed complete consumption of the isocyanide. The product was precipitated in MeOH/water (1:1 v/v), filtered off, redissolved in CH<sub>2</sub>Cl<sub>2</sub> and precipitated again with Et<sub>2</sub>O resulting in a pale brown solid, which was dried in vacuo.

For polymers **1**, **2** and **3** similar spectral data were obtained, only differences in intensities of the overlapping signals originating from the dendritic segment were present. Data for **3** is shown.

**3**: <sup>1</sup>H NMR (CDCl<sub>3</sub>, 300 MHz, TMS) δ = 9.6 - 9.0 (br, NH), 5.77 (m, H<sub>2</sub>C=CH-CH<sub>2</sub>-), 4.87 (t, H<sub>2</sub>C=CH-CH<sub>2</sub>-), 4.9 - 4.0 (br, CH(CH<sub>3</sub>)), 3.6 (br, OCH<sub>3</sub>), 1.58 (d, H<sub>2</sub>C=CH-CH<sub>2</sub>-), 1.7 - 1.0 (br, CH(CH<sub>3</sub>) + Si-CH<sub>2</sub>-CH<sub>2</sub>-CH<sub>2</sub>-Si), 0.87 (br, CH<sub>2</sub>-Si), 0.63 (br, Si-CH<sub>2</sub>) ppm; <sup>13</sup>C NMR (CDCl<sub>3</sub>, 75 MHz, TMS) δ = 175 - 171 (br, C=O), 165 - 160 (br, C=N), 135 (H<sub>2</sub>C=CH-CH<sub>2</sub>-), 114 (H<sub>2</sub>C=CH-CH<sub>2</sub>-), 64 - 61 (br, CN-CH(CH<sub>3</sub>)), 53 - 51 (br, OCH<sub>3</sub>), 49 - 43 (br, NH-CH(CH<sub>3</sub>)), 34-32 (br, CCH<sub>3</sub>), 26 (CH<sub>2</sub>-CH<sub>2</sub>-NH), 24 - 20 (br, CN-CH(CH<sub>3</sub>)), 20 (H<sub>2</sub>C=CH-CH<sub>2</sub>-), 19 - 16 (br, NH-CH(CH<sub>3</sub>)), 19 + 18 + 17 (Si-(CH<sub>2</sub>)<sub>3</sub>-Si), 6 (Si-CH<sub>2</sub>-(CH<sub>2</sub>)<sub>2</sub>-NH) ppm; IR (KBr) ν = 3279 (N-H), 3076, 2992, 2914, 2877 (C-H), 1750 (C=O ester), 1657 (amideI), 1629 (C=C), 1532 (amideII) cm<sup>-1</sup>.

**4**: <sup>1</sup>H NMR (CDCl<sub>3</sub>, 300 MHz, TMS) δ = 9.6 - 9.0 (br, NH), 5.1 - 4.0 (br, CH(CH<sub>3</sub>)), 3.6 (br, OCH<sub>3</sub>), 2.0 - 0.9 (br, CH(CH<sub>3</sub>) + Si-CH<sub>2</sub>-CH<sub>2</sub>), 0.6 (br, Si-CH<sub>2</sub>), 0.0 (br, CH<sub>3</sub>-Si) ppm; <sup>13</sup>C NMR (CDCl<sub>3</sub>, 75 MHz, TMS) δ = 174 - 171 (br, C=O), 165 - 160 (br, C=N), 64 - 61 (br, CN-CH(CH<sub>3</sub>)), 53 - 51 (br, OCH<sub>3</sub>), 50 - 46 (br, NH-CH(CH<sub>3</sub>)), 34-32 (br, CCH<sub>3</sub>), 24 - 20 (br, CN-CH(CH<sub>3</sub>)), 19 - 16 (br, NH-CH(CH<sub>3</sub>)), 19 + 18 + 17 (Si-(CH<sub>2</sub>)<sub>3</sub>-Si), 0 (Si-CH<sub>3</sub>) ppm; IR (KBr) ν = 3280 (N-H), 2952 (C-H), 1751 (C=O ester), 1657 (amideI), 1532 (amideII) cm<sup>-1</sup>.

For catalysts **6** - **9** spectral data were found that were identical within the experimental error. Signals related to the dendritic part were similar to those observed for the unreacted wedges. Data for **6** are shown, since for this compound the applied weight ratio initiator / nickel allowed the most accurate assignment of the observed signals.

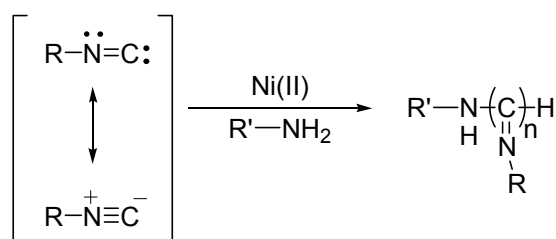
**6**: <sup>1</sup>H NMR (CDCl<sub>3</sub>, 300 MHz, TMS) δ = 8.08 + 6.84 (t, 1H, NHCH<sub>2</sub>), 7.95 + 7.00 (s, 1H, NHC(CH<sub>3</sub>)<sub>3</sub>), 5.79 (m, 9H, CH=CH<sub>2</sub>), 4.87 (m, 18H, CH=CH<sub>2</sub>), 4.01 + 3.37 (m, 2H, NHCH<sub>2</sub>), 1.9 - 1.25 (m, 2H, CH<sub>2</sub>CH<sub>2</sub>CH<sub>2</sub>), 1.74 + 1.45 (s, 9H, NHC(CH<sub>3</sub>)<sub>3</sub>), 1.58 (s, 27H, CH<sub>3</sub>), 0.7 - 0.6 (m, 2H, CH<sub>2</sub>Si) ppm; <sup>13</sup>C NMR (CDCl<sub>3</sub>, 75 MHz, TMS) δ = 178.0 + 176.1 (NCN), 134.9 + 134.7 (CH=CH<sub>2</sub>), 123 (Ni-C=N), 114,6 + 114,4 (CH=CH<sub>2</sub>), 61 (CN-C(CH<sub>3</sub>)<sub>3</sub>), 57.1 + 56.3 (NH-C(CH<sub>3</sub>)<sub>3</sub>), 54.8 + 48.4 (NH-CH<sub>2</sub>), 31.8 + 30.3 + 29.4 (CH<sub>3</sub>), 25.2 + 23.0 (CH<sub>2</sub>CH<sub>2</sub>CH<sub>2</sub>), 20.1 (CH<sub>2</sub>-CH=CH<sub>2</sub>), 9.9 + 9.1 (CH<sub>2</sub>Si) ppm; IR (KBr) ν 3293 (N-H), 2985, 2926 (C-H), 2254 + 2228 (C=N), 1630 (C=C), 1587 + 1544 (N-C-N), 1095 (ClO<sub>4</sub><sup>-</sup>) cm<sup>-1</sup>. UV/Vis (CH<sub>2</sub>Cl<sub>2</sub>) λ (ε) = 251 (11300), 290 (4600) nm.

## 6.5 References and Notes

- 1 a) S. I. Stupp, V. LeBonheur, K. Walker, L. S. Li, K. E. Huggins, M. Keser, A. Amstutz *Science* **1997**, 276, 384. b) S. Förster, M. Antonietti *Adv. Mater.* **1998**, 10, 195. c) J. Ruokolainen, R. Mäkinen, M. Torkkeli, T. Mäkelä, R. Serimaa, G. ten Brinke, O. Ikkala *Science* **1998**, 280, 557.
- 2 a) P. J. Flory *J. Phys. Chem.* **1942**, 10, 51. b) M. J. Huggins *J. Phys. Chem.* **1942**, 46, 151. c) M. J. Huggins *J. Am. Chem. Soc.* **1942**, 64, 1721.
- 3 a) F. S. Bates *Science* **1991**, 251, 898. b) F. S. Bates, M. F. Schulz, A. K. Khandpur, S. Förster, J. H. Rosedale, K. Almdal, K. Mortensen *Faraday Discuss.* **1994**, 98, 7.
- 4 a) J. C. M. van Hest, D. A. P. Delnoye, M. W. P. L. Baars, M. H. P. van Genderen, E. W. Meijer *Science* **1995**, 268, 1592. b) C. J. Hawker, K. L. Wooley, J. M. J. Fréchet, *J. Chem. Soc., Perk. Trans. I* **1993**, 1287. c) J. Iyer, K. Fleming, P. Hammond, *Macromolecules* **1998**, 31, 8757. d) Y. Chang, Y. C. Kwon, S. C. Lee, C. Kim *Macromolecules* **2000**, 33, 4496.
- 5 a) L. Zhang and A. Eisenberg *Science* **1995**, 268, 1728. b) L. Zhang, C. Bartels, H. Shen, A. Eisenberg *Phys. Rev. Lett.* **1997**, 79, 5034. c) B. M. Discher, Y.-Y. Won, D. S. Ege, J. C.-M. Lee, F. S. Bates, D. E. Discher, D. A. Hammer *Science* **1999**, 284, 1143.
- 6 a) M. A. Hempenius, B. M. W. Langeveld-Voss, J. A. E. H. van Haare, R. A. J. Janssen, S. S. Sheiko, J. P. Spatz, M Möller, E. W. Meijer *J. Am. Chem. Soc.* **1998**, 120, 2798. b) J. T. Chen, E. L. Thomas, C. K. Ober, G.-P. Mao *Science* **1996**, 273, 343. c) S. A. Jenekhe and X. L. Chen *Science* **1998**, 279, 1903.
- 7 a) S. J. Holder, R. C. Hiorns, N. A. J. M. Sommerdijk, S. J. Williams, R. G. Jones, R. J. M. Nolte *Chem. Commun.* **1998**, 1445. b) N. A. J. M. Sommerdijk, S. J. Holder, R. C. Hiorns, R. G. Jones, R. J. M. Nolte *Macromolecules* **2000**, 33, 8289.
- 8 J. J. L. M. Cornelissen, M. Fischer, N. A. J. M. Sommerdijk, R. J. M. Nolte *Science* **1998**, 280, 1477.
- 9 R. J. M. Nolte *Chem. Soc. Rev.* **1994**, 23, 11.
- 10 van Heerbeek, R.; Reek, J. N. H.; Kamer, P. C. J.; van Leeuwen, P. W. N. M. *Tetrahedron Let.* **1999**, 40, 7127.
- 11 R. W. Stephany, W. Drenth, *Recl. Trav. Chim. Pays-Bas* **1972**, 91, 1453. b) P. C. J. Kamer, R. J. M. Nolte, W. Drenth, *J. Chem. Soc., Chem. Commun.* **1986**, 1789. c) P. C. J. Kamer, R. J. M. Nolte, W. Drenth, *J. Am. Chem. Soc.* **1988**, 110, 6818.
- 12 Chapter 2 of this thesis.
- 13 a) J. J. L. M. Cornelissen, J. J. J. M. Donners, W. S. Graswinckel, R. de Gelder, A. E. Rowan, N. A. J. M. Sommerdijk, R. J. M. Nolte *Science*, **293**, 676 (2001). b) Chapter 3 of this thesis.
- 14 P. de Witte, internal report (1998).
- 15 R. B. Heslop, P. L. Robinson *Inorganic Chemistry. A guide to Advanced Study* 3th ed., Elsevier, Amsterdam, **1967**, p. 726-731.
- 16 a) S. Mössmer, J. P. Spatz, M. Möller, T. Aberle, J. Schmidt, W. Burchard *Macromolecules* **2000**, 33, 4791. b) T. Thurn-Albrecht, J. Schotter, G. A. Kästle, N. Emley, T. Shibauchi, L. Krusin-Elbaum, K. Guarini, C. T. Black, M. T. Tuominen, T. P. Russel *Science* **2000**, 290, 2126.
- 17 a) P. J. A. Kenis, R. F. Ismagilov, G. M. Whitesides, *Science* **1999**, 285, 83. b) J. Sloan, D. M. Wright, H. G. Woo, S. Bailey, G. Brown, A. P. E. York, K. S. Coleman, J. L. Hutchison, M. L. H. Green, *Chem. Commun.* **1999**, 699. c) Y. Zhou, S. H. Shu, X. P. Cui, C. Y. Wang, Z. Y. Chen, *Chem. Mater.* **1999**, 11, 545.

# Summary

In this thesis a study towards higher structural order in macromolecular systems is presented. It can be described as an exploration at the boundaries between organic, supramolecular and polymer chemistry. Highly ordered macromolecular systems (e.g. proteins, DNA) play crucial roles in Nature and their structure and self-assembling behaviour are a source of inspiration for an increasing number of scientists. The investigations presented in this thesis, deal with the hierarchical transfer of (chiral) structural information present in monomeric peptide derived isocyanides to higher levels of molecular organization, i.e. in polymers of these isocyanides and in aggregates formed by them. Polyisocyanides have a rather well-defined helical conformation and are accessible in an optically active form by a nickel catalyzed polymerization reaction (Scheme 1). This polymerization is initiated by a nucleophile, e.g. an amine, and during the reaction the isocyanide monomers coordinate to the metal center and are incorporated into the growing chain by a series of consecutive insertion reactions. In this way only a minor rearrangement of the chemical bonds is required to form the  $4_1$  (4 repeat units per helical turn) helical polymeric backbone.



**Scheme 1** Nickel(II) catalyzed polymerization of isocyanides.

Previous research has shown that the  $4_1$  polyisocyanide helix is only stable when sterically demanding side chains are present. For the majority of the polyisocyanides the persistence length, i.e. a measure of the stiffness of the polymer chain, is limited. The



first part of this thesis describes research efforts aimed at preparing optically active polyisocyanides in which the helix stability is improved and the persistence length increased through the introduction of non-covalent interactions between the side chains.

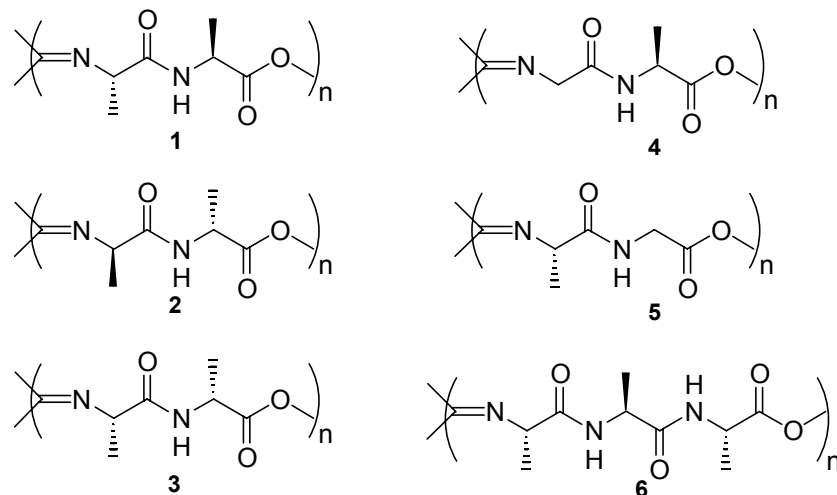


**Figure 1** Isocyanopeptide based polymers investigated. **1**: poly(L-isocyanalanyl-L-alanine methyl ester); **2**: poly(D-isocyanalanyl-D-alanine methyl ester); **3**: poly(L-isocyanalanyl-D-alanine methyl ester); **4**: poly(isocyanoglycyl-L-alanine methyl ester); **5**: poly(L-isocyanalanyl-glycine methyl ester); **6**: poly(L-isocyanalanyl-L-alanyl-L-alanine methyl ester).

A number of peptide derived isocyanides has been synthesized and polymerized (Figure 1). These polyisocyanopeptides have amide groups in their side chains, which have the possibility to form intramolecular hydrogen bonds. As a result of the helical structure of polyisocyanides, side chain  $n$  is more or less above side chain  $(n + 4)$  with a distance suited for the formation of hydrogen bonds. Polymers **1** – **6** (Figure 1) have been synthesized to investigate whether hydrogen bonds between the side chains are indeed formed and how these bonds affect the conformational properties of the polymers. Polyisocyanopeptide **6** has two amide groups per side chain and is able to form a  $\beta$ -sheet-like architecture, mimicking the interactions present in naturally occurring  $\beta$ -helices.

Detailed infrared and <sup>1</sup>H NMR spectroscopic investigations showed that *all* amide groups present in the polymers participate in hydrogen bonding. The single crystal X-ray structure of L-isocyanalanyl-L-alanine methyl ester (the monomer for **1**) served as a reference in these investigations (Figure 2). It appeared that in the dipeptide

derived polyisocyanides, except in **5**, ordered arrays of hydrogen bonds along the polymeric backbone are present. Analogous to the denaturation of proteins, the hydrogen bonds present in these polymers can be disrupted. This was, however, only possible with strong acids like trifluoroacetic acid and not with hydrogen bonding solvents (e.g. methanol, DMSO), demonstrating the robust character of the hydrogen bonding arrays. Powder X-ray diffraction experiments showed that in the solid state the rigid polyisocyanopeptides are organized in a pseudo-hexagonal arrangement. The acidified samples, which were studied for comparison, only gave broad signals pointing to a decrease in the level of organization of the polymeric molecules. The conformational properties in solution were studied by CD spectroscopy, which showed that polymers **1** – **3** are stable up to 40 °C and subsequently unfold in a non-linear (cooperative) process upon increasing the temperature. In the case of **4** this process was significantly faster and started already at room temperature. The CD spectrum of polyisocyanide **5** did not display notable changes upon increasing the temperature

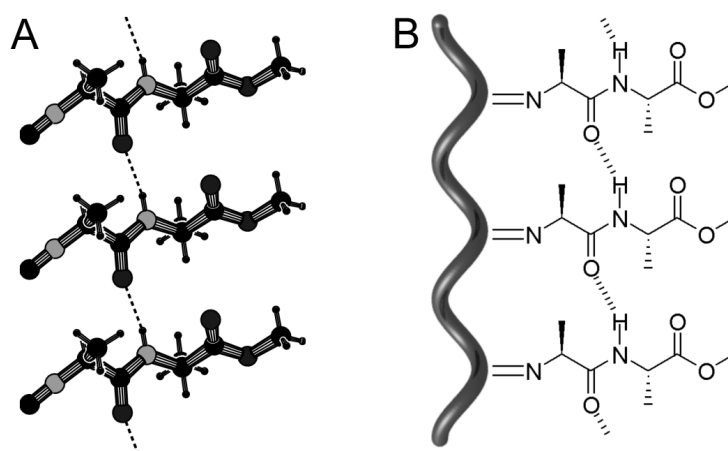


**Figure 2** Crystal structure of the monomer of **1**, showing the intermolecular hydrogen bonds between the stacked molecules (**A**). Schematic representation of the hydrogen bonds between side chains  $n$  and  $(n + 4)$  in polyisocyanopeptide **1** (**B**).

or by adding acid, pointing to the absence of a secondary organization in this polymer. Based on the experimental data it was concluded that the introduction of hydrogen bonding units in the polyisocyanopeptide side chains has a positive effect on the conformational properties of these macromolecules. Peptide derived polyisocyanides

are stable in solution at room temperature and as a result of the increased rigidity it is possible to visualize the individual macromolecules by AFM. Measuring the contour length of the macromolecules allowed the determination of the molecular weights and the polydispersities of the samples, which was not possible by more conventional techniques.

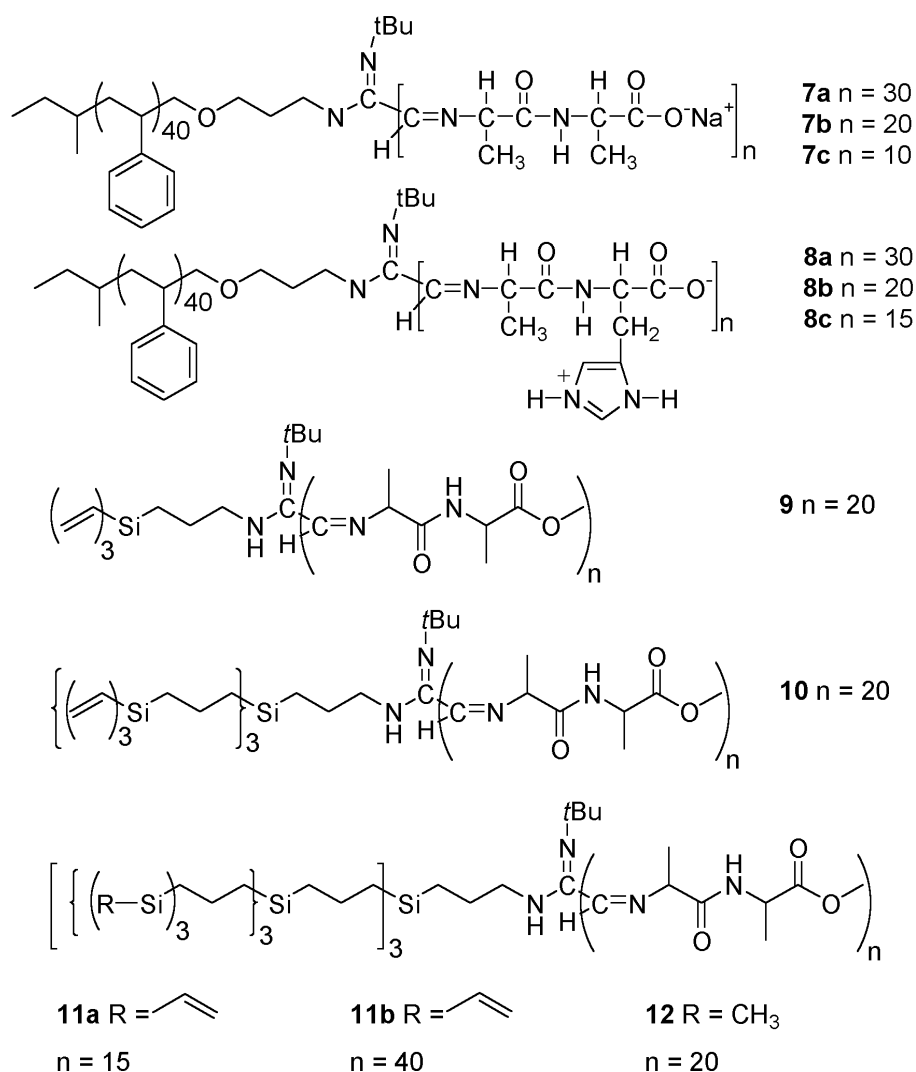


**Figure 3** Block copolymers of isocyanopeptides and styrene and dendritic carbosilanes.

Relatively small changes in the side chain configuration, as in **1** (L-Ala, L-Ala) and **3** (L-Ala, D-Ala), resulted in significant differences in the properties of the macromolecules. For **3** a higher molecular weight and polydispersity was found than for **1** prepared under identical conditions. The former polymer also showed an increased tendency to form aggregates. A protein-like folding seems to take place during the

polymerization reaction, since it has been found that polyisocyanopeptide **3** can also be prepared with the help of a small amount of acid as a catalyst, which is exceptional.

An interesting similarity is present between the mechanism by which chirality is transferred in polyisocyanopeptides and the way proteins are built up and are folded in aqueous solution. To investigate whether the polyisocyanopeptides retain their structure in water, the methyl esters present in polymers **1**, **3** and **6** were removed by base to yield the water-soluble polyisocyanopeptides. Using IR and  $^1\text{H}$  NMR spectroscopy it could be shown that the hydrogen bonds remain intact in water. The conformational aspects in water have been studied in detail with the help of CD spectroscopy. A helix geometry maintained by hydrogen bonds can be expected to unfold in a cooperative process when the temperature is increased. For the three polymers investigated cooperativity was indeed observed in the decrease of the intensities of the Cotton effects, both in the bands corresponding to the polymer backbone (260 – 400 nm) and in the amide transitions (200 – 260 nm). In the case of polymer **6** the unfolding process appeared to be more complex than in the case of **1** and **2**. The two types of hydrogen bonding arrays present in the former polymers are disrupted at different temperatures.

In the second part of this thesis the assembly of polyisocyanides into large supramolecular architectures is presented. Block copolymers containing a polyisocyanide segment have been synthesized by using macromolecular initiators in the Ni(II) catalyzed polymerization reaction. These initiators consisted of amine terminated polystyrene and amine derived carbosilane dendrimers (Figure 3). Removal of the methyl ester functionalities in block copolymers **7** and **8** resulted in chiral ‘superamphiphiles’ consisting of a charged, helical polyisocyanopeptide headgroup and a hydrophobic polystyrene tail. These superamphiphiles have properties comparable to traditional amphiphiles, but differ in size (about one order of magnitude larger). Under optimized conditions the macromolecules of negatively charged **7b** self-assembled in aqueous solution to yield micellar rods having lengths up to several micrometers. Block copolymer **8** displayed a similar behaviour. Interestingly, in this case it was possible to change the stiffness of the rods by varying the type of counter ion.

As with traditional surfactants it was found that the ratio between the hydrophobic and hydrophilic segments in the macromolecules influences the aggregation behavior of the superamphiphiles. Compounds **7c** and **8c** formed in addition to bilayer-type assemblies like plates and vesicles, also helical assemblies (superhelices, Figure 4). The observed differences in the supramolecular structures

formed by the negatively charged and zwitterionic copolymers suggest that the helices are formed by a complex formation mechanism, involving the hierarchical transfer of chirality from the monomeric building blocks to the superstructures.

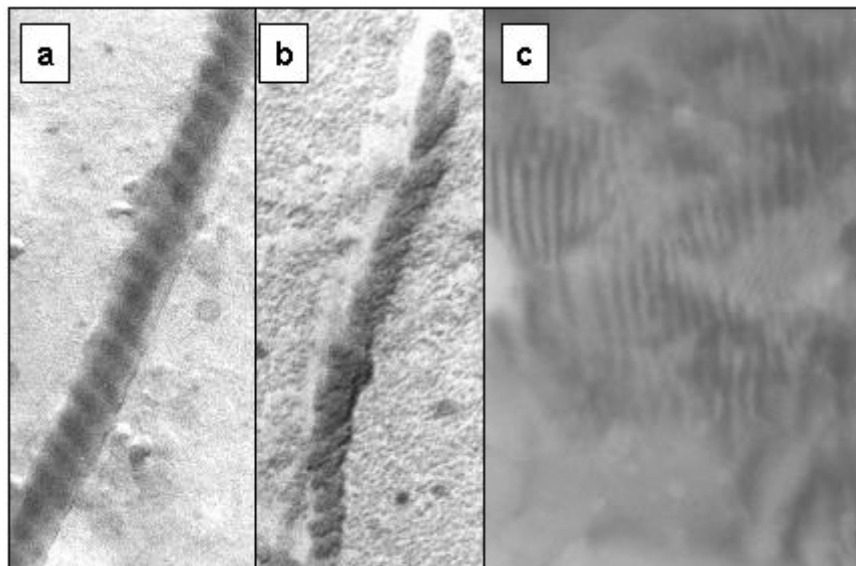


**Figure 4** Left handed superhelix formed by **7c** in an aqueous environment (a). Right handed helical architecture formed by **8c** in water (b). Striped pattern formed by **12** in the presence of  $\text{Ag}^+$  ions (c).

The block copolymers prepared from the polyisocyanopeptides and the carbosilane dendrimers (Figure 3) were expected to display interesting properties because of the large differences of the two component blocks: the dendrimer has a convex architecture and is flexible, whereas the polyisocyanopeptide part is rod-like and rigid. Block copolymers built from third generation dendrimers (**11** and **12**) appeared to selectively bind metal ions, like silver ions. These ions were complexed to the polyisocyanide segment and as a result aggregates were formed with dimensions ranging from hundreds of nanometers to over one micron (determined by light scattering). These aggregates were further investigated by electron microscopy, which showed a pattern of alternating dark and lighter stripes (Figure 4). It was shown that the dark stripes are rich in silver and that upon irradiation with the electron beam nanowires of metallic silver are formed.

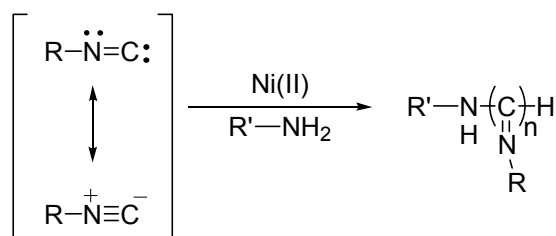
The investigations described in this thesis show that by introducing non-covalent, i.e. hydrogen bonding interactions between the side chains of a polymer new

properties can be introduced. It appeared to be possible to stepwise transfer chiral information from a peptide building block to a macromolecule and eventually to a large assembly of macromolecules. The availability of a large number of natural and synthetic amino acids opens the possibility for the future synthesis of a wide array of well-defined isocyanopeptide polymers and block copolymers. Possible applications for these compounds are their use as reference compounds for structural studies on natural occurring ( $\beta$ -sheet) proteins and their use as scaffolds for metal catalysts and non-linear optical chromophores. Furthermore, initial work has shown that the materials can be used as a matrices for the formation of mesoscopic silver wires.



# Samenvatting

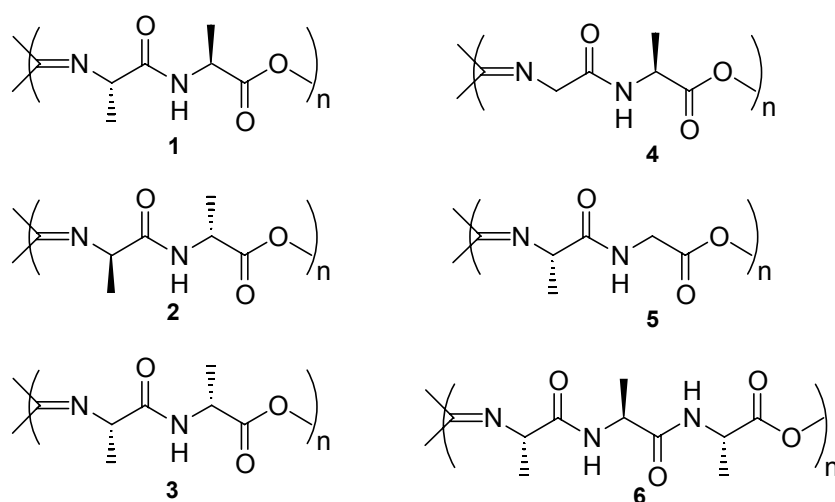
Het onderzoek dat in dit proefschrift wordt beschreven omvat een studie naar het verkrijgen van structurele ordening in macromoleculaire systemen. Men kan het omschrijven als onderzoek op de grensvlakken van de organische chemie, de supramoleculaire chemie en de polymeerchemie. Hoog geordende macromoleculaire verbindingen (zoals b.v. eiwitten en DNA) spelen een cruciale rol in natuurlijke processen. De structuur van deze biomacromoleculen alsmede de wijze waarop deze aggregaten tot supramoleculaire structuren vormen een bron van inspiratie en onderzoek van een toenemend aantal wetenschappers. Meer specifiek behandelt dit proefschrift de hiërarchische overdracht van chirale informatie aanwezig in isocyaniden afgeleid van peptiden naar hogere niveaus van organisatie, te weten polymeren en aggregaten opgebouwd uit deze polymeren. Polymeren van isocyaniden hebben een goed gedefinieerde helixvormige structuur en zijn toegankelijk in optische actieve vorm door gebruik te maken van een door nikkel-gekatalyseerde polymerisatiereactie. Deze reactie wordt geïnitieerd door een nucleofiel molecuul, zoals een amine, en de monomeren worden via een serie van opeenvolgende inschuivingsreacties aan het nikkelcentrum in de groeiende polymeerketen ingebouwd. Op deze manier is slechts een minimale herschikking van de chemische bindingen nodig om de helixvormige polymere ruggegraat te vormen, die bestaat uit 4 repeterende eenheden per winding (4<sub>1</sub>-helix).



**Schema 1** *Nikkel(II)-gekatalyseerde polymerisatie van isocyaniden.*



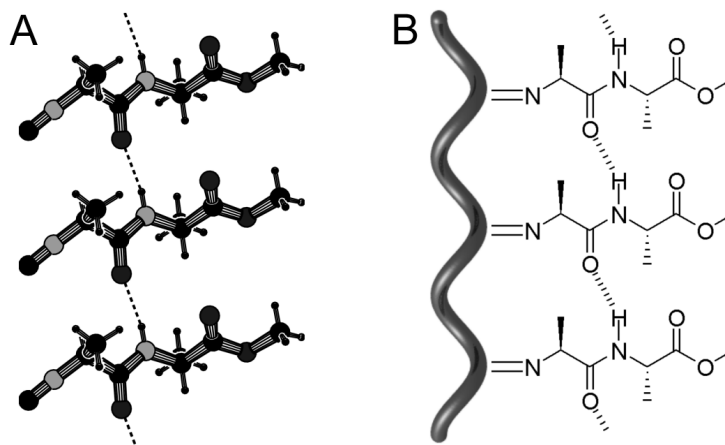
Eerder onderzoek heeft laten zien dat de  $4_1$  helixstructuur van polyisocyaniden slechts stabiel is wanneer de zijketens sterisch omvangrijke groepen bevatten. Voor het merendeel van de thans bekende polyisocyaniden is de z.g.n. persistentielengte, een maat voor de stijfheid van de polymeerketen, beperkt. In het eerste deel van het hier gepresenteerde onderzoek is onderzocht of het mogelijk is om optisch actieve polyisocyaniden te verkrijgen, waarbij de twee voorgenoemde eigenschappen, conformationele stabiliteit en persistentielengte, significant zijn verbeterd. Dit is gedaan door tussen de zijketens van de polymeren niet-covalente interacties, te weten waterstofbruggen, aan te brengen.



**Figuur 1** Bestudeerde homopolymeren op basis van isocyanopeptiden. **1:** poly(L-isocyanoalanyl-L-alaninemethylester); **2:** poly(D-isocyanoalanyl-D-alaninemethylester); **3:** poly(L-isocyanoalanyl-D-alaninemethylester); **4:** poly(isocyanoglycyl-L-alaninemethylester); **5:** poly(L-isocyanoalanyl-glycinemethylester); **6:** poly(L-isocyanoalanyl-L-alanyl-L-alaninemethylester)

Ten behoeve hiervan zijn een aantal van peptiden afgeleide isocyaniden vervaardigd en gepolymeriseerd (Figuur 1). Deze polyisocyanopeptiden bevatten amidegroepen in de zijketens, welke de mogelijkheid hebben tot het aangaan van onderlinge waterstofbruggen. Als gevolg van de schroeflijnvormige structuur van een polyisocyanide bevindt zijketen  $n$  zich min of meer boven zijketen  $(n + 4)$  en de afstand tussen deze zijketens is zeer geschikt voor de vorming van zulke waterstofbruggen (Figuur 2). De in Figuur 1 weergegeven verbindingen **1 – 6** zijn gesynthetiseerd om te bestuderen of er inderdaad interzijketen-waterstofbruggen worden gevormd en of deze waterstofbruggen de conformatie van de polymeren beïnvloeden. Polymeer **6** heeft twee

amidegroepen en kan daarmee een  $\beta$ -sheet-achtige structuur geven, waarmee interacties aanwezig in natuurlijk voorkomende  $\beta$ -helices worden nagebootst. Gedetailleerde infraroodstudies en  $^1\text{H-NMR}$  spectroscopische onderzoeken hebben aangetoond dat *alle* in de polymeren aanwezige amidegroepen inderdaad participeren in waterstofbruggen. De kristalstructuur van L-isocyanoalanyl-L-alaninemethylester, het monomeer van polymeer **1**, diende hierbij als referentiekader (Figuur 2). Het blijkt dat



**Figuur 2** Kristalstructuur van het monomeer van **1**, waarbij de intermoleculaire waterstofbruggen tussen de gestapelde moleculen te zien zijn (A). Schematische weergave van waterstofbruggen tussen zijketens  $n$  en  $(n + 4)$  in polyisocyanopeptide **1** (B).

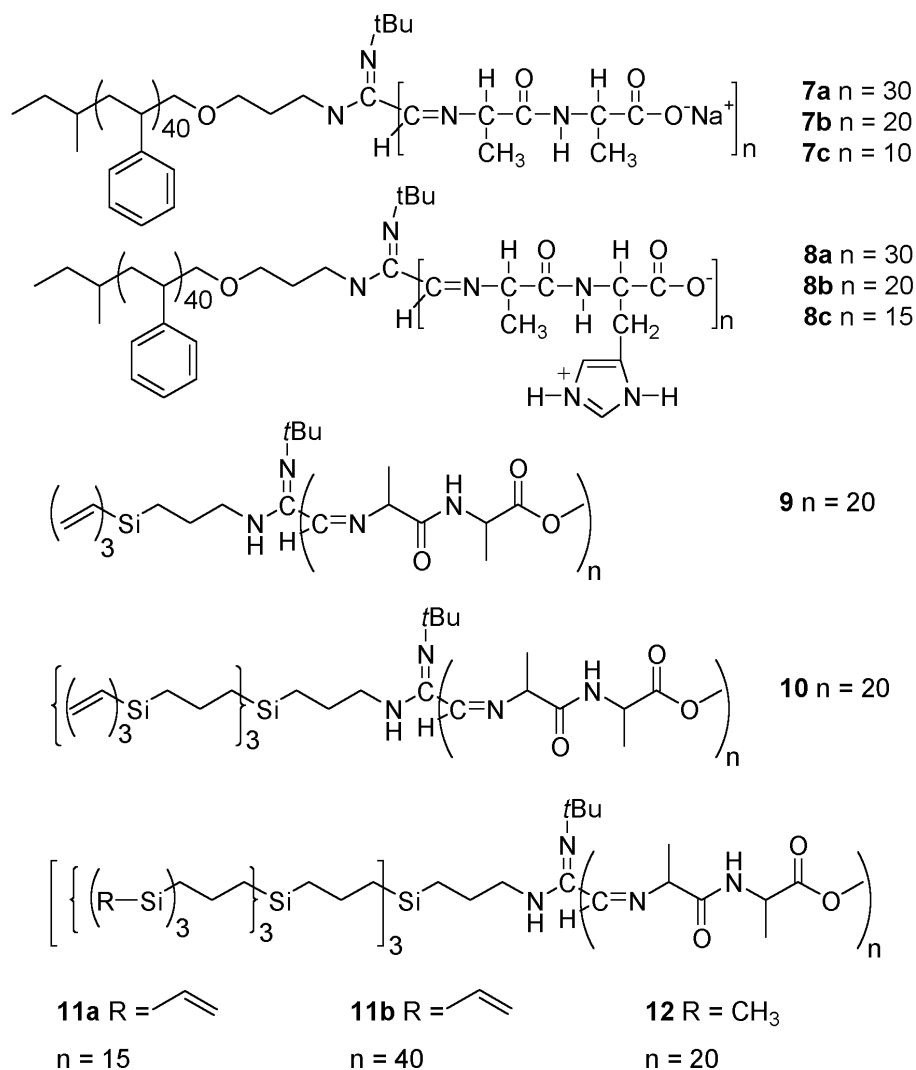
van dipeptiden afgeleide polyisocyaniden, met uitzondering van polymeer **5**, geordende strengen van waterstofbruggen bezitten die parallel aan de polymere ruggegraat lopen. Net als bij eiwitten kunnen ook in de synthetische polymeren de waterstofbruggen door een proces van denaturatie worden verbroken. Dit was echter alleen mogelijk onder tamelijk extreme omstandigheden, namelijk met sterke zuren zoals trifluoroazijnzuur en niet met waterstofbrugbrekende oplosmiddelen zoals methanol en DMSO, hetgeen een indicatie geeft van het robuuste karakter van de nieuwe polymeren. Röntgen-diffractie-experimenten toonden aan dat de polymeren zich in de vaste fase op een kristallijne manier ordenen en wel als starre cilinders in een pseudo-hexagonale pakking. Ter vergelijking hiervan gaven de aangezuurde monsters, waarin de waterstofbruggen verbroken zijn, slechts brede signalen, hetgeen duidt op een sterke afname van de macromoleculaire ordening. De conformationele eigenschappen van de polymeren in oplossing zijn bestudeerd met ondermeer CD-spectroscopie. Uit deze studies bleek dat

polymeren **1** – **3** stabiel zijn tot circa 40 °C en daarna langzaam in een niet-lineair (coöperatief) proces ontvouwen. In het geval van polymeer **4**, verliep dit proces beduidend sneller en begon het al bij kamertemperatuur. Het CD spectrum van verbinding **5** vertoonde nauwelijks veranderingen bij opwarmen of toevoegen van zuur, hetgeen wijst op de afwezigheid van een secundaire organisatie in dit polymeer. Op grond van de uitgevoerde experimenten kan worden geconcludeerd dat het introduceren van waterstofbruggende groepen in de zijketens de conformationele eigenschappen van de polyisocyaniden gunstig beïnvloedt. De polyisocyanopeptiden zijn stabiel in oplossing bij kamertemperatuur en de toename in rigiditeit maakt het zelfs mogelijk de macromoleculen zichtbaar te maken met ‘Atomic Force Microscopy’. Door de contourlengte van de polymeren te meten, was het met behulp van deze techniek mogelijk het moleculair gewicht en de polydispersiteit te bepalen, iets wat met meer gangbare procedures niet goed mogelijk bleek, onder meer door het rigide karakter van de verbindingen.

Relatief kleine verschillen in de configuratie van de zijketens, zoals in **1** (L-Ala, L-Ala) en **3** (L-Ala, D-Ala), bleken significante verschillen in de eigenschappen van de macromoleculen te geven. Zo werd voor **3** een hoger molecuulgewicht en polydispersiteit gevonden dan voor **1** en bleek dit polymeer een sterkere neiging tot aggregatie te vertonen. Tevens werd gevonden dat polyisocyanopeptide **3** ook gevormd kan worden met behulp van een kleine hoeveelheid zuur als katalysator, hetgeen erg uitzonderlijk is en aangeeft dat de polymeerketen zich als een eiwit opvouwt.

De opbouw van polyisocyanopeptiden en de overdracht van chirale informatie van het monomeer naar het polymeer vertoont overeenkomsten met de wijze waarop eiwitten worden opgebouwd. Om te bekijken of polyisocyanopeptiden ook in water hun structuur behouden, danwel ontvouwen, zijn in polymeren **1**, **3** en **6** de methylestergroepen omgezet in carboxylaatgroepen door hydrolyse met base. Met behulp van IR- en <sup>1</sup>H-NMR-experimenten is aangetoond dat in dit oplosmiddel de waterstofbruggen tussen de zijketens nog geheel intact zijn. De conformationele aspecten in water zijn in detail bestudeerd met behulp van CD-spectroscopie. Te verwachten is dat een door waterstofbruggen in stand gehouden helix-geometrie zich in een coöperatief proces zal ontvouwen wanneer de temperatuur wordt verhoogd. Voor de drie bestudeerde polyisocyanopeptiden werd inderdaad coöperativiteit waargenomen in de afname van de verschillende Cottoneffecten bij toenemende temperatuur. Deze afname werd gevonden zowel in de banden die corresponderen met de polymere

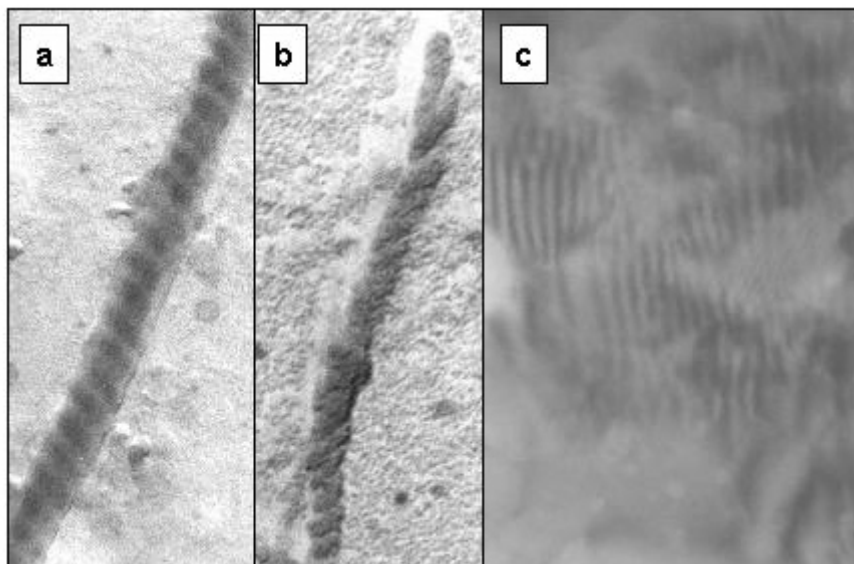
ruggegraat (260 – 400 nm) als in de amide-overgangen (200 - 260 nm). In het geval van polymeer **6** blijkt de ontvouwing complexer te zijn dan in geval van polymeren **1** en **3**, omdat de waterstofbruggen tussen de twee verschillende soorten amidegroepen niet bij dezelfde temperatuur worden verbroken.



**Figuur 3** Blokcopolymeren van isocyanopeptiden en styreen en dendrimere carbosilanen.

In het tweede deel van het onderzoek is de assemblage van polyisocyaniden tot grote supramoleculaire architecturen onderzocht. Hiertoe zijn blokcopolymeren vervaardigd door uit te gaan van macromoleculaire initiatoren in de door nikkel-gekatalyseerde polymerisatie van de isocyanopeptiden. Deze initiatoren bestonden uit polystyreen, dat aan één keteneinde was voorzien van een aminofunctie, en uit dendrimere carbosilanen, eveneens voorzien van een eindstandige aminofunctie (Figuur

3). Ontscherming van het polyisocyanopeptide-gedeelte in de gevormde blokkopolymeren **7** en **8**, resulteerde in chirale 'superamfifielen', bestaande uit een geladen polyisocyanide-gedeelte en een hydrofobe polystyreen-staart. Deze superamfifielen bleken eigenschappen te bezitten die vergelijkbaar zijn met traditionele amfifielen, enkel de afmetingen van de moleculen verschillen een ordegrrootte. Onder optimale condities bleken de moleculen van negatief geladen **7b** in water te aggregeren tot micellaire staafjes met lengtes van soms wel meerdere micrometers. Blokkopolymeer **8b** vertoonde een vergelijkbaar gedrag. In het laatste geval was het opmerkelijk dat door variatie van het tegenion de flexibiliteit van de gevormde staafjes kon worden gestuurd.



**Figuur 4** Linkshandige superhelix gevormd door **7c** in water (a). Rechtshandige dubbelhelix-architectuur gevormd door **8c** in water (b). Strepenpatroon gevormd door **12** in aanwezigheid van  $\text{Ag}^+$ -ionen (c).

Evenals in het geval van traditionele amfifiele moleculen, bleek de verhouding hydrofoob/hydrofiel-gedeelte in het macromolecuul het aggregatiegedrag in grote mate te beïnvloeden. Superamfifielen **7c** en **8c** vormden bilaag-achtige structuren zoals platen en vesicles. Daarnaast werden, zeer verrassend, in beide gevallen schroeflijnvormige assemblages (superhelices, Figuur 4) waargenomen. De waargenomen verschillen in de supramoleculaire structuren gevormd door de negatief geladen en de zwitterionische copolymeren bleken op een complex vormingsmechanisme te wijzen, waarbij op een

hiërarchische wijze de chiraliteit in de monomeren wordt overgedragen naar de suprastructuren.

Van de blokcopolymeren afgeleid van isocyanopeptiden en carbosilaandendrimeren werd verwacht dat ze interessante eigenschappen zouden bezitten, vanwege het grote verschil in karakter van de twee typen blokken: het dendriemere heeft een convexe opbouw en is flexibel, het polyisocyanopeptide daarentegen is staafvormig en rigide. De blokcopolymeren opgebouwd uit een derde-generatie dendriemere (**11** en **12**) bleken in chloroform metaalionen, zoals zilverionen, te complexeren. Deze ionen werden selectief gebonden aan het polyisocyanopeptide-gedeelte en als gevolg daarvan ontstonden supramoleculaire aggregaten met afmetingen in de orde van honderden nanometers tot zelfs meer dan een micrometer (bepaald met lichtverstrooiing). Deze aggregaten zijn bestudeerd met elektronenmicroscopie, waarbij strepenpatronen van alternerend lichte en donkere banen werden gevonden (Figuur 4C). Verder onderzoek toonde aan dat de donkere strepen rijk zijn aan zilverionen en dat onder invloed van de elektronenbundel nanodraden van metallisch zilver worden gevormd.

Het in dit proefschrift beschreven onderzoek laat zien dat door de introductie van niet-covalente interacties (waterstofbruggen) tussen de zijketens de eigenschappen van polymeren kunnen worden beïnvloed. Verder is het mogelijk gebleken om op basis van goed gedefinieerde blokcopolymeren nieuwe supramoleculaire architecturen te maken, waarbij (chirale) informatie stapsgewijs wordt overgedragen van een monomere bouwsteen naar uiteindelijk een groter aggregaat van macromoleculen. De beschikbaarheid van een grote verscheidenheid aan natuurlijke en niet-natuurlijke aminozuren, maakt het mogelijk om in de toekomst een grote diversiteit aan goed gedefinieerde polymeren en blokcopolymeren te synthetiseren. Mogelijke toepassingen van deze verbindingen kunnen worden voorzien in de studie naar de structuur van natuurlijk voorkomende eiwitten, die een schroeflijnvormige opbouw van  $\beta$ -sheets bezitten (prion-eiwitten). Verder kunnen de polymeren dienen als ankerpunt voor het vastleggen van metaalkatalysatoren of als mal voor de organisatie van chromoforen met niet-lineaire optische eigenschappen. Initieel werk heeft reeds aangetoond dat de (blokco)polymeren kunnen worden toegepast als matrijs voor de vorming van mesoscopische zilverdraden.



# Dankwoord

Na het schrijven van een proefschrift is het -uiteindelijk- nadenken over een dankwoord een welkome verademing, zelfs al gebeurt dat inmiddels in de (hectische) rust van het mooie Californië. Zodra je dan eenmaal begonnen bent, lijkt het plotseling toch op het schrijven van een hoofdstuk; je wilt origineel zijn, toch redelijk beknopt en zeker volledig. Om dan toch maar in die stijl te blijven, beschouw ik dit gedeelte als de inleiding die leidt tot het volgende doel: het bedanken van iedereen die in de breedste zin van het woord een bijdrage heeft geleverd aan de voltooiing van het in dit proefschrift beschreven promotieonderzoek.

Onderzoek naar polyisocyaniden, de verbindingen beschreven in dit proefschrift, is historisch sterk verbonden met professor Roeland Nolte. Het was dan ook een hele uitdaging om me vast te bijten in een project waarin deze moleculen de hoofdrol speelden en opnieuw geïntroduceerd werden in de vakgroep. Roeland, bedankt voor het vertrouwen, je motiverende en inspirerende manier van begeleiden en de geboden vrijheid. Het was één grote leerervaring die ik met plezier heb ondergaan.

Goed en wel uit de startblokken kwam copromotor Nico Sommerdijk om me met raad en daad bij te staan. Nico, jouw kritische noten, luisterend oor en de efficiëntie in de afwerking hebben een aanzienlijke bijdrage gehad in de succesvolle afronding van dit proefschrift.

Een gedeelte van het hier beschreven werk is mede uitgevoerd door een aantal studenten, waarvan ik het begeleiden (al spreek ik liever van samenwerken) als erg boeiend heb ervaren. Zondermeer heb ik van jullie erg veel geleerd. Matthias Fischer, you were the first and straight away quite succesfull one, working with the difficult histidine derivatives. Your enthusiastic working attitude has led to fine results and a paper which was worth the effort. Medio 1997 kwam Sander Graswinckel erbij. Rustig maar gestaag werkte jij eerst aan blokcopolymeren en daarna aan waterstofbruggende homopolymeren. Onze initiële wetenschappelijke 'onenigheden' hebben uiteindelijk toch geresulteerd in een beter begrip van het gedrag van isocyanopeptiden. Weloverwogen ging Rens van Waes aan de slag met de superamfifielen, je verzamelde gedurende je stage een indrukwekkende hoeveelheid foto's van 'superstructuren' en flesjes bier van het tourspel. Sander en Rens jullie hielpen ook met het verhuizen van ons werkterrein naar het andere eind van het gebouw. Naast het verrichten van een hoop niet-chemisch werk, voorkwamen jullie ook een sociaal isolement van mij en Jack aldaar. Peter van Rijnsbergen kwam vrij onaangekondigd binnen en stond enkele dagen



later met U2-muziek mooie verbindingen in elkaar te sleutelen. Vooral de ‘harige borstels’ lijken interessante eigenschappen te hebben, alleen waren er nog teveel losse eindjes om het werk in dit boekje op te nemen. Thank you, guys!

Verder wil ik natuurlijk alle collega’s binnen de afdeling Organische Chemie in Nijmegen bedanken. In ons nieuwe lab: Jack, Pieter, Dennis, Joan, Jurry, Kelly en Geoffrey en de andere studenten voor korte of langere tijd aanwezig. De rest van de nolte-groep: Martin, Bert, Peter, Hans, Alexander, Hans, Jantien, Bastienne, Rob, Bart, Edward, Simon, Simon, Vera, Bea, Cristina, Mark, Paul, Femke, Isabelle, Gerald en Marga. Hans Adams en Annie Roelofsen wil ik ook bedanken voor hun experimentele bijdragen en Alan Rowan voor een scala aan berekeningen en NMR-experimenten (en niet in het minst voor een gezamenlijke ‘vaderschaps-voorbereiding’). Prof. Tesser ben ik erkentelijk voor legio synthetische adviezen. Verder gaat mijn dank uit naar de technische ondersteuning van de analytische groep: Pieter, Peter, Ad en Helene, de secretaresses Désirée van der Weij en Sandra Tijdink en naar Wim en Cris die altijd zorgden voor een constante aanvoer van chemicaliën en ander spul. Evenals naar dr. René de Gelder voor de opheldering van een kristalstructuur en de hulp bij de interpretatie van de diffractie-gegevens. Huub Geurts, Dick Klepper en Jan Gerritsen ben ik erkentelijk voor hun hulp bij de microscopie experimenten. Gerda Nachtegaal en prof. Arno Kentgens wil ik bedanken voor het uitvoeren van NMR-experimenten in de vaste stof.

De leden van de vakgroep Macromoleculaire en Organische Chemie van de TU Eindhoven wil ik bedanken voor hun gastvrijheid tijdens talloze experimenten en bezoeken, zeker toen een groot deel van de ‘nico-club’ haar thuis in het vertrouwde Brabant had gevonden. Met name: prof. Bert Meijer, voor alle tips en adviezen gedurende de rit en het voorwerk voor de transfer naar Almaden. Tonny, voor de hulp op verschillende vlakken; ik heb plezier gehad in onze pogingen om dendrimeren van stokjes te voorzien. Joost van Dongen wil ik bedanken voor de diverse analyses en dr. Rint Sijbesma voor het verschaffen van inzicht in de ordening van onze polymeren. Tijdens het opnieuw opbouwen van de ‘grote-schaal-polymerisatie-opstelling’ en de daaropvolgende experimenten heb ik veel gehad aan de kennis van prof. Jan van Hest, waarvoor mijn dank.

Mijn dank gaat ook uit naar dr. Joost Reek, Rieko van Heerbeek en dr. Paul Kamer (Universiteit van Amsterdam) voor de prettige samenwerking waarvan de resultaten beschreven staan in Hoofdstuk 6. Een aantal mensen ben ik erkentelijk voor het verrichten van metingen ten behoeve van het in dit proefschrift beschreven onderzoek. Dr. Harmut Fischer (TNO TPD Eindhoven) voor het doen van röntgen-diffractie- en microscopie-experimenten aan onze blokcopolymeren. Prof. André Persoons, dr. Thierry Verbiest en dr. Martti Kauranen (Katholieke Universiteit Leuven, België) voor

een introductie op het gebied van de niet-lineaire optica en een aantal initiële metingen. I would also like to thank prof. Manfred Schmidt and dr. Karl Fischer (Universiteit Mainz, Duitsland) for performing some insightfull light scattering measurements. Prof. Cor Koning (TU Eindhoven/DSM) wil ik bedanken voor het verschaffen van een aantal preparaten.

Thuis gekomen van een dag in het lab, zijn er een aantal mensen buiten de chemie die ik hier graag wil bedanken. Zonder hun steun, gezelschap, belangstelling en serieuze pogingen om mijn uiteenzettingen over linker- en rechterhanden, schroeven en het ‘in elkaar klikken’ van moleculen te begrijpen, was het verloop van mijn promotieonderzoek anders en zeker minder plezierig geweest. De broodnodige ontspanning was er altijd op feestjes, avondjes uit, tijdens concerten en vakanties met de ‘kamereuj uit Lôsbroek’, ‘Scouting Boekel’, met Bas, Wieske en Tijnl en overige vrienden en kennissen. De muzikale uitlaatklep was er met Mike en Toni en later met de ‘Fatburger boys’. Op sportief gebied is het misschien het beste om de hele zwem- en polovereniging ‘Gorgo’ te bedanken, de collega bestuursleden en in het bijzonder de zwemvrienden van Heren 1. De belangstelling van mijn (schoon)familie heb ik altijd erg gewaardeerd. Piet en Tilly, Ingrid en Richard jullie worden bedankt voor de interesse, de steun en het regelmatig oppassen tijdens ‘de laatste loodjes’. Mijn zus Arianne stond (en staat) zo goed als altijd voor mij/ons klaar voor de meest uiteenlopende dingen; van mij naar huis brengen in enigzins benevelde toestand (‘Hee, er lopen hier kangaroes!’) tot het regelen van belastingzaken als wij er ‘even’ niet zijn. Broer en paranimf Robert (en Claudy), in dezelfde periode hebben we onze opleidingen afgerond en daarbij hebben we zeker allebei profijt gehad van mijn eerste didactische ervaringen ten behoeve van jouw scheikundige tentamens. Mijn ouders hebben me altijd vrij gelaten in mijn keuzes, gestimuleerd om die keuzes door te zetten en geholpen waar nodig, ik zou bovendien nog zoveel meer kunnen zeggen. Voor nu, pap en mam, bedankt voor alles!

Tot slot wil ik mijn fantastische vrouw Sandra bedanken. Tijdens het lopende onderzoek was je altijd geïnteresseerd en belangstellend naar de gang van zaken. Gedurende het schrijven van dit proefschrift heeft alles (je werk, de voorbereidingen voor de reis naar het buitenland, de tijdsdruk) jou, volgens mij, nog meer energie gekost dan mij. Ik had zonder je hulp waarschijnlijk nu dan ook nog in Nijmegen achter de zuurkast gestaan om experimenten te doen. Dit is eigenlijk dus ook een beetje jouw proefschrift. Het bewijs van onze liefde staat nu in bed liedjes te zingen en daarvoor kan ik je nooit genoeg bedanken. Lieve Sam, -ons kleine dochttertje, je kunt nu nog niet lezen maar voor later...- jouw ‘Paapaa, mmmmm’ met daarbij de kussende beweging, maakt een dag vol beroerde resultaten en slecht nieuws in één klap goed!



# List of Publications

J.J.L.M. Cornelissen, M. Fischer, N.A.J.M. Sommerdijk, R.J.M. Nolte "Helical Superstructures from Charged Poly(styrene)-Poly(isocyanodipeptide) Block Copolymers" *Science* **280**, 1427 (1998).

J.J.L.M. Cornelissen, E. Peeters, R.A.J. Janssen, E.W. Meijer "Chiroptical Properties of a Chiral-substituted Poly(thienylene vinylene)" *Acta Polym.* **49**, 471 (1998).

J.J.L.M. Cornelissen, J.J.J.M. Donners, R. de Gelder, W.S. Graswinckel, G.A. Metselaar, A.E. Rowan, N.A.J.M. Sommerdijk, R.J.M. Nolte " $\beta$ -Helical Polymers from Isocyanopeptides" *Science* **293**, 676 (2001).

J.J.L.M. Cornelissen, R.J.H. Hafkamp, N.A.J.M. Sommerdijk, M.C. Feiters, R.J.M. Nolte "Helical Superstructures from Low Molecular Weight and Polymeric Building Blocks" *Polym. Prep.* **40**, 517 (1999).

J.J.L.M. Cornelissen, W.S. Graswinckel, N.A.J.M. Sommerdijk, R.J.M. Nolte "Polyisocyanopeptides: a new class of helical polypeptides" *Polym. Prep.* **40**, 548 (1999).

R.J.M. Nolte, A.E. Rowan, M.C. Feiters, P.J.J.A. Buijnsters, J.J.L.M. Cornelissen, J.M. Hannink, N.A.J.M. Sommerdijk "Helical Macromolecular Programming" *Polym. Prep.* **41**, 889 (2000).

J.J.L.M. Cornelissen, W.S. Graswinckel, A.E. Rowan, R. de Gelder, N.A.J.M. Sommerdijk, R.J.M. Nolte "Artificial  $\beta$ -Sheet Helices" *Polym. Prep.* **41**, 953 (2000).

R.J.M. Nolte, J.J.L.M. Cornelissen, J.J.J.M. Donners, R. van Heerbeek, J.N.H. Reek, A.E. Rowan, N.A.J.M. Sommerdijk " $\beta$ -Helical Polymers and Copolymers" *PMSE* **84**, 676 (2001).

J.J.L.M. Cornelissen, R.J.M. Nolte, A.E. Rowan, N.A.J.M. Sommerdijk "Chiral Architectures from Macromolecular Building Blocks" *Chem. Rev.* in press.

J.J.L.M. Cornelissen, W.S. Graswinckel, P.J.H.M. Adams, G.H. Nachttegaal, A.P.M. Kentgens, N.A.J.M. Sommerdijk, R.J.M. Nolte "Synthesis and Characterization of Polyisocyanides Derived from Alanine and Glycine Dipeptides" *J. Pol. Sci., Part A: Pol. Chem.* in press.

J.M. Hannink, J.J.L.M. Cornelissen, J.A. Farrera, P. Foubert, F.C. De Schryver, N.A.J.M. Sommerdijk, R.J.M. Nolte "Protein-Polymer Hybrid Amphiphiles" *Angew. Chem.* in press.

J.J.L.M. Cornelissen, N.A.J.M. Sommerdijk, R.J.M. Nolte "Determination of the Helical Sense in Alanine Based Polyisocyanides" *Macrom. Chem. Phys.* submitted.

J.J.L.M. Cornelissen, R. van Heerbeek, P.C.J. Kamer, J.N.H. Reek, N.A.J.M. Sommerdijk, R.J.M. Nolte "Silver Nanoarrays templated by Block Copolymers of Carbosilane Dendrimers and Polyisocyanopeptides" *Adv. Mat.* submitted.

# Curriculum Vitae

Jeroen Cornelissen werd geboren op 12 augustus 1972 in Veghel. Na het doorlopen van de middelbare school, startte hij in 1988 met de opleiding Procestechniek aan het Technisch Lyceum Eindhoven. Na de afronding van deze studie, doorliep hij de propadeuse van de studie Milieukunde aan het Prof. H.C. van Hall Instituut te Groningen, waarna in augustus 1992 werd begonnen met de studie Scheikunde aan de Katholieke Universiteit Nijmegen. In augustus 1996 behaalde hij het doctoraal diploma met als hoofdvakrichting Fysisch-Organische Chemie (prof. dr. R. J. M. Nolte) en als bijvakrichting Polymeerchemie (prof. dr. E. W. Meijer, TU Eindhoven). In de periode van oktober 1996 tot januari 2001 was de auteur in dienst van CW-NWO en voerde hij het in dit proefschrift beschreven onderzoek uit. Sinds juni 2001 is hij werkzaam als post-doctoraal onderzoeker bij het IBM Almaden Research Center in San Jose, U.S.A.

Jeroen Cornelissen was born on August 12 1972 in Veghel, the Netherlands. In 1988 he started a training in Process Technology at the Technisch Lyceum Eindhoven. After finishing this course, he joined the first year of an Environmental Science school at the Prof. H.C. van Hall Insituut in Groningen, whereafter he started to study chemistry at the University of Nijmegen in August 1992. He graduated in August 1996 with a major in Physical Organic Chemistry (prof. dr. R. J. M. Nolte) and a minor in Polymer Chemistry (prof. dr. E. W. Meijer, TU Eindhoven). From October 1996 untill January 2001 the author was employed by CW-NWO. In this period the research described in this thesis was completed. Since June 2001 he is working as a post-doctoral fellow at the IBM Almaden Research Center in San Jose, U.S.A.